Treatment of Hydrocarbon-rich and Complex Refinery Wastewater in Aerobic Granular Reactors (AGR) with Polyhydroxyalkanoates (PHA) Biopolymer Production

Thesis Submitted
in Partial Fulfillment of the Requirements for the Degree of

Doctor of Philosophy

by

Sayanti Ghosh

Centre for the Environment

Indian Institute of Technology Guwahati

Guwahati-781039, Assam, India

November, 2021

Dedicated to my parents

Centre for the Environment

Indian Institute of Technology Guwahati

STATEMENT

I hereby declare that the work contained in this thesis entitled **"Treatment of Hydrocarbon-rich and Complex Refinery Wastewater in Aerobic Granular Reactors (AGR) with Polyhydroxyalkanoates (PHA) Biopolymer Production"** is carried out by me at Centre for the Environment, Indian Institute of Technology Guwahati, under the supervision of **Prof. Saswati Chakraborty** and **Prof. Manabendra Ray**.

Sayanti Ghosh

Date: 10th November, 2021

Place: Guwahati

(Sayanti Ghosh)
Centre for the Environment
Indian Institute of Technology Guwahati
Guwahati-781039, Assam, India

November, 2021

Centre for the Environment

Indian Institute of Technology Guwahati

CERTIFICATE

It is certified that the work contained in this thesis entitled **"Treatment of Hydrocarbon-rich and Complex Refinery Wastewater in Aerobic Granular Reactors (AGR) with Polyhydroxyalkanoates (PHA) Biopolymer Production"** by **Sayanti Ghosh** (Roll No.156152003) has been carried out under our supervision in Centre for the Environment, Indian Institute of Technology Guwahati. We certify that she has fulfilled all the requirements according to the rules of this institute regarding the investigations embodied in her thesis and this work has not been submitted elsewhere for a degree.

(Prof. Saswati Chakraborty)
Professor
Department of Civil Engineering
Indian Institute of Technology Guwahati
Guawahati-781039, Assam, India

(Prof. Manabendra Ray)
Professor
Department of Chemistry
Indian Institute of Technology Guwahati
Guwahati-781039, Assam, India

ACKNOWLEDGEMENTS

Since, I reached towards the completion of my Ph.D journey, I take the opportunity to acknowledge to all the wonderful people who have been supportive during my research work and thesis writing.

It is a pleasure to express my deepest thanks and most sincere gratitude to my thesis supervisor **Prof. Saswati Chakraborty**, for her excellent guidance throughout my Ph.D work. Her kindness, dedication, hard work, patience and attention to minute details have been a great inspiration to me. Her deep knowledge of the subjects and guidance on the moral principles of high quality research is exemplary. She has always motivated me to be an independent thinker and contemplate the logics that lead to reasons, which is the biggest takeaway of her supervision. Her competence to deal with difficult situations is tremendous and always helped me to tackle complicated situations.

I sincerely thank my co-supervisor **Prof. Manabendra Ray** for his encouragement and valuable suggestions in every stage of my research work. His wisdom and immense technical knowledge always helped me to improve my work.

I express my heartfelt gratitude to the Chairman of my Doctoral Committee, **Prof. Kannan Pakshirajan**, and the members of my Doctoral Committee, **Prof. Ajay Kalamdhad** and **Prof. Subrata Kumar Majumder**, for their valuable time, precious suggestions and right directions to improve the quality of my research work. I would like to thank the current head **Prof. U. Bora** and former heads **Prof. M. K. Purkait**, **Prof. V. K. Dubey** and **Prof. G. Das** of Centre for the Environment, IITG for support and facilities provided during my research.

I am also grateful to **Dr. Deepmoni Deka** (Scientific Officer, Centre for the Environment, IITG), **Mr. Partha Protim Bakal** and **Mr. Kaustubh Rakshit** (Technical Superintendent, Centre for the Environment, IITG) and other non-technical staffs of Centre for the Environment, IITG for their help and cooperation in instrumental facilities and official matters. I am thankful to **Central Instruments Facility**, IITG and **Guwahati Biotech Park** for the allowance of sample analysis to accomplish my thesis objectives. I acknowledge **Ministry of Education (MoE), India** for providing me the research scholarship.

I gratefully acknowledge for the continuous help and encouragement I received from my senior **Dr. Sachin Kumar Tomar** from establishing my work to experimental analysis and

thesis writing. I also deeply thank my other senior **Dr. Subrat Kumar Mallick** for his help and valuable suggestions in performing experiments.

I was fortunate enough to complete my journey with my dearest friend **Poulami** who has been always there as a source of love and mental support. I am thankful to have so many nice memories with my batchmates and friends **Arnab, Jaya Krishnan, Tanushree, Himali, Anupama**, **Jinat, Udaratta and Rahul** during my Ph.D days. I acknowledge **Jaya Krishnan** for his help and encouragement in HPLC analysis. I appreciate the help and affection rendered by my juniors **Anjishnu, Agnibha, Christy** and **Shweta**. My acknowledgement would be incomplete without expressing my deepest regards to **Dr. Dibyajyoti Halder, Mr. Somnath Chanda, Mr. Rajneesh Kumar, Miss Deepa Sachan, Mr. Tanmay Dutta** and other members of Centre for the Environment, IITG for their continuous motivation, help in learning instruments and writing articles.

I would like to thank my entire classical dance group **Dr. Needhi Kotoky, Dr. Jayshree Hazarika, Dr. Poulomi Dey** and **Dr. Priyanka Talukdar** from several departments of IITG and I will always cherish the memories of our rejuvenating dance rehearsals and stage performances.

I sincerely acknowledge **Mr. Shah Alam Siddiqui**, **Mr. Hasim Ahmed** and **Mr. Shekhar Shakya** of Indian Oil Corporation Limited, Guwahati, **Mr. Girish Chandra** of Master India Brewing Company, Guwahati and **Mr. Vikas Biswas** of IIT Guwahati sewage treatment plant for providing the initial sludge and wastewater for my study.

Finally, I am very much indebted to my parents **Mr. Susanta Ghosh** and **Mrs. Swapna Ghosh** for their selfless love, patience, sacrifice and belief which helped me to achieve my goal. My research would not have been completed without their moral support, confidence and endurance. Above all, I am thankful to **The Almighty** and my **Gurudev** for bestowing blessings with a sound health, mental strength and tenacity to complete my Ph.D work.

Sayanti Ghosh

November, 2021

ABSTRACT

The modern era of bioremediation has been practicing aerobic granulation technology since last three decades in various recalcitrant industrial wastewater treatments. Compact granular structure, excellent settling property, presence of numerous pollutant degrading microbes and high tolerance to toxicity made granulation a promising biotechnology. Petroleum industries are the producers of toxic and poorly-biodegradable hydrocarbon polluted wastewater. Our first study provides extensive information about oily wastewater treatment in aerobic granular reactors (AGR) using three different inocula from sewage, refinery and brewery. Initially, sodium acetate was used for granule formation while AGR with brewery inoculum had maximum granule size. But, during emulsified diesel exposure, previous oil adaptation helped the refinery sludge granules to achieve maximum granule size of 3.49±0.01 mm and extracellular polymeric substances (EPS: 404 mg/g volatile suspended solids (VSS)) with maximum 67.39±0.15% oil removal efficiency. *Brevibacterium paucivorans* strain SG001, *Micrococcus aloeverae* strain SG002 and *Staphylococcus hominis* strain SG003 were identified as the major pollutant degraders isolated from sewage, refinery and brewery granules. *Micrococcus aloeverae* exhibited maximum hydrocarbon removal efficiencies (oil: 61.34±0.85%) among the three species. Re-addition of sodium acetate restored granule structure and stability.

We further checked the impacts of hydraulic retention time (HRT) on granule characteristics, reactor activity, hydrocarbon removal efficiency and removal mechanism while treating emulsified diesel wastewater in AGRs. AGR with shortest HRT (12 h) achieved maximum 4.72±0.05 mm granule size, 400.31±0.01 mg/g VSS of EPS with maximum biomass activity of 8.33±0.21 mg COD/mg VSS.day among the AGRs. But longest HRT (48 h) played major role providing longer reaction time for 90.31±0.26% hydrocarbon removal. Degradation of short and long chain alkanes (C_6-C_7, C_9-C_{10}, C_{11}-C_{13}, C_{15}-C_{18}, C_{27}) were observed in the AGRs which further produced fatty acids as metabolites. About 24-48 h HRT with 0.125-0.25 kg/m^3.day hydrocarbon loadings providing below 77 mg/L effluent hydrocarbon was recommended for successful AGR treatment to avoid phytotoxicity after disposal.

Rapid granulation of oil degrader *Micrococcus aloeverae* strain SG002 was conducted with investigation of its most efficient approach of bioaugmentation in AGRs to reduce granule rupture and enhance pollutant removal in multiple hydrocarbon laden refinery wastewater treatment. Highly settleable *Micrococcus* granules with 0.5±0.02 mm size formed in 15 days

achieving 80% organics removal. In control AGR, recalcitrant hydrocarbons deteriorated size and stability of aerobic granules. About 2 doses of 10% (w/w) granular augmentation of *Micrococcus* facilitated cocci abundant granule microstructure with 404.65±1.45 mg/g VSS of EPS and 7.63±0.41 mg COD/mg VSS.day of reactor activity. Granular augmentation ensured simultaneous 99% phenolics removal and 19% nitrification in 2 h within 63 days of AGR operation. Degradation of C_8-C_{15} *n*-alkanes with partial fatty acid conversion occurred in control reactor and C_6-C_{36} removal was observed indicating β-oxidation of fatty acids in bioaugmented AGRs.

Thereafter, accumulation of polyhydroxyalkanoates (PHA) biopolymers was observed in aerobic granules having mixed sludge and pure strain inoculum,. Small sized (0.71±0.04 mm) *Micrococcus aloverae* strain SG002 granules achieved 81.40±0.2% hydrocarbon removal efficiency accumulating 0.47±0.01 mg PHA/mg cell dry weight (CDW) due to cocci populated strong microbial structure. Changing organic loading (0.6-1.8 kg COD/m^3.day) and high C/N (8-24) ratio stimulated 0.71±0.04 mg PHA/mg CDW yield in the refinery granules with 90% hydrocarbon removal. Long and short chain *n*-alkanes (C_{16}-$C_{36,}$ C_6-C_{10}) were mostly biotransformed into PHA. Granule extracted PHA was characterized as copolymer P(3HB-co-3HV) having 3.5-4.5 of butyrates and valerates (PHB:PHV) ratios.

At last, a batch scale study was conducted to produce salt tolerant aerobic granules of *Brevibacterium paucivorans*, *Staphylococcus hominis* and *Micrococcus aloeverae* evaluating organics removal and nitrification efficiencies in refinery wastewater treatment. Each strain separately formed granules in 20-25 days. In *Brevibacterium,* granule size and VSS deteriorated at 20 g/L NaCl influence. *Micrococcus* granules had cocci enriched smallest granules (0.9±0.02 mm) with maximum granule strength (integrity coefficient: 12±0.12%). Refinery sludge origin and thick layer of 226 mg/g VSS EPS prevented saline inhibition in *Micrococcus* granules improving nitrification up to 28% with 93% hydrocarbon removal in 12 h. Hence, Bioaugmentation of *Micrococcus* granules can be recommended for AGR scale treatment of refinery wastewater.

Keywords: Aerobic granular reactor; Refinery wastewater; Inoculum variation; HRT variation; Bioaugmentation; Hydrocarbon biodegradation; Polyhydroxyalkanoates; Salinity tolerance.

Table of Contents

List of Tables

List of Figures

List of Abbreviations

^{1}H NMR	Proton nuclear magnetic resonance
AGR	Aerobic granular reactor
AGS	Aerobic granular sludge
AHL	N-acyl homoserine lactones
ALE	Alginate-like exopolymers
AOB	Ammonia-oxidizing bacteria
AOP	Advanced oxidation process
ASP	Activated sludge process
BIS	Bureau of Indian Standards
BOD	Biochemical oxygen demand
BSA	Bovine serum albumin
BTEX	Benzene, toluene, ethylbenzene and xylene
$CDCl_3$	Deuterated chloroform
CDW	Cell dry weight
CLSM	Confocal laser scanning microscopy
COD	Chemical oxygen demand
CON A	Concanavalin A
CPCB	Central Pollution Control Board
D	Diesel
DO	Dissolved oxygen
EDTA	Ethylenediaminetetraacetic acid
EPS	Extracellular polymeric substances
F/M	Food/microorganism ratio
FESEM	Field emission scanning electron microscope
Fig	Figure
FISH	Fluorescence in situ hybridization
FLU	Fluorines
FTIR	Fourier-transform infrared spectroscopy
FW	Fresh weight

GAO	Glycogen Accumulating Organisms
GC-MS	Gas chromatography- mass spectrocopy
GSV	Granule settling velocity
H/D	Height/diameter ratio
H_2O_2	Hydrogen peroxide
HBR	Hybrid bioreactors
HLR	Hydrocarbon loading rate
HMSA	2-hydroxymuconic semialdehyde
HPLC	High performance liquid chromatography
HRT	Hydraulic retention time
IC	Integrity coefficient
MBBR	Moving bed bioreactors
MBR	Membrane bioreactors
MFC	Microbial fuel cells
MLSS	Mixed liquor suspended solids
MLVSS	Mixed liquor volatile suspended solids
MMC	Mixed microbial culture
MoEF	Ministry of environment and forest
NaOAc	Sodium acetate
NAP	Naphthalene
NH_4^+-N	Ammonia nitrogen
NIOSH	National Institute for Occupational Safety and Health (USA)
NLR	Nitrogen loading rate
NO_2^--N	Nitrite-nitrogen
NO_3^--N	Nitrate-nitrogen
NOB	Nitrite-oxidizing bacteria
OD	Optical density
OLR	Organic loading rate
OSHA	Occupational Safety and Health Administration (USA)
P(3HB-*co*-3HV)	Co-polymer of polyhydroxybutyrates and polyhydroxyvalerates
PAC	Poly aluminum chloride

PAH	Polycyclic aromatic hydrocarbons
PHA	Polyhydroxyalkanoates
PHB	Polyhydroxybutyrates
PHE	Phenanthrene
PHV	Polyhydroxyvalerates
PN	Proteins
POME	Palm oil mill effluent
PS	Polysaccharides
QQ	Quorum quenching
QS	Quorum sensing
R1, R2, R3	Reactor 1, reactor 2, rector 3
rpm	Revolution per minute
SBR	Sequencing/ sequential batch reactor
SND	Simultaneous nitrification and denitrification
SOUR	Specific oxygen uptake rate
SRT	Solids retention time
SVI	Sludge volume index
TDS	Total dissolved solids
TN	Total nitrogen
TOC	Total organic carbon
TP	Total phosphorous
TPH	Total phenolic hydrocarbon
TSS	Total suspended solids
UASB	Up-flow anaerobic sludge blanket
USEPA	United States Environment and Protection Agency
VER	Volume exchange ratio
VFA	Volatile fatty acid
VSS	Volatile suspended solids
WWBR	Wastewater biorefineries

List of Symbols

%	Percentage
°C	Degree Celsius
µL	Microlitre
µM	Micromolar
µm	Micrometre
cm	Centimetre
g	Gram
h	Hour
kg	Kilogram
L	Litre
m	Metre
mg	Milligram
min	Minute
mL	Millilitre
mM	Millimolar
mS	Millisiemens
s	Second

Chapter 1

Introduction, literature review and objectives

CHAPTER 1

Introduction, literature review and objectives

This chapter encompasses research background, detailed literature survey on hydrocarbon-rich wastewater, recent advancements in aerobic granulation technology with our objectives and research protocol.

1.1 Introduction

Aerobic granulation technology is a modified activated sludge process (ASP) contributing smooth, compact granules having high settling velocity, high biomass retention, high tolerance to chemical toxicity consisting billions of microbial pollutant degraders facilitating simultaneous nutrient (C, N, P) and recalcitrant pollutant removals (Winkler et al., 2018). Granulation is an established biological technique for both low and high strength organic wastewater. Approximately, 20-75% energy and space reductions in aerobic granular reactors (AGR) are the added benefits to this process in comparison of conventional ASPs (de kruek et al., 2004).

Petroleum industry is the biggest energy sector which deals with refining of the crude oil to produce diesel, petrol, kerosene, gasoline, lubricants and other byproducts. Oil procurement from reservoir to final fuel production goes through a lengthy process with uncontrollable production of hydrocarbon-rich wastewater having toxic impacts on the environment. To reach the global demand, 99.93 million barrels of oil consumption has been reported in 2018 with generation of 6500 million litres wastewater per day (U.S. Energy Information Administration, 2020). Environmental regulation determined 5-40 mg/L oil as the permissible limit to discharge effluent (Daud et al., 2015). In India, according to Environmental Protection Act, 2002, the permissible limit of oil and grease in effluent is 10 mg/L and in drinking water it is 0.2 mg/L.

Crude oil and refinery wastewater consist of oil, phenol, cresols, benzene, toluene, ethyl-benzene, xylene (BTEX), poly aromatic hydrocarbons (PAH) and dissolved minerals. Oil can block sunlight and oxygen transfer in surface water hampering the marine biodiversity (Chavan and Mukherjee, 2008). Phenolic compounds are responsible for kidney, liver damage and even cancer in a human body (Zhang et al., 2016a). Moreover, crude oil extraction and distillation involve use of saline water which can even reach 300 g/L of hypersalinity in refinery effluents (Mallick and Chakraborty, 2020). Incidents of oil spillage toxicity on macro-benthic invertebrates of Suez Bay, Egypt (Belal, 2019); on coral reefs of Gulf of Mexico, South Kuwait and Taiwan (Turner and Reneger, 2017) and BTEX exposure

on tropical marine microcrustacean *Mysidopsis juniae* further reflected the detrimental effects of petroleum hydrocarbons on environment (Nascimento et al., 2020). The "2020 Assam oil and gas leak" took place in Baghjan oilfield of Tinsukia, India which hampered two important biodiversity regions named Dibru-Saikhowa National Park and Maguri Motapung Beel. In 2017, Malaysia alone was the producer of 19.86 million tons of crude palm oil releasing huge volume of palm oil mill effluent (POME) with high organic loads which could be a source of severe environmental pollution (Najib et al, 2017). Moreover, metal industry wastewater and oily effluents released from food industries are also potential sources of hydrocarbon-rich wastewaters.

Since last few decades, research and developments in physicochemical treatments like advanced oxidation process (AOP), membrane separation, nanotechnology, electrocoagulations have been carried out. Ultrafiltrations and reverse osmosis techniques are the conventional oil-water separation methods which have been further upgraded with hydrophilic polymer membranes or nanomaterial attached membranes (Ismail et al., 2020). Hydrophobic and oleophilic surfaces of bismuth vanadate ($BiVO_4$) and Fe_3O_4 magnetic nanoparticles enhanced oil adsorptions (Goh et al., 2019). Hybridization of AOP with membrane reactors enhanced 29-37% oxidation rate with antifouling abilities and 85% removal percentage in phenolic and oily wastewater (Rostam and Taghizadeh, 2020). Membrane separation and electrocoagulation are commonly known processes to treat saline wastewaters. On other hand, electrocoagulation technique achieved 71-89% oil removals from oily wastewater generated from ocean vehicles or oil drilling sites (Aswathy et al., 2016; Changmai et al., 2018). To mitigate the alarming water pollution, even United Nations (UN) has assigned "Clean Water and Sanitation" as the sixth goal to achieve the Sustainable Development Goals (SDG) by 2030 (Tahreen et al, 2020).

However, large chemical requirement, high energy consumption, costly raw materials, membrane fouling and short lifetime are the major disadvantages of these physicochemical processes. Hence, from economic and environmental aspects, biological processes are more acceptable for oil remediation. Activated sludge process (ASP), membrane bioreactors (MBR), moving bed reactors (MBBR), sequencing batch reactors (SBR), hybrid bioreactors (HBR), airlift and bubble column bioreactors, up-flow anaerobic sludge blankets (UASB), aerobic or anaerobic granular sludge and constructed wetlands are the various popular biotechnologies successfully employed in oily wastewater treatment providing 60-99% oil removal (Jain et al., 2020). Due to the longer start-up period, less sensitivity in low strength

organic wastewater and generation of odorous gases in anaerobic treatments, aerobic biological processes became more attractive to the environmentalists (Lim and Kim, 2014).

Literature on AGR mediated petroleum, coal gasification and hypersaline oily wastewater are reported to achieve about 90% oil removal at 5.6-200 mg/L oil concentrations (Zhang et al., 2011; Milia et al., 2016; Corsino et al., 2015). Chen et al. (2019) observed 95% oil remediation but nitrogen removal was only 30-39% in 100% synthetic oily wastewater where *Propioniciclava*, *Micropruina*, *Alphaproteobacteria*, *Flavobacterium* and *Sulfuritalea* bacteria were predominant. Corsino et al. (2015) achieved small granules providing large surface area for oil biosorption in hypersaline oily wastewater. Bio-adsorption of hydrocarbons in salt-adapted granules helped in petroleum slop wastewater treatment (Campo and Di Bella, 2019). POME treatments are documented to accumulate biodegradable polymer PHA at the end of feast phase of the AGR cycle. Extensive studies on sea water, fish canning and other saline wastewater have also been carried out by the researchers (Viviani, 2016; Wu et al., 2020; Sarvajith and Nancharaiah, 2020). Tomar and Chakraborty, 2018a, b and Jemaat et al, 2014 have undertaken advanced AGR studies in phenol and cresol contaminated wastewater treatment by either varying cycle time and air flow velocity or by applying bioaugmentation technique.

However, most of the cases were conducted with low hydrocarbon content (5.6-200 mg/L) which focused on AGR performances by changing loading or operating conditions rather than exploring role of inocula in changing granule characteristics and AGR performance. Studies on granulation from specific oil degrading bacteria may increase granule stability and reduce biomass washout from reactors. Moreover, Bioaugmentation of that particular strain generated granules in AGR system may further improve granule properties and oil removal efficiencies which is not well addressed in literature. Prolonged granulation time, granule rupture and hindrance in nitrification are the drawbacks in hydrocarbon-rich wastewater treatment. AGR mediated hydrocarbon degrading mechanism and recovery of biodegradable plastics polyhydroxyalkanoates (PHA) from waste sludge granules in petroleum wastewater are not discussed.

Hence our study involved with determination of role of inoculum, microorganisms, hydrocarbon loading threshold and hydrocarbon degradation pathway in aerobic granules while treating oily wastewater. Bioaugmentation aspects of specific oil degrader originated granules were thoroughly investigated in complex refinery wastewater. Salinity impacts were also examined in bio-granules. Production of PHA in oil degrading granules explored potential product recovery from recalcitrant oily wastewater.

1.2 Thesis organization

The entire thesis is divided into seven chapters. **Chapter 1** gives the introduction with literature survey, knowledge gaps and objectives of the study. **Chapter 2** is about the influence of inoculum variation and microbes in formation, stability and performance of aerobic granules in oily wastewater treatment. **Chapter 3** describes about the role of HRT, hydrocarbon degradation pathway and phytotoxicity of AGR treated effluent for a safe disposal. **Chapter 4** provides an extensive study of rapid granulation of oil degrader *Micrococcus* and its appropriate mode of bioaugmentation to enhance granule stability and hydrocarbon removal efficiency in multi-pollutant laden refinery wastewater. **Chapter 5** comprises the recovery of biodegradable polymer PHA in both refinery sludge granules and *Micrococcus* originated granules in hydrocarbon-rich wastewater. **Chapter 6** includes a batch scale granulation study separately in three types of oil degrading bacterial strains in refinery wastewater under salinity exposure. Finally, **chapter 7** presents the conclusions and future scope of the entire work.

1.3 Literature review

Aerobic granulation has been studied in low to high strength hydrocarbon-rich aromatic wastewater where granule properties, criteria of granulation, impacts of AGR operating conditions, microbial hydrocarbon degrading mechanism, nitrification phenomena, biopolymer recovery and current research trends were emphasized on. The detailed literature review on above mentioned aspects is given here in a nutshell.

1.3.1 Granulation mechanism

Aerobic granules are assemblies of diverse bacterial population which are interlinked through biological, physical and chemical actions (Winkler et al., 2018). Granulation is a gradual conversion of floccular biomass to compact spherical structure which depends on AGR configuration, feeding strategy, substrate characteristics and type of microbial population. Granulation mechanisms have been hypothesized by many researchers. Some of the proposed mechanisms are described below.

1.3.1.1 Triggering forces in aerobic granules

Liu and Tay (2002) and Winkler et al. (2018) proposed that granulation takes place in four different steps:

- Bacterium to bacterium interaction mediated by physical processes such as diffusion, gravity, hydrodynamic and/or thermodynamic forces;

- Bacterial aggregation by either physical forces like thermodynamic forces, Van der Waals, or by chemical forces like inter-particulate bridging ionic bonding or by biochemical forces such as cell surface dehydration, fusion of the cell membranes, cell to receptor attraction and so on;
- Cell aggregation by cellular forces like cell clustering or extracellular polymeric substances production;
- Granule structure stabilization by hydrodynamic shear force. This shear force was found to be responsible to provide a final three-dimensional granular structure to the microbial communities.

Different steps of aerobic granulation are described by Hailei et al. (2006) which are illustrated in Fig.1.1.

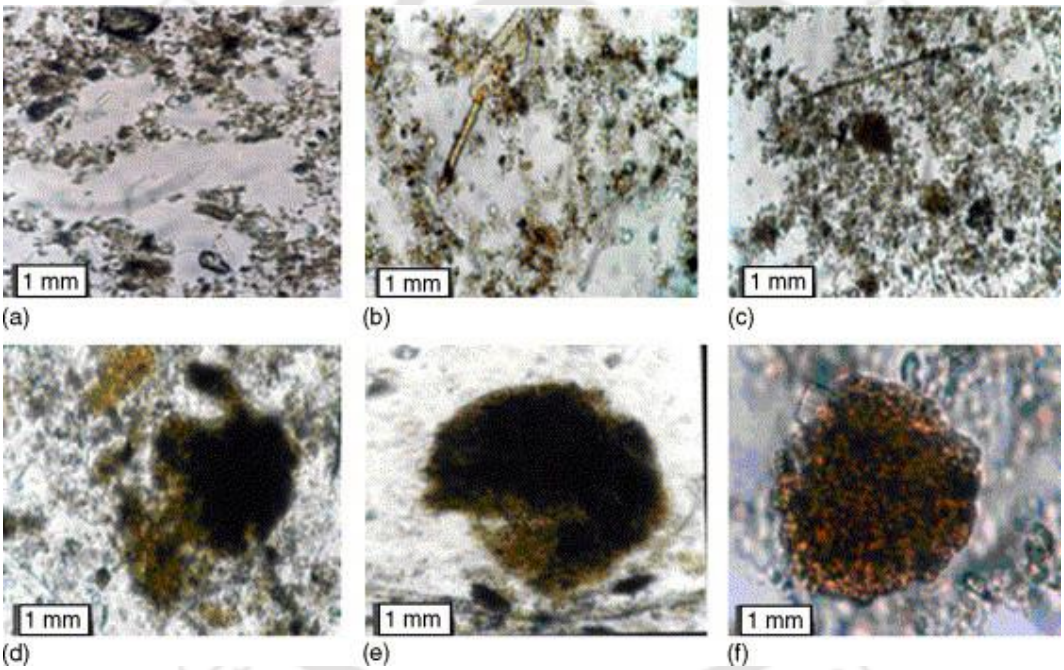

Fig.1.1 Micrograms of the granulation phenomena. Picture depicting (a) initial sludge; (b) multiplication of sludge bacteria; (c) appearance of bacterial floc; (d) cohesion of the floc; (e) maturation of floc; (f) formation of aerobic granule (Hailei et al. 2006).

1.3.1.2 Extracellular polymeric substances mediated granulation

Extracellular polymeric substances (EPS) are gummy materials secreted on the outer surfaces of microbial cells, which promote cell to cell adhesion and granule formation providing long term granule stability (Nancharaiah and Reddy, 2018, Feng et al., 2021). EPS consist of different exopolysaccharides, exoproteins, humic acid, uronic acid and DNA (deoxyribonucleic acid) which enhance granulation process (Wang et al. 2015). Proteins and polysaccharides are the major constituents of EPS which are extractable up to 60% and 40–

95%, respectively (Dubé and Guiot, 2019). In literature, PN fraction was usually found dominant over PS fractions. Hence PN/PS ratio ranged between 3-8 suggesting formation of highly hydrophobic granules (Feng et al., 2019)

However, in real and synthetic petroleum wastewater treatment, Zhang et al. (2011) and Cheng et al. (2019) observed higher proportion of PS than PN in granules. In recalcitrant hydrocarbon exposure, PS content rapidly rose up whereas the synthesis of bigger and complex PN molecules was hindered. PS was the sticky gel like substance to provide cell mechanical energy forming a protein and lipid embedded granular structure (Adav and Lee, 2008). Monosaccharides like α-D-glucopyranose and β-D-glucopyranose had a major role in organic structure composition of those oil tolerant granules. On other hand, in hypersaline oily wastewater and petroleum slop wastewater treatment, cell metabolism triggered high EPS production which facilitated enhanced hydrocarbon adsorption and degradation in granules (Corsino et al., 2015; Campo and Di Bella, 2019). Moreover, oil degrading aerobic granules were reported to have 6 to 9 times higher PN values than PS values promoting more binding PN to form stable granules (Corsino et al., 2015; Campo and Di Bella, 2019).

1.3.1.3 Role of hydrophobicity

Liu et al. (2003a) reported surface hydrophobicity as the primary factor behind aerobic granulation. Increasing cell hydrophobicity can decrease the excess Gibbs free energy of bacterial cell surface enhancing cell to cell adhesion in granulation process (Tay et al. 2002a). Greater proportion of PN in saline hydrocarbon-rich wastewater increased cell hydrobhobicity promoting granule stability (Corsino et al., 2015; Campo and Di Bella, 2019).

1.3.1.4 Cell-to-cell adhesion

Zheng et al. (2006) hypothesized that aerobic granulation promotes cell to cell adherence which regulates different cellular reactions. Bacterial aggregation is further classified into two categories:

- Auto aggregation: Adhesion between the cells of genetically identical strains.
- Co-aggregation: Aggregation between genetically different bacterial strains.

1.3.1.5 Other mechanisms

Influence of dominating microbial species (Barr et al. 2010) and addition of crushed granules inside a sequencing batch reactor (SBR) are the other granulation mechanisms reported so far (Verawaty et al. 2012). Lv et al., (2014) explored the role of bacteria (like *Pseudomonas* sp., *Acinetobacter* sp. etc.) producing autoinducer molecules, quorum sensing (QS) molecules (like Autoinducer-2 or N-acyl-homoserine lactones (AHL)) or quorum

quenching (QQ) enzymes enhancing granule formation. As autoinducers and QS molecules are interlinked with EPS synthesis in aerobic granules, they can initiate granulation of microbial flocs. Literature evidence of 10-100-fold increase in C4-C8 AHLs concentration indicated simultaneous granule initiation inside reactor (Nancharaiah and Reddy, 2018). A generalized granulation mechanism is discussed in Fig.1.2 given by Sarma et al. (2017) and Lv et al. (2014).

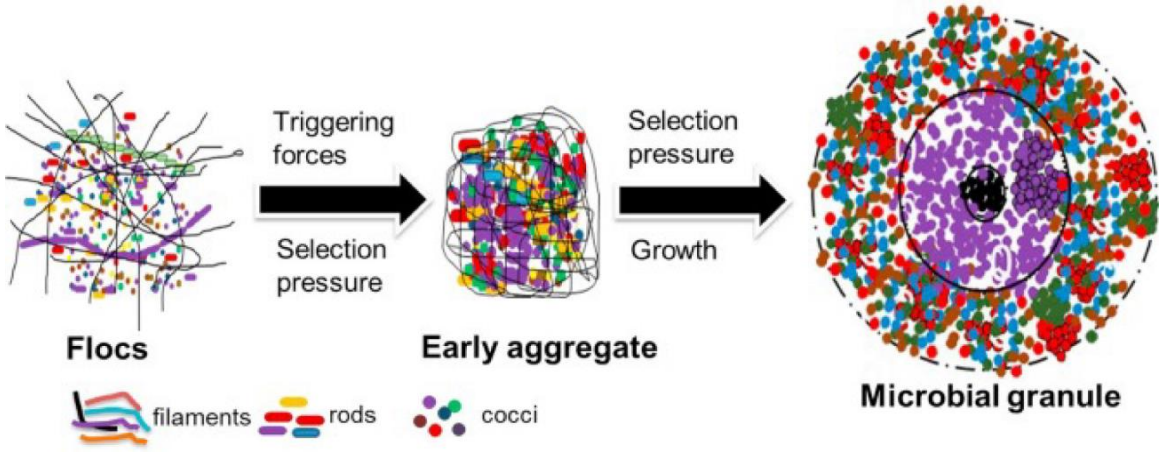

Fig.1.2 Granule formation mechanism in sequencing batch reactors (SBR) (Sarma et al., 2017; Lv et al., 2014)

1.3.2 Characteristics of aerobic granules

Characteristics of aerobic granules are determined by physical, chemical and biological parameters. Stable granulation is dependent on optimum values of several parameters like granule size, settling velocity, sludge volume index, granule strength, density, EPS concentration, microstructure etc. which are elaborated in this section.

1.3.2.1 Physical parameters

1.3.2.1.1 Size of granules

The approximate average granule diameter range lies between a wide range of 0.2 to 16 mm (Beun et al. 1999; Zheng et al. 2006). High organic loading rate promotes larger granules whereas, smaller granules can be formed under high shear forces (Gao et al. 2011). Zhang et al. (2011) faced granule size reduction in presence of 100% petrochemical wastewater. The average granule size during steady state of an AGR ranged between 0.46 to 2.7 mm in phenolic, coal gasification and saline hydrocarbon-rich wastewaters (Tomar and Chakraborty, 2020a; Milia et al., 2016; Campo and Di Bella, 2019).

1.3.2.1.2 Granule settling velocity (GSV)

Granule settling velocity corresponds with granule size and structure which lies between 30 to 70 m/h and is three times greater than the settling velocity of conventional activated

sludge (Liu and Tay 2004). Aerobic granulation is also achievable at settling velocity below 9.5 m/h (Val del Río et al. 2013). During *o*-cresol, coal gasification and hypersaline oily wastewater treatment, 5 min of average settling time provided a wide range 40-85 m/h of GSV value and petroleum sludge granules had better settleability than municipal sludge originated granules (Jemaat et al., 2014; Corsino et al., 2015; Milia et al., 2016).

1.3.2.1.3 Sludge volume index (SVI)

SVI determines the volume (in milliliters) required for 1 g of settled sludge after a specific settling time such as 5, 10 or 30 min, respectively. Granule setteability is generally represented by SVI. Shorter SVI denotes more compact and stable granular structure. Liu et al. (2003a) observed excellent granule hydrophobicity at SVI values lower than 50 mL/g. In petrochemical wastewater treatment, recalcitrance of hydrocarbon often decreased granule settling with increasing SVI values (Zhang et al., 2011; Corsino et al., 2015). However, for stable granulation, 14-40 mL/g SVI value was suggested in petroleum, phenolic, POME and hypersaline oily wastewaters (Chen et al. 2019; Tomar and Chakraborty, 2020a; Najib et al., 2017; Corsino et al., 2015). The SVI_{30}/SV_{I5} ratio of 1 recommends highly settleable granules which were observed during gradual increase of salinity in *p*-nitrophenol, phenol and *o*-cresol contaminated wastewater (Ramos et al., 2015).

1.3.2.1.4 Physical strength and density

According to literatures, approximately 1 g/mL granule density is observed for matured aerobic granules (Etterer and Wilderer 2001). During *p*-nitrophenol removal stability in granule density was achieved at 210 g $VSS/L_{granules}$ in 100 days (Jeemat et al., 2013). In petroleum slop and hypersaline oily wastewater treatment, granule density was observed within the range 70-75 g $TSS /L_{granules}$ (Corsino et al., 2015; Campo and Di Bella, 2019).

1.3.2.1.5 Integrity coefficient

Granule strength was determined in terms of integrity coefficient (IC) by calculating the ratio of solids (TSS) present in the supernatant to the total weight (TSS) of the residual granular sludge, expressed in percent (Ghangrekar et al., 2005). Rosman et al. (2014) observed that in rubber wastewater treatment, with decreasing operating HRT from 24 to 6 h, IC values of aerobic granules decreased from 18 to 9% denoting increasing granule compactness. Lower IC indicated higher granule strength. Granules having photosynthetic pigments achieved high stability and strength with 2% IC values while treating POME (Najib et al., 2017).

1.3.2.1.6 Physical structure

Aerobic granules are either spherical or rod-shaped. They are mainly yellow, brown and black in colour (Zheng et al. 2006) which is dependent on type of carbon source, feed composition and microbial population. Small brownish aerobic granules appeared in glucose-fed AGR when the settling time was decreased from 35 to 3 min and it gradually changed into yellow after granule maturation but further turned to be brownish in real petrochemical wastewater (Zhang et al., 2011).

1.3.2.2 Chemical parameters

1.3.2.2.1 Specific oxygen utilization rate (SOUR)

SOUR denotes the activity of microorganisms expressed as milligrams of oxygen consumed by a milligram of cellular protein per hour. In a case study, SOUR values in glucose-fed and acetate-fed granules ranged between 55.9 to 69.4 mg O_2/g MLVSS.h (Tay et al. 2002a). In floccular sludge, salinity intrusion can exert osmotic shock which can reduce SOUR hampering cell growth rate however granular sludge was proven to be more effective in salinity tolerance. Wu et al. (2020) observed that aerobic granules could withstand 40 g/L saline shock where 0.70 to 0.75 mg O_2/g VSS.min specific oxygen uptake rate (SOUR) recovered granule biological activities.

1.3.2.2.2 Extracellular polymeric substances (EPS)

EPS are metabolic polymers secreted by aerobic granules which help in granule formation. EPS mainly contain β-polysaccharides and proteins. In aerobic granules proteins/polysaccharides (PN/PS) ratios are generally found nearly 3.4 to 6.2 which are about 0.9 time higher than flocculent activated sludge (Adav and Lee 2008). Relatively higher protein fractions are required for matured granule formation (McSwain et al. 2005). Corsino et al. (2015) observed that in presence of new feed and high shear force, EPS synthesis increased in granules treating hypersaline oily wastewater but Zhang et al. (2011) faced initial deterioration of EPS content in granules due to hydrocarbon recalcitrance. Hydrocarbon exposure and salinity shock were proven to be responsible to enhance EPS production to form salinity resistant granules (Campo and Di Bella, 2019).

1.3.2.3 Biological parameters

Different light and electronic micrograms like light microscopy, scanning electron microscopy (SEM), Field emission scanning electron microscopy (FESEM), fluorescence in situ hybridisation (FISH) along with confocal laser scanning microscopy (CLSM) are mainly employed to study aerobic granular structures. The granule microscopic SEM image obtained by Zhang et al. (2011) is given in Fig.1.3 which indicated that in presence of glucose,

granules were dominated by cocci bacteria whereas change of substrate from glucose to petrochemical wastewater provided short and long rod-shaped bacterial population in aerobic granules (Zhang et al., 2011).

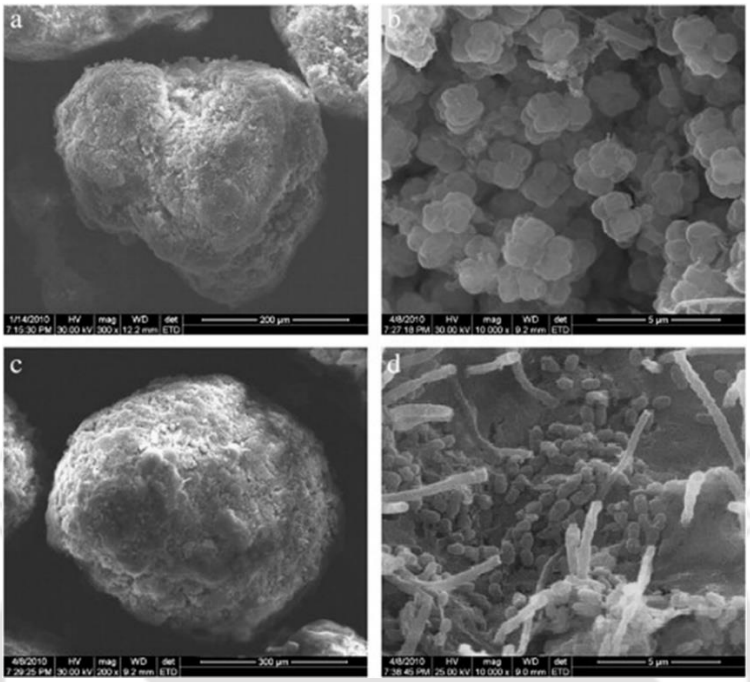

Fig.1.3 SEM images for granules developed in (a, b) glucose and (c, d) petrochemical wastewater on day 60 and 180, respectively (Zhang et al., 2011).

Bioaugmentation of 15% (w/w) VSS of *p*-nitrophenol degrading floccular sludge provided stable granulation in AGR and FISH-CLSM analysis revealed the dominance of *Acinetobacter* genus and low occurrence of *Nitrobacter* sp. in bioaugmented granules (Jemaat et al., 2013).

1.3.3 Role of microorganisms in aerobic granulation

Aerobic granules are the self-immobilized clusters of numerous bacteria having different characteristics and pollutant degrading properties. In wastewater treatment, determination of the role of inoculum and consisting microorganisms is very essential for the understanding of the probable pollutant degrading catabolic pathway. Literature addressed several groups of microorganisms in aerobic granules responsible for cell attachment, pollutant removal, nitrification and salt tolerance in industrial wastewater treatment. Some are discussed here.

1.3.3.1 Inoculation of cell aggregating bacteria

Bacterial cells can aggregate with each other to form granular structure. When cell to cell attachment occurs between two genetically similar strains it is called auto-aggregation and when it is between two genetically different species is called co-aggregation. Two co-aggregated cells can undergo joint metabolic activity and can receive biochemical cell

signalling which enhances the bio-granulation process (Lin et al., 2020). By selecting specific co-aggregating strains as inoculum, cell surface hydrophobicity for granule formation was accelerated which was reported by Ivanov et al. (2008).

Jiang et al. (2006) inoculated two co-aggregating strains *Propioniferax*-like PG-02 and *Comamonas* sp. PG-08 where *Propioniferax* was a phenol degrader and *Comamonas* had strong aggregation ability. The combination achieved fast granulation in 7 days with complete removal of 250 mg/L phenol in 2 days of AGR operation. Ivanov et al. (2006) observed about 58% co-aggregation index in aerobic granules inoculated with *Klebsiella pneumoniae* strain B and *Pseudomonas veronii* strain F with high self-aggregating properties. *Pseudomonas veronii* was further used as the starter culture for AGR system by Ivanov et al. (2008) which helped to achieve granulation in 3 days with 500 μm granule size and 70 mL/g of SVI.

Liu et al. (2015a) seeded an AGR with 2 g (dry weight) of pyridine degrading and auto-aggregating *Rhizobium sp*. NJUST18 which was capable of forming 0.5-1 mm sized granules with 37 m/h settling velocity and achieved complete removal of 4000 mg/L of pyridine in 7.5 h of study. In another study, AGR was inoculated with 2 g (dry weight) of pyridine degrading or coaggregating strains *Rhizobium sp.* NJUST18, *Shinella granuli* NJUST29 and *Paracoccus versutus* NJUST32. The combination of NJUST18+NJUST29 had the strongest coaggregation having 62.08% of coaggregation index which helped in forming 0.2-0.5 mm granules with high EPS content of 232.79 mg/g VSS achieving complete 1000 mg/L pyridine removal in AGR within 50 h (Liang et al., 2018).

Inoculation of denitrifier TN-14, in continuous flow AGR enhanced EPS production with high quantity PN fraction in granules (Xin et al., 2017). The major fact which revealed from these studies was that the extracellular PN of EPS was the major contributor of self and co-aggregation in aerobic granules.

1.3.3.2 Role of pollutant degraders

Inoculation of slow growing bacteria is essential to achieve stable granulation (Zhang et al., 2019). Bioaugmentation approaches were extensively studied by adding a particular pollutant degrading strain or mixed sludge in order to enhance pollutant removal efficiency of the aerobic granules (Herrero and Stuckey, 2015). Literature evidences of inoculation of *p*-nitrophenol degrading floccular sludge, *Pseudomonas putida* SM1443 carrying plasmid pJP4 and pyridine degrading species *Rhizobium sp*. NJUST18 provided successful bioremediation of *p*-nitrophenol, *o*-cresol, 2,4-dichlorophenoxyacetic acid, chlorophenols and pyridine contaminated wastewater, respectively (Jemaat et al., 2013, 2014; Quan et al., 2010, 2011;

Ma et al., 2012; Liu et al., 2015a). However, the pollutant degrading strains should also possess cell aggregating and EPS producing properties to maintain granule strength and to prevent biomass washout from the reactors.

1.3.3.3 Nitrifying, denitrifying bacteria and PAOs

Nitrosomonas are found to be predominant among ammonium oxidizing bacteria (AOB) population and has a low affinity towards oxygen (Poot et al., 2016). On the other hand, *Nitrobacter*, *Nitrosomonas* and *Nitrosospira* generally coexist with *Nitrosomonas* on outer oxygen saturated layer of aerobic granules whereas, *Nitrosospira* and *Nitrobacter* are found in deeper granule layers due to their stratified growth in low oxygen availability (Winkler at al., 2013). In nitrifying-denitrifying bio-granules *Nitrobactor* is considered to be the major nitrite oxidizing bacteria (NOB) as they are capable to grow mixotropically during nitrite reduction. Heterotrophic denitrifiers play a major role in nitrite reduction. Imbalance in AOB and NOB population are majorly observed in granular sludge (Poot et al., 2016).

Zhang et al. (2011) observed that in presence of real petrochemical wastewater, aerobic granules faced partial disintegration and instability which reduced nitrogen removal due to the probable rupture in outer AOB layer of granules. In another study, Jemaat et al. (2014) bioaugmented heterotrophic *o*-cresol degrading sludge in AGR to enhance cresol removal. As a result, the cresol degrader prevailed on the outer layer of granules and acted as a shield for the AOBs ensuring high rate of nitrification during cresol treatment.

In phosphate removal the influence of pH, salinity, temperature and organic loading, type of substrates and AGR parameters are proven to be effective in aerobic granules (Bassin et al., 2011). Hypersalinity caused gradual depletion in phosphate accumulating organisms (PAOs) like *Accumulibacter* from granular sludge. *Candidatus*, *Accumulibacter* and *phosphatis* are the major species responsible for enhanced P removal by aerobic granules (Gonzalez-Gil and Holliger, 2011). However, in presence of volatile fatty acids like acetate and priopionate, PAO growth was observed to outcompete the glycogen-accumulating organisms (GAOs) as PAOs were successful to utilize the organic substrates at a pH range of 6.5-7.5 and temperatures between 15-30 °C (Nancharaiah and Reddy, 2018).

1.3.3.4 Filamentous bacteria

Excessive filamentous growth in aerobic granules is unfavourable as it provides loose granular structure which is vulnerable and can be easily washed out from the AGR (Kent et al., 2018). Zhang et al. (2006) observed significant reduction in granule density and hydrophobicity hampering granule settleability when filamentous bacteria were dominant in granules. But presence of filamentous bacteria in the initial stage of granulation helps in

bridging between the microbial cells to form bigger sludge flocs. Due to increased surface area, filamentous bacteria can outcompete other microbes at low substrate and dissolved oxygen concentration (DO) resulting into filamentous dominance during granule formation phase. Gradually with time, sufficient oxygen supply in the AGRs suppresses the overgrowth of filaments, high shear forces detach the filaments from the granule surfaces and helps in non-filamentous dense granule formation (Tay et al., 2002b; Show et al., 2012; Tomar and Chakraborty, 2018a). Short settling time can further wash out the filamentous bacteria from the reactors.

1.3.3.5 Other Microorganisms

Activated sludge is mainly composed of hydrophobic and hydrophilic bacterial population. Hydrophobic species help in granule maturation and improves the granule settleability in AGRs. Hydrophilic bacteria remain in effluent as free biomass and don't participate in cell aggregation (Winkler et al., 2018). There are numerous microbial species which take part in granulation and pollutant degradation. One such most common phylum in aerobic granules is *Proteobacteria*. Multiple bacterial genera under the phyla of *Bacteroidetes, Firmicutes* and *Actinobacteria* have been isolated from active granules (Amorim et al., 2014). Several heterotrophic bacteria were identified as fast-growing EPS producers. However, *Pseudomonas, Zoogloea, Flavobacterium, Stenotrophomonas* and *Acinetobacter* had major role in EPS matrix formation, which belong to PAO, GAO, autotrophic nitrifier and ANAMMOX bacterial category (Amorim et al., 2014).

During salinity exposure, several halotolerant and halophiles became predominant in aerobic granules to prevent biomass washout from AGRs. *Marinobacter, Halomonas, Azoarcus, Sphingomonas* and *Muricauda* were some halotolerant species isolated from saline shock resistant granules treating seawater or saline aromatic wastewater within 2-40 g/L NaCl concentration (Ramos et al., 2015; Li et al., 2020; Sarvajith and Nancharaiah, 2020).

Table 1.1 represents presence of several microbial species responsible for maintaining granule stability, hydrocarbon removal, salt tolerance and nitrogen removal during different types of oily wastewater treatment studied so far.

Table 1.1 Role of inoculum and major bacterial population present in AGRs in several hydrocarbon-rich wastewater treatment

Type of wastewater	Seed sludge	Pollutant range	Effective degrading microorganism	Microbial removal mechanism	References
Petrochemical wastewater	Activated municipal sewage sludge	COD: 282±20 Phenol: 13 mg/L Oil: 5.6 mg/L, NH_4^+-N: 42.9 mg/L	Cocci dominance: in synthetic wastewater; rod shaped bacteria: in real petrochemical wastewater with co-substrates	Petrochemical wastewater was treated by co-metabolism with glucose, sodium acetate and propionate. Propionate was the most efficient in degrading refractory compounds and NH_4^+-N.	Zhang et al. (2011)
o-cresol wastewater	Bioaugmentation of *p*-nitrophenol-degrading activated sludge	*o*-cresol: 100 mg/L, NH_4^+-N: 950 ±25 mg/L	Dominance of *Acinetobacter* and low amount of *Nitrobacter*	*Acinetobacter* was *o*-cresol degrader and *Nitrobacter* helped in partial nitration	Jemaat et al. (2014)
Hypersaline oily wastewater	Activated municipal sludge and from a membrane reactor	COD: 900-1350 mg/L, TPH: 6.8 mg/L, NH_4^+-N: 90-105 mg/L	Salinity and hydrocarbon exposure inhibited [1]AOB and [2]NOB growths reducing nitrification; anaerobic granule layer helped in phosphorus removal; [3]PAO growth was further deteriorated by chlorides	Granule microbes enhanced EPS production which helped in oil inclusion inside granules indicating adsorption of hydrocarbons	Corsino et al. (2015)
Saline aromatic wastewater	Phenol degrading aerobic granules of a continuous airlift reactor	COD: 2890±240 mg/L, (phenol, *p*-nitrophenol, *o*-cresol: 563±21, 350±17, 95±6 mg/L), glucose and sucrose	At low salinity: *Sphingobium*, *Cythophaga* and *Comamona* and at high salinity: *Devosia*, *Sphingomonas* and *Muricauda* were the most abundant genera	*Sphingobium*, *Cythophaga* and *Comamona* were the aromatic compound degrader; *Devosia*, *Sphingomonas* and *Muricauda* were halotolerant EPS producers	Ramos et al. (2015)
Palm oil mill effluent (POME)	Mixed sludge from sewage oxidation pond, POME facultative pond and POME	Organic loading rate: 2.75 kg COD/m^3.day	*Enterobacter cloacae*, *Bacillus cereus* and *Lysinibacillus* sp. with photosynthetic pigments, bacteriochlorophyll *a* and carotenoids.	Reduction of carbon dioxide (CO_2) from POME by the photosynthetic pigments of biogranules	Najib et al. (2016)

Petroleum wastewater	Petrochemical sludge from secondary clarifier	COD: 600-900 mg/L, oil: 50-200 mg/L, NH_4^+-N: 25-40 mg/L	Oil degrading genera *Propioniciclava*, *Micropruina*, *Alphaproteobacteria*, *Flavobacterium* and *Sulfuritalea*.	*Propioniciclava* and *Micropruina*, utilized carbohydrates in feed; *Alphaproteobacteria*, *Flavobacterium* and *Sulfuritalea* were aromatic hydrocarbon degraders and *Flavobacterium* took part in nitrification in AGR	Chen et al. (2019)

[1]AOB: ammonium oxidizing bacteria
[2]NOB: Nitrite oxidizing bacteria
[3]PAO: Polyphosphate accumulating organisms

1.3.4 Impacts of operating conditions in granulation

Granulation is a complex microbial phenomenon which depends upon several reactor operational conditions like organic loading, hydraulic retention time (HRT), settling time, feeding patterns etc. Since the major regulating factors are difficult to predict, the operational conditions are considered as the accessible 'window' to optimize a stable granulation inside an AGR. The AGR operating conditions affecting granule characteristics and performance are discussed in this section.

1.3.4.1 Organic loading rate (OLR)

Aerobic granulation is achievable at different OLRs. Moy et al. (2002) and Liu et al. (2003a, b) successfully achieved aerobic granulation at high loading of 15 kg COD/m^3.day as well as low loading of 2.5 kg COD/m^3.day organic loading rates. It indicates that aerobic granulation is almost independent of OLR values. However, Tay et al. (2004) suggested that about 4 kg COD/m^3.day as an optimal OLR of aerobic granulation for achieving 99% of COD removal efficiency. In palm oil mill effluent treatment by aerobic granules, COD removal was independent of OLRs between 3-6 kg COD/m^3.day. Rapid granulation occurred at 2 kg COD/m^3.day and 1.6-1.7 kg COD/m^3.day OLR range in petrochemical and petroleum slop wastewater treatment, respectively.

1.3.4.2 Settling time

Approximately 5 minutes settling time is required to achieve effective granulation. According to literatures, short settling time around 5 minutes helps to provide high cell proteins to the polysaccharides and a rise in granule hydrophobicity (Qin et al. 2004). In petrochemical and POME wastewater treatment, granule settling velocity decreased from 15 to 0.5 min with increasing granule size and stability (Gobi et al., 2011; Chen et al., 2019; Campo and Di Bella, 2019).

1.3.4.3 Intermittent feeding strategy

According to the literatures, aerobic granules had been mostly reported in sequencing batch reactor (SBR). SBR operation mode consists of feeding, aeration, sludge settling and effluent decanting in each cycle. In a cycle the settling time and volume exchange ratio (VER) provide a specific pressure to washout loose and non-granular biomass from the reactor eliciting mature granulation (Liu et al. 2007). Fig.1.4 provides a schematic diagram of SBR for aerobic granulation fed with two different substrates, phenol and sodium acetate acetate studied by Tomar and Chakraborty (2019).

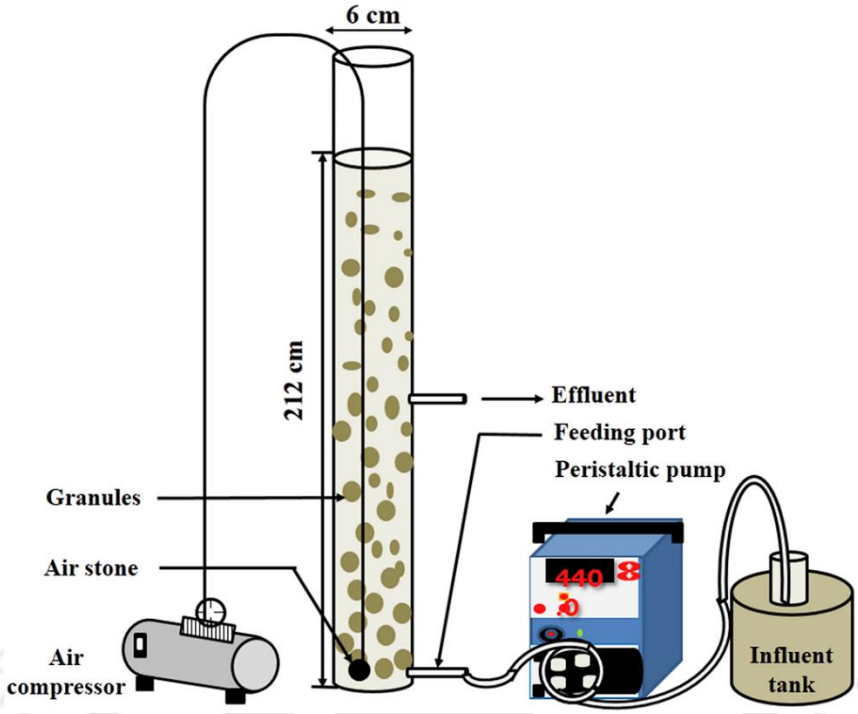

Fig.1.4 Schematic of SBR operated with refinery sludge inoculum by using two substrates, phenol and sodium acetate (Tomar and Chakraborty, 2019).

1.3.4.4 Hydrodynamic force

High hydrodynamic shear force enhances stable and compact granule formation (Khan et al. 2009). Superficial air velocity above 1.2 cm/s is required for aerobic granulation inside a sequencing batch reactor (Liu and Tay 2004). Hence, higher shear force, promotes faster microbial aggregation leading to rapid biogranulation (Beun et al. 1999). Corsino et al. (2015) observed significant PS and PN productions in aerobic granules during start-up phase in presence of high shear force and new feed in hypersaline oily wastewater treatment.

1.3.4.5 Augmentation of cations and toxic chemicals

Cations and chemicals were not directly associated in pollutant removal mechanisms of aerobic granules but they are reported to trigger the granulation process. Dosing of 100 mg Ca^{2+}/L was reported to provide more compact granules structure than in control reactor (Jiang et al., 2003) and about 500 mg/L of poly aluminum chloride (PAC) augmentation reduced average granulation period from 17 to 7 days (Liu et al., 2014). PAC augmented granules had 3.2 mm granule size with better EPS production than control system. Role of mineral cations like Ca^{+2} was explored in granule formation by improving EPS synthesis to protect the granules against increased salinity shock (Ma et al., 2020). Restoration of any supressed biological activity and microbial population could also be achieved by Ca^{2+} dosing. Zhang et al. (2016b) achieved restoration of metabolic growth of damaged ANAMMOX cells. Liu et

al. (2020) conducted an experiment where effluent sludge was conditioned with Ca^{+2} before reintroducing in AGR which further increased granule EPS concentration. Tomar and Chakraborty (2020b) conducted reformation of disintegrated aerobic granules treating phenolic wastewater by adding 340 mg/L of thiocyanate which with increased granule size up to 1.8 mm and evoked EPS content till 101 mg/g VSS.

1.3.4.6 Seed sludge

The properties of the initial seed sludge affect aerobic granule formation. Two sequencing batch reactors were seeded with two different types of sludge. One was inoculated with 100% flocculent sludge and another one was added with 10% crushed granules (and 90% flocculent sludge) for studying the aerobic granulation enhancement. Aerobic granules developed faster in 90%-floc sequencing batch reactor and were fully granulated than 100% floc sequencing batch reactor. However, the mean granule diameter was almost similar. The removal rate of nitrogen, phosphorous and organic matter were 75%, 93% and 85%, respectively in 100% floc sequencing batch reactor, while in 90% floc sequencing batch reactor pollutant removals were found to be 84%, 99% and 80%, respectively (Coma et al. 2012). To achieve matured granulation in 18 days, Pijuan et al. (2011) and Verawaty et al. (2012) suggested inoculation of 50% (dw/dw) crushed granules and a mixture of flocculent sludge and crushed granules, respectively. Milia et al (2016) observed that use of oil acclimatized petrochemical sludge provided faster granulation and higher total organic carbon (TOC) removal than sewage sludge in coal gasification wastewater treatment.

1.3.4.7 Food to microorganism (F/M) ratio

F/M ratio determines the ratio of incoming food (influent COD) and microorganisms (suspended solids) available in the reactor. In most of the cases, high F/M ratio accelerates faster and larger granulation, and a low F/M ratio results into slower and smaller granule formation. Moreover, a high F/M ratio enhances granule stability and size (Lobos et al. 2008). But Moy et al. (2002) reported that large and compact granules suffered from air diffusion limitations. Hence, F/M ratios should keep changing at different phases of SBR operation to achieve proper granulation. Li et al. (2011) suggested high F/M ratio in the initial phase and low F/M ratio in the final phase to be optimum for aerobic granulation. During start-up phase of petroleum wastewater treatment, granule MLVSS was reduced in oil exposure increasing F/M ratio from 0.11 to 0.45 kg COD/kg MLVSS.day with decreased cycle time from 24 to 15 h in AGR (Caluwé et al., 2017).

1.3.4.8 Feast/famine feeding strategy

In substrate abundance, microorganisms (feast phase) accumulate it and synthesize EPS which is utilized as the energy source to conduct metabolic activities of microbes in carbon deficient phase (famine phase). A long starvation period can reduce treatment efficiency of an AGR but can also enhance PN production in EPS matrix (Rusanowska et al., 2019). In low organic loading, aerobic granules were observed to rapidly consume the yeast feed which resulted into high EPS production (Kang and Yuan, 2017). At lowest organic loading, granules rapidly consumed the substrate in a short period leading to longer famine phase where the EPS provided the carbon and energy for endogenous respiration. In contrast, Campo et al., (2018) indicated high energy requirement of aerobic granules to adapt hypersaline environment which resulted into EPS consumption by granules during feast phase. Caluwé et al. (2017) operated two AGRs in two different modes of aerobic feast/famine, and anaerobic famine/aerobic feast to treat petrochemical wastewater. Both AGRs obtained matured granules in 30 days with 95% COD removal efficiency but anaerobic AGR had comparatively smaller granules than the aerobic one.

1.3.4.9 Height to diameter (H/D) ratio

Height to diameter ratio (H/D) of an AGR column is the major controlling parameter for granular shape and microstructure formation. Zhu et al. (2008) observed that when the H/D ratio was very high in an AGR, internal flow patterns helped in strong granule formation. In contrast, Kong et al. (2009) reported that in AGR, H/D ratio and granule settling velocity had no significant effect on granulation. In petroleum, POME and petroleum slop wastewater the H/D ratio of AGR was maintained for stable granulation at 5.71, 6.67, 10, respectively (Chen et al., 2019; Gobi et al., 2011; Campo and Di Bella, 2019).

1.3.4.10 Hydraulic retention time (HRT)

HRT determines the average contact time between microbes and soluble compound or pollutant remains in a bioreactor. For SBR performance optimization, an effective HRT should be carefully selected (Fang and Yu, 2001). Beun et al. (1999) observed that shorter HRTs promote stable granulation. However, a very short HRT can suppress the biomass growth due to excessive washout of the flocculent biomass from the reactors. Rosman et al. (2014) observed that low HRT (12 h) enhanced COD and nitrogen removal in rubber wastewater treatment whereas, Tomar and Chakraborty (2018b) reported that granule size and EPS content were inversely proportional to HRT and pollutant removal was independent of the HRT while treating phenol and ammonia in AGRs. In petrochemical wastewater treatment 12 h HRT was effective to form oil degrading granules (Zhang et al., 2011; Chen et

al., 2019). Aerobic granulation was also achieved at short and longer HRTs of 6 and 24 h in POME and hypersaline oily wastewater, respectively (Gobi et al., 2011; Corsino et al., 2015).

1.3.4.11 Volumetric exchange ratio (VER)

VER defines the volume of the effluent withdrawn in every cycle of the SBR. An exchange ratio of 40, 50 or 80% was found favourable for granulation. Wang et al. (2006) observed that rapid granulation was possible in AGRs having high VERs and good settling properties. If settling velocity was less, high VER caused excessive biomass washout causing poor granulation. In petrochemical, POME and petroleum slop wastewater treatments, AGRs were operated with a fixed 50% VER as reported in literature (Zhang et al., 2011; Najib et al., 2017; Campo and Di Bella; 2019).

1.3.4.12 Substrate composition

Aerobic granulation occurred in wide varieties of simple carbon substrates like glucose, sucrose, acetate, molasses and ethanol (Adav et al., 2008). Granulation was also observed with recalcitrant compounds like phenol (Tomar and Chakraborty, 2018b), thiocyanate (Tomar and Chakraborty, 2018a), hydrocarbons (Zhang et al,. 2011; Chen et al., 2019) and aniline (Winkler et al., 2018). Granules cultivated in inorganic carbon source with nitrifyning bacteria exhibited excellent nitrification efficiencies (Tay et al. 2002b). Aerobic granulation was successfully employed in treating low strength to high strength real domestic and industrial effluents generated from municipal, petrochemical, brewery, textile, paper mill, dairy products, seafood, manure and pharmaceutical sectors (Winkler et al. 2018).

However, Granule microscopic structure and bacterial community are largely dependent upon types of substrates in which they are cultivated. Literature evidences proved that glucose-fed granules obtained loosely bound and filamentous structure whereas acetate-fed granules achieved compact and non-filamentous structures with more stability (Liu and Tay 2004).

1.3.4.13 Effects of environmental factors

1.3.4.13.1 pH

According to Hailei et al. (2006), slightly alkaline pH nearly 7.5 is essential for matured granule formation. However, granulation might be hindered at pH values above 8.5. Acidic pH is favourable for fungi growth inside the granules, whereas an alkaline pH produces bacteria dominating granules ensuring compact microbial structure (Yang et al. 2008). Considering the alkaline pH of petroleum wastewater, Milia et al. (2016) treated coal gasification wastewater in two different phases having pH 7.2 and 7.8, respectively. But no significant impact of pH variation was observed in NH_4^+-N removal efficiency of AGRs.

1.3.4.13.2 Effect of temperature

Temperature is a key factor in granulation, microbial population and reactor performance. According to Hailei et al. (2006), temperatures below 41 °C and above 26 °C are favourable for granule formation. Zhiwei et al. (2009) optimized 30 °C temperature essential for matured granulation. At low temperature (16 °C) a stepwise increase of salinity enhanced aerobic granulation till 14 g/L NaCl concentration. Petroleum and coal gasification wastewater were mostly reported to be treated at an average of 25 °C temperature in AGRs (Zhang et al., 2011; Milia et al., 2016).

1.3.4.13.3 Dissolved oxygen concentration (DO)

Granules are observed to be formed across lower DO concentration range of 0.7 to 1.0 mg/L (Dangcong et al. 1999) and at higher concentration of 2 mg/L (Tay et al. 2002c) in SBRs. It proves that DO is not a significant parameter for aerobic granules. On other hand, Hailei et al. (2006) found that below 2.5 mg/L DO concentration resulted into unstable poor granulation. However, Sturm and Irvine (2008) demonstrated more importance of DO concentration on substrate removal kinetics than hydrodynamic shear force in aerobic granulation. Gobi and Vadivelu (2014) reported decrease in DO level during accumulation of PHA in aerobic granules whereas it further reached saturation level in famine phase. Vijayan and Vadivelu (2017) also observed that despite of continuous aeration of 2 L/min, DO level in AGR went below saturation level in feast phase as oxygen was required to convert volatile fatty acids (VFA) in PHAs. At the end of feast phase, DO level reached saturation level (8.6 mg/L) as less oxygen was needed to oxidize less amount of remaining substrate.

In AGR system for oily wastewater, granulation occurred mainly in oil-acetate or oil-glucose co-substrate feeding strategy (Zhang et al., 2011; Chen et al., 2019). Table 1.2 summarizes the effective AGR operating strategies along with significant outcomes studied in various types of hydrocarbon-rich wastewater treatment.

Table 1.2 Effective AGR operating strategies along with significant outcomes studied in different hydrocarbon-rich wastewater treatment

Type of effluent	Major operational strategy	AGR operating parameters	Results obtained	References
Petrochemical wastewater	Oil acclimation and co-metabolism methods	AGR volume: 3 L; OLR: 2 kg COD/m^3.d; NLR: 0.16 kg NH_4^+-N/m^3.day; VER: 50%; cycle time: 6 h; superficial air velocity: 2.2 cm/s operation time: 223 days	Granule size: 220 µm, SVI: 26.1-41.5 mL/g, COD removal: 89% ([1]I: 500 mg/L), NH_4^+–N: (I: 42.9 mg/L) 94%	Zhang et al. (2011)
Palm oil mill effluent (POME)	Integrated biological and adsorption removal method	AGR volume: 8 L; OLR: 3-6 kg COD/m^3.d; VER: 25%; superficial air velocity: 5 L/min; cycle time: 6 h; operation time: 170 days; biological removal: in AGR, adsorption: in waste granules	Granule size: 0.9 mm, granulation time: 110 days; [2]MLSS: 3.6-2.5 g/l; SVI: 30 mL/g, COD removal: by AGR: 88-90%; by adsorption: 10%	Gobi et al. (2011)
p-nitrophenol wastewater	Bioaugmentation of 15% (w/w) of *p*-nitrophenol degrading floccular sludge	AGR volume: 2.6 L, air flow-rate: 125-500 mL/min, *p*-nitrophenol: 15 mg/L, Operation time: 111 day	Size: 1.5±0.2 mm,VSS: 2.4-3.2 g/L, GSV: 70±5 m/h, SVI_5: 13±2 mL/g TSS, EPS: 60±7 mg/g VSS	Jeemat et al. (2013)
Saline aromatic wastewater	Long term salinity, co-substrate feeding and granule reconstruction by adding anaerobic granules	AGR volume: 2.6 L, air flow-rate: 150 to 250 mL/min, influent COD: 2890 mg/L (Phenol, *o*-cresol, *p*-nitrophenol, glucose, sucrose), salinity: 2-29 g salt/L, operation time: 250 days	Granule size: 0.22 mm. SVI_{30}: 26±2 mL/g, SVI_{30}/SVI_5: 1, EPS: 61 g/g [3]VSS, COD removal: 96%, halotolerant granule bacteria were EPS producers and degraded aromatics at low salinity	Ramos et al. (2015)
Petrochemical wastewater	Aerobic and anaerobic feast/famine regimes were varied in AGRs	[4]SBR_{ae}: aerobic regime; [5]SBR_{an}: anaerobic famine and aerobic feast regime; OLR: 1.0-1.35 kg COD/m^3.d	Granule size: 264.7-07.4 µm, SVI: 71-56 mL/g MLSS; GSV: 10 m/h. COD removal: 96% (I: 94.0±26.2 mg/L; 80.4± 27.8 mg/L)	Caluwé et al. (2017)

Palm oil mill effluent (POME)	Carbon dioxide (CO_2) reduction of POME by using photosynthetic bacteria in aerobic granules	AGR volume: 1.2 L; OLR: 2.75 kg COD/m^3.d; VER: 50%; air velocity: 2.07 cm/s; cycle time: 4 h; operation time: 120 days	Granule size: 0.3-2.36 mm, MLSS: 6.90-8.25 g/L; GSV: 18.0-103.0 m/h; integrity coefficient: 2%; granule bacteria having photosynthetic pigments like bacteriochlorophyll *a* and carotenoids consumed POME as nutrient	Najib et al. (2017)
Coal gasification wastewater	By varying seed sludge, pH control range and superficial gas flow velocity	AGR volume: 3 L; VER: 50%; cycle time: 4 h; HRT: 8 h; operation time: 480 days, sludge: municipal and petrochemical [6]WWTP, pH: 7-7.8, superficial gas flow velocity: 2-3 cm/S	Granule size: 1300-250 µm, SVI_8: 30±8 mL/g.TSS; VSS: 4.9±0.6 g/L; [7]TSS: 260±20 mg/L; GSV: 1.1-6 m/h; COD removal: 92-94% (I: 240–630 mg/L); NH_4^+-N: 78% (I: 340–610 mg/L)	Milia et al. (2016)
Petroleum wastewater	Correlation of organic/nitrogen removal was established with microbial communities	AGR volume: 71 L; VER: 50%; H/D: 5.71; cycle time: 4.8-6 h; operation time: 130 days	Granule size: 0.46–0.9 mm, EPS: 128 mg/g.VSS; SVI_{30}: 30 mL/g; integrity coefficient: 99.8%; COD removal: 95% (I: 900 mg/L); NH_4^+-N: 30–39% (I: 25-40 mg/L); Oil: 90% (I: 200 mg/L)	Chen et al. (2019)
Petrochemical slop wastewater	slop was treated with (i) matured salt-adapted granules and (ii) by cultivating aerobic granules in slop wastewater	AGR volume: 3.5 L, air flow velocity: 3.3 cm/s, cycle time: 6 h, VER: 50%, COD: 816 mg/L, TPH: 151 mg/L, NaCl: 37.8±1.5 g/L	More oil adsorption and degradation in granules grown in slop, Size: 1-1.15 mm, VSS: 2.5 g/L, SVI_5: 10 mL/g, PN: 80-100 mg/g VSS, PS: 5-25 mg/g VSS; COD removal: 67%, [8]TPH removal: 83%	Campo and Di Bella (2019)

[1]I: influent (mg/L), [2] MLSS: Mixed liquor suspended solids (g/L), [3]VSS: volatile suspended solids (g/L), [4]SBR_{ae}: Sequencing batch reactor aerobic, [5]SBR_{an}: Sequencing batch reactor anaerobic, [7]TSS: Total suspended solids (mg/L), [8]TPH: Total phenolic hydrocarbons (mg/L)

Aerobic granulation technology has been regarded as an emerging technology. Other than petroleum wastewater is has been widely used in different induatrial wastewater treatment. Some are listed below in Table 1.3

Table 1.3 Wide range of application of aerobic granulation in for various wastewater treatment systems

Type of wastewater	**Opearating conditions**	**Observation**	**Reference**
Phenolic wastewater treatment	AGRs with 6 L working volume were operated with refinery and brewery sludge at 6 and 12 h HRTs and 5 min settling time. Phenol loading varied between 1-2.4 kg phenol/m^3/day	Brewery sludge provided 2.7 mm sized granules having 114 mg/g VSS of EPS content but refinery granules disintegrated beyond 3.32 kg COD m/day of organic loading.	Tomar and chakraborty (2020)
Malting wastewater	AGRs treated malting wastewater with an OLR (COD_{total}) of 3.4 kg/m^3·d with cycle time of 8 h, settling time of 5-2 min, HRT of 0.5 days and volumetric flow rate of 600-800 L/h.	AGRs achieved 80%. COD removal efficiency.	Schwarzenbeck et al. (2004)
Anabattoir (slaughterhouse) wastewater	Granules were developed for treating nutrient rich abattoir wastewater with with cycle time of 8 h, settling time of 2 min, HRT of 13-3 h.	Removal efficiencies for the total COD, total N and total P were found to be only 68%, 86% and 74%, respectively.	Lemaire et al. (2008)
Pharmaceutical wastewater	manganese-oxidizing aerobic granular sludge (Mn-AGS) were cultivated in AGRs with 18 to 9 h HRT and addition of *Pseudomonas putida* MnB1 bacteria	ASRs removed pharnmaceutacals at 8-127 µg/h/g SS of removal rate.	He et al. (2019)
Dairy wastewater	Successful cultivation of AGS in a SBR for treating dairy wastewater was carried out at a 50% volumetric exchange ratio, a cycle duration of 8 h, settling time of 15-4 min and a volumetric flow rate of 600 L/h.	Removal efficiencies of 90% COD_{total}, 80% N_{total} and 67% P_{total} can be achieved after complete granulation process.	Schwarzenbeck et al. (2005)

Brewery wastewater	AGs with sizes of 2–7, volumetric exchange ratio of 50%, cycle duration of 6 h, settling time of 18-4 min and superficial air flow velocity of 1.77 cm/s were cultivated in a SBR.	A high and stable removal efficiencies of 88.7% COD_t and 88.9% NH_4^+-N were achieved.	Wang et al. (2007)
Swine slurry	A SBR for treating swine slurry was operated with cycle time of 3h, settling time of 10-4 min and HRT of 6 h. During stage 1 the OLR was set to be 1.9 kg CODs/ m^3d for promoting granule formation while in stage 2, swine slurry content was increased.	Granule size in stage 1: 1.1 to 2.3 mm, in stage 2: 2.0 to 2.8 mm. The removal efficiencies for organic and ammonia were found to be 61–73% and 56–77%, respectively.	Morales et al. (2013)
Livestock wastewater	AGS in SBR for treating wastewater from a cattle farm was cultivated with a SVI of 42 mL/g, cycle time of 4 h, settling time of 15 min and air flow rate of 1 L/m.	Granule size range: 3.5 to 4.1 mm Maximum COD, TN and TP removal efficiencies: 74%, 73% and 70%, respectively.	Othman et al. (2013)
Rubber wastewater	Granules with diameter 1.5 mm**,** settling velocity of 33 m/h, SVI of 22.3 mL/g, settling time of 15 min and with air velocity of 1.7 cm/s were developed in SBR for treating rubber wastewater.	Granules showed excellent settling ability, The removal efficiencies for COD, ammonia and total nitrogen were 96.5%, 94.7 and 89.4%.	Rosman et al. (2014)
Seafood industry wastewater	AGs were cultivated with OLR applied between 2 to 13, with cycle time of 3 h, settling time of 3-1 min and HRT of 0.25 days to treat Seafood industry wastewater.	The Total nitrogen removal efficiency was around 30% and the maximum ammonia removal was reached up to 65%.	Val del Río et al. (2013)
Textile industry wastewater	AGs were successfully cultivated inside a SBR with SVI of 19 ml/g and 19ml/g after 5min and 30 min settling, volume exchange ratio was 50%, OLR was 20 kg COD/m.d while treating textile wastewater.	Stable azo dye (Acid Red 14) removal yield was above 90% and the sludge retention time (SRT) in 15 days triggered a 30% reduction in the bio decolorization yield.	Franca et al. (2015)

Pulp mill wastewater	Aerobic granules were cultivated inside AGRs by using bioaugmentation technique	High BOD (97%) and COD (90%) removal efficiencies have been observed.	Morais et al. (2016)
Resource use of spend aerobic granules (a) PHA accumulation	Aerobic granules were treated with an aerobic dynamic feeding (ADF) strategy with a feast period of 50–120 min and a period of starvation.	The accumulated Polyhydroxyalkanoate (PHA) yield was around 0.7 mg PHA/mg biomass.	Gobi and Vadivelu (2014)
(b) MB removal and adsorption	Methylene blue (MB) adsorption by the EPS content of granules was studied.	The removal of MB by EPS was responsible for 9.38% of the adsorption capacity.	Wei et al. (2015)
(c) Ammonium adsorption	Adsorption capacity of ammonium by aerobic granules was observed.	Maximum adsorption: 24.5 mg NH_4^+-N/g-volatile suspended solids at >2000 mg NH_4^+-N/L.	Yu et al. (2014)
(d) Strontium (II) adsorption	Strontium (II) adsorption by AGs was affected by solution pH, biomass quantity, temperature and mixing intensity.	Ion exchange, physical adsorption and surface complexation were responsible for adsorption.	Wang et al. (2015)

1.3.5 Hydrocarbon and recalcitrant pollutant degradation mechanisms

Hydrocarbon removal occurred either by adsorption in granule EPS matrix or by biodegradation by hydrocarbon degrading microorganisms. Bio-adsorption approach is an alternative to conventional membrane separation or coagulation processes for heavy metals, recalcitrant and emerging pollutants removal and it is closely related to the EPS content in aerobic granules (Kong et al., 2014). The adsorption process is dependent on several factors. Firstly, the surface charge and aerobic granule surfaces are generally found to be negatively charged. Secondly, the functional groups present on granule surfaces.

Granule EPS layer is mainly composed of carboxyl, amine and hydroxyl groups which take active role in pollutant bio-adsorption. Lastly, the surface area of the granules and it is observed to be decreased with granule maturation from seed sludge. However, the porosity and presence of multiple functional groups enhance pollutant bio-adsorption in granules (Wang et al., 2018).

In POME treatment, about 88% COD removal was biologically achieved by aerobic granules and the remaining 21% was bio-adsorbed by waste aerobic granules (Gobi et al., 2011). Corsino et al. (2015) observed that in hypersaline oily wastewater treatment, TPH removal increased from 30 to 50% with oil droplet inclusion inside aerobic granules. Within 55 days of the study, hydrocarbon removal efficiency reached 90% with decreased granule size which increased granule surface area providing active sites for oil adsorption. On other hand, increase in EPS concentration (340 mg/g VSS) also provided several functional groups enhancing oil inclusion in granules. Fig.1.5 provides an image of oil droplet inclusion in granule cultivated in hypersaline oily wastewater (Corsino et al., 2015).

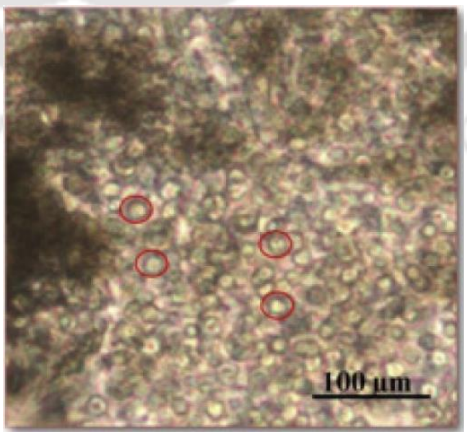

Fig.1.5 Oil droplet inclusion inside aerobic granules by bio-adsorption in hypersaline oily wastewater treatment (Corsino et al., 2015)

Oil adsorption in granules provided more contact time with granule bacteria for biodegradation of oil. Rise in PN and PS fractions at end of feast and famine phase further

indicated slow degradation of hydrocarbons in granules. Aerobic granules grown in petroleum slop had rapid synthesis of binding PN in presence of salinity and hydrocarbon stress (Campo and Di Bella, 2019). The enhanced EPS production further ensured bio-aggregation for granulation and bio-adsorption of hydrocarbons in granules. The dual mechanism acted as a physical and biological selector promoting robust aerobic granules containing salt adapted hydrocarbon degrading bacteria. Gradual adaptation in saline aromatic wastewater provided complete biodegradation of phenol, *o*-cresol and *p*-nitrophenols without producing any intermediate compound (Ramos et al., 2015).

Several microorganisms were observed to play major role in biodegradation of hydrocarbons. *Propioniciclava*, *Micropruina*, *Alphaproteobacteria*, *Flavobacterium* and *Sulfuritalea* were identified as the oil degrading genera present in granules treating petroleum wastewater (Chen et al., 2019). *Acinatobacter* was the main phenol degrading species isolated from bioaugmented AGR fed with *o*-cresol wastewater (Jeemat et al., 2014). In phenol, *o*-cresol and *p*-nitrophenol contaminated saline wastewater, dominance of *Sphingobium*, *Cythophaga* and *Comamona* were observed as the aromatic compound degrader whereas, *Devosia*, *Sphingomonas* and *Muricauda* were the EPS producers (Ramos et al., 2015). The probable aerobic phenol biodegradation is described in equation 1.1.

$$C_6H_5OH+7O_2 \rightarrow 3H_2O+6CO_2 \quad (1.1)$$

During *p*-cresol degradation in AGR, Basheeer and Farooqi (2012) observed the conversion of phenols to catechols (1, 2-hydroxybenzene) which further followed either *ortho* or *meta* pathway. In *ortho* pathway of cathechol, cis, cis-muconate is produced via catechol-1,2-dioxygenase which can be further utilized in TCA cycle. In *meta* pathway, catechol ring is cleaved by catechol-2,3-dioxygenase to 2-hydroxymuconic semialdehyde (HMSA). HMSA can be either oxidized or hydrolyzed to 4-oxalocrotonate and 2-oxopent-4-enoate and cis-muconate is finally converted to muconolactone.

In AGR treatment of pulp mill wastewater *Pseudomonas* sp. degraded high molecular weight lignin and tannin into lower molecular weight fractions and *Corynebacteriaceae* and *Flavobacterium* were identified as aromatic compound degraders and excellent EPS producers (Vashi et al., 2018). In azo dye removal process, biosorption and biodegradation were effective in aerobic granules. Azo dye reduction was initiated with azo bond breakage in anaerobic mode in presence of electron donor co-substrates. The byproducts and amines were further consumed by granules as carbon and nitrogen sources providing CO_2, water and nitrogenous compounds as end products of the pathway (Sarvajith et al., 2018). Pyridine degradation was reported by *Paracoccus* sp. in aerobic layer of granules with simultaneous

denitrification (Wang et al., 2018). According to Tomar and Chakraborty (2018a), in AGR system thiocyanate was degraded by following hydrolysis to cyanate (OCN^-) and sulfide (S^2), then another round of hydrolysis of OCN^- was observed into NH_4^+ and bicarbonates (HCO_3^-). Sulfides were finally oxidized to sulfates (SO_4^{2-}).

Ion exchange and bio-adsorption in EPS are the most probable metal removal mechanisms in AGRs. Removals of hypotoxic heavy metals like Zn (II), Cu (II), Mn (II), Fe (II), Ni (II), Co (II), Cr (III) and highly toxic cationic metals like Pb, Cd, Be etc. were studied in AGRs (Wu et al., 2019; Liu and Xu 2008; Liu et al., 2015b). pH, granule surface charge and temperature were the key factors in metal bio-adsorption process. By adding manganese oxidizing aerobic granules redox sensitive heavy metals like As (III) and Sb (III) were oxidized into less toxic As (V) and Sb (V) whereas, Cr (VI) was reduced to less harmful Cr (III). *Paracoccus* was identified as the major acetate utilizing bacteria which was probably responsible for oxidizing Mn (II) (He et al., 2019).

Other recalcitrant pollutants like 2,4-dichlorophenoxyacetic acid, *p*-nitrophenol, aniline were also reported to be biodegraded by aerobic granules (Quan et al., 2011; Jeemat et al., 2013; Jiang et al., 2017) and methylparaben was removed by bio-adsorption (Argenta et al., 2020). Emerging pollutants like estrogen, estradiol, pharmaceutical and personal care products were also treated in AGRs where changes in bacterial population were observed during toxic pollutant exposure (Amorim et al., 2018).

1.3.6 Nitrogen removal and nitrification

Conventionally, during nitrification process, NH_4^+-N is initially converted into NO_2^- by ammonia-oxidizing bacteria (AOB) (*Nitrosomonas*) which is considered as partial nitrification and it is further transformed into NO_3^- by nitrite-oxidizing bacteria (NOB) (*Nitrobactor*) called complete nitrification (Metcalf and Eddy, 2003). The overall reactions (Metcalf and Eddy, 2003) involved in nitrifications are summarized below in equation 1.2a-c.

$$2NH_4^+ + 3O_2 \rightarrow 2NO_2 + 4H^+ + 2H_2O \quad (1.2a)$$

$$2NO_2^- + O_2 \rightarrow 2NO_3^- \quad (1.2b)$$

$$NH_4^+ + 2O_2 \rightarrow NO_3^- + 2H^+ + H_2O \quad (1.2c)$$

Sludge retention time (SRT) determines average time the activated sludge solids retain inside a reactor and it is a useful parameter to design a reactor. Long SRT (10-30 days) favours the growth of NOBs (Wan et al., 2013). Hence, in recalcitrant pollutant exposure, granule rupture may increase effluent biomass washout which can decrease SRT values and

NOB populations which may further hamper the complete nitrification in AGRs. Winkler et al. (2015) observed that unlike flocculent activated sludge, aerobic granules had *Nitrobacter* NOB dominance but not *Nitrospira*. They further explained two probable pathways.

i) Nitrite-loop: The pathway can supply additional NO_2^- from partial denitrification and can elevate NOB/AOB ratio in AGR. The pathway is described in equation 1.3.

$$NH_4^+ \xrightarrow{AOB} NO_2^- \xrightarrow[Nitrobacter]{Nitrospira} NO_3^- \xrightarrow{DPAOs} N_2 \qquad (1.3)$$

ii) Ping-pong: This pathway provides mixotrophic growth of *Nitrobacter* in presence of acetate and predominance of mixotrophic *Nitrobacter* growth is observed among the NOBs (equation 1.4). Moreover, the mixotrophic *Nitrobacter* enables NO emission from AGR. Variation in temperature and oxygen level leads to increase in NOB/AOB ratio with NO emission.

$$NH_4^+ \xrightarrow{AOB} NO_2^- \xrightarrow[Nitrobacter]{Nitrospira} NO_3^- \begin{cases} \xrightarrow[DPAOs]{Nitrobacter} N_2 \\ \xrightarrow{} NO \end{cases} \qquad (1.4)$$

Probable nitrogen removal pathways in aerobic granules are given in Fig.1.6.

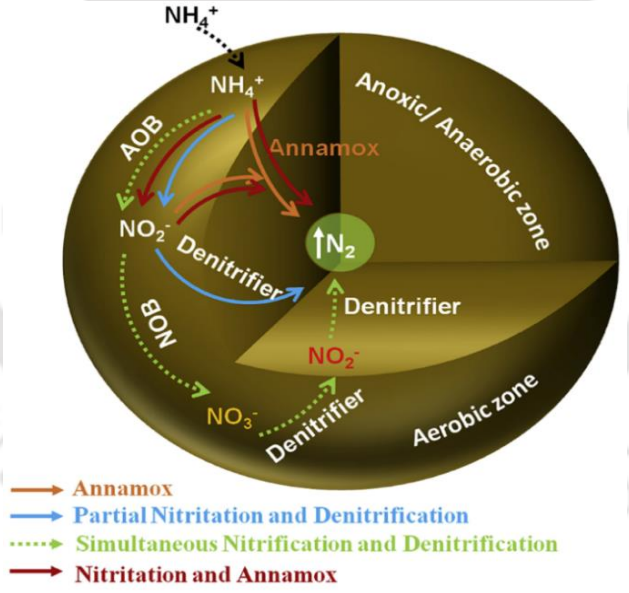

Fig.1.6 Summary of probable biological nitrogen removal pathways like ANAMMOX, partial nitrification and denitrification, simultaneous nitrification and denitrification in aerobic granular sludge (Nancharaiah and Sarvajith, 2019).

Simultaneous nitrification and denitrification (SND) were evident in aerobic granules even during continuous aeration in AGR (Nancharaiah and Reddy, 2018). Under same reactor conditions, micro scale granules performed SND where nitrification and denitrification occured concurrently which wass dependent on coexistence of aerobic and anoxic regions.

Aerobic granular size, availability of electron donor, microbial activity and DO level were the major parameters controlling SND process (Coma et al., 2012).

However, in hydrocarbon-rich wastewater treatment granules often suffer from partial disintegration and reduced nitrogen removal. Tomar and Chakraborty (2020a) observed partial nitrification at 700 mg/L phenol concentration due to phenol toxicity. It increased biomass washout, supressed NOB population and reduced SRT (9-9.7 days) which finally resulted into patrial nitrification. Corsino et al. (2015) observed only 45% NH_4^+-N removal but nitrification was absent in hypersaline oily wastewater as AOB growth was inhibited by aromatic hydrocarbons and NOB population was inhibited by salinity. Similarly, Chen et al. (2019) faced very low NH_4^+-N removal (30-39%) due to presence of nitrifying and denitrifying bacteria inhibitory compounds like alkanes and heterocyclic nitrogen in petroleum wastewater. However, addition of glucose co-substrate provided electron donors for the activation of microbes providing 100% NH_4^+-N removal. Partial nitration was also observed during *p*-nitrophenol and *o*-cresol removals in AGRs (Jemaat et al., 2013, 2014). Presence of *Acinetobacter* confirmed phenolic compound removal and low occurrence of *Nitrobacter* confirmed that NOB growth was supressed by AOB populations in granules.

1.3.7 Salinity tolerance mechanism in aerobic granules

Increase of salinity in wastewater stream can increase cell osmotic shock which can hamper specific oxygen uptake rate (SOUR) and reduce bacterial cell metabolism, cell growth rate and can further disrupt the enzymatic pathway for pollutant removal. As a result, the COD removal capacity of activated sludge microbes is reduced in salinity exposure (Wu et al., 2020). Hence, fabrication of a stable activated sludge process in increasing salt concentration is a challenging task. Presence of 20 and 30 g/L of salinity in wastewater or industrial effluent are considered as saline and hypersaline wastewater, respectively (Sarvajith and Nancharaiah, 2020).

High salinity was responsible to increase water density leading to high biomass washout in flocculent sludge whereas due to high stability and biomass retention, granular sludge could withstand in salinity stress (Wu et al., 2020). In granular sludge, hypersalinity stress also triggered EPS synthesis increasing cell surface hydrophobicity which provided a protective layer on granules (Corsino et al., 2017). Some literature indicated presence of high PN concentration consisting porin or periplasmic binding PN which are associated with transmembrane transport under saline shock (Wang et al., 2017). It further enhanced microbial activity for pollutant degradation under saline environment.

Corsino et al. (2015) observed hydrocarbon adsorption and biodegradation in aerobic granules while treating hypersaline oily wastewater. In 2-29 g/L of salinity exposure, complete removal of phenol, *o*-cresol, *p*-nitrophenol from aromatic wastewater was achieved by Ramos et al. (2015) where AGR was simultaneously fed with co-substrates. Fish canning wastewater and hypersaline seawater promoted saline shock resisted granules at 30-70 g/L NaCl range (Viviani, 2016; Sarvajith and Nancharaiah, 2020). Two types of seed sludge, i) salt-adapted bio-granules and ii) flocculent sludge exposed to petroleum slop for granulation were used to treat petroleum slop wastewater (Campo and Di Bella, 2019). The second type of sludge had higher EPS content for TPH adsorption which achieved 67% COD and 83% TPH removals, respectively. He et al. (2021) observed complete phenol removal (10-100 mg/L) with phenol favoured P removal than N in AGR fed with phenolic wastewater at low salinity (2% NaCl).

Presence of several halophilic microorganisms was prominent in those studies. *Halomonas* and *Nitzschia* strains in synthetic saline wastewater (Meng et al., 2020), autochthonous seawater-born microbes, *Stappiaceae* and *Rhodobacteraceae* (Sarvajith and Nancharaiah, 2020), EPS producing *Devosia*, *Sphingomonas* and *Muricauda* were dominant in aerobic granules treating saline aromatic wastewater (Ramos et al., 2015).

1.3.8 Recent advancements in aerobic granulation technology

Since last decade, extensive research and development was carried out by coupling and hybridizing several technologies for performance enhancement of wastewater treatment processes. Simultaneous waste treatment with resource and energy recovery, incorporation of different microbial species or adsorbents to achieve multipollutant degrading shock resistant granules are the few methods which are currently being studied in aerobic granulation. Some of the popular techniques are discussed here.

1.3.8.1 Bioaugmentation

Previously, biological reactors were considered as “black boxes” because their functionality was hugely dependent on empirical knowledge of microbial ecology. The major disadvantage of bioreactors was the lack of sufficient number of specific pollutant degraders. However, non-specific sludge or consortium augmentation mostly had unpredictable outcomes (Herrero and Stuckey, 2015).

Bioaugmentation process ensures the process efficiency of reactor by adding a specific bacterial strain or a consortium having pollutant degrading properties. Bioaugmentation reinforced the AGR system by reducing slow granulation and maturation problems faced by mixed sludge inoculum. Addition of pollutant degrading or cell aggregating strains further

improved granule structural stability, AGR performance and nitrogen removal by preventing depletion of ammonia-oxidizing outer granule layer during recalcitrant pollutant exposure. Ma et al. (2012) suggested above 5% (w/w VSS) augmentation to be effective in reducing biomass washout from AGRs. Bioaugmentation was carried out by

- pre-adapted pure strain,
- pre-acclimatized consortia,
- genetically engineered bacteria,
- biodegradation-relevant genes or by
- plasmid mediated augmentation (Herrero and Stuckey, 2015).

Bioaugmentation was introduced in AGRs by the experiments of Jiang et al. (2006, 2007) where co-aggregating *Propioniferax*-like PG-02 and *Comamonas* sp. PG-08 and similar phenol degrader strains *Pandoraea* sp. PG-01 and *Rhodococcus erythropolis* PG-03 were utilized to enhance aerobic granulation. The bioaugmented granules had 0.3-1.8 mm size with 34-47 mL/g SVI determining high granule stability. The augmentation also improved phenol removal up to 100% for 250 mg/L phenol concentration within 2 h. Further experiments were carried out by pre-adapted activated sludge or gene augmentations. Bioaugmentation of 12% (w/w) VSS of *p*-nitrophenol degrading activated sludge (Jemaat et al., 2014) and *Pseudomonas putida* SM1443 carrying plasmid pJP4 augmented in 10% inoculation ratio (Quan et al., 2011) in two different studies helped in complete removal of 100 mg/L *o*-cresol and 500 mg/L 2,4-dichlorophenoxyacetic acid, respectively. Fig.1.7 obtained from Quan et al. (2011) showed that control AGR had dominance of *Pseudoxanthomonas taiwanensis*, uncultured *proteobacteria*, uncultured *Sphingobium* sp. and *Novosphingobium* sp. (c, d) whereas after *Pseudomonas* augmentation, presence of *Aquincola*, *tertiaricarbonis* and *Sphingobium* sp. were also observed in bioaugmented granules (a, b).

In case of pyridine removal, bioaugmentation potential of self-aggregating *Rhizobium sp.* NJUST18 was explored in AGR system (Liu et al., 2015a) which was further modified by Liang et al. (2018) where a combination of *Rhizobium sp.* NJUST18 and *Shinella granuli* NJUST29 strains showed high coaggregation index of 62.08%. Both cases achieved complete pyridine removal in 1000-4000 mg/L of pyridine influent. The granulation coaggregation mechanism observed by Liang et al. (2018) is described in Fig.1.8.

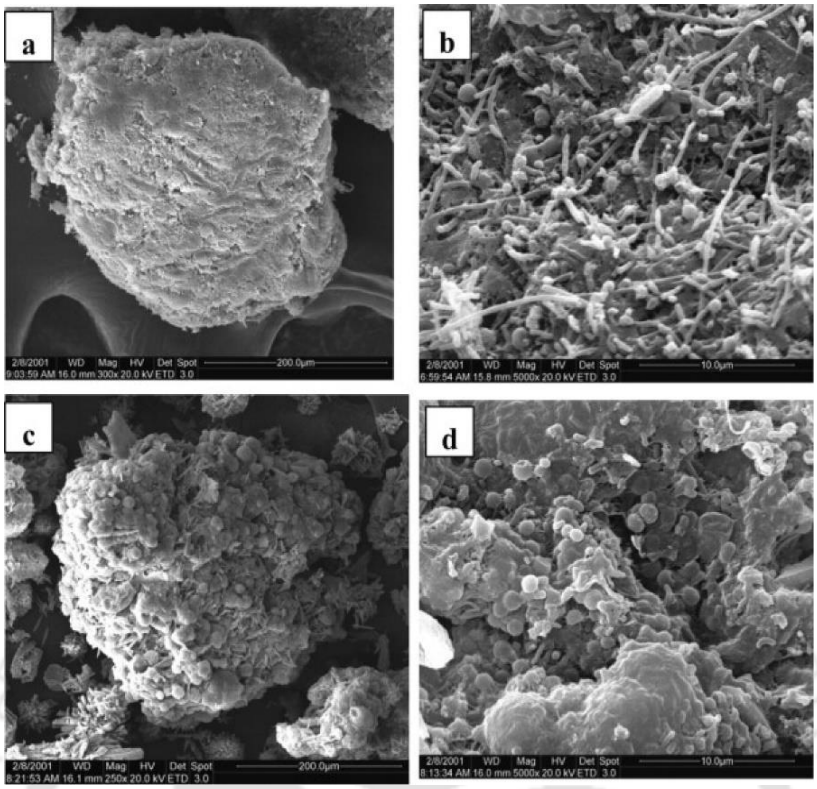

Fig.1.7 SEM micrograms of aerobic granules grown in (a, b) *Pseudomonas* bioaugmented reactor and (c, d) control reactor (Quan et al., 2011).

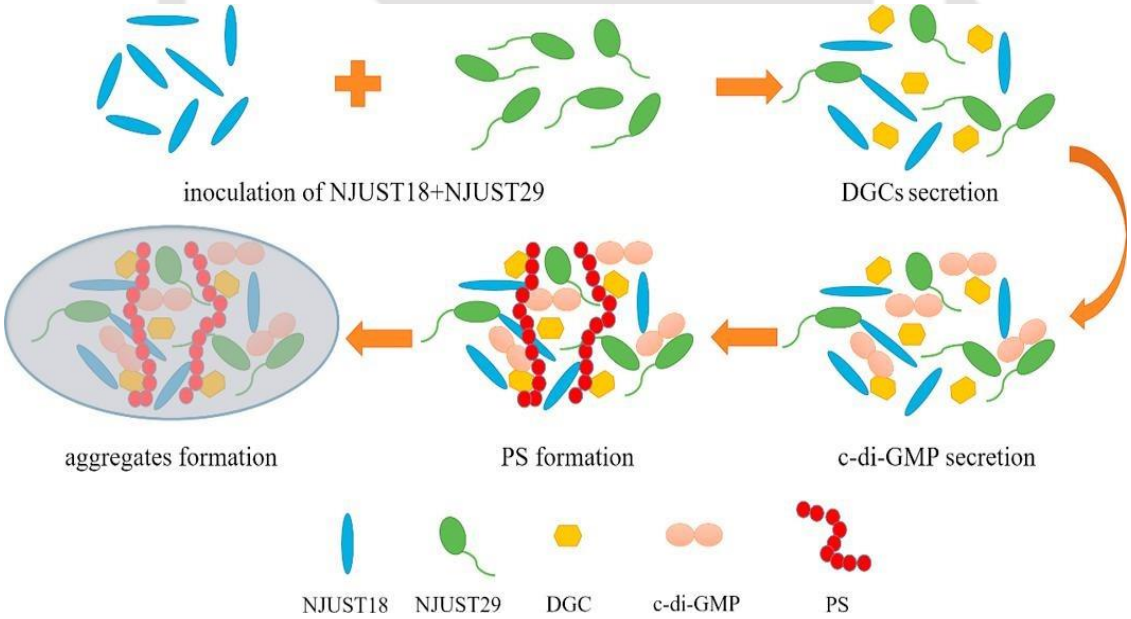

Fig.1.8 Granulation mechanism based on coaggregation of *Rhizobium sp.* NJUST18 and *Shinella granuli* NJUST29 for pyridine contaminated wastewater treatment (Liang et al., 2018).

Seed granules, biofilm and temporary inorganic carrier (like activated carbon) augmentation are studied for granulation in continuous flow reactors (Kent et al., 2018). Repeated bioaugmentation is essential to maintain stability of newly introduced strains which

is a lengthy process. Not only a strain or consortium selection, but also the way of introducing and survival the specialized consortia by maintaining DO, nutrient and growth environment are the key factors for successful bioaugmentation (Herrero and Stuckey, 2015). Emerging areas of research like protein engineering, in vitro compartmentalization, surface area sequestration, nanotechnology can be incorporated in developing new bioaugmented AGRs for recalcitrant wastewater treatments.

1.3.8.2 Algal-bacterial aerobic granules

AGRs are capable of minimizing space and energy requirements by 50-75% and 30-48% while compared to conventional activated sludge plants (Nancharaiah et al., 2019). However, the 60% energy cost is spent for providing aeration in AGRs (Bengtsson et al., 2018). Since last three years, use of microalgae in wastewater treatment is attracting the environmentalists as they are fast growing and can reduce aeration cost by providing oxygen supply through photosynthesis. Utilization of algal-bacterial aerobic granules is documented in photo sequencing batch reactors in saline seawater-based wastewater and wastewater having low C/N ratio (Liu et al., 2017; He et al., 2018; Rajitha et al., 2020; Huang et al., 2020). Algal-bacterial granules are also proven to be capable of enhanced nitrogen and phosphorus removal along with lipid producing biomass suitable for biofuel production.

Liu et al. (2017) inoculated *Chlorella* and *Scenedesmus* algae with bacterial sludge in photo reactors. Dissolved oxygen (DO) level played a crucial role in lipid synthesis from algal-bacterial granules. Finally, maximum total nitrogen and phosphate removal were correlated with higher algal biomass fraction in granules but not proportionally increased with fatty acid methyl esters yield. *Cyanobacteria* and *Comamonadaceae* communities occupied up to 5.2–36% population in the granular sludge.

In low strength synthetic domestic wastewater, algal-bacterial granules developed in 7 days by overproduction of sticky PS, binding PN with tryptophan with humic acids (He et al., 2018). Illumina pyrosequencing technology revealed that fast growing algal community supressed the diversity of bacterial population. Initial predominant algae *Diatomea* was shifted to green algae *Chlorophyceae* after granule maturation. Huang et al. (2020) observed significant increase in unsaturated fatty acid methyl ester content in algal-bacterial granules due to the rapid growth of *Stigeoclonium*, *Navicula* and *Scenedesmus* algal genera.

Autochthonous phototrophic biofilm was used to produce microalgae-colonized aerobic granules (Rajitha et al., 2020). Morphology of algal-bacterial granules in phototrophic and non-phototrophic conditions revealed that granules in 12 h/12 h light/dark and 24 h dark condition formed clear boundary with green microalgae. But in 24 h light condition, granules

had hairy growth. Autofluorescence indicated presence of bacteria (green) and bacteria and algae overlap (yellow) in 12 h/12 h light/dark, bacterial colony (green) was observed under 24 h dark condition and no autofluorescence was seen in 24 h dark condition (Fig.1.9). The algal-bacterial granules were highly settleable which reached 20 mL/g SVI_5 and achieved 95% and 97% of total nitrogen and phosphate removals in salinity influence. Hence, algal-bacterial granular sludge system offers a multi-functional water-resource-energy recovery with carbon sequestration providing both economic and environmental sustainability (Zhang et al., 2021).

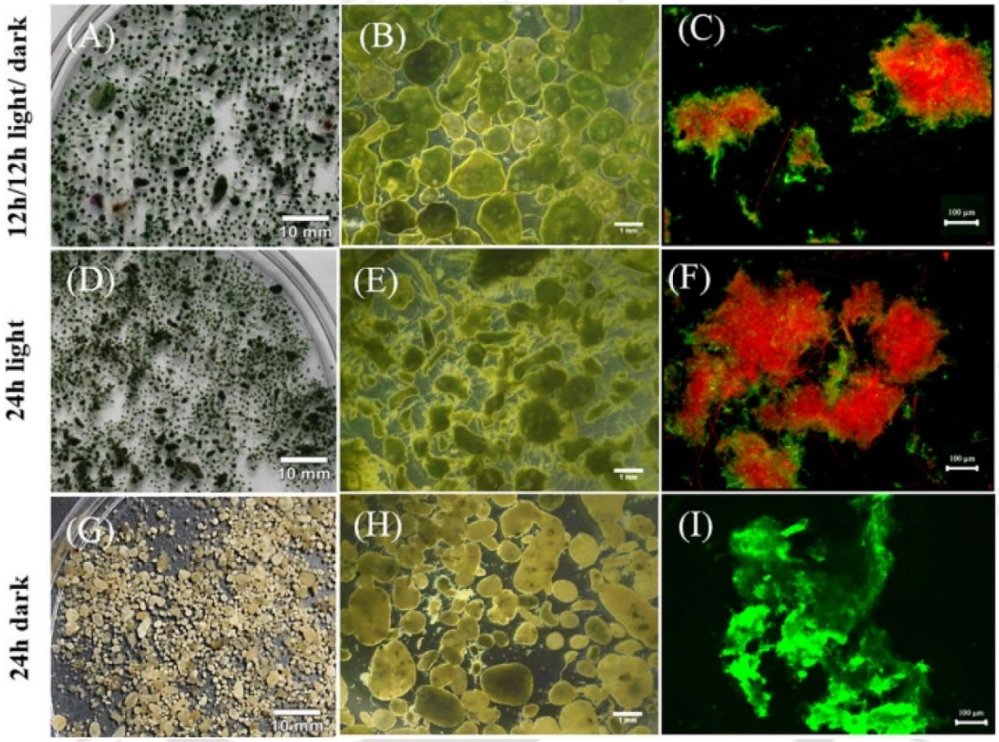

Fig.1.9 Algal-bacterial granules in phototrophic (24 h and 12 h/12 h light/dark) and non-phototrophic (dark) conditions. A, D, G: Bird's eye view images; B, E, H: Stereo-zoom microscopic images; C, F, I: Fluorescence microscopic images (Rajitha et al., 2020).

1.3.8.3 Drying of aerobic granules

Currently, use of dried granules is frequent as an inoculum for a rapid AGR start-up, long term granule storage or as supplement to AGR for reactivation of treatment efficiency (Show et al., 2012). Bone dried granules with high proteins/polysaccharide ratio was obtained by following seven different procedures at 37, 60 and 4 °C temperatures and also by keeping the granules in sunlight, in dark, in flowing air stream and by dipping in acetone, respectively (Hu et al., 2016). Even though dried granules faced 80% volume loss and reduction of volatile organic matters, after recovery they almost recovered their structural integrity with restoration of previous organics removal efficiency. Zhang et al. (2019b) suggested that after

dry storage of granules in agar at 4° C temperature for 30 days, granule efficiency can be restored within 11 days in AGR operation with real wastewater. This process was effective for the recovery of the *Streptococcus* (43.64%) as dominant genera along with 99% recovery of methanogens whereas anaerobes and facultative anaerobes were also proliferated in stored granules.

In a recent study, Ogura et al. (2020) demonstrated a process for fast AGR start-up and reactivation by using dehydrated granules. Dried granules were reactivated within 1 day of inoculation in synthetic wastewater achieving above 90% COD and NH_4^+-N removal efficiencies. Granule drying process is described in Fig.1.10. Recovered granules had 90% granulation percentage with excellent settling property having below 60 mL/g of SVI_{30} value.

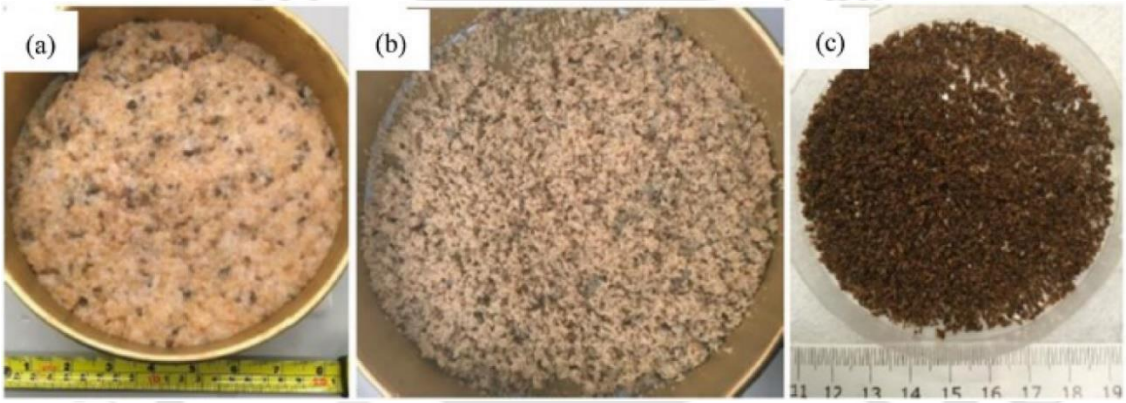

Fig.1.10 Methods of drying of granules (a) sieved granules (b) dehydrated granules and (c) dried granules (Ogura et al., 2020).

1.3.8.4 Biochar accelerated granulation

Biochar is an agricultural waste derived microporous biostable adsorbent which is used as a cost-effective replacement of activated carbon (Huggins et al., 2016). Biochar has high carbon sequestration capacity which was initially used as a soil quality enhancer. As granulation required long start-up period and also faced disintegration in recalcitrant wastewater, biochar was used for rapid granulation. AGR seeded with *Rhizobium* sp. NJUST18 and activated sludge was further added with 4 g/L of rice husk derived biochar to accelerate granulation and treat high strength pyridine contaminated wastewater (Zhang et al., 2017a). The granular sludge composed of biochar had high biomass concentration (2.6 g/L), high settleability (SVI: 31 mL/g) and could degrade 1500 mg/L of pyridine in 220 min. Microbial analysis revealed the presence of both coaggregating and pyridine degrading microbial strains in biochar containing aerobic granules with high concentration of EPS.

In another study, Ming et al. (2019) used three different types of biochar obtained from rice husk, rice bran and walnut shell which helped in forming the nucleus of the aerobic

granules and became matured after EPS secretion. Biochar incorporation increased granule surface area and pore size which facilitated polarity, high oil adsorption capacity and reduced the toxicity of petroleum wastewater. Moreover, biochar addition increased microbial diversity of the AGR with dominance of petroleum degrading and denitrifying bacterial population. Biochar mediated granulation process is described in Fig.1.11.

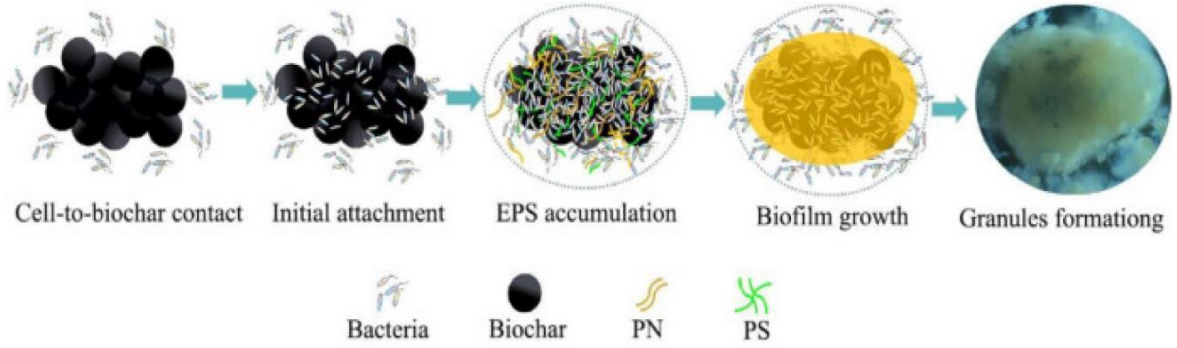

Fig.1.11 Biochar stimulated probable granulation mechanism (Zhang et al., 2017a)

1.3.8.5 Combined aerobic granules and microbial fuel cells

Studies in microbial fuel cells (MFCs) are in core interest of the researchers as a unique platform for simultaneous wastewater treatment and energy harvesting. Electricity generation in MFCs depends on the aggregation of electrochemical bacteria on anode surfaces which can covert the organic pollutants into electricity. Hence, MFC efficiency is related to degradation efficiency of the pollutant (Cheng et al., 2017). As aerobic granules are combinations of several bacteria and provide high organic removal performances, combined AGR and MFC process can lead to a pathbreaking research. Aerobic granules grown in MFC cathode chamber have been characterized by Yang et al. (2014). Treatment of epoxy reactive diluent (ERD) wastewater was conducted in a combined AGR-MFC system in presence of sodium acetate co-substrate which acted as energy provider electron donor. The AGR start-up time was between 7 to 13 days and lesser time required in domestic wastewater. Toxicity tolerant granules had about 77% COD removal where pollutant degradation was achieved by a synergic effect of both MFC anode aggregated biofilm and active aerobic granules.

Other advances in aerobic granular membrane reactors by changing HRT or organic loading (Tanava et al., 2019) and application of electric pulse (Guo et al., 2019) or ferrous ion dosing are proved to be effective in rapid granulation and enhancing organics removal efficiency (Cai et al., 2018). Broken granule structure restoration was achieved by addition of anaerobic granules in saline aromatic wastewater (Ramos et al., 2015) and about 340 mg/L of thiocyanate dosing reformed disintegrated aerobic granules in phenolic wastewater (Tomar and Chakraborty, 2020b).

1.3.9 Recovery of value-added products and their application

Among the 300 million tonnes of worldwide annual polymer production, about the 99% is based on fossil fuels which are non-biodegradable and causes CO_2 emission (Payne et al., 2019). With increasing environmental concerns, biodegradable biopolymer production is becoming popular among biotechnologists. Currently, the research trends in wastewater treatment plants (WWTPs) have been gradually shifted to wastewater biorefineries (WWBR) to utilize the wastewater as a renewable feedstock to establish a simultaneous waste treatment and valuable resource recovery process. Excessive waste sludge generation and its eco-friendly management is an important aspect to practice a sustainable granular sludge treatment. According to de Valk et al. (2019), the excess sludge processing may cost nearly to the half of the total operational cost of the wastewater treatment plant. To reduce the sludge handling expense, some economic sludge managements can be achieved by

i) utilizing dewatered sludge as manure,

ii) using waste sludge granules as cheap bio-adsorbents,

iii) recovering biodegradable biopolymers like alginate-like exopolymers (ALE) and polyhydroxybutarytes (PHB) from waste biogranules and by

iv) energy recovery in biomethanation process by anaerobic sludge digestion

To achieve a circular economy, some promising resource recovery options are discussed here.

1.3.9.1 Recovery of EPS

The major proportion of the dry weight of granular sludge biomass consists of EPS which are the sticky base materials for granulation. The most common classifications for EPS are bound EPS (B-EPS) and soluble EPS (S-EPS). B-EPS are closely attached with microbial cells which can be further divided into two categories, loosely-bound (LB-EPS) and tightly-bound EPS (TB-EPS). The TB-EPS are found in high proportion in granules which contribute major properties of the biofilm or granular sludge (Sheng and Yu, 2006). PS and PN are the major constituents of EPS which are observed between 40-95% in extractable biopolymer form. EPS can play a major role in bio-adsorption of oil, metals and dyes like methylene blue (Nancharaiah and Reddy, 2018). The presence of several chemical groups, EPS binding site and ion-exchange process facilitate the pollutant bio-adsorption in EPS. The high pollutant adsorption capacity was observed even in wide range of pH and temperature variation. The heavy metal adsorbed granules even achieved high settling velocity indicating stability in AGR system. EPS can also be used as a biomaterial for medical implants or as a rheological and sizing chemical additive (Feng et al., 2019).

1.3.9.2 Alginate-like exopolymers (ALE)

Chemical characterization determined that the 15-25% of the organic fraction of municipal sludge granules is the ALE (Felz et al., 2016). However, ALE is also reported to be extracted from floccular sludge (Sam and Dulekgurgen, 2015). ALE possess a hydrogel forming property in presence of divalent cation Ca^{+2} which increases granule strength, hydrophobicity and elasticity providing encapsulation to the microbial cells (Lin et al., 2013; Sam and Dulekgurgen, 2015). ALE mainly contain neutral and amio sugars, uronic acids, PN and polyphenolic compounds which make it a suitable biomaterial to be utilized in paper coating, bio-cement, textile, medical implants and agricultural industries (Felz et al., 2019). ALE can also play a role of a soil-enhancer to increase the water retention capacity of the soil in the semi-arid environments (Nancharaiah and Reddy, 2018).

Based on current research trend and market exposure, ALE production from wastewater can be coupled with AGR systems where the ALE recovery can reach nearly 50% turnover of the entire treatment plant (Van Leeuwen et al., 2018). Recently a research group in the Netherlands estimated that 10 different WWTPs are expected to produce 85 ktons of ALE compounds by 2030 generating profits nearly 170 million euros (Van Leeuwen et al., 2018).

However, according to a study conducted by Schambeck et al. (2020), EPS synthesis was not correlated with granule maturation whereas, ALE production increased with increasing granule stability and settleability during municipal wastewater treatment. Maximum 236 and 187 mg VS_{ALE}/g VS_{sludge} were recovered from granular and flocculent sludge, respectively. Though ALE recovery was less in flocculent sludge, the production could have been compensated by higher sludge production rates. ALE production was dependent on the nutrient and substrate conversion. Microbial analysis explored that a stable microbial group (like *Xanthomonadaceae*, *Sphingomonadaceae*, *Flavobacteriaceae* etc.) was responsible for the enhanced ALE production in granules. No clear difference in elemental and functional groups were observed in granule and flocculent sludge derived ALE and both had hydrogel forming properties indicating their potential application in paper and textile coating industries. In a pilot-scale AGR, Rollemberg et al. (2020) achieved 0.219 g ALE/g VSS recovery with phosphorous and tryptophan while treating low-strength municipal wastewater in tropical climate.

1.3.9.3 Polyhydroxyalkanoates (PHA)

PHAs are biodegradable polyesters with a hydroxyl-acid group which is exactly similar to the conventional petroleum-based plastics in properties. PHA are usually found in a copolymer form P(3HB-*co*-3HV) composed of two derivatives hydroxybutyrates (HB) and hydroxyvalerates (HV) (Amulya et al., 2016). Due to the non-biodegradable nature and CO_2

gas emission, conventional plastics impose a detrimental environmental pollution (Amulya et al., 2016). Bioplastics are eco-friendly alternatives to petroleum-based plastics to mitigate the pollution. To avoid the use of costly sugar substrates wastewater can be utilized as the precursor of PHA synthesis by granular sludge bacteria. At the end of a AGR feast phase, sludge bacteria are capable of accumulating PHA as an energy storage in absence of external carbon source which they oxidize and utilize in carbon deficient phase (famine phase) as the cell metabolic energy (Salehizadeh and Van Loosdrecht, 2004). Currently, PHA based products are being used in making films, packaging, medical implants and drug delivery carriers (Zheng et al., 2020).

Palm oil mill effluent (POME) and acetate wastewater were utilized as sole substrate for PHA production by aerobic granules. Literature suggested several volatile fatty acids (acetic, propionic, butyric, and valeric acids) in POME as the proven precursors of PHA production. Limiting nitrogen condition, high C/N ratio or implementation of aerodynamic feeding and changing feast-famine ratio promoted stress in AGRs to enhance PHA production (Fang et al., 2009; Wang et al., 2014; Gobi and Vadivelu, 2014; Vijayan and Vadivelu, 2017). Granule size variation with changing loading rate and aeration in AGR promoted 0.683–0.87 mg PHA/mg cell dry weight (CDW) in POME treatment by Gobi and Vadivelu (2014, 2015).

However, market availability of limited PHA variants (mainly poly-3-hydroxybutyrate (PHB), poly-4-hydroxybutyrate (P4HB) and their copolymers), low productivity, low molecular weight, crystallinity and poor tensile strength and high production cost (about 3-folds higher than the conventional plastics) are the major drawbacks to large scale PHA production (Lettner et al., 2017). Hence, utilization of waste sludge biomass or feedstock (lignocellulosic biomass, wastewater etc.) and engineering new biosynthesis pathways to design high quality PHA can be the potential future research prospect for biopolymer recovery (Yadav et al., 2020). Some potential future prospects and applications of the AGR derived bio-based polymers are summarized in Table 1.4.

Table 1.4 Applications of aerobic granule derived biopolymers recovered from AGRs

Application	Biopolymer	Characteristics	Practical implementation	References
hydrogel as coating materials	Granular sludge-based ALE	ALE forms hydrogels with Ca^{+2}; Presence of sugar, PN, polyphenols and uronic acid resembles to sodium alginate (Felz et al., 2020c)	Used in paper industries as raw material of paper coating for waterproof grease resistant surface	Lotti et al. (2019), Karakas et al. (2020)
Curing of cement	Granule derived EPS	hydrophilic EPS reduces moisture loss during curing process avoiding cracking and shrinkage in construction	Lab-scale feasibility of EPS is tested as cure cement	Zlopasa et al. (2014); Karakas et al. (2020)
Biosorbent materials	Granule derived EPS	EPS binds with heavy metal and organic pollutant by physisorption, ion-exchange, chemical precipitation or at binding sites	Adsorption of Pb^{2+}, Cd^{2+}, and Zn^{2+} by -COOH and -OH groups of EPS; Cu^{2+} by -COOH group of PN and Ni^{2+} adsorption by amino groups	Liu et al. (2015a); Li et al. (2020) and Li et al. (2017)
Flame retardant materials	EPS extracted from granular and flocculent sludge	Self-extinguishing properties of EPS was suitable to be flame retardant material of flax fabrics (Kim et al., 2020)	Bio-based EPS is potential alternative to dioxins and furans containing hazardous commercial flame retardants	Kim et al. (2020)
Membrane fabrication using EPS	Granule derived EPS	Ion exchange property of EPS facilitated monovalent ion selective membrane properties	EPS-membrane had more selectivity for K^{+} over Na^{+} ions, multi monovalent or divalent ions selectivity analysis is further required	Sudmalis et al. (2020)
Bioplastics	Granule accumulated PHA and PHB	Thermostatic biodegradable polyester resembles to petroleum-based plastics	Used in packing industries and medical implants	Vijayan and Vadivelu (2017)

1.4 Advantages and challenges of aerobic granulation

Since the last three decades, literature revealed unknown facts of probable granulation mechanism, impacts of operational strategies, environmental conditions, pollutant degradation, variation in growth substrates and active microbial populations for a successful wastewater treatment. Major advantages of the aerobic granulation technology include

i) Aerobic granules provide **compact, dense and highly settleable structure** (GSV: 30-90 m/h) having similar SVI values at 5 and 30 min allowing smaller AGR size selection, with reduced footprint and operational cost providing simultaneous C, N, P and recalcitrant pollutant removal potential and shock loading tolerance capacities (Liu and Tay, 2004; Winkler et al., 2018).

ii) **Presence of numerous microbial populations** like heterotrophic pollutant degraders, AOB, NOBs, PAOs and halotolerant bacteria achieved synergism in aerobic granules providing several inter-linked pathways to degrade multiple pollutants inside AGRs.

iii) Aerobic granulation is an established method to treat **a huge diversity of wastewaters** ranging from several industrial effluents (like Rubber, textile, dairy, brewery, swine slurry, palm oil mill, pulp and paper mill wastewater etc.) to metal adsorption (Yao et al., 2009; Wu et al., 2019), toxic recalcitrant wastewaters (like phenolics, petroleum refinery, pyridine, hypersaline petroleum slop wastewater) and emerging pollutants like pesticides, pharmaceuticals etc. (Rosman et al., 2014; Schwarzenbeck et al., 2005; Wang et al., 2007; Gobi and Vadivelu 2015; Morales et al., 2013; Vashi et al., 2018; Chen et al., 2019; Campo and Di Bella., 2019; Ma et al., 2012; Liang et al., 2018; Sarvajith et al., 2018).

iv) **Integration of aerobic granular sludge processes with other treatment** units, such as anaerobic digester, anoxic denitrifying reactor, membrane bioreactor or the implementation of advanced technologies like bioaugmentation, algal-bacterial granules further enhanced the process efficiencies of AGRs.

v) Moreover, **recoveries of value-added polymers** like, ALE or PHA ensured a sustainable sludge management with conversion of wastewater **"Treatment plants" to wastewater "Biorefineries"** in AGR systems.

However, there are still some lacuna in understanding of the exact granulation mechanism and maintenance of granule structural integrity in recalcitrant wastewater. Conversion of lab-scale to full-scale granular sludge mediated wastewater treatment is still a challenging task. The major challenges in granulation which need specific attention to improve for application in real wastewater treatment are as follows

i) In **pilot-scale studies**, plants go through instabilities and fluctuations in organic loading, pollutant concentrations, pH imbalance and operational failures. Hence, AGR system requires stability at wide range of OLR, operational pH and temperature to achieve a successful remediation. Most of the literature addressed lab-scale studies where the wastewater was defined synthetic wastewater with controlled operating conditions (Sharma et al., 2017; Chen et al., 2019). Very few pilot-scale plants are already established in China, the Netherlands and Portugal to treat sewage and industrial wastewater providing insignificant output on wastewater composition, reactor parameters and operational conditions (Nancharaiah and Reddy, 2018).

ii) There are very few studies reporting successful granulation during **low strength real sewage treatment** (Li et al., 2014). This process took almost 10-13 months for matured granulation which is a major drawback to achieve stable treatment process.

iii) **Maintaining granule structural integrity** is another challenge in recalcitrant wastewater treatment. Granules may disintegrate due to some unknown toxicity or environmental factors and easy methods of granule structure reconstruction are still under investigation stage.

iv) Poor understanding of **granulation mechanism** results into lack of knowledge about molecular level interaction, biochemical pathways and cell to cell aggregation to enhance granulation process. It further affects the designing process of full-scale AGR process in real wastewater treatment.

v) The **removal mechanism of N and P** along with optimization of favourable conditions to achieve simultaneous complete nitrification and denitrification in AGR system is not well discussed and indicates a potential future research scope.

vi) Challenges are encountered during **extraction and purification of recovered biopolymers** from AGR. Instead of following traditional protocols, cost-effective, eco-friendly and efficient advanced method should be established. Hitches in EPS purification process is another bottleneck in current biopolymer recovery scenario.

1.5 Source and characteristics of hydrocarbon-rich wastewater

1.5.1 Petroleum refinery wastewater

Petroleum refinery and petrochemical industries are the producers of massive amount of toxic, recalcitrant and heterogenous hydrocarbon-rich wastewater. Petroleum oil exploration to refining undergo a series of processes such as bore-well drilling, crude desalting, distillation, thermal cracking, catalytic cracking, hydrocracking, isomerization, polymerization, alkylation, hydro treatment, transportation etc (Jain et al., 2020). Each and

every step releases a large volume of wastewater containing free oil, phenolic compounds, ammonia, sulfides, metals and even H_2S gas which are finally discharged into the water bodies after physicochemical and biological treatments (Karray et al., 2020).

The accidental pollutant release may result into fire explosion and the oily wastewater can contaminate land and water with hazardous impacts on ecosystem. Moreover, ground seepage of petroleum wastewater and marine oil spillage are another potential hazard generated from oil industries (Karray et al., 2020). The chemical toxicity and multiple pollutant loads require a simultaneous nutrient and hydrocarbon removal method which is stable, shock load tolerant, economic and eco-friendly. The characteristics of the major constituents of refinery wastewater are as follows.

- **Oil and grease** are the primary pollutants in a petroleum wastewater which are composed of long carbon chains (till C_{44}) having high molecular weight providing poor biodegradability, high viscosity and heat resistance. Oil can exist in four forms in discharged wastewater. Free oils are having greater than 150 µm droplet diameter, dispersed oil ranges within 20-150 µm droplet size, emulsified oil has droplets smaller than 20 µm, and dissolved oil does not exist in droplet form (Tanudjaja et al., 2019). They are basically a hydrocarbon mixture with inorganic compounds and minerals.
- **Phenols, chlorophenols and cresols** are aromatic compounds with benzene ring in structure. They impose severe genotoxicity, carcinogenicity and mutagenicity due to strong bioaccumulation and persistence into both human and aquatic animals (Jain et al., 2020).
- **Polyaromatic hydrocarbons (PAHs)** are specific group of organic compounds having low solubility with high boiling and melting points. Naphthalene (NAP), phenanthrene (PHE) and fluorines (FLU) are the most common PAHs often found as dispersed oil in refinery effluent (Gaurav and Yadav, 2020).
- **BTEX** are aromatic hydrocarbons referring a mixture of benzene, toluene, ethylbenzene and xylene produced during catalytic reforming of naphtha in petroleum refining process. BTEX are highly flammable and mainly used as solvents (Mikhak et al., 2019).
- **Cyanides** are generated from catalytic cracking in petroleum refinery, they are major source of nitrogen in refinery wastewater and highly toxic in nature (Tian et al., 2020).
- Cationic and anionic **emulsifiers** are added during enhanced oil recovery in the oil drilling sites. The emulsifiers further come in contact with ground water causing water pollution (Siyal et al., 2020).

- Desulfurization unit and alkylation process releases several **sulfur compounds** like H_2S, mercaptans, spent caustic (in form of Na_2S and R-SH) etc. which further increases pollutant loads in oily wastewater (Mallick and Chakraborty, 2017).
- **Ammonia (NH_3)** in refinery wastewater represents the nitrogen fraction of pollutants which is very toxic for human and animal health [6].
- **Heavy metals like Pb, Cr, Ni, Cu** etc. are present in petroleum refinery wastewater which imposes toxic impacts on ecosystem (Mikhak et al., 2019).
- **Saline water** is often used to maintain the pressure in aquifer zone while extracting crude oil. Moreover, **chlorides** can increase salinity of refinery wastewater till 300 g/L in refinery effluent (Razavi and Miri, 2015).
- **Total suspended solids (TSS)** determine the organic and inorganic suspended matters larger than 2 µm size. TSS are often released from cooling tower blowdown, ballast water and tank bottom drainage of the petroleum refinery and sometimes associated with turbidity of wastewater. Central pollution control board (CPCB, 2019) recommended 100 mg/L as the permissible limit of TSS in refinery wastewater
- **Chemical oxygen demand (COD)** is defined as the oxygen required to chemically oxidize organic matters into inorganic end products. CPCB (2019) and Ministry of Environment and Forests (MoEF, 2008) suggested permissible COD limits in refinery effluent are 250 and 125 mg/L, respectively. Chang et al (2005) reported presence of maximum 266,000 mg/L of COD concentration in wastewater generated by petrochemical industries of Taiwan.
- **Biochemical oxygen demand (BOD)** indicates amount of dissolved oxygen utilized by aerobic microorganisms to biologically degrade organic matters present in wastewater. BOD_5 of a wastewater sample is measured after 5 days at 20 °C temperature. Increasing BOD suggests high pollutant concentrations in wastewater. CPCB (2019) and MoEF (2008) suggested permissible BOD_5 limits in refinery effluent at 30 and 15 mg/L, respectively.

Table 1.5 gives details of the major components of petroleum refinery wastewater generated at different stages of the refining process with their properties and permissible discharge limits in refinery effluent or occupational exposure limits.

Table 1.5 Components of petroleum refinery wastewater generated at different stages of the refining process with their properties and permissible discharge limits in refinery effluent or occupational exposure

Name of the pollutant	Sources	Primary properties	Permissible discharge limit in drinking water	Permissible discharge limit in effluent/ occupational exposure	References
Oil and grease (mg/L)	Crude desalting, distillation, catalytic cracking, alkylation	Long carbon chain, hydrophobic, viscous liquid	0.2	10	EPA (2002), CPCB (2019)
Phenolic compounds	Crude distillation, thermal and catalytic cracking, isomerization and hydro-treating	Aromatic, volatile liquid, causes skin burns	0.001	0.35	BIS (2012), CPCB (2019)
Polycyclic aromatic hydrocarbons (PAH) (m/L^3)	Coal gasification, catalytic cracking, vehicle exhaust	Nonpolar, soluble in organic solvents, volatile, high boiling and melting point	0.0001-0.0004	0.0001-0.0004	USEPA (2021)
Benzene (mg/L)	Catalytic reforming and steam cracking	Aromatic, colourless liquid, highly flammable	0.005	0.5 (exposure limit)	USEPA (2021), OSHA (2021)
Toluene (mg/L)	A byproduct during gasoline production by catalytic reforming	Colourless, odorous liquid used as solvent		100 ([1]TWA [2]PEL)	NIOSH (2021)
Xylene (mg/L)	Derived from aromatics of catalytic reforming of naphtha	Colourless, flammable liquid used as solvent		100 (TWA PEL)	NIOSH (2021)
Ethylbenzene (mg/L)	Produced from coal tar and petroleum industry	Colourless, flammable liquid with gasoline like odour		100 (TWA PEL)	NIOSH (2021)
Cyanide (mg/L)	Catalytic cracking	Highly toxic compound	0.05	0.2	(BIS, 2012; CPCB, 2019)
Ammonia (mg/L)	Crude desalting, thermal cracking, distillation	Colourless, odorous gas	0.5	Free ammonia: 5, ammonia nitrogen: 50	(BIS, 2012; CPCB, 2019)

Sulphides	Crude desalting, distillation, catalytic and hydrocracking, alkylation	Highly flammable, toxic	0.05	2	(BIS, 2012; CPCB, 2019)
Metals (mg/L)	Petroleum source rock, storage tank, pipelines	High density and atomic weight, toxic	0.01-0.05	0.05-3	(BIS, 2012; CPCB, 2019)
Chromium		Brittle, toxic (hexa)	0.05 (hexa), 1 (total)	0.1 (hexa), 2 (total)	(BIS, 2012; CPCB, 2019)
Lead		Soft, ductile, highly poisonous	0.01	0.1	(BIS, 2012; CPCB, 2019)
Copper		Highly conductive, toxic	0.05	3	(BIS, 2012; CPCB, 2019)
Nickel		Hard, ductile, toxic	0.02	3	(BIS, 2012; CPCB, 2019)
Emulsifiers (mg/L)	Drilling and exploration	Polar or non-polar in nature	Not defined	Not defined	
Salinity (mg/L)	Crude oil recovery, distillation and alkylation	Increases water density, inhibits bacterial nitrification	250 (for chlorides)	1000 (for chlorides)	(BIS, 2012; CPCB, 2019)

EPA: Environmental Protection Act (India)
CPCB: Central Pollution Control Board
BIS: Bureau of Indian Standards
USEPA: United States Environmental Protection Agency
OSHA: Occupational Safety and Health Administration (USA)
NIOSH: National Institute for Occupational Safety and Health (USA)
[1] TWA: Time-weighted average
[2]PEL: Permissible exposure limit

1.5.2 Palm oil mill effluent (POME)

Palm oil mills are another source of oily wastewater production. About 1 tonne of crude palm oil production requires 5 to 7.5 tonnes of water from which almost 50% is reported to be released as POME into fresh water streams (Najib et al., 2017). Malaysia, Indonesia and Nigeria are the major palm oil producers in the world. Malaysia used to produce 80 million tonnes of solid waste from palm oil mills which increased till 85-110 million tonnes in 2020 (Agensi Inovasi Malaysia, 2013). POME contains high organic loads with plant nutrients contributing approximately 50 g/L COD and 25 g/L BOD concentrations (Norfadilah et al., 2016). Hence, discharge of untreated POME can cause serious environmental hazards. POME is conventionally treated by ponding system in Malaysia which generates large amount harmful greenhouse gases (GHG) like 65% methane (CH_4), 35% carbon dioxide (CO_2) with sulphur dioxide (SO_2) and hydrogen sulphide (H_2S) contributing to the detrimental global warming (Najib et al., 2016).

1.5.3 Other potential sources

Food, dairy, tannery and textile industries involve the use of large amount of water for several steps of processing, washing, mixing and pasteurizing which may further release oily wastewater into the environment. Poultry, dairy, sea food industries are oily wastewater producers with high organic loadings (Tanudjaja et al., 2019). Cutting oils are required in metal processing which is an emulsion of oil, water and other additives like surfactants, fatty acids and heavy metals (Perez et al., 2007). Use of cutting oil as flushing fluid and coolants in metals industries are another major source of oily wastewater (Seo et al., 2007).

The major disadvantage of the oily wastewater is the poor biodegradability. Hence, it is difficult to design a stable treatment process for recalcitrant hydrocarbon-rich wastewater. In some cases, the oil concentration is very low to remove by incineration but the biological toxicity of the oily wastewater indicates the requirement of a case-specific biological treatment process.

1.6 Toxic effects on environment

1.6.1 Oils

As oil is immiscible in water, oil can reduce oxygen carrying capacity of water, hinder photosynthesis and is also harmful for fish and birds (Chavan and Mukherjee, 2008). Aliphatic and aromatic hydrocarbons were proved to be responsible in growth retardation and mortality of aquatic species. Prolonged hydrocarbon exposure was proved to be toxic in human bodies causing cancer, liver and kidney diseases (Biswal et al., 2009; Zhang et al.,

2016a). Due to long carbon chains and complex chemical structure oils impose recalcitrance to be degraded in biological system.

1.6.2 Phenolics

Phenolics are reported to be ecotoxic, genotoxic, and mutagenic in nature (Jain et al., 2020). The lethal dose for phenol is assigned within 1 to 32 g by the U.S. Department of Health and Human Services. Even at very low concentration, phenolic compounds can disrupt enzymatic and metabolic activities of aquatic animals and prolonged exposure may cause biomagnification, can paralyse the central nervous system of human and also has harmful effects on liver and kidney (Mustapha and Lens, 2018). Phenolic compounds can easily penetrate the skin and directly enter into the body by inhalations. They are corrosive to eyes and can cause skin burn. Phenol toxicity was observed in *Eucyclops agilis* and it reduced photosynthesis and motility in euglena (Kottuparambil et al., 2014).

1.6.3 PAH

PAH compounds are considered as genotoxic, carcinogenic and mutagenic. *Chlamys farreri*, a species of scallop suffered from enzymatic disruption causing DNA damage, protein denaturation and lipid peroxidation in benzopyrene, benzofluoranthene and chrysene exposure (Xiu et al., 2014). PAH can enter in body by both inhalation and drinking route and their overall concentration can exceed cancer risk standards regulated by USEPA increasing cancer risk in human body (Li and Li, 2017). PAH can also cause oxidative stress increasing risk of cardiovascular diseases.

1.6.4 BTEX

BTEX are categorized as class-A carcinogenic pollutants by USEPA (Carvajal et al., 2018). They can enter into the nerve tissues by ingestion and can cause serious damage to the nervous system. They are also reported to be mutagenic. Benzene can reduce counts of both red and white blood cells (Dehghani et al., 2018). Toluene ingestion can cause fatigue and cerebral atrophy which can further affect the respiratory system, central nervous system, kidney and liver. Xylene and ethylbenzene can be absorbed by gastrointestinal tract and can cause enzymatic disruption, skin inflammation and damage of nervous system (Pubchem, 2020).

1.6.5 Sulfur compounds

In crude oil, sulfur is present with carbon and hydrocarbon molecules. Sulfur can also exist in form of sulfates and mercaptans in refinery wastewater. Spent caustic mainly releases huge amount of sulphides (S^{2-}) having pH value about 12 which is corrosive and hazardous in nature and can increase effluent COD concentration (Townsend et al., 2003). Sulphides are

volatile compounds which react with hydrogen and form odorous and toxic hydrogen sulphide (H_2S) gas (Mallick and Chakraborty, 2017). Sulphides can also chemically react with dissolved oxygen (DO) present in water and can inhibit methanogenic activity of anaerobic bacteria.

1.6.6 Nitrogenous compounds

Ammonia (NH_3) can react with H_2S to produce ammonium sulphide (NH_4HS) in distillation unit of petroleum refinery. About 1 to 25 mg/L of ammonia was proven to be toxic to aquatic lives and about 1 mg/L hindered the oxygen carrying capacity of haemoglobin. Even trace amount of 200 µmol/L of ammonium is responsible to affect the plasma pH and sodium, potassium ions transportation in nerve cells (USEPA, 1985). Ammonia is further converted to nitrite-N (NO_2^--N) and nitrate-N (NO_3^--N) which is a possible reason for eutrophication. Consumption of water having more than 10 mg/L NO_3^--N concentration is reported to cause methemoglobinemia, commonly known as blue baby disease and NO_3^-N concentration above 500 mg/L can damage intestines as a symptom of diarrhea (USEPA, 1985).

1.6.7 Metals

Heavy metals like Fe, Cu, Pb, Cr, Ni are found as priority pollutants in refinery effluent which are toxic, carcinogenic and their long-term exposure may cause several health damages. Metal accumulation in *Oreochromis niloticus* fish was reported due to the exposure in petroleum refinery wastewater generated from a petroleum plant of Nigeria (Jain et al., 2020). Cr toxicity is responsible for delayed wound healing, irritation of the respiratory tract and even increases risk for oral carcinoma and pharynx cancers (Bhattacharya et al., 2016). Lower memory, epithelium or oral mucosal atrophy, hypochromic anaemia, dermatitis and lymph node fibrosis are reported as the outcomes of Fe, Cu and Ni toxicity (Paithankar et al., 2021). Pb can cross the blood–brain barrier causing dyslexia, a neurological damage in children due to shortening attention span and can even cause anaemia in middle-aged and older people (Xue et al., 2020).

1.6.8 Salinity

Salinity intrusion in refinery wastewater is responsible for sludge biomass washout from treatment plants and disruption of enzymatic and metabolic activity of microbes which can further increase COD concentration (Wu et al., 2020). Short term salinity exposure may hinder PAO metabolism and decrease SOUR capacity of activated sludge (Zhang et al., 2017b). Consumption and use of saline water may cause skin diseases, respiratory infection,

diarrhea and can even increase health risks of cardiac problems, high blood pressure and kidney diseases (Rakib et al., 2019).

1.7 Summary of literature and knowledge gaps in oily wastewater treatment

Aerobic granulation technology has been extensively studied in several industrial and domestic wastewater treatment by focusing on AGR operating properties, microbial profiling, role of EPS or pollutant degradation pathways. Granulation is initiated by aggregation potential of microbes which is triggered by physical, chemical and biological forces and EPS synthesis to form a protective layer. Granule properties are determined by size, density, settling capacity, EPS, hydrophobicity, integrity coefficients and microstructure is observed by microscopic analysis. Literature suggested organic loading, HRT, feast famine ratio and settling times to be the major factors in granulation.

In recalcitrant pollutant removal, combined effects of bio-adsorption, aromatic pollutant degraders, PAO and nitrifying bacteria were effective in simultaneous organics removal and partial nitrification denitrification, ANAMMOX or nitrification and denitrification together. Salinity stress enhanced the activity of halophilic and EPS producing strains which reduced biomass washout from AGRs and formed salinity resistant stable granules. Since last decade, hybridization of new technologies like algal-bacterial granules, bioaugmentation, MFC, and biochars were implemented in AGRs to enhance process efficiency of waste treatment with resource and energy recovery. The current research trends of shifting wastewater treatment plants (WWTPs) into wastewater biorefineries (WWBR) suggested the recovery of biodegradable biopolymers like EPS, ALE, PHAs and their potential application as hydrogel coating, biomedical implants, bio-adsorption or in making membranes and flame retardant materials. However, maintaining granule stability in high concentration recalcitrant pollutant, establishment of cost-effective biopolymer purification protocol and scaling up AGR from lab to pilot scale treatment are still the major challenges to be achieved.

Aerobic granular treatment of petroleum, coal gasification and diesel wastewater provided significant removal of bulk parameters like COD, phenol, nitrogen or phosphate (Milia et al., 2016; Chen et al., 2019, Tomar and Chakraborty, 2020a). Most of the cases had low hydrocarbon content (5.6-200 mg/L) and faced granule rupture with poor nitrification. However, the knowledge gaps in previous literature raised the following questions.

i) What is the role of inoculum and how does its previous exposure to toxic hydrocarbons helps in granule formation and oily wastewater treatment?
ii) Once granule disintegration occurs, will it be possible to regenerate/reformulate granular sludge from the ruptured granules or new sludge addition is necessary?

iii) What is the threshold hydrocarbon and organic loading to prevent granule rupture and to make effluent suitable for discharge or what is the desirable treatment efficiency of oily wastewater?

iv) Major bottlenecks of AGR are long time requirement for development of granular sludge and to maintain granule stability. Does bioaugmentation of oil degrading microorganism in AGR shorten granulation time, improve granule stability and reactor performance?

v) If bioaugmentation is helpful, what should be the best way to achieve that? Is it possible to generate granular sludge using specific bacterial strain?

vi) Oil refinery wastewater has significant amount of salinity present in it. What is the effect of salinity on oil degrading microbial strains and what is the threshold limit?

vii) Aerobic wastewater treatment generates large amount of sludge and waste sludge which need appropriate sludge management. Is it possible to make any value added product from the waste sludge generated in oily wastewater treatment?

1.8 Objective of the study and research protocol

The objective of our study was

- **to degrade oily wastewater in AGR using different inoculum,**
- **to determine the threshold hydrocarbon loading to prevent granule rupture,**
- **to study on probable hydrocarbon degradation pathway in AGR and**
- **rapid granule formation with specific oil degrading bacterial culture and to develop the most efficient bioaugmentation approach with those granules, and**
- **finally, utilization of waste sludge from AGR for polyhydroxyalkanoates (PHA), a biopolymer production.**

The **scope of the work** includes the necessity of filling the knowledge gaps of aerobic granular treatment of oily wastewater such as, slow granule formation, granule rupture, role of inoculum in oil removal, and bioplastic recovery by establishing a rapid granulation technique promoting hydrocarbon and saline shock resistant aerobic granules with easy reconstruction of broken granules while treating high strength refinery wastewater. Recovery of biodegrdable biopolymers from waste sludge granules indicates towards an economical sludge management and also an added advantage of cost saving in the oi1 refinery waste treatment system.

Detail research protocol to achieve the research objectives is shown in Fig.1.12.

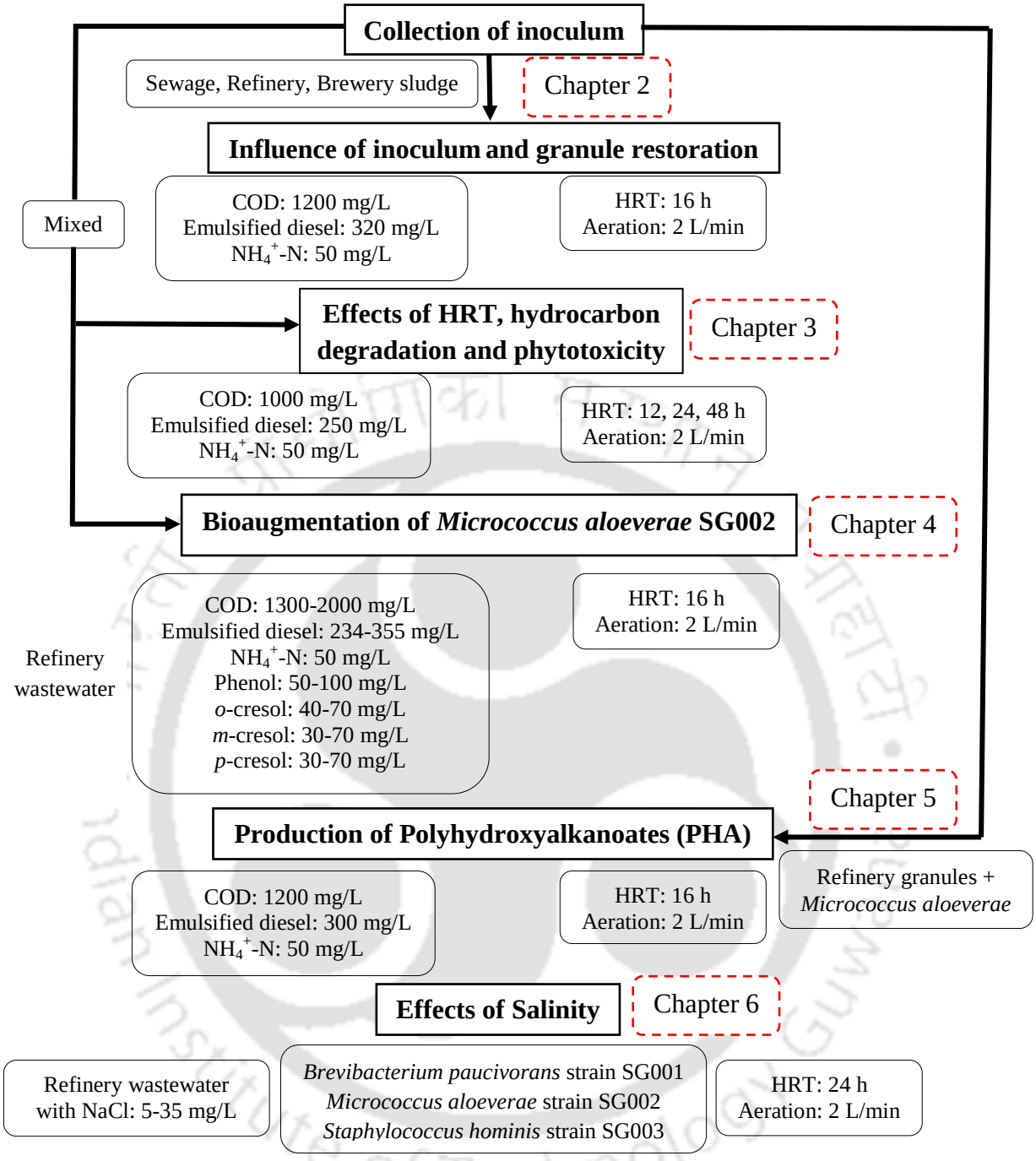

Fig.1.12 Research protocol of the work

References

Adav, S.S. and Lee, D.J., 2008. Extraction of extracellular polymeric substances from aerobic granule with compact interior structure. Journal of Hazardous materials 154, 1120-1126.

Adav, S.S., Lee, D-J, Show, K-Y, Tay, J-H., 2008. Aerobic granular sludge: recent advances. Biotechnology Advances 26, 411-423.

Agensi Inovasi Malaysia, 2013. National Biomass Strategy 2020: New Wealth Creation for Malaysia's Palm Oil Industry, Version 2.0.

Amorim, C.L., Alves, M., Castro, P.M. and Henriques, I., 2018. Bacterial community dynamics within an aerobic granular sludge reactor treating wastewater loaded with pharmaceuticals. Ecotoxicology and Environmental safety 147, 905-912.

Amorim, C.L., Maia, A.S., Mesquita, R.B., Rangel, A.O., van Loosdrecht, M.C., Tiritan, M.E. and Castro, P.M., 2014. Performance of aerobic granular sludge in a sequencing batch bioreactor exposed to ofloxacin, norfloxacin and ciprofloxacin. Water Research 50, 101-113.

Amulya, K., Reddy, M.V., Rohit, M.V. and Mohan, S.V., 2016. Wastewater as renewable feedstock for bioplastics production: understanding the role of reactor microenvironment and system pH. Journal of Cleaner Production 112, 4618-4627.

Argenta, T.S., Barros, A.R.M., de Carvalho, C.D.A., Dos Santos, A.B. and Firmino, P.I.M., 2020. Parabens in aerobic granular sludge systems: Impacts on granulation and insights into removal mechanisms. Science of The Total Environment 753, 142105.

Aswathy, P., Gandhimathi, R., Ramesh, S.T. and Nidheesh, P.V., 2016. Removal of organics from bilge water by batch electrocoagulation process. Separation and Purification Technology 159, 108-115.

Barr, J.J., Cook, A.E. and Bond, P.L., 2010. Granule formation mechanisms within an aerobic wastewater system for phosphorus removal. Applied and Environmental Microbiology 76, 7588-7597.

Basheer, F. and Farooqi, I.H., 2012. Biodegradation of p-cresol by aerobic granules in sequencing batch reactor. Journal of Environmental Sciences, 24.

Bassin, J.P., Pronk, M., Muyzer, G., Kleerebezem, R., Dezotti, M. and Van Loosdrecht, M.C.M., 2011. Effect of elevated salt concentrations on the aerobic granular sludge process: linking microbial activity with microbial community structure. Applied and Environmental Microbiology 77, 7942-7953.

Belal, A.A.M., 2019. Spatial and temporal changes in the population of macro-benthic invertebrates exposed to oil spillage in Suez Bay, Red Sea, Egypt. The Egyptian Journal of Aquatic Research 45, 353-358.

Bengtsson, S., de Blois, M., Wilén, B.M. and Gustavsson, D., 2018. Treatment of municipal wastewater with aerobic granular sludge. Critical Reviews in Environmental Science and Technology 48, 119-166.

Beun, J.J., Hendriks, A., Van Loosdrecht, M.C.M., Morgenroth, E., Wilderer, P.A. and Heijnen, J.J., 1999. Aerobic granulation in a sequencing batch reactor. Water Research 33, 2283-2290.

Bhattacharya, P.T., Misra, S.R. and Hussain, M., 2016. Nutritional aspects of essential trace elements in oral health and disease: an extensive review. Scientifica, 2016.

Biswal, B.K., Tiwari, S.N. and Mukherji, S., 2009. Biodegradation of oil in oily sludges from steel mills. Bioresource Technology 100, 1700-1703.

Cai, W., Jin, M., Zhao, Z., Lei, Z., Zhang, Z., Adachi, Y. and Lee, D.J., 2018. Influence of ferrous iron dosing strategy on aerobic granulation of activated sludge and bioavailability of phosphorus accumulated in granules. Bioresource Technology Reports 2, 7-14.

Caluwé, M., Dobbeleers, T., D'aes, J., Miele, S., Akkermans, V., Daens, D., Geuens, L., Kiekens, F., Blust, R. and Dries, J., 2017. Formation of aerobic granular sludge during the treatment of petrochemical wastewater. Bioresource Technology 238, 559-567.

Campo, R. and Di Bella, G., 2019. Petrochemical slop wastewater treatment by means of aerobic granular sludge: effect of granulation process on bio-adsorption and hydrocarbons removal. Chemical Engineering Journal 378, 122083.

Campo, R., Corsino, S.F., Torregrossa, M. and Di Bella, G., 2018. The role of extracellular polymeric substances on aerobic granulation with stepwise increase of salinity. Separation and Purification Technology 195, 12-20.

Carvajal, A., Akmirza, I., Navia, D., Pérez, R., Muñoz, R. and Lebrero, R., 2018. Anoxic denitrification of BTEX: Biodegradation kinetics and pollutant interactions. Journal of environmental management 214, 125-136.

Central Pollution Control Board India 1986. The Environment (Protection) Rules. Schedule VI

Chang, B.V., Chiang, F., Yuan, S.Y., 2005. Anaerobic degradation of nonylphenol in sludge. Chemosphere 59, 1415–1420.

Changmai, M., Pasawan, M. and Purkait, M.K., 2019. Treatment of oily wastewater from drilling site using electrocoagulation followed by microfiltration. Separation and Purification Technology 210, 463-472.

Chavan, A. and Mukherji, S., 2008. Treatment of hydrocarbon-rich wastewater using oil degrading bacteria and phototrophic microorganisms in rotating biological contactor: effect of N: P ratio. Journal of Hazardous Materials 154, 63-72.

Chen, C., Ming, J., Yoza, B.A., Liang, J., Li, Q.X., Guo, H., Liu, Z., Deng, J. and Wang, Q., 2019. Characterization of aerobic granular sludge used for the treatment of petroleum wastewater. Bioresource Technology 271, 353-359.

Cheng, K., Hu, J., Hou, H., Liu, B., Chen, Q., Pan, K., Pu, W., Yang, J., Wu, X. and Yang, C., 2017. Aerobic granular sludge inoculated microbial fuel cells for enhanced epoxy reactive diluent wastewater treatment. Bioresource Technology 229, 126-133.

Coma, M., Verawaty, M., Pijuan, M., Yuan, Z. and Bond, P.L., 2012. Enhancing aerobic granulation for biological nutrient removal from domestic wastewater. Bioresource Technology 103, 101-108.

Corsino, S.F., Campo, R., Di Bella, G., Torregrossa, M. and Viviani, G., 2015. Cultivation of granular sludge with hypersaline oily wastewater. International Biodeterioration & Biodegradation 105, 192-202.

Corsino, S.F., Capodici, M., Torregrossa, M. and Viviani, G., 2017. Physical properties and extracellular polymeric substances pattern of aerobic granular sludge treating hypersaline wastewater. Bioresource Technology 229, 152-159.

Dangcong, P., Bernet, N., Delgenes, J-P, Moletta, R., 1999. Aerobic granular sludge—a case report. Water Research 33, 890-893.

Daud, N.M., Abdullah, S.R.S., Hasan, H.A. and Yaakob, Z., 2015. Production of biodiesel and its wastewater treatment technologies: a review. Process Safety and Environmental Protection 94, 487-508.

de Kreuk, M.V. and Van Loosdrecht, M.V., 2004. Selection of slow growing organisms as a means for improving aerobic granular sludge stability. Water Science and Technology, 49, 9-17.

de Sousa Rollemberg, S.L., de Oliveira, L.Q., de Barros, A.N., Firmino, P.I.M. and Dos Santos, A.B., 2020. Pilot-scale aerobic granular sludge in the treatment of municipal wastewater: optimizations in the start-up, methodology of sludge discharge, and evaluation of resource recovery. Bioresource Technology 311, 123467.

de Valk, S., Feng, C., Khadem, A.F., van Lier, J.B. and de Kreuk, M.K., 2019. Elucidating the microbial community associated with the protein preference of sludge-degrading worms. Environmental Technology 40, 192-201.

Dehghani, M., Fazlzadeh, M., Sorooshian, A., Tabatabaee, H.R., Miri, M., Baghani, A.N., Delikhoon, M., Mahvi, A.H. and Rashidi, M., 2018. Characteristics and health effects of BTEX in a hot spot for urban pollution. Ecotoxicology and Environmental Safety 155, 133-143.

Drinking Water specifications of BIS (IS: 10500:2012).

Dubé, C.D. and Guiot, S.R., 2019. Characterization of the protein fraction of the extracellular polymeric substances of three anaerobic granular sludges. AMB Express 9, 23.

Environmental protection act, 2002, Regulations made by the Minister under sections 39 and 96 of the Environment Protection Act 2002.

Environmental protection agency (EPA) (1975), Patuxent Wastewater Treatment Facilities: Environmental Impact Statement, Philadelphia, Pennsylvania.

Etterer, T. and Wilderer, P.A., 2001. Generation and properties of aerobic granular sludge. Water Science and Technology 43, 19-26.

Fang, F., Liu, X.W., Xu, J., Yu, H.Q. and Li, Y.M., 2009. Formation of aerobic granules and their PHB production at various substrate and ammonium concentrations. Bioresource Technology 100, 59-63.

Fang, H.H., Yu, H., 2001. Acidification of lactose in wastewater. Journal of Environmental Engineering 127, 825-831.

Felz, S., Al-Zuhairy, S., Aarstad, O.A., van Loosdrecht, M.C. and Lin, Y.M., 2016. Extraction of structural extracellular polymeric substances from aerobic granular sludge. JoVE (Journal of Visualized Experiments) 115, 54534.

Feng, C., Lotti, T., Canziani, R., Lin, Y., Tagliabue, C. and Malpei, F., 2020. Extracellular biopolymers recovered as raw biomaterials from waste granular sludge and potential applications: A critical review. Science of the Total Environment 142051.

Feng, C., Lotti, T., Lin, Y. and Malpei, F., 2019. Extracellular polymeric substances extraction and recovery from anammox granules: Evaluation of methods and protocol development. Chemical Engineering Journal 374, 112-122.

Gao, D., Liu, L., Liang, H. and Wu, W.M., 2011. Aerobic granular sludge: characterization, mechanism of granulation and application to wastewater treatment. Critical Reviews in Biotechnology 31, 137-152.

Gaurav, G.K. and Yadav, D., 2020. Probing the excellence of wastewater PAHs removal approaches: A critical review. Journal of Contaminant Hydrology 103715.

Ghangrekar, M.M., Asolekar, S.R. and Joshi, S.G., 2005. Characteristics of sludge developed under different loading conditions during UASB reactor start-up and granulation. Water Research 39, 1123-1133.

Gobi, K. and Vadivelu, V.M., 2014. Aerobic dynamic feeding as a strategy for in situ accumulation of polyhydroxyalkanoate in aerobic granules. Bioresource Technology 161, 441-445.

Gobi, K. and Vadivelu, V.M., 2015. Dynamics of polyhydroxyalkanoate accumulation in aerobic granules during the growth–disintegration cycle. Bioresource Technology 196, 731-735.

Gobi, K., Mashitah, M.D. and Vadivelu, V.M., 2011. Development and utilization of aerobic granules for the palm oil mill (POM) wastewater treatment. Chemical Engineering Journal 174, 213-220.

Goh, P.S., Ong, C.S., Ng, B.C. and Ismail, A.F., 2019. Applications of emerging nanomaterials for oily wastewater treatment. In Nanotechnology in Water and Wastewater Treatment. Elsevier, pp. 101-113.

Gonzalez-Gil, G. and Holliger, C., 2011. Dynamics of microbial community structure of and enhanced biological phosphorus removal by aerobic granules cultivated on propionate or acetate. Applied and Environmental Microbiology 77, 8041-8051.

Guo, Y., Zhang, B., Zhang, Z., Shi, W., Zhang, R., Cheng, J., Li, W. and Cui, F., 2019. Enhanced aerobic granulation by applying the low-intensity direct current electric field via reactive iron anode. Water Research 149, 159-168.

Hailei, W., Guangli, Y., Guosheng, L. and Feng, P., 2006. A new way to cultivate aerobic granules in the process of papermaking wastewater treatment. Biochemical Engineering Journal 28, 99-103.

He, Q., Chen, L., Zhang, S., Chen, R., Wang, H., Zhang, W. and Song, J., 2018. Natural sunlight induced rapid formation of water-born algal-bacterial granules in an aerobic bacterial granular photo-sequencing batch reactor. Journal of Hazardous Materials 359, 222-230.

He, Z., Zhang, Q., Wei, Z., Zhao, Y. and Pan, X., 2019. Cultivation of a versatile manganese-oxidizing aerobic granular sludge for removal of organic micropollutants from wastewater. Science of The Total Environment, 690, 417-425.

He, Q., Xie, Z., Fu, Z., Wang, H., Chen, L., Gao, S., Zhang, W., Song, J., Xu, P., Yu, J. and Ma, J., 2021. Effects of phenol on extracellular polymeric substances and microbial communities from aerobic granular sludge treating low strength and salinity wastewater. Science of The Total Environment 752, 141785.

He, Z., Wei, Z., Zhang, Q., Zou, J. and Pan, X., 2019. Metal oxyanion removal from wastewater using manganese-oxidizing aerobic granular sludge. Chemosphere 236, 124353.

Herrero, M. and Stuckey, D.C., 2015. Bioaugmentation and its application in wastewater treatment: a review. Chemosphere 140, 119-128.

Hu, J., Zhang, Q., Chen, Y.Y. and Lee, D.J., 2016. Drying and recovery of aerobic granules. Bioresource Technology 218, 397-401.

Huang, W., Liu, D., Huang, W., Cai, W., Zhang, Z. and Lei, Z., 2020. Achieving partial nitrification and high lipid production in an algal-bacterial granule system when treating low COD/NH4–N wastewater. Chemosphere 248, 126106.

Huggins, T.M., Haeger, A., Biffinger, J.C. and Ren, Z.J., 2016. Granular biochar compared with activated carbon for wastewater treatment and resource recovery. Water Research 94, 225-232.

Ismail, N.H., Salleh, W.N.W., Ismail, A.F., Hasbullah, H., Yusof, N., Aziz, F. and Jaafar, J., 2020. Hydrophilic polymer-based membrane for oily wastewater treatment: A review. Separation and Purification Technology 233, 116007.

Ivanov, V., Wang, X.H. and Stabnikova, O., 2008. Starter culture of Pseudomonas veronii strain B for aerobic granulation. World Journal of Microbiology and Biotechnology 24, 533-539.

Ivanov, V., Wang, X.H., Tay, S.T.L. and Tay, J.H., 2006. Bioaugmentation and enhanced formation of microbial granules used in aerobic wastewater treatment. Applied Microbiology and Biotechnology 70, 374-381.

Jain, M., Majumder, A., Ghosal, P.S. and Gupta, A.K., 2020. A review on treatment of petroleum refinery and petrochemical plant wastewater: a special emphasis on constructed wetlands. Journal of Environmental Management 272, 111057.

Jemaat, Z., Suárez-Ojeda, M.E., Pérez, J. and Carrera, J., 2013. Simultaneous nitritation and p-nitrophenol removal using aerobic granular biomass in a continuous airlift reactor. Bioresource Technology 150, 307-313.

Jemaat, Z., Suárez-Ojeda, M.E., Pérez, J. and Carrera, J., 2014. Partial nitritation and o-cresol removal with aerobic granular biomass in a continuous airlift reactor. Water Research 48, 354-362.

Jiang, H.L., Maszenan, A.M. and Tay, J.H., 2007. Bioaugmentation and coexistence of two functionally similar bacterial strains in aerobic granules. Applied Microbiology and Biotechnology 75, 1191.

Jiang, H.L., Tay, J.H., Liu, Y. and Tay, S.T.L., 2003. Ca^{2+} augmentation for enhancement of aerobically grown microbial granules in sludge blanket reactors. Biotechnology Letters 25, 95-99.

Jiang, H.L., Tay, J.H., Maszenan, A.M. and Tay, S.T.L., 2006. Enhanced phenol biodegradation and aerobic granulation by two coaggregating bacterial strains. Environmental Science & Technology 40, 6137-6142.

Jiang, Y., Wei, L., Yang, K., Shi, X. and Wang, H., 2017. Rapid formation of aniline-degrading aerobic granular sludge and investigation of its microbial community succession. Journal of Cleaner Production 166, 1235-1243.

Kang, A.J. and Yuan, Q., 2017. Long-term stability and nutrient removal efficiency of aerobic granules at low organic loads. Bioresource Technology 234, 336-342.

Karakas, I., Sam, S.B., Cetin, E., Dulekgurgen, E. and Yilmaz, G., 2020. Resource recovery from an aerobic granular sludge process treating domestic wastewater. Journal of Water Process Engineering 34, 101148.

Karray, F., Aloui, F., Jemli, M., Mhiri, N., Loukil, S., Bouhdida, R., Mouha, N. and Sayadi, S., 2020. Pilot-scale petroleum refinery wastewaters treatment systems: Performance and microbial communities' analysis. Process Safety and Environmental Protection 141, 73-82.

Kent, T.R., Bott, C.B. and Wang, Z.W., 2018. State of the art of aerobic granulation in continuous flow bioreactors. Biotechnology advances 36, 1139-1166.

Khan, F., Zain Khan, M., Qamar Usmani, S. and Sabir, S., 2009. Biodegradation of phenol by aerobic granulation technology. Water Science and Technology 59, 273-278.

Kim, N.K., Mao, N., Lin, R., Bhattacharyya, D., van Loosdrecht, M.C. and Lin, Y., 2020. Flame retardant property of flax fabrics coated by extracellular polymeric substances recovered from both activated sludge and aerobic granular sludge. Water Research 170, 115344.

Kong, Q., Ngo, H.H., Shu, L., Fu, R.S., Jiang, C.H., Miao, M.S., 2014. Enhancement of aerobic granulation by zero-valent iron in sequencing batch airlift reactor. Journal of Hazardous Materials 279, 511-517.

Kong, Y., Liu, Y-Q., Tay, J-H., Wong, F-S., Zhu, J., 2009. Aerobic granulation in sequencing batch reactors with different reactor height/diameter ratios. Enzyme and Microbial Technology 45, 379-383.

Kottuparambil, S., Kim, Y.J., Choi, H., Kim, M.S., Park, A., Park, J., Shin, W. and Han, T., 2014. A rapid phenol toxicity test based on photosynthesis and movement of the freshwater flagellate, Euglena agilis Carter. Aquatic toxicology 155, 9-14.

Lemaire, R., Webb, R. I., Yuan, Z. 2008. Micro-scale observations of the structure of aerobic microbial granules used for the treatment of nutrient-rich industrial wastewater. The ISME journal, 2(5), 528-541

Lettner, M., Schöggl, J.P. and Stern, T., 2017. Factors influencing the market diffusion of bio-based plastics: Results of four comparative scenario analyses. Journal of Cleaner Production 157, 289-298.

Li, A.J., Li, X.Y., Yu, H.Q., 2011. Effect of the food-to-microorganism (F/M) ratio on the formation and size of aerobic sludge granules. Process Biochemistry 46, 2269-2276.

Li, G.F., Ma, W.J., Cheng, Y.F., Li, S.T., Zhao, J.W., Li, J.P., Liu, Q., Fan, N.S., Huang, B.C. and Jin, R.C., 2020. A spectra metrology insight into the binding characteristics of Cu2+ onto anammox extracellular polymeric substances. Chemical Engineering Journal, 124800.

Li, J., Ding, L.B., Cai, A., Huang, G.X. and Horn, H., 2014. Aerobic sludge granulation in a full-scale sequencing batch reactor. BioMed Research International 2014.

Li, N., Wei, D., Wang, S., Hu, L., Xu, W., Du, B. and Wei, Q., 2017. Comparative study of the role of extracellular polymeric substances in biosorption of Ni (II) onto aerobic/anaerobic granular sludge. Journal of Colloid and Interface Science 490, 754-761.

Li, X., Luo, J., Guo, G., Mackey, H.R., Hao, T. and Chen, G., 2017. Seawater-based wastewater accelerates development of aerobic granular sludge: A laboratory proof-of-concept. Water research 115, 210-219.

Liang, J., Li, W., Zhang, H., Jiang, X., Wang, L., Liu, X. and Shen, J., 2018. Coaggregation mechanism of pyridine-degrading strains for the acceleration of the aerobic granulation process. Chemical Engineering Journal 338, 176-183.

Lim, S.J. and Kim, T.H., 2014. Applicability and trends of anaerobic granular sludge treatment processes. Biomass and Bioenergy 60, 189-202.

Lin, H., Ma, R., Hu, Y., Lin, J., Sun, S., Jiang, J., Li, T., Liao, Q. and Luo, J., 2020. Reviewing bottlenecks in aerobic granular sludge technology: Slow granulation and low granular stability. Environmental Pollution, 114638.

Lin, Y.M., Sharma, P.K. and Van Loosdrecht, M.C.M., 2013. The chemical and mechanical differences between alginate-like exopolysaccharides isolated from aerobic flocculent sludge and aerobic granular sludge. Water research 47, 57-65.

Liu, J., Li, J. and Piché-Choquette, S., 2020. The combination of external conditioning and Ca^{2+} addition prior to the reintroduction of effluent sludge into SBR sharply accelerates the formation of aerobic granules. Journal of Water Process Engineering 36, 101269.

Liu, L., Fan, H., Liu, Y., Liu, C. and Huang, X., 2017. Development of algae-bacteria granular consortia in photo-sequencing batch reactor. Bioresource Technology 232, 64-71.

Liu, Q.S., Tay, J.H. and Liu, Y., 2003b. Substrate concentration-independent aerobic granulation in sequential aerobic sludge blanket reactor. *Environmental Technology 24*, 1235-1242.

Liu, W., Zhang, J., Jin, Y., Zhao, X. and Cai, Z., 2015b. Adsorption of Pb (II), Cd (II) and Zn (II) by extracellular polymeric substances extracted from aerobic granular sludge: efficiency of protein. Journal of Environmental Chemical Engineering 3, 1223-1232.

Liu, X., Chen, Y., Zhang, X., Jiang, X., Wu, S., Shen, J., Sun, X., Li, J., Lu, L. and Wang, L., 2015a. Aerobic granulation strategy for bioaugmentation of a sequencing batch reactor (SBR) treating high strength pyridine wastewater. Journal of Hazardous materials 295, 153-160.

Liu, Y. and Tay, J.H., 2002. The essential role of hydrodynamic shear force in the formation of biofilm and granular sludge. Water Research 36, 1653-1665.

Liu, Y. and Tay, J.H., 2004. State of the art of biogranulation technology for wastewater treatment. Biotechnology Advances 22, 533-563.

Liu, Y., Yang, S.F., Liu, Q.S. and Tay, J.H., 2003a. The role of cell hydrophobicity in the formation of aerobic granules. Current Microbiology 46, 0270-0274.

Liu, Y.Q., Wu, W.W., Tay, J.H. and Wang, J.L., 2007. Starvation is not a prerequisite for the formation of aerobic granules. Applied Microbiology and Biotechnology 76, 211-216.

Liu, Z., Liu, Y., Zhang, A., Zhang, C. and Wang, X., 2014. Study on the process of aerobic granule sludge rapid formation by using the poly aluminum chloride (PAC). Chemical Engineering Journal 250, 319-325.

Lobos, J., Wisniewski, C., Heran, M., Grasmick, A., 2008. Sequencing versus continuous membrane bioreactors: effect of substrate to biomass ratio (F/M) on process performance. Journal of Membrane Science 317, 71-77.

Lotti, T., Carretti, E., Berti, D., Montis, C., Del Buffa, S., Lubello, C., Feng, C. and Malpei, F., 2019. Hydrogels formed by anammox extracellular polymeric substances: structural and mechanical insights. Scientific Reports 9, 1-9.

Lv, Y., Wan, C., Lee, D.J., Liu, X. and Tay, J.H., 2014. Microbial communities of aerobic granules: granulation mechanisms. Bioresource Technology 169, 344-351.

Ma, H., Guo, C., Yao, M., Wu, M., Wang, Z. and Wang, S., 2020. Calcium ions affect sludge digestion performance via changing extracellular polymeric substances in anaerobic bioreactor. Biomass and Bioenergy 137, 105548.

Ma, J.Y., Quan, X.C., Yang, Z.F. and Li, A.J., 2012. Biodegradation of a mixture of 2, 4-dichlorophenoxyacetic acid and multiple chlorophenols by aerobic granules cultivated through plasmid pJP4 mediated bioaugmentation. *Chemical Engineering Journal 181*, 144-151.

Mallick, S.K. and Chakraborty, S., 2017. Treatment of synthetic refinery wastewater in anoxic–aerobic sequential moving bed reactors and sulphur recovery. Journal of Environmental Science and Health, Part A 52, 1257-1268.

Mallick, S.K. and Chakraborty, S., 2020. Salinity footprint on anoxic-aerobic sequential moving bed reactors during petroleum refinery wastewater treatment: Effects on the dominant species. Journal of Water Process Engineering 37, 101376.

"Massive blast at oil field in Assam's Tinsukia district". India Today. Retrieved 8 June 2020.

McSwain, B.S., Irvine, R.L., Hausner, M. and Wilderer, P.A., 2005. Composition and distribution of extracellular polymeric substances in aerobic flocs and granular sludge. Applied and Environmental Microbiology 71, 1051-1057.

Meng, F., Huang, W., Liu, D., Zhao, Y., Huang, W., Lei, Z. and Zhang, Z., 2020. Application of aerobic granules-continuous flow reactor for saline wastewater treatment: Granular stability, lipid production and symbiotic relationship between bacteria and algae. Bioresource Technology 295, 122291.

Metcalf, E., Eddy, H.I. 2003. Wastewater engineering; treatment and reuse. McGraw-Hill, Boston.

Mikhak, Y., Torabi, M.M.A. and Fouladitajar, A., 2019. Refinery and petrochemical wastewater treatment. In Sustainable Water and Wastewater Processing, Elsevier, 55-91.

Milia, S., Malloci, E. and Carucci, A., 2016. Aerobic granulation with petrochemical wastewater in a sequencing batch reactor under different operating conditions. Desalination and Water Treatment 57, 27978-27987.

Ming, J., Wang, Q., Yoza, B.A., Liang, J., Guo, H., Li, J., Guo, S. and Chen, C., 2020. Bioreactor performance using biochar and its effect on aerobic granulation. Bioresource Technology 300, 122620.

Morales, N., Figueroa, M., Fra-Vázquez, A., Del Río, A.V., Campos, J.L., Mosquera-Corral, A. and Méndez, R., 2013. Operation of an aerobic granular pilot scale SBR plant to treat swine slurry. Process Biochemistry 48, 1216-1221.

Morais, I.L.H., Silva, C.M. and Borges, C.P., 2016. Aerobic granular sludge to treat paper mill effluent: organic matter removal and sludge filterability. Desalination and Water Treatment, 57, 8119-8126.

Moy, B.P., Tay, J.H., Toh, S.K., Liu, Y. and Tay, S.L., 2002. High organic loading influences the physical characteristics of aerobic sludge granules. Letters in Applied Microbiology 34, 407-412.

Mustapha, H.I. and Lens, P.N., 2018. Constructed Wetlands to Treat Petroleum Wastewater. In Approaches in Bioremediation. Springer, Cham, pp. 199-237.

Najib, M.M., Ujang, Z., Salim, M.R., Ibrahim, Z. and Muda, K., 2016. Reduction and biofixation of carbon dioxide in palm oil mill effluent using developed microbial granules containing photosynthetic pigments. Bioresource Technology 221, 157-164.

Najib, M.Z.M., Ujang, Z., Salim, M.R. and Ibrahim, Z., 2017. Developed microbial granules containing photosynthetic pigments for carbon dioxide reduction in palm oil mill effluent. International Biodeterioration & Biodegradation 116, 163-170.

Nancharaiah, Y.V. and Reddy, G.K.K., 2018. Aerobic granular sludge technology: mechanisms of granulation and biotechnological applications. Bioresource Technology 247, 1128-1143.

Nancharaiah, Y.V. and Sarvajith, M., 2019. Aerobic granular sludge process: a fast growing biological treatment for sustainable wastewater treatment. Current Opinion in Environmental Science & Health 12, 57-65.

Nancharaiah, Y.V., Sarvajith, M. and Mohan, T.K., 2019. Aerobic granular sludge: the future of wastewater treatment. CURRENT SCIENCE 117, 395.

Nascimento, M.K.S., Loureiro, S., dos Reis Souza, M.R., da Rosa Alexandre, M. and Nilin, J., 2020. Toxicity of a mixture of monoaromatic hydrocarbons (BTX) to a tropical marine microcrustacean. Marine Pollution Bulletin 156, 111272.

Norfadilah, N., Raheem, A. and Harun, R., 2016. Bio-hydrogen production from palm oil mill effluent (POME): A preliminary study. International Journal of Hydrogen Energy 41, 11960-11964.

Occupational Safety and Health Standards, Toxic and Hazardous Substances, 1910.1028. Osha.gov. Retrieved on 2011-11-23.

Ogura, S., Hamza, R.A. and Tay, J.H., 2020. Dried aerobic granules for fast startup of aerobic granular sludge reactors: Reactivation and performance. Journal of Water Process Engineering 36, 101298.

Othman, I., Anuar, A. N., Ujang, Z., Rosman, N. H., Harun, H., Chelliapan, S. 2013. Livestock wastewater treatment using aerobic granular sludge.Bioresource technology, 133, 630-634.

Paithankar, J.G., Saini, S., Dwivedi, S., Sharma, A. and Chowdhuri, D.K., 2021. Heavy metal associated health hazards: An interplay of oxidative stress and signal transduction. Chemosphere 262, 128350.

Payne, J., McKeown, P. and Jones, M.D., 2019. A circular economy approach to plastic waste. Polymer Degradation and Stability 165, 170-181.

Perez, M., Rodriguez-Cano, R., Romero, L.I., Sales, D., 2007. Performance of anaerobic thermophilic fluidized bed in the treatment of cutting-oil wastewater. Bioresource Technology 98, 3456-3463.

Pijuan, M., Werner, U., Yuan, Z., 2011. Reducing the startup time of aerobic granular sludge reactors through seeding floccular sludge with crushed aerobic granules. Water Research 45, 5075–5083.

Poot, V., Hoekstra, M., Geleijnse, M.A., van Loosdrecht, M.C. and Pérez, J., 2016. Effects of the residual ammonium concentration on NOB repression during partial nitritation with granular sludge. Water Research 106, 518-530.

Qin, L., Tay, J.H. and Liu, Y., 2004. Selection pressure is a driving force of aerobic granulation in sequencing batch reactors. Process Biochemistry 39, 579-584.

Quan, X.C., Ma, J.Y., Xiong, W.C. and Yang, Z.F., 2011. Effects of gene-augmentation on the formation, characteristics and microbial community of 2, 4-dichlorophenoxyacetic acid degrading aerobic microbial granules. Journal of Hazardous Materials 196, 278-286.

Quan, X.C., Ma, J.Y., Xiong, W.C. and Yang, Z.F., 2011. Effects of gene-augmentation on the formation, characteristics and microbial community of 2, 4-dichlorophenoxyacetic acid degrading aerobic microbial granules. Journal of Hazardous Materials 196, 278-286.

Rajitha, K., Sarvajith, M., Venugopalan, V.P. and Nancharaiah, Y.V., 2020. Development and performance of halophilic microalgae-colonized aerobic granular sludge for treating seawater-based wastewater. Bioresource Technology Reports 100432.

Rakib, M.A., Sasaki, J., Matsuda, H. and Fukunaga, M., 2019. Severe salinity contamination in drinking water and associated human health hazards increase migration risk in the southwestern coastal part of Bangladesh. Journal of Environmental Management 240, 238-248.

Ramos, C., Suárez-Ojeda, M.E. and Carrera, J., 2015. Long-term impact of salinity on the performance and microbial population of an aerobic granular reactor treating a high-strength aromatic wastewater. Bioresource Technology 198, 844-851.

Razavi, S.M.R. and Miri, T., 2015. A real petroleum refinery wastewater treatment using hollow fiber membrane bioreactor (HF-MBR). Journal of *Water Process* Engineering 8, 136-141.

Rosman, N.H., Anuar, A.N., Chelliapan, S., Din, M.F.M., Ujang, Z., 2014. Characteristics and performance of aerobic granular sludge treating rubber wastewater at different hydraulic retention time. Bioresource technology 161, 155-161.

Rostam, A.B. and Taghizadeh, M., 2020. Advanced oxidation processes integrated by membrane reactors and bioreactors for various wastewater treatments: A critical review. Journal of Environmental Chemical Engineering 104566.

Rusanowska, P., Cydzik-Kwiatkowska, A., Świątczak, P. and Wojnowska-Baryła, I., 2019. Changes in extracellular polymeric substances (EPS) content and composition in aerobic granule size-fractions during reactor cycles at different organic loads. Bioresource Technology 272, 188-193.

Salehizadeh, H. and Van Loosdrecht, M.C.M., 2004. Production of polyhydroxyalkanoates by mixed culture: recent trends and biotechnological importance. Biotechnology Advances 22, 261-279.

Sam, S.B. and Dulekgurgen, E., 2016. Characterization of exopolysaccharides from floccular and aerobic granular activated sludge as alginate-like-exoPS. Desalination and Water Treatment 57, 2534-2545.

Sarma, S.J., Tay, J.H. and Chu, A., 2017. Finding knowledge gaps in aerobic granulation technology. Trends in Biotechnology 35, 66-78.

Sarvajith, M. and Nancharaiah, Y.V., 2020. Biological nutrient removal by halophilic aerobic granular sludge under hypersaline seawater conditions. Bioresource Technology, 318, 124065.

Sarvajith, M., Reddy, G.K.K. and Nancharaiah, Y.V., 2018. Textile dye biodecolourization and ammonium removal over nitrite in aerobic granular sludge sequencing batch reactors. Journal of Hazardous Materials 342, 536-543.

Schambeck, C.M., Magnus, B.S., de Souza, L.C.R., Leite, W.R.M., Derlon, N., Guimarães, L.B. and da Costa, R.H.R., 2020. Biopolymers recovery: dynamics and characterization of alginate-like exopolymers in an aerobic granular sludge system treating municipal wastewater without sludge inoculum. Journal of Environmental Management 263, 110394.

Schwarzenbeck, N., Borges, J.M. and Wilderer, P.A., 2005. Treatment of dairy effluents in an aerobic granular sludge sequencing batch reactor. Applied Microbiology and Biotechnology 66, 711-718.

Seo, D.C., Lee, H.J., Hwang, H.N., Park, M.R., Kwak, N.W., Cho, I.J., Cho, J.S., Seo, J.Y., Joo, W.H., Park, K.H., Heo, J.S., 2007. Treatment of non-biodegradable cutting oil wastewater by ultrasonication-Fenton oxidation process.Water Science and Technology 55, 251-259.

Sheng, G.P. and Yu, H.Q., 2006. Characterization of extracellular polymeric substances of aerobic and anaerobic sludge using three-dimensional excitation and emission matrix fluorescence spectroscopy. Water Research 40, 1233-1239.

Show, K.Y., Lee, D.J. and Tay, J.H., 2012. Aerobic granulation: advances and challenges. Applied Biochemistry and Biotechnology 167, 1622-1640.

Siyal, A.A., Shamsuddin, M.R., Low, A. and Rabat, N.E., 2020. A review on recent developments in the adsorption of surfactants from wastewater. Journal of Environmental Management 254, 109797.

Standards for Effluent Discharge Regulations, General Notice No. 44. of 2003, The NIOSH Pocket Guide to Chemical Hazards. National Institute for Occupational Safety and Health (NIOSH).

Sudmalis, D., Mubita, T.M., Gagliano, M.C., Dinis, E., Zeeman, G., Rijnaarts, H.H.M. and Temmink, H., 2020. Cation exchange membrane behaviour of extracellular polymeric substances (EPS) in salt adapted granular sludge. Water Research 178, 115855.

Tahreen, A., Jami, M.S. and Ali, F., 2020. Role of electrocoagulation in wastewater treatment: A developmental review. Journal of Water Process Engineering 37, 101440.

Tanudjaja, H.J., Hejase, C.A., Tarabara, V.V., Fane, A.G. and Chew, J.W., 2019. Membrane-based separation for oily wastewater: A practical perspective. Water Research 156, 347-365.

Tavana, A., Pishgar, R. and Tay, J.H., 2019. Impact of hydraulic retention time and organic matter concentration on side-stream aerobic granular membrane bioreactor. Science of The Total Environment 693, 133525.

Tay, J.H., Jiang, H.L. and Tay, S.T.L., 2004. High-rate biodegradation of phenol by aerobically grown microbial granules. Journal of Environmental Engineering, 130, 1415-1423.

Tay, J.H., Liu, Q.S. and Liu, Y., 2002a. Characteristics of aerobic granules grown on glucose and acetate in sequential aerobic sludge blanket reactors. Environmental Technology 23, 931-936.

Tay, J.H., Liu, Q.S. and Liu, Y., 2002c. Aerobic granulation in sequential sludge blanket reactor. Water Science and Technology 46, 13-18.

Tay, J-H, Yang, S-F, Liu Y., 2002b. Hydraulic selection pressure-induced nitrifying granulation in sequencing batch reactors. Applied Microbiology and Biotechnology 59, 332-337.

Tian, X., Song, Y., Shen, Z., Zhou, Y., Wang, K., Jin, X., Han, Z. and Liu, T., 2020. A comprehensive review on toxic petrochemical wastewater pretreatment and advanced treatment. Journal of Cleaner Production 245, 118692.

Tomar, S.K. and Chakraborty, S., 2018b. Characteristics of aerobic granules treating phenol and ammonium at different cycle time and up flow liquid velocity. International Biodeterioration & Biodegradation 127, 113-123.

Tomar, S.K. and Chakraborty, S., 2019. Comparison of rapid granulation developed from the same industrial sludge with two different substrates. International Biodeterioration & Biodegradation 142, 218-226.

Tomar, S.K. and Chakraborty, S., 2020a. Impact of high phenol loading on aerobic granules from two different kinds of industrial sludge along with thiocyanate and ammonium. Bioresource Technology 315, 123824.

Tomar, S.K. and Chakraborty, S., 2020b. Impact of thiocyanate on the reformation of aerobic granules from the disintegrated granules treating phenol-contained wastewater along

with the recovery of nitritation efficiency. Journal of Water Process Engineering 36, 101260.

Tomar, S.K., Chakraborty, S., 2018a. Effect of air flow rate on development of aerobic granules, biomass activity and nitrification efficiency for treating phenol, thiocyanate and ammonium. Journal of Environmental Management 219, 178-188.

Townsend, G.T., Prince, R.C. and Suflita, J.M., 2003. Anaerobic oxidation of crude oil hydrocarbons by the resident microorganisms of a contaminated anoxic aquifer. Environmental Science & Technology 37, 5213-5218.

Turner, N.R. and Renegar, D.A., 2017. Petroleum hydrocarbon toxicity to corals: A review. Marine Pollution Bulletin 119, 1-16.

U.S. Energy Information Administration, 2020. Short-Term Energy Outlook (STEO) Forecast Highlights. EIA.

Val del Río, A., Figueroa, M., Mosquera-Corral, A., Campos, J.L. and Méndez, R., 2013. Stability of aerobic granular biomass treating the effluent from a seafood industry. International Journal of Environmental Research 7, 265-276.

Van Leeuwen, K., De Vries, E., Roest, K. and Koop, S., 2018. The energy & raw materials factory of the Dutch water authorities: its role in the circular economy of the Netherlands. Environmental Management 61, 786-795.

Vashi, H., Iorhemen, O.T. and Tay, J.H., 2018. Degradation of industrial tannin and lignin from pulp mill effluent by aerobic granular sludge technology. Journal of water Process Engineering 26, 38-45.

Verawaty, M., Pijuan, M., Yuan, Z., Bond, P., 2012. Determining the mechanisms for aerobic granulation from mixed seed of floccular and crushed granules in activated sludge wastewater treatment. Water Research 46, 761-771.

Viviani, G., 2016. Simultaneous nitritationedenitritation for the treatment of high-strength nitrogen in hypersaline wastewater by aerobic granular sludge. Water Research 88, 329-336.

Vjayan, T. and Vadivelu, V.M., 2017. Effect of famine-phase reduced aeration on polyhydroxyalkanoate accumulation in aerobic granules. Bioresource Technology 245, 970-976.

Wan, C., Sun, S., Lee, D.J., Liu, X., Wang, L., Yang, X. and Pan, X., 2013. Partial nitrification using aerobic granules in continuous-flow reactor: rapid startup. Bioresource Technology 142, 517-522.

Wang, J., Jiang, X., Liu, X., Sun, X., Han, W., Li, J., Wang, L. and Shen, J., 2018. Microbial degradation mechanism of pyridine by Paracoccus sp. NJUST30 newly isolated from aerobic granules. *Chemical Engineering Journal 344*, 86-94.

Wang, J., Li, W.W., Yue, Z.B. and Yu, H.Q., 2014. Cultivation of aerobic granules for polyhydroxybutyrate production from wastewater. Bioresource Technology, 159, pp.442-445.

Wang, L., Liu, X., Chen, X. F., Lee, D. J., Tay, J. H., Zhang, Y., Wan, C. L. 2015. Biosorption of Sr (II) from aqueous solutions using aerobic granules: equilibrium and mechanisms. Journal of Radioanalytical and Nuclear Chemistry, 306, 193-202.

Wang, L., Liu, X., Chen, X.F., Lee, D.J., Tay, J.H., Zhang, Y. and Wan, C.L., 2015. Biosorption of Sr (II) from aqueous solutions using aerobic granules: equilibrium and mechanisms. Journal of Radioanalytical and Nuclear Chemistry 306, 193-202.

Wang, L., Liu, X., Lee, D.J., Tay, J.H., Zhang, Y., Wan, C.L. and Chen, X.F., 2018. Recent advances on biosorption by aerobic granular sludge. Journal of Hazardous Materials 357, 253-270.

Wang, S.G., Liu, X.W., Gong, W.X., Gao, B.Y., Zhang, D.H. and Yu, H.Q., 2007. Aerobic granulation with brewery wastewater in a sequencing batch reactor. Bioresource Technology 98, 2142-2147.

Wang, X., Yang, T., Lin, B. and Tang, Y., 2017. Effects of salinity on the performance, microbial community, and functional proteins in an aerobic granular sludge system. Chemosphere 184, 1241-1249.

Wang, Z-W., Li, Y., Zhou, J-Q., Liu, Y., 2006. The influence of short-term starvation on aerobic granules. Process Biochemistry 41, 2373-2378.

Wei, D., Wang, B., Ngo, H. H., Guo, W., Han, F., Wang, X., Wei, Q., 2015. Role of extracellular polymeric substances in biosorption of dye wastewater using aerobic granular sludge. Bioresource technology, 185, 14-20.

Winkler, M.H., Kleerebezem, R., De Bruin, L.M.M., Verheijen, P.J.T., Abbas, B., Habermacher, J. and Van Loosdrecht, M.C.M., 2013. Microbial diversity differences within aerobic granular sludge and activated sludge flocs. Applied Microbiology and Biotechnology 97, 7447-7458.

Winkler, M.K., Le, Q.H. and Volcke, E.I., 2015. Influence of partial denitrification and mixotrophic growth of NOB on microbial distribution in aerobic granular sludge. Environmental Science & Technology 49, 11003-11010.

Winkler, M.-K.H., Meunier, C., Henriet, O., Mahillon, J., Suárez-Ojeda, M.E., Del Moro, G., De Sanctis, M., Di Iaconi, C., Weissbrodt, D.G., 2018. An integrative review of granular sludge for the biological removal of nutrients and recalcitrant organic matter from wastewater. Chemical Engineering Journal 336, 489-502.

Wu, X., Li, H., Lei, L., Ren, J., Li, W. and Liu, Y., 2020. Tolerance to short-term saline shocks by aerobic granular sludge. Chemosphere 243, 125370.

Wu, X., Li, W., Ou, D., Li, C., Hou, M., Li, H. and Liu, Y., 2019. Enhanced adsorption of Zn^{2+} by salinity-aided aerobic granular sludge: Performance and binding mechanism. Journal of Environmental Management 242, 266-271.

Xin, X., Lu, H., Yao, L., Leng, L. and Guan, L., 2017. Rapid formation of aerobic granular sludge and its mechanism in a continuous-flow bioreactor. Applied Biochemistry and Biotechnology 181, 424-433.

Xiu, M., Pan, L. and Jin, Q., 2014. Bioaccumulation and oxidative damage in juvenile scallop Chlamys farreri exposed to benzo [a] pyrene, benzo [b] fluoranthene and chrysene. Ecotoxicology and Environmental Safety 107, 103-110.

Xu, H. and Liu, Y., 2008. Mechanisms of Cd^{2+}, Cu^{2+} and Ni^{2+} biosorption by aerobic granules. Separation and Purification Technology 58, 400-411.

Xue, Q., Zhou, Y., Gu, H., Xie, X., Hou, F., Liu, Q., Wu, H., Zhu, K., Wan, Z. and Song, R., 2020. Urine metals concentrations and dyslexia among children in China. Environment International 139, 105707.

Yadav, B., Pandey, A., Kumar, L.R. and Tyagi, R.D., 2020. Bioconversion of waste (water)/residues to bioplastics-A circular bioeconomy approach. Bioresource Technology 298, 122584.

Yang, P., Chen, T. and Li, H.Q., 2016. Aerobic granular sludge stabilization in biocathode chamber of newly constructed continue flow microbial fuel cell system treating synthetic and pharmaceutical wastewater. Desalination and Water Treatment 57, 3414-3423.

Yao, L., Ye, Z.F., Tong, M.P., Lai, P. and Ni, J.R., 2009. Removal of Cr3+ from aqueous solution by biosorption with aerobic granules. Journal of Hazardous Materials 165, 250-255.

Yu, X., Wan, C., Lei, Z., Liu, X., Zhang, Y., Lee, D. J., Tay, J. H., 2014. Adsorption of ammonium by aerobic granules under high ammonium levels. Journal of the Taiwan Institute of Chemical Engineers, 45, 202-206.

Zhang, D., Li, W., Hou, C., Shen, J., Jiang, X., Sun, X., Li, J., Han, W., Wang, L. and Liu, X., 2017a. Aerobic granulation accelerated by biochar for the treatment of refractory wastewater. Chemical Engineering Journal 314, 88-97.

Zhang, H., He, Y., Jiang, T. and Yang, F., 2011. Research on characteristics of aerobic granules treating petrochemical wastewater by acclimation and co-metabolism methods. Desalination 279, 69-74.

Zhang, L., Long, B., Wu, J., Cheng, Y., Zhang, B., Zeng, Y., Huang, S. and Zeng, M., 2019b. Evolution of microbial community during dry storage and recovery of aerobic granular sludge. Heliyon 5, p.e 03023.

Zhang, M., Ji, B. and Liu, Y., 2021. Microalgal-bacterial granular sludge process: A game changer of future municipal wastewater treatment?. Science of The Total Environment 752, 141957.

Zhang, R., Yu, S., Shi, W., Tian, J., Jin, L., Zhang, B., Li, L. and Zhang, Z., 2016a. Optimization of a membrane cleaning strategy for advanced treatment of polymer flooding produced water by nanofiltration. RSC advances 6, 28844-28853.

Zhang, Y., Dong, X., Nuramkhaan, M., Lei, Z., Shimizu, K., Zhang, Z., Adachi, Y., Lee, D.J. and Tay, J.H., 2019a. Rapid granulation of aerobic granular sludge: A mini review on operation strategies and comparative analysis. Bioresource Technology Reports 7, 100206.

Zhang, Y., Jiang, W.L., Xu, R.X., Wang, G.X. and Xie, B., 2017b. Effect of short-term salinity shock on unacclimated activated sludge with pressurized aeration in a sequencing batch reactor. Separation and Purification Technology 178, 200-206.

Zhang, Z.Z., Cheng, Y.F., Zhou, Y.H., Buayi, X. and Jin, R.C., 2016b. Roles of EDTA washing and Ca^{2+} regulation oan the restoration of anammox granules inhibited by copper (II). Journal of Hazardous Materials 301, 92-99.

Zheng, Y., Chen, J.C., Ma, Y.M. and Chen, G.Q., 2020. Engineering biosynthesis of polyhydroxyalkanoates (PHA) for diversity and cost reduction. Metabolic Engineering 58, 82-93.

Zheng, Y.M., Yu, H.Q., Liu, S.J. and Liu, X.Z., 2006. Formation and instability of aerobic granules under high organic loading conditions. Chemosphere 63, 1791-1800.

Zhiwei, S., Nanqi, R., Zhang, K. and Longyan, T.O.N.G., 2009. Influence of temperature on the characteristics of aerobic granulation in sequencing batch airlift reactors. Journal of Environmental Sciences 21, 273-278.

Zhu, L., Xu, X., Luo, W., Tian, Z., Lin, H., Zhang, N., 2008. A comparative study on the formation and characterization of aerobic 4-chloroaniline-degrading granules in SBR and SABR. Applied Microbiology and Biotechnology 79, 867-874.

Zlopasa, J., Koenders, E.A.B. and Picken, S.J., 2014. Using bio-based polymers for curing cement-based materials. In AMS 14: Proceedings of the 1st Ageing of Materials & Structures Conference, Delft, The Netherlands, 26-28 May 2014. DCMat Ageing Centre, Delft University of Technology.

Chapter 2

Role of inoculum in aerobic granular reactors for oily wastewater treatment

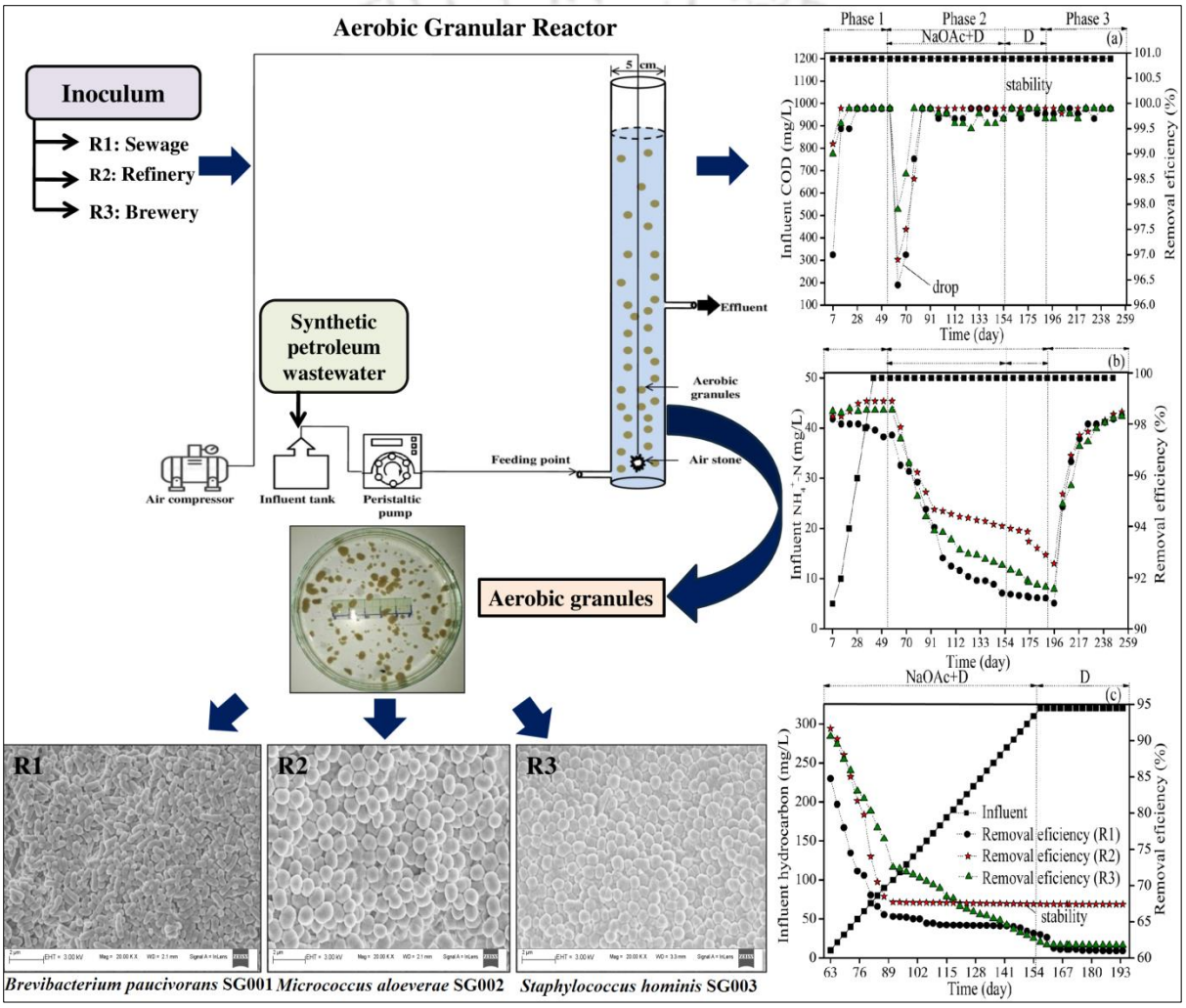

CHAPTER 2

Role of inoculum in aerobic granular reactors for oily wastewater treatment

This chapter provides extensive information about oily wastewater treatment in AGRs using three different inocula from sewage, refinery and brewery with detailed microbial analysis.

2.1 Introduction

Most of the published literature on oily wastewater treatment focused on AGR performance with changing volumetric loading or operating conditions. However, performance of a bioreactor largely depends on seeding sludge and pollutant degrading microbial species. Activated sludge collected from municipal (Zhang et al., 2011; Corsino et al., 2015), petrochemical (Chen et al., 2019) or palm oil mill effluent (POME) treatment plants (Abdullah et al., 2013) were mostly used for granulation in oily wastewater treatment. Chen et al. (2019) reported the presence of petroleum degrading *Propioniciclava*, *Micropruina*, *Alphaproteobacteria*, *Flavobacterium* and *Sulfuritalea* genera in aerobic granules. Uncultured *Methylobacillus*, *Bacterium* and *Flavobacterium* were dominant during granule formation whereas *Bacteriodetes* and uncultured *Propionibacteriaceae* were active after granule maturation in POME treatment (Abdullah et al., 2013). Previous exposure with wastewater may effect granulation from a particular sludge. Milia et al., (2016) observed irreversible granule breakage with domestic wastewater treatment plant sludge whereas, oil acclimatized sludge of petrochemical wastewater treatment plant provided faster granulation in coal gasification wastewater treatment. But how the granule characteristics, performance and oil tolerance threshold may vary with different inocula dominated by different bacterial population was largely unknown.

Three different inocula originating from sewage having heterogeneous microbes, from refinery which were previously acclimatized with recalcitrant hydrocarbons and from brewery industry may differently behave in granulation in oily wastewater. This aspect was not well addressed in literature.

So, the main objective of this chapter was to perform a comparative study to thoroughly investigate the role of sewage, refinery and brewery sludge on granule formation and stability while treating high concentration oily wastewater along with determination of threshold oil concentration for different sludge granules and identification of major pollutant degrading

microbial species in different inoculum. Probable restoration process of partially ruptured granules was also explored.

2.2 Materials and methods

2.2.1 Chemicals and reagents

All the chemicals used in this study were either of analytical grade (AR) or laboratory grade (LR). For synthetic wastewater, chemicals like sodium acetate, potassium di hydrogen phosphate (KH_2PO_4), di potassium hydrogen phosphate (K_2HPO_4), sodium bi-carbonate (for pH adjustment), $MgSO_4.7H_2O$, $CaCl_2.2H_2O$, $FeCl_3.6H_2O$, $CuCl_2$, $ZnCl_2$, $NiCl_2.6H_2O$ and $CoCl_2$ were used which were purchased from HiMedia, India. Other chemicals for analytical procedures like phenol, sodium nitroprusside, tri-sodium citrate, sodium hypochlorite, ferrous ammonium sulfate, potassium dichromate, mercuric sulfate, silver sulfate, ferroin indicator, sodium chloride, glucose, bovine serum albumin (BSA), sodium potassium tartrate, sodium carbonate, copper sulfate, Folin-Ciocalteu reagent, potassium chloride, sodium hydroxide, silica gel, nutrient broth, glutaraldehyde etc. were also purchased from HiMedia and SRL, India. Sulfuric acid, nitric acid and hydrochloric acid were procured from HiMedia, India. Other analytical grade solvents like n-heaxane (for gravimetric analysis), n-hexadecane, ethanol, chromatography grade n-hexane and another chemical nonylphenolethoxylate were mostly purchased from Merck, India.

Diesel was purchased from the nearby petrol pump of Hindustan Petroleum Corporation Limited. Tap water was used for feed preparation whereas, for reagents or stock/standard solution preparation and analysis of samples deionized water or millipore water were used wherever applicable.

2.2.2 Experimental set-up

A photograph and schematic of fabricated AGR is shown in Fig.2.1 and 2.2. Three acrylic pipes with 3.0 L working volume were used to design the AGRs (R1, R2, R3). The inner diameter, working height and H/D (Height/Diameter) ratio of the reactors were 5.0 cm, 153.0 cm and 30.5, respectively. Aeration (2 L/min) was provided by oil-free air compressor through air stones at the bottom of the reactors. One four channel peristaltic pump was employed for reactor feeding. Effluent was withdrawn from outlet pipe placed at 76.5 cm from the base of the rectors. The reactors were maintained at room temperature (20-30 °C).

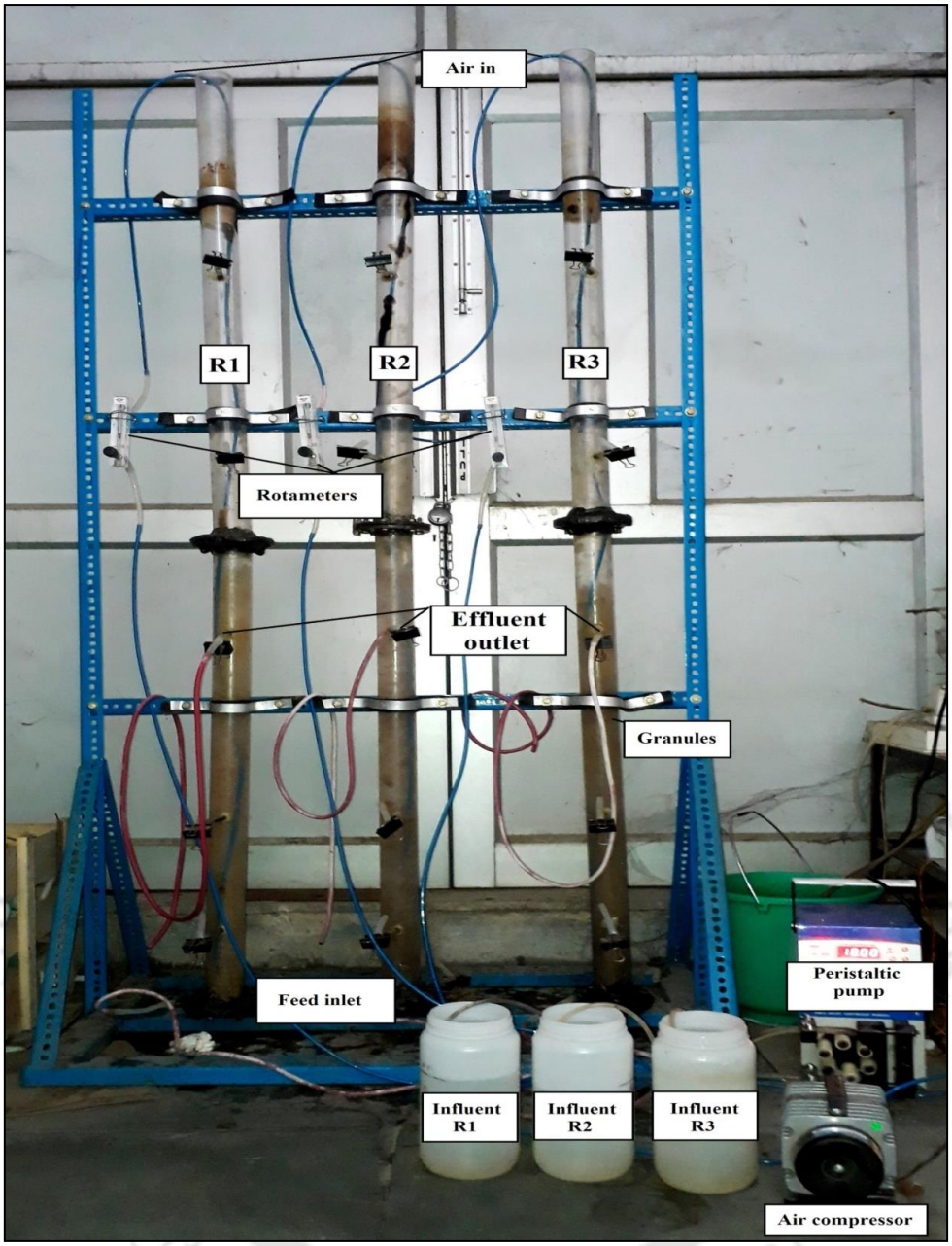

Fig.2.1 Photograph of the fabricated aerobic granular reactors (AGR) during feeding time

2.2.3 Inoculum collection

R1, R2 and R3 were inoculated with sludge collected from the aeration tanks of Indian Institute of Technology Guwahati sewage treatment plant, Indian Oil Corporation Limited effluent treatment plant, Guwahati and Master India Brewing Company, Guwahati, respectively. Initial pH, sludge volume index (SVI) and settling velocity of sewage, refinery and brewery sludge were 8.36, 8.29, 8.44; 89.76±0.05 mL/g, 76.87±0.15 mL/g, 73.56±0.33 mL/g and 1.4±0.02 m/h, 3.7±0.11 m/h, 4.2±0.17 m/h, respectively. To maintain uniformity, initial volatile suspended solid (VSS) was diluted at 0.4±0.03 g/L for all three types of sludge.

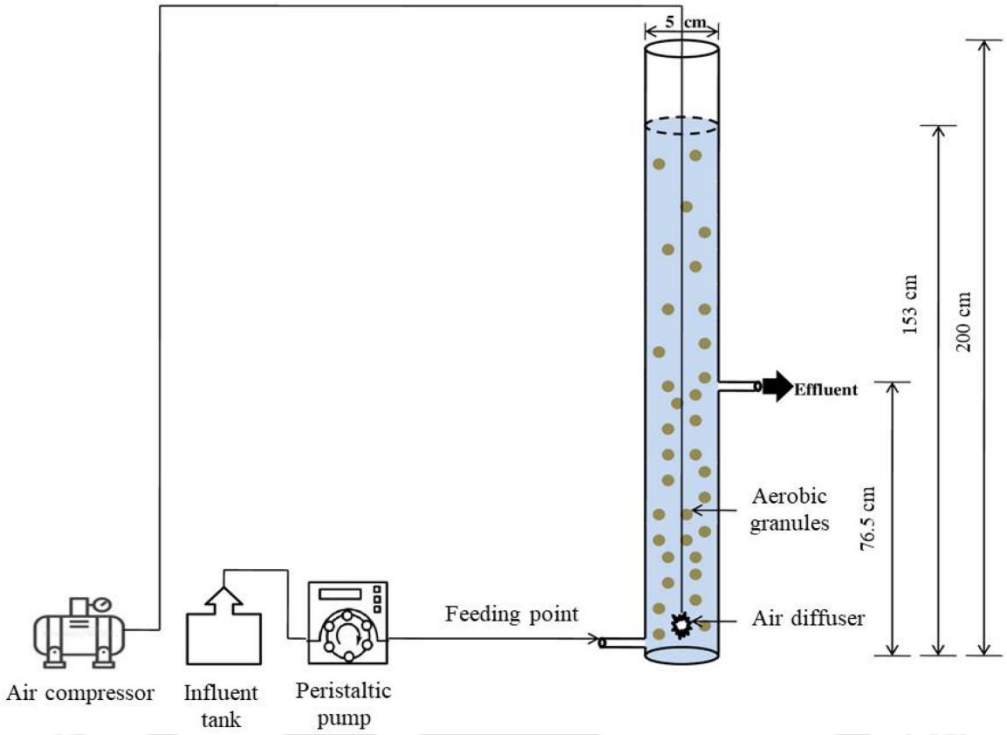

Fig.2.2 Schematic of the fabricated aerobic granular reactor (AGR).

2.2.4 Feed composition

Fig.2.3 depicts the changing feed compositions in phase 1 (granule formation phase), phase 2 (oil removal phase) and phase 3 (granule restoration phase). In phase 1 (day 1-56), AGRs were fed with sodium acetate (1540 mg/L) with 1200 mg/L influent COD and 5-50 mg/L NH_4^+-N as nitrogen source. The COD:NH_4^+-N ratio was maintained at 20:1 throughout the study. Feed pH was maintained at 7±0.2 by using phosphate buffer (containing 72 g/L KH_2PO_4 and 104.5 g/L K_2HPO_4) which also worked as a phosphate source. About 1 mL/L of trace metal solution composed of 10,000 mg/L $MgSO_4.7H_2O$, 10,000 mg/L $CaCl_2.2H_2O$, 5000 mg/L $FeCl_3.6H_2O$, 1000 mg/L $CuCl_2$, 1000 mg/L $ZnCl_2$, 500 mg/L $NiCl_2.6H_2O$, 500 mg/L $CoCl_2$ was used as mineral source for bacterial growth (Tomar and Chakraborty, 2018). In phase 2 (day 57-190), a mixture of diesel oil (collected from Hindustan Petroleum Corporation Limited petrol pump with 782.5 kg/m^3 density at 30 °C temperature) and nonylphenol ethoxylate emulsifier (diesel: emulsifier v/v ratio 200:1) along with sodium acetate was used to maintain a COD of 1200 mg/L. Oil concentration ranged between 10 to 320 mg/L in phase 2. Diesel concentration gradually increased in every 3 days and acetate concentration was correspondingly decreased. From day 157-190, only emulsified diesel was used as carbon source providing 1200 mg/L COD in the AGRs. In phase 3 (day 191-246), diesel application was stopped in the AGRs and sodium acetate (1540 mg/L) having 1200 mg/L COD was re-added in feed for granule restoration.

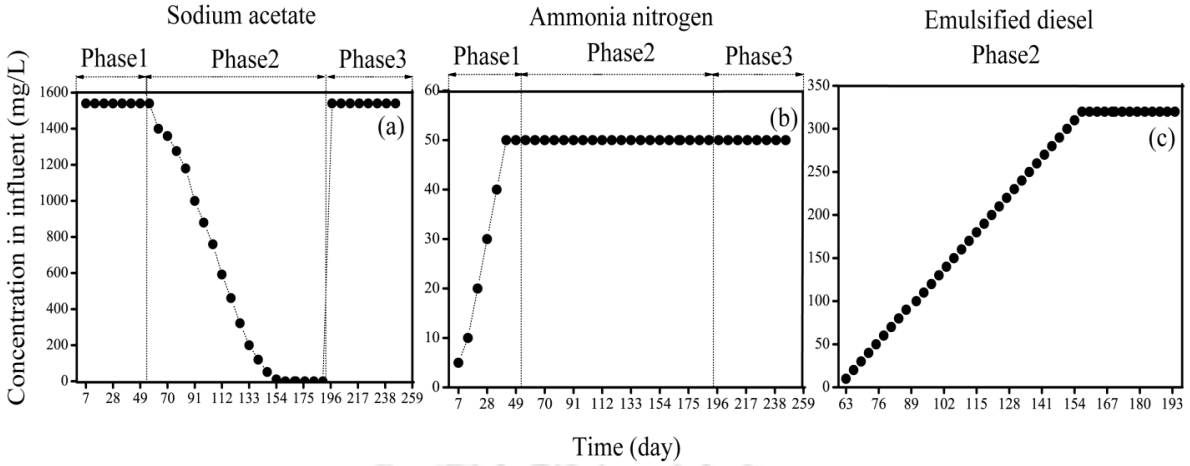

Fig.2.3 (a) Sodium acetate, (b) ammonia nitrogen and (c) diesel concentration variation in inflluent (HRT, VER and air flow rate were maintained at 16 h and 50% and 2 L/min, respectively).

2.2.5 Reactor operating conditions

All three AGRs were operated in 3 cycles per day with of 8 h cycle time and 16 h of hydraulic retention time (HRT). Volume exchange ratio (VER) was maintained at 50% which determined that 50% of reactor working volume was decanted in each cycle and same volume of fresh feed was added to the reactor. Continuous oxygen supply provided 2 L/min of air flow rate. Liquid up-flow velocity (ULV) is the liquid velocity at which influent feed moves in the upward direction in the AGR during feeding and feed up-flow velocity was controlled at 2.07 m/h in the AGRs. In each cycle, 22 min for feeding, 450 min for reaction, 3-5 min for settling, 2 min for decanting and 3 min idle time were used. The effluent pH remained within 7.5 to 8.5. The initial F/M ratio in all three AGRs were 2.96 g COD/g SS.day as high F/M value at reactor start-up is essential for fast granulation and to increase granule size (Li et al., 2011). HRT, ULV, loading rate and removal (%) were calculated by using equation 2.1 to 2.4.

$$\text{HRT (day)} = \frac{\text{Reactor volume,L}}{(\text{Volume decanted per cycle,L}) \times (\text{No.of cycles per day})} \quad (2.1)$$

$$\text{ULV (m/h)} = \frac{\text{Flowrate } (\text{m}^3/\text{cycle})}{\text{Feeding time per cycle (h)} \times \text{Cross sectional area of reactor } (\text{m}^2)} \quad (2.2)$$

$$\text{Loading rate } (\text{kg/m}^3.\text{day}) = \frac{S_0}{\text{HRT}} \quad (2.2)$$

$$\text{Removal (\%)} = \frac{(S_0 - S_e) \times 100}{S_0} \quad (2.4)$$

Where, S_0 is the influent concentration (mg/L), S_e is the effluent concentration (mg/L),

2.2.6 Analytical procedures

2.2.6.1 Analysis of effluent and sludge

Effluent samples were filtered and analysed. **pH, conductivity** and **atmospheric temperature** were measured by pH meter (Extech), conductivity meter (Thermo Scientific) and a thermometer, respectively. pH meter was adjusted with bufefer solutions (pH 4.0, 7.0 and 9). **Granule size** was measured by using ImageJ softwere, version 1.47 (Tijani et al., 2015). Granule samples were taken on a Petri dish and photograph was taken. The photograph was further analyzed by ImageJ to measure the equivalent diameter from the projected surface area of the granules. The average diameter of minimum 50 granules were considered from each AGR. The **granule density** (g/L) was determined according to Beun et al. (1999) dividing dry weight of granules by granule volume using volumetric displacement method. **Total suspended solid** (TSS) (g/L), and volatile suspended solid (VSS) (g/L) and **sludge volume index** (SVI) (mL/g) were calculated according to standard methods (APHA, 2005). Granule samples were taken out from the AGRs at aeration phase and dried up at 105 °C in a hot air oven (IKON) for **TSS** analysis. For **VSS**, the sample was further ignited at 550 °C in a muffle furnace (Thermo Scientific). To measure **granule settling velocity** (GSV), ten random aerobic granules were chosen and they were allowed to settle down inside a 1 L measuring cylinder. Finally, the GSV was calculated by dividing the distance travelled by the granules to the average time required for settling down (Yu et al., 2009). **SVI_{30}** was determined by taking 1 L of granular sludge sample in a measuring cylinder and allowing it to settle down in 30 min and was calculated from the ratio of the settled sludge volume (mL) to the TSS of the granular biomass (g).

Extracellular polymeric substances (EPS) were extracted by using modified heat extraction process along with conductivity adjustment of sample (Li and Yang, 2007). About 50 mL of granular sludge sample was taken out from the AGR and was centrifuged at 4000 rpm for 5 min. The pellet was suspended at 0.05% NaCl solution to adjust the conductivity. The sample is then kept in a water bath at 60 °C temperature for 30 min and was further centrifuged for 15 min at 4000 rpm. The supernatant was collected as EPS extract.

The **Polysaccharides** (PS) were measured (mg/g VSS) according to phenol-sulfuric acid method (Dubois et al., 1956). About 2 ml EPS extract was taken in a test tube and was rapidly mixed with 1 mL of 5% phenol solution and 5 mL concentrated H_2SO_4. Test tube was allowed to stand for 10 minutes and was vortexed for 30 s. Then, the test tube was placed in a water bath at room temperature (25-30 °C) for 20 min for colour development. Absorbance was measured at 490 nm. Standard curve (Fig.A1) for carbohydrate was prepared between

the range of 20 to 100 µg/mL glucose concentration (at 490 nm wavelength) with a R^2 (coefficient of determination) value of 1.

Proteins (PN) were analysed (mg/g VSS) by using Folin method (Lowry et al., 1951). For protein assay, reagent A (about 2 g sodium potassium tartrate tetrahydrate and 500 mL of 1N NaOH in 1L distilled water), B (consisting 2 g sodium potassium tartrate tetrahydrate, 1 g copper sulfate and 10 mL of 1N NaOH in 100 mL distilled water) and C (one volume of Folin-Ciocalteau reagent was mixed with 15 volumes of distilled water) were freshly prepared. Approximately, 1 mL EPS extract was added with 0.9 mL of reagent A in a test tube was placed in a water bath for 10 min at 50 °C and was cooled down at room temperature. Thereafter, about 0.1 mL reagent B was mixed with the test tube sample and was incubated for 10 min at room temperature. Finally, about 3 mL of reagent C was rapidly added to the test tube and was incubated in water bath for 10 min at 50 °C. Afterward, the sample was allowed to cool down at room temperature for 30-60 min to develop the blue colour and absorbance was measured at 650 nm. BSA was used as a standard to prepare calibration curve (Fig.A2) for protein.

Cell hydrophobicity (%) was measured by a spectrophotometric method based on the affinity between n-hexadecane and granules following 10 minutes of pre-incubation of sample (n-hexadecane and granules) at 30 ºC temperature, vigorous mixing for 2 min and 15 min of partitioning time (Rosenberg et al., 1989). Finally, the absorbance was measured at 400 nm.

Microscopic images of granules were analysed under field emission scanning electron microscope (FESEM, Make: Zeiss, Model: Sigma). For FESEM analysis, granules were prepared by consecutive technique of buffer washing, glutaraldehyde fixing and dehydration by gradients (30-90%) of ethanol (Wang et al., 2007).

COD (mg/L) was measured using closed reflux titrimetric method by titrating the acidified sample with ferrous ammonium sulfate as a titrant (APHA, 2005). As diesel was insoluble in water, 8 h of digestion time was required for complete diesel digestion before COD measurement (Mallick and Chakraborty, 2017). **Ammonia-nitrogen** (NH_4^+-N) was analysed by Phenate method using phenol solution (11 mL phenol dissolved in 100 mL ethanol), oxidising solution (Alkaline citrate+sodium hypochlorite) and sodium nitroprusside solution with absorbance measured at 640 nm (APHA, 2005) in a UV-visible spectrophotometer (Agilent Technologies). A calibration curve (Fig.A3) in the range of 0.2 to 1 mg/L was drawn which followed good linearity with a R^2 value of 0.991.

Nitrate (NO_3^-) and nitrite (NO_2^-) concentrations (mg/L) were analysed by ion chromatograph (792 Basic IC, Metrohm) using anion column (Metrosep A Supp 5, 250/4.0 mm) and carbonate eluent maintaining a flow-rate of 0.7 mL/min and column pressure of 11–13 MPa.

2.2.6.2 Hydrocarbon removal

Diesel concentration was measured (in terms of total hydrocarbon) by partition-gravimetric method (APHA, 2005). Effluent sample was centrifuged at 8000 rpm for 5 minutes and supernatant was used for analysis of diesel. About 10 mL of the acidified sample (1:1 HCl) was subjected to be extracted with 30 mL n-hexane in a separating funnel and shaken vigorously for 2 minutes. The funnel was kept unmoved for the separation of distinct aqueous and n-hexane layers. The aqueous layer was carefully separated and extracted again with the above mentioned procedure. Then the n-hexane (which dissolved hydrocarbons) was filtered through anhydrous sodium sulfate to eliminate residual water and was collected in a distillation flask. To determine the diesel concentration, the solution was transferred to a closed container and mixed with silica gel (3 g/100 mg diesel) for 5 minutes by a magnetic stirrer to absorb the polar compounds. The remaining solution was filtered with filter paper pre-moistened with n-hexane. The n-hexane was evaporated at 85 ºC and hydrocarbon was estimated as per equation 2.5.

$$\mathrm{TH}\left(\frac{\mathrm{g}}{\mathrm{L}}\right) = \frac{W_{Total} - W_{Empty}}{V_s} \qquad (2.5)$$

Where, W_{Total} = Total weight of distillation flask and residue (g);

W_{Empty} = Empty weight of distillation flask (g);

V_s = Volume of sample (L).

Hydrocarbon degradation was confirmed by gas chromatograph mass spectroscope (GC-MS) (PerkinElmer (USA); Model: Claurus 680 Gas Chromatograph/Claurus 600C Mass spectrometer) analysis of feed and effluent by using Elite-5MS Capillary Column of 60 mm length and inner diameter of 0.25 mm. The temperatures of both the injector and detector were kept at 250 °C. The initial temperature was 60 °C for 5 min, followed with a ramp of 5 °C/min to 200 °C and then a ramp of 10 °C/min to 300 °C kept for 10 min. Transfer and source temperatures were 200 °C and 180 °C, respectively. Mobile phase was helium (He) gas and the main GC-MS software was Turbomass Version 5.4.2.

2.2.6.3 Volatilization and adsorption study

Volatilization study was carried out by using 500 mL feed (containing 320 mg/L emulsified diesel, 50 mg/L NH_4^+-N, phosphate buffer and all micro nutrients) in a 1 L glass beaker for 8 h cycle time with 2 L/min aeration. Samples were taken out after 8 h to estimate average oil removal (mg/L). Adsorption study was carried out by autoclaving 2 g of biogranules taken out from each reactor. Hundred millilitre of feed (same as abiotic study) was taken inside conical flasks, dead granules were added and were kept in orbital shaker at 120 rpm for 8 h. Initial and final samples were analyzed to check oil removal (mg/L) by dead granules. Volatilization and adsorption studies were done in triplicates.

2.2.6.4 Reactor activity study

For reactor activity study, a known amount of granular sludge (VSS ≈ 2.5 to 3.5 g/L) sample from each AGR was taken into 1 L beakers and 500 mL of sodium acetate (1540 mg/L) solution was added as carbon source providing 1200 mg/L COD and aeration (2 L/min) was provided. Effluent samples were taken out from the beakers in every 5 min, 10 min, 15 min, 30 min, 1 hour, 2 hour and up to 6 hours interval to check COD removals. Experiment was carried out in 3 feeding cycles of 6 hours each. After 3rd feeding, the final granule VSS value was estimated. From the three feeding cycle, the average reactor biomass activity was calculated from the slope of linear portion of cumulative COD removal and time graph (Jawed and Tare, 1999). Activity was expressed in terms of mg COD/ mg VSS.day which is described in equation 2.6.

$$\text{Activity } \left(\frac{\text{mg COD removed}}{\text{mg VSS day}}\right) = \text{Slope of graph } \left(\frac{\text{mg of COD removed}}{\text{h}}\right) \times \frac{24\text{h}}{\text{day}} \times \frac{1}{\text{mg VSS}} \quad (2.6)$$

2.2.6.5 Microbial identification

For microbial identification, phase 2 granules were collected from the AGRs. Granules were suspended in 0.5% sterile NaCl solution and sonicated to prepare bacterial suspension. Cell suspensions were serially diluted (from 10^{-1} to 10^{-10} time dilution) and 1 µL of each sample was spread over nutrient agar (NA) plates. Plates were incubated at 37 °C temperature overnight. Different single bacterial colonies were selected on basis of morphology, pigmentation and Gram staining results and were further isolated using repeated streak plate procedure. Isolated pure colonies were sub-cultured in a liquid media containing 320 mg/L of emulsified diesel. Three white, yellow and pale golden coloured strains were isolated as major pollutant degrading bacteria from R1, R2 and R3, respectively and were sent to Genombio Technologies Pvt. Ltd. for microbial identification. After genomic DNA extraction and PCR amplification (by using 27F and 1492R primers), gel electrophoresis

provided clear DNA bands. DNA was sequenced by using ABI PRISM Big Dye Terminator V3.1 kit (Applied Biosystems, USA) and was analysed by Analysis 5.2 software. Evolutionary history was inferred by using Neighbor-Joining method and finally phylogenetic trees were prepared by using MEGA X software.

2.2.6.6 Pollutant removal by isolated strains

Isolated pure strains were individually subjected to varying COD, NH_4^+-N and diesel concentrations to check their pollutant removal efficiencies. COD, NH_4^+-N and diesel concentrations of the feed ranged between 200 to 1200, 10 to 50 and 50 to 320 mg/L, respectively. Pollutant removals were checked in every 12 h intervals and continued up to 48 h from inoculation time.

2.3 Results and discussion

2.3.1 Volatilization and adsorption study

Approximately 0.021±0.10% oil removal (influent oil: 320 mg/L) was observed by volatilization (without granules) in 8 h. Adsorption study proved that only 0.076±0.03% oil removal was possible by autoclaved dead granules. This study ensured that oil removal was dependent upon biological functions of granule bacteria which cannot be performed abiotically. The results of the abiotic studies are given in Table 2.1

Table 2.1 Abiotic oil removal in volatilization and adsorption study

Abiotic study	Influent oil (mg/L)	Effluent oil (mg/L)	Removal efficiency (%)
Volatilization study	320	319.93±0.32	0.021±0.10
Adsorption study	320	319.76±0.96	0.076±0.33

*Volatilization and adsorption studies were conducted without granules and with dead granules respectively. Effluent oil concentration was checked after 8 h cycle time.

2.3.2 Granule formation

Small round and rod-shaped aerobic granules appeared in the AGRs within 7 days. Initially, granule colour was brownish due to flocculent biomass wash-out (Zhang et al., 2011). Gradually, sodium acetate promoted matured yellowish granules with less flocculent biomass (Fig.2.4). Increasing granule size reduced granule settling time from 5 to 3 min. At the end of phase 1 (day 56), R1, R2 and R3 achieved maximum granule size of 5.16±0.02 mm, 5.42±0.03 mm and 5.44±0.05 mm, respectively. Fig.2.5a describes granule size profile in the AGRs.

In phase 2, decreasing acetate and increasing diesel concentration caused partial granule rupture. Granules turned to be brownish again. Average granule size decreased from 5.34±0.03 mm to 4.02±0.05 mm on day 91 in presence of 100 mg/L influent oil. Granule

disintegration in real petrochemical wastewater was also reported by Zhang et al. (2011). Between day 157-190, in complete absence of acetate and presence of 320 mg/L of diesel, initially granules became unstable. On day 190, final granule size reached up to 3.11±0.01 mm; 3.49±0.01 mm and 2.42±0.01 mm, in R1, R2 and R3, respectively. In presence of 100 mg/L of diesel, maximum granule size was observed in R3, having brewery sludge. But finally, R2 containing refinery sludge granules had biggest granules in presence of 320 mg/L of diesel. It indicated higher oil tolerance threshold in refinery granules than sewage and brewery granules.

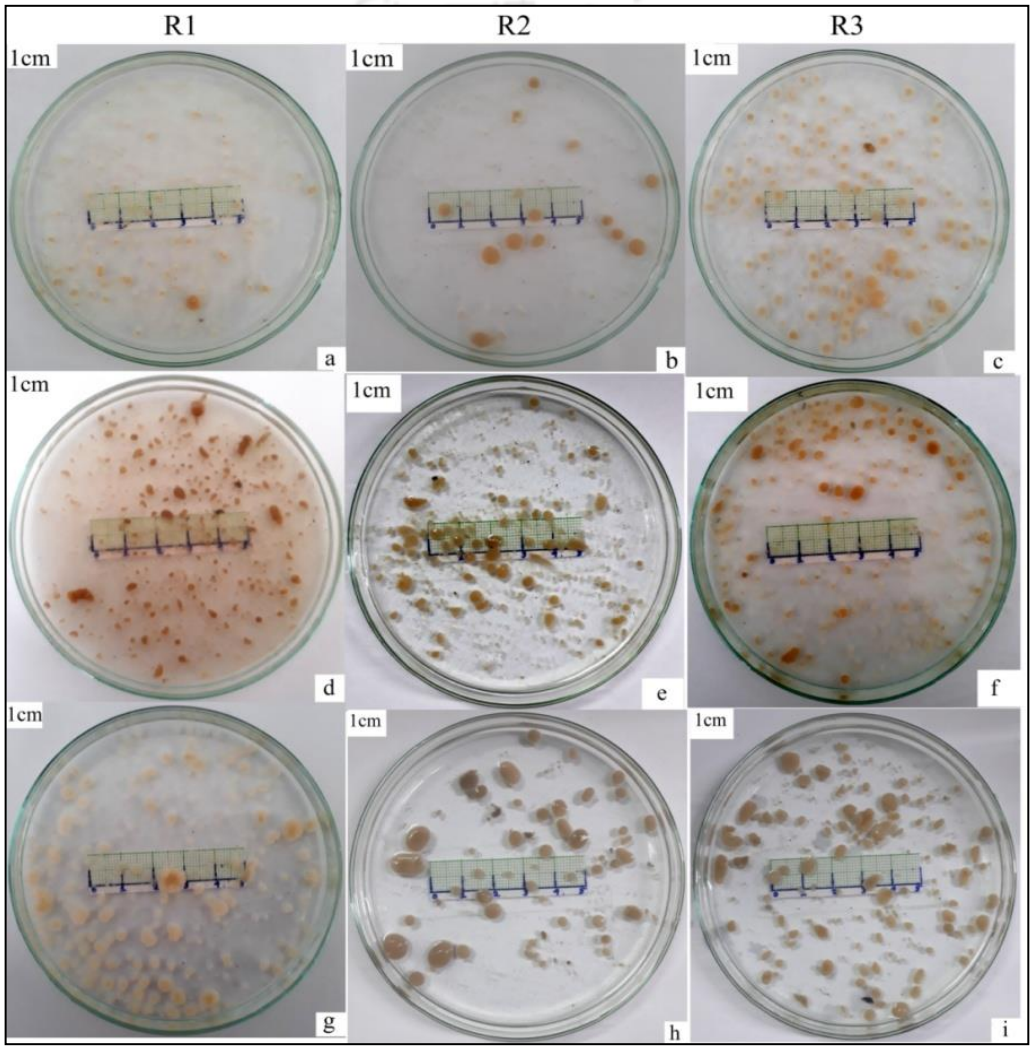

Fig.2.4 (a, b, c) Matured yellowish aerobic granules in phase 1, (d, e, f) slightly ruptured brownish granules in phase 2 and (g, h, i) reconstructed yellowish granules in phase 3.

Table 2.2 elaborates a literature survey on approximate granule size in acetate and oil-fed granules which depicts that comparatively bigger sized granules were formed due to lower HRT in our AGRs both in acetate-fed and oil-fed wastewater than the reported granule sizes.

Table 2.2 Variation in size in acetate-fed and oil-fed granules

Acetate-fed granule size (mm)	References	Oil-fed granule size (mm)	References
0.3-0.5	Dongcong et al. (1999)	1.13	Zhang et al. (2011)
2.5-2.7	Beun et al. (2002)	1.3	Milia et al. (2016)
1.5	Corsino et al. (2016)	0.31	Caluwé et al. (2017)
0.8-1.1	Deng et al. (2016)	0.46–0.9	Chen et al. (2019)
4.37±0.03	Current study	3.71±0.05	current study

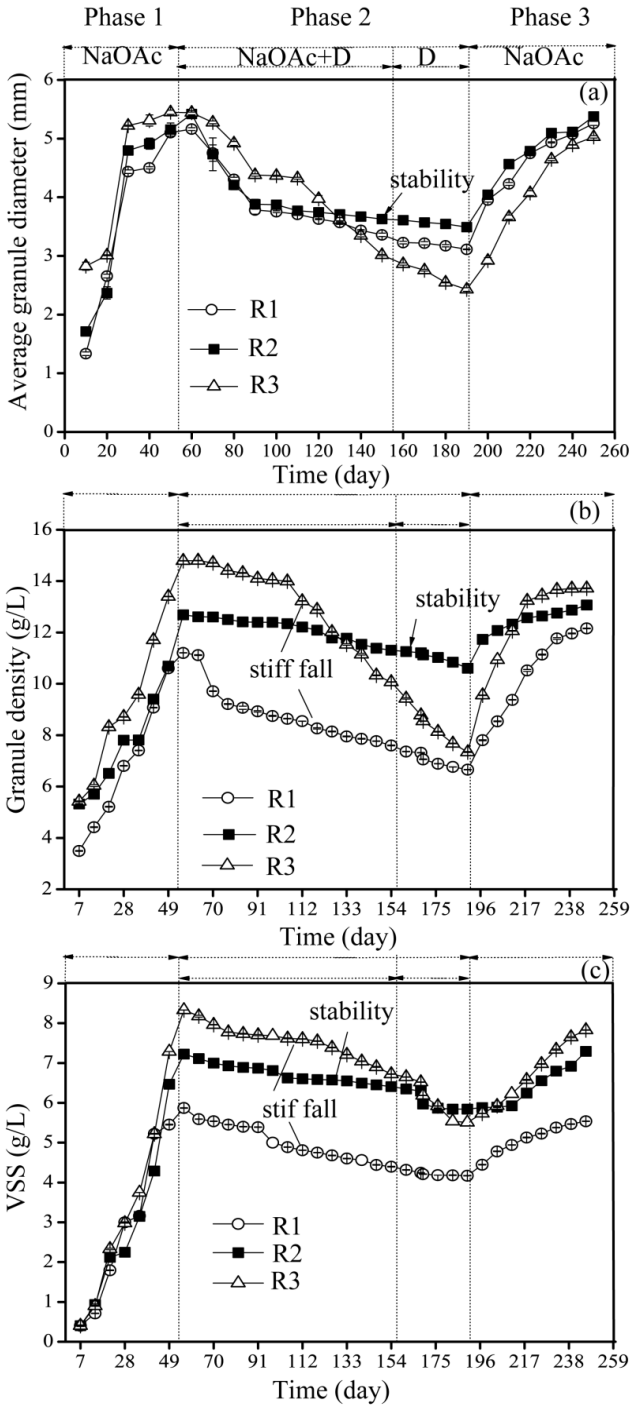

Fig.2.5 (a) Granule size, (b) density and (c) VSS content profile in the AGRs. [NaOAc represents sodium acetate and D represents diesel].

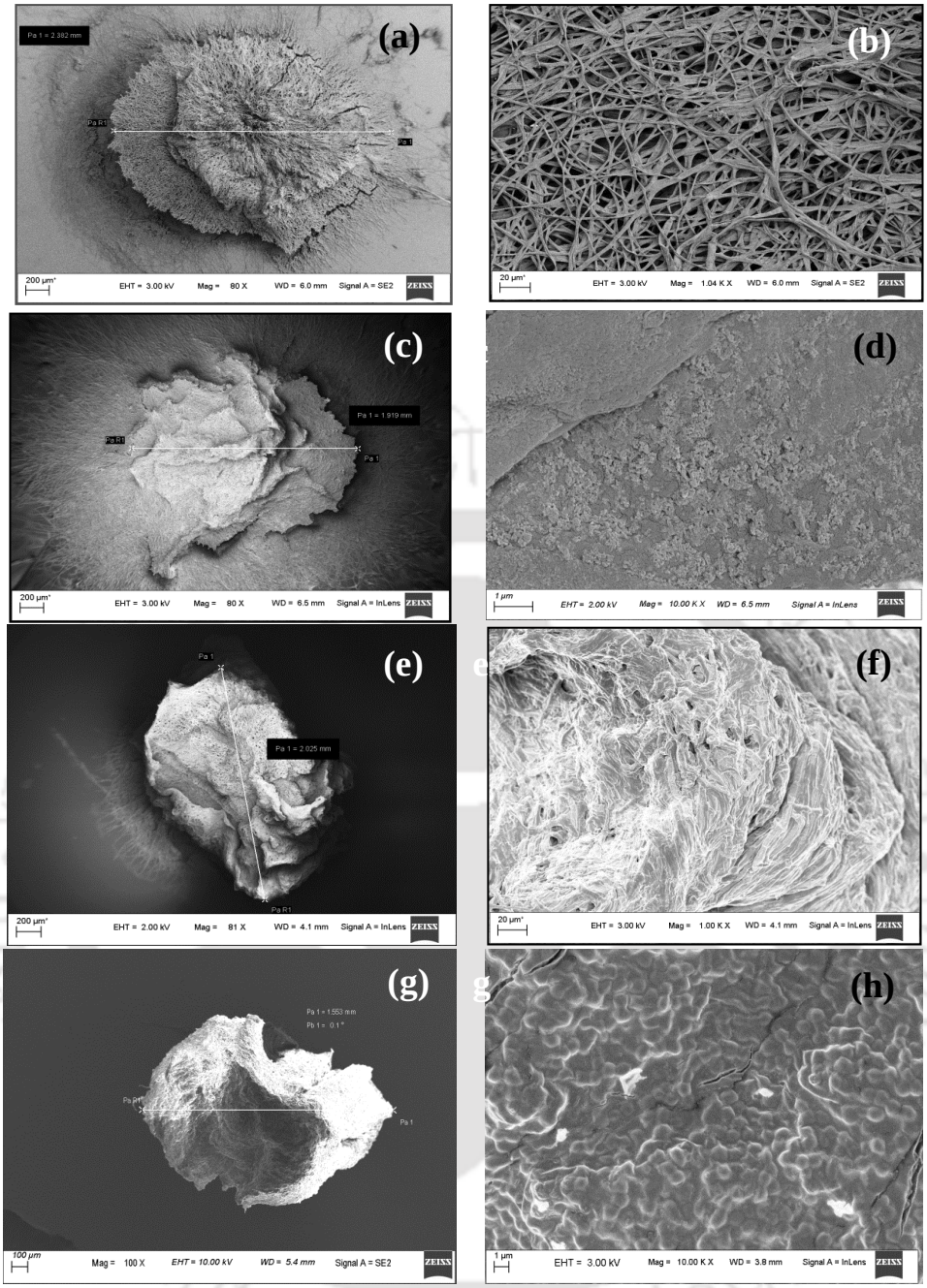

Fig.2.6 (a, b) FESEM image of R2 granule on day 25 showed filamentous structure, (c, d) which became non-filamentous on day 53. (e, f) Granules became partially filamentous due to oil exposure on day 74. (g, h) Non-filamentous granule structure restored on day 246.

VSS determines the amount of organic matter present in the granules. At the end of phase 1, R3 exhibited maximum VSS content (8.33±0.13 g/L) and granule density (14.79±0.1 g/L) denoting maximum granule stability. In phase 2, a stiff fall in granule density and VSS profile were observed in R1 and R3 (Fig.2.5b and c). But in R2, VSS and granule density were comparatively stable. R2 granules with refinery origin had maximum tolerance in high oil concentration (320 mg/L) which resulted into less granule rupture and high granule

density. As, sewage and brewery inocula were not previously exposed to oily wastewater, R1 and R3 granules suffered from partial granule rupture in presence of emulsified diesel. At the end of phase 2, R2 promoted maximum granule density (10.61±0.01 g/L) and VSS concentration (5.84±0.03 g/L) among the AGRs. In phase 3 (day 191 to 246), re-addition of sodium acetate helped to restore average granule size, density and VSS content up to 5.22±0.07 mm, 12.97±0.05 g/L and 6.89±0.11 g/L in the AGRs suggesting recovery of ruptured granules. Similarly, as phase 1, granule colour further changed from brown to yellowish.

FESEM images of most oil tolerant R2 granules are described in Fig.2.6. Microscopic images revealed that initially (day 25) the aerobic granules were dominated by filamentous bacteria. But after maturation, granules became non-filamentous (day 53). In increasing diesel concentration granules became partially filamentous (day 74). Finally, re-addition of acetate restored non-filamentous granule structure (day 246). Similar microscopic structures were found for R1 and R3 granules.

2.3.3 Characterization of aerobic granules

2.3.3.1 Settling of granules

GSV and SVI are the key parameters to check granule setteability. Qin et al. (2004) established that below 50 mL/g of SVI value was necessary for excellent hydrophobicity in aerobic granules. At the end of phase 1, SVI values reached 35.49±1.84 mL/g in R1, 30.35±2.32 mL/g in R2 and 20.54±1.26 mL/g in R3, respectively suggesting stable granules. Eventually, GSV values increased up to 25.49±0.13 m/h, 32.89±2.01 m/h and 51.32±1.02 m/h in R1, R2 and R3, respectively in phase 1. Liu and Tay (2004) proved that the settling velocity corresponds with size and structure of granule and ranged from 30 to 70 m/h. Similarly, in current study, GSV values were proportional to the granule diameters (Fig.2.5a). Comparative granule SVI and GSV profiles are described in Fig.2.7a. In phase 1, the F/M ratio in AGRs was 0.14-0.2 g COD/g SS.day which provided matured granulation with high settleability. In phase 2, granule settleability was initially affected by recalcitrant diesel. It resulted into increasing SVI and decreasing GSV trends in granules. Zhang et al. (2011) also observed that SVI increased with decreased granule stability in real petrochemical wastewater. F/M ratio signifies the ratio of incoming food (influent COD) and microorganisms (suspended solids) available in the reactor. As, average F/M ratio sharply increased from 0.17 g COD/g SS.day to 0.24 g COD/g SS.day causing biomass washout from AGRs it hampered granule settling properties which was similar to the results observed by Hamza et al. (2018) in high strength organic wastewater.

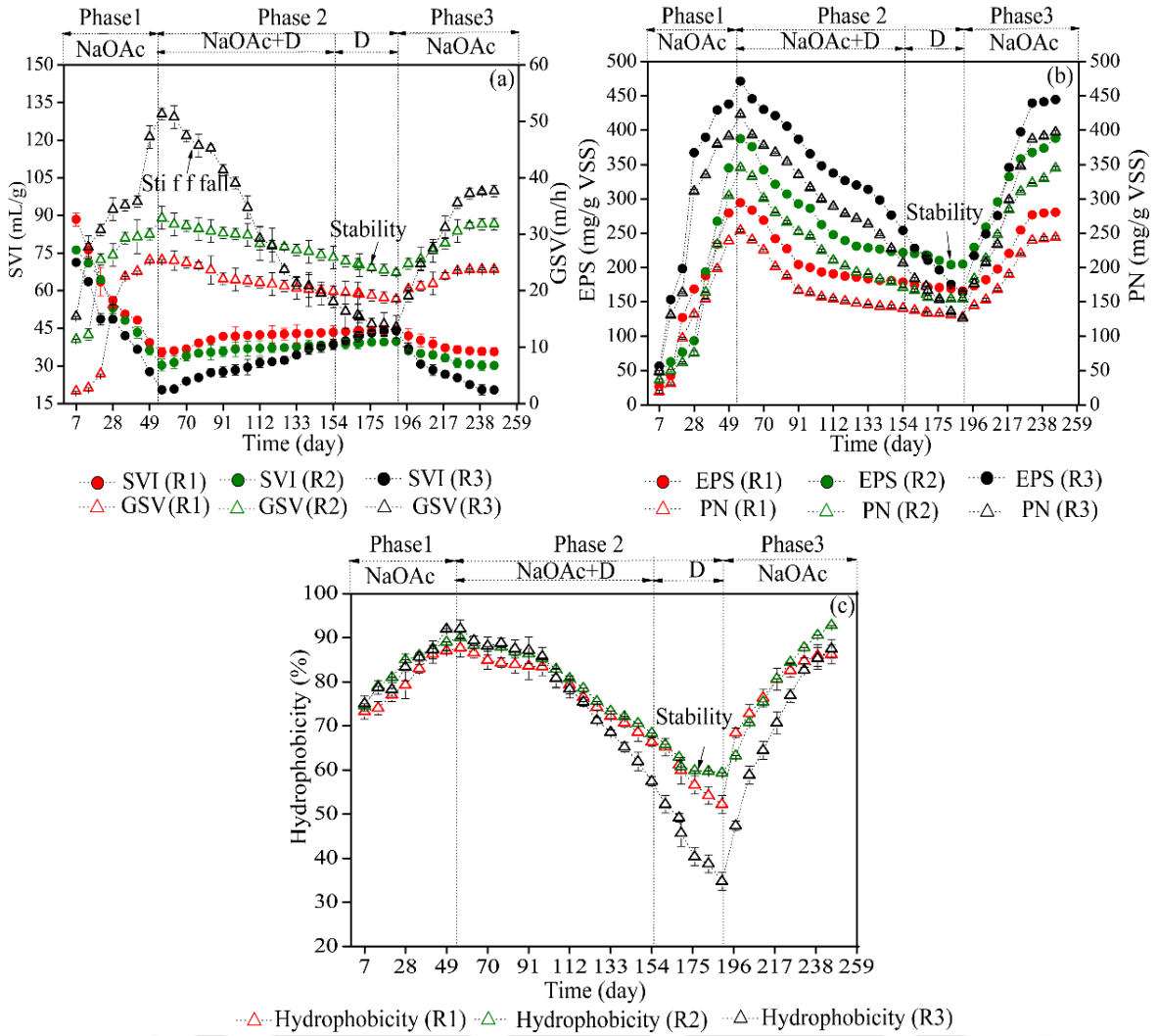

Fig.2.7 (a) SVI with GSV, (b) EPS with PN and (c) granule hydrophobicity profile in the AGRs. [NaOAc represents sodium acetate and D represents diesel].

After day 168, at 320 mg/L oil concentration, SVI gradually became stable near 41.56±2.01 mL/g in the AGRs. Val del Río et al. (2013) observed granulation at GSV below 9.5 m/h. In our case also granules survived at lower GSV. However, R2 granules containing refinery inocula were capable to withstand high diesel concentration with comparatively lower (0.21 g COD/g SS.day) F/M ratio and obtained maximum GSV (23.21±0.58 m/h) and minimum SVI (39.80±0.57 mL/g) values among the AGRs at the end of phase 2. Similarly, switching of municipal sludge to petroleum sludge provided faster and stable granulation in coal gasification wastewater treatment (Milia et al., 2016). In phase 3, sodium acetate restored granule stability. F/M ratio further decreased (0.16-0.15 COD/g SS.day) with enhanced biomass concentration with an increasing GSV and a decreasing SVI trend in the AGRs.

2.3.3.2 EPS and hydrophobicity

EPS are metabolic polymers consisting of proteins and β-polysaccharides secreted on outer granule surfaces (Liu and Tay, 2002). In cultivation phase, the microorganisms try to adjust their cell metabolisms with the new feed and high shear forces (Zhang et al., 2011). Hence, in phase 1 EPS increased significantly in the AGRs.

PN are hydrophobic in nature. They elicit cell hydrophobicity which favour granule formation and PS provide cell mechanical energy. Granule PN fraction was found higher than PS fraction. In phase 1, PN:PS ratio varied between 2.45±0.01 to 8.78±0.01. Comparative EPS and PN profiles in the AGRs are shown in Fig.2.7b. In phase 2, initially diesel addition hampered EPS synthesis. Glucose-fed granules also faced lower EPS and PN production while treating real petrochemical wastewater conducted by Zhang et al. (2011). However, Zhang et al. (2011) and Chen et al. (2019) reported oil treating granules with greater PS content than PN which contradict our result. AGRs gradually acclimatized themselves in 320 mg/L of diesel which stabilized EPS and PN:PS values between 172 to 218 mg/g VSS and 3.56–3.96, respectively (on day 168). At the end of phase 2, R2 containing oil acclimatized refinery granules achieved maximum 204.85±2.01 and 154.23±2.0 mg/g VSS of EPS and PN contents due to higher oil tolerance threshold than the other two sludge. In phase 3, sodium acetate re-constructed granule structure which increased EPS content and PN:PS ratio.

High cell hydrophobicity contributes to lower SVI and compact microbial structure (Qin et al., 2004). Initial average sludge hydrophobicity was 50.27±1.72% which rapidly increased up to 89.89±2.12% in phase 1 but deteriorated in phase 2 (48.77±2.04%) and further restored at 88.78±2% in phase 3. In phase 1, R3 achieved maximum cell hydrophobicity (92.01±2.03%) among the AGRs. But in phase 2, refinery sludge granules in R2 achieved maximum cell hydrophobicity (59.34±0.15%) denoting most oil tolerant stable granules among the three AGRs. Hydrophobicity profiles in the AGRs are described in Fig.2.7c.

2.3.4 Performance of AGR

2.3.4.1 Performance in COD and NH_4^+-N removal

COD and NH_4^+-N removal patterns are described in Fig.2.8a and b. Organic loading rate (OLR) was fixed at 1.8 kg COD/m^3.day. Nitrogen loading rate (NLR) gradually increased from 0.0075 kg NH_4^+-N/m^3.day to 0.075 kg NH_4^+-N /m^3.day between day 1-42 and remained unchanged throughout the experiment. In phase 1, aerobic granules easily consumed sodium acetate and achieved 99.9±0.05% (influent COD: 1200 mg/L) COD removal efficiency.

According to literature, aerobic granulation was achievable across a wide range from 15 kg COD/m^3.day to 2.5 kg COD/m^3.day without affecting granule integrity which proved that

COD removal by aerobic granules was independent of OLRs (Moy et al., 2002). Initially in phase 2, the change in carbon source (from acetate to recalcitrant diesel) probably reduced the carbon metabolism of granules (Milia et al., 2016). Hence, COD removal efficiency slightly dropped from 99.9±0.05% to 96±0.06% between day 57-66. After diesel acclimatization, aerobic granules achieved a stable COD removal efficiency of 99±0.05% in presence of 320 mg/L diesel as sole carbon source. Irrespective of reduced VSS content (Fig. 2c), COD removal remained unaffected in phase 2 which is agreeing with the result observed by Chen et al. (2019) in aerobic granular treatment of petroleum wastewater. In phase 3, COD removal efficiencies remained unchanged at 99.9±0.05%. It proved that COD removal was independent of inoculum and carbon source.

Influent NH_4^+-N increased between 10 to 50 mg/L from day 1-42. At the end of phase 1, R1, R2 and R3 achieved approximately 98.34±0.02% NH_4^+-N removal efficiency with 1.22 mg/L, 0.55 mg/ L and 0.73 mg/L effluent NH_4^+-N concentrations.

In phase 2, NH_4^+-N removal efficiencies slightly dropped from 97% to 91% in the AGRs. Previous literature reported very poor nitrogen removal performances of aerobic granules in petroleum wastewater treatment (Zhang et al., 2011; Corsino et al., 2015; Chen et al., 2019). But comparatively stable and higher NH_4^+-N removal efficiencies (91.67±0.14%) were observed in our AGRs. Granule disintegration increased biomass washout providing 0.35-0.4 g/L of effluent VSS. Sludge retention time (SRT) determines the average time activated sludge solid retains in a reactor which is calculated by equation 2.7.

$$\text{SRT (day)} = \frac{V_t \times X \times t_c}{V_W \times X_W \times 24} \quad (2.7)$$

Where V_t is the reactor working volume (L), t_c is the cycle duration (h), X is the VSS in the reactor (g/L), X_W is the VSS in effluent (g/L) and V_W is the effluent volume (L).

Low F/M ratio is correlated with high SRT values in AGRs (Hamza et al., 2018). SRTs in R1, R2 and R3 were 8, 10 and 8.5 days, respectively. R2 granules were more oil competent than R1 and R3 achieving maximum 92.54±0.01% NH_4^+-N removal and it had the maximum 10 days SRT for having the lowest F/M ratio (0.21 g COD/g SS.day) among the AGRs. R1 and R3 had maximum 91% of NH_4^+-N removals in presence 320 mg/L of emulsified diesel. The initial granule breakage might have induced partial disruption of aerobic layer containing ammonia oxidizing bacteria (AOB) (Tay et al., 2002). At the end of phase 2, the final effluent NH_4^+-N concentrations in R1, R2 and R3 were 4.5, 3.73 and 4.25 mg/L, respectively. Nitrogen utilized in biomass growth was calculated according to equation 2.8.

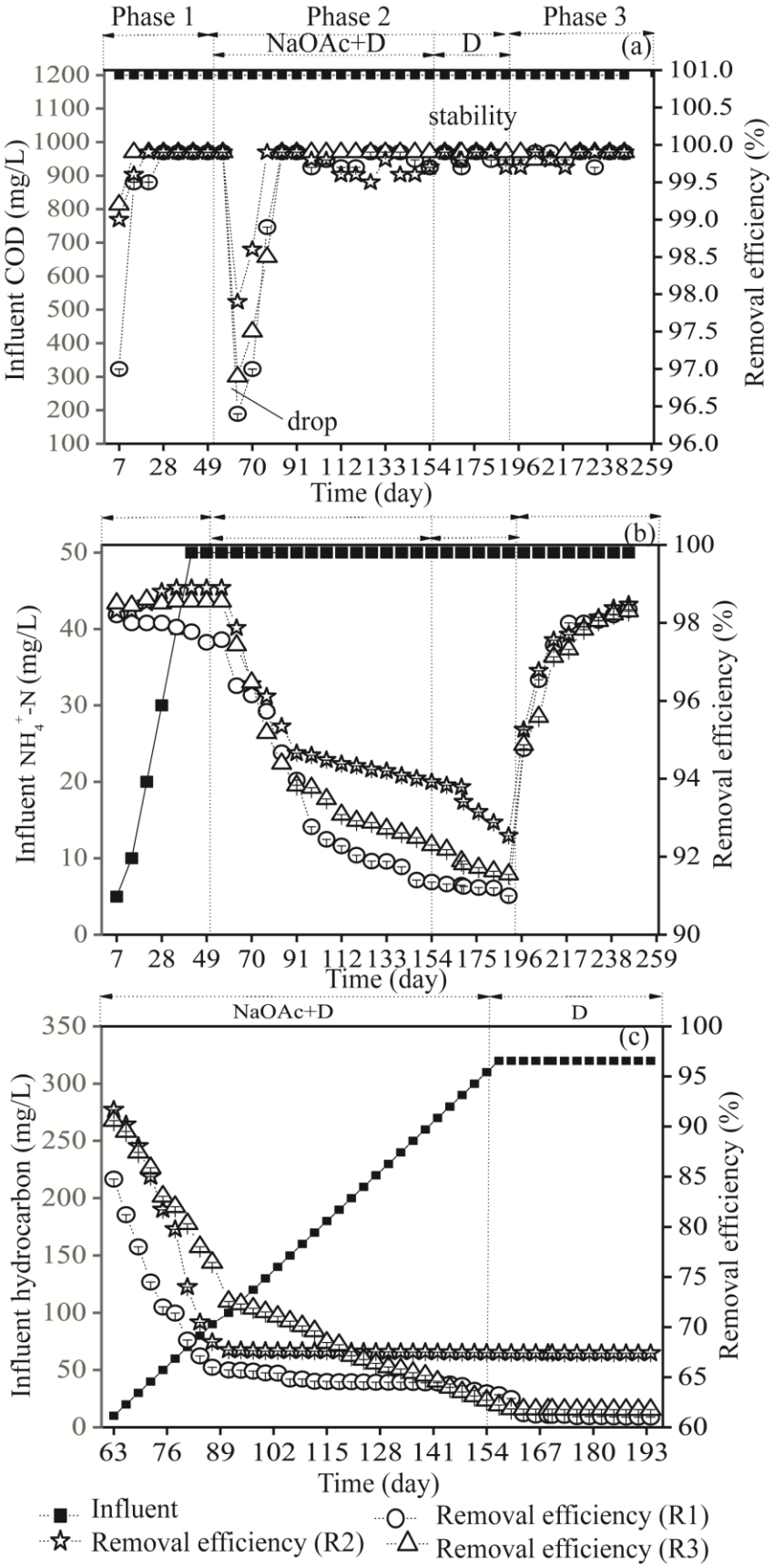

Fig.2.8 (a) COD, (b) NH_4^+-N, (c) hydrocarbon removal profiles in the AGRs. [NaOAc represents sodium acetate and D represents diesel].

Nitrogen utilized for biomass growth (mg/L) = 0.12 $P_{X,\,bio}/Q$ (2.8)

Where, $P_{X,bio}$ = biomass wasted per day (mg VSS/day) calculated by equation 2.9 (Metcalf and Eddy, 2003) and Q = Flow rates inside R1, R2 and R3 which was 4.5 L/day.

$$P_{X,bio} = \frac{X}{SRT} \times V_t \quad (2.9)$$

The details of F/M ratio, SRT, biomass wasted per day and nitrogen consumed in biomass growth in the AGRs on day 190 of phase 2 in presence of 320 mg/L of emulsified diesel are summarized in Table 2.3.

Table 2.3 F/M ratio, SRT, biomass wasted per day and nitrogen consumed in biomass growth accounts in the AGRs in phase 2

Parameters	**R1**	**R2**	**R3**
F/M ratio (g COD/g SS.day)	0.29	0.23	0.21
SRT (day)	8	10	8.5
$P_{X,bio}$ (mg VSS/day)	1563.75	1752	1650
Nitrogen utilized for biomass growth (mg/L)	41.7	46	44

As, 10-30 days SRT is considered as favourable for growth of nitrite-oxidizing bacteria (NOB) (Wan et al., 2013), NO_2^--N production was almost null and approximately 0.6-12 mg/L of NO_3^--N was produced in the AGRs. This result ensured that maximum 80-90% NH_4^+-N was consumed in biomass growth. While treating petroleum wastewaters containing 5.6-200 mg/L of hydrocarbons, Zhang et al. (2011), Corsino et al. (2015) and Chen et al. (2019) achieved only 30-60% NH_4^+-N removals due to granule disintegration and nitrogen removal efficiency which was recovered only after adding co-substrates (glucose or acetates). Whereas, in current study, 92% stable NH_4^+-N removal in refinery sludge granules in 320 mg/L emulsified diesel substrate indicated use of refinery inoculum appropriate for granulation in oily wastewater. In phase 3, after granule restoration again 98±0.01% NH_4^+-N removal was obtained in the AGRs.

2.3.4.2 Performance in hydrocarbon removal

Hydrocarbon loading rate increased from 0.015 kg/m^3.day to 0.48 kg/m^3.day in 134 days. Increasing diesel and decreasing acetate concentration reduced the oil removal efficiencies of the AGRs. Hydrocarbon removal patterns are described in Fig.2.8c. Between day 57-190, the increase in F/M ratio (0.17 g COD/g SS.day to 0.24 g COD/g SS.day) in the AGRs was associated with presence of surplus substrate in effluent when the amount of the organic pollutant exceeded the consumption capacity of the available granule bacteria in the system (Hamza et al., 2018). Between day 63-72, in presence of 10-40 mg/L diesel, oil removal efficiencies varied between 90±0.5% (R2, R3) to 85±0.5% (R1). On day 91, maximum

72.54±0.14% (for 100 mg/L diesel) oil removal was achieved by R3 due to more granule stability than R1 and R2, respectively. But when 320 mg/L oil was used (between day 157-190) as sole carbon source, refinery granules in R2 became more stable than sewage and brewery granules in R1 and R3 due to previous oil exposure.

Hence, at the end of phase 2 (on day 190), R2 achieved maximum 67.39±0.15% oil removal (influent: 320 mg/L) whereas, R1 and R3 achieved 61.02±0.08% and 61.76±0.26% removals, respectively. Similarly, between 10 to 100 mg/L oil exposure, maximum oil removal rate (3.41±0.13 to 28.26±0.07 mg oil/g VSS.day) was observed in R3. But in presence of 320 mg/L diesel, oil tolerant refinery granules (R2) achieved stable and maximum removal rate of 140.43±0.23 mg oil/g VSS.day followed by removal rates of 110.88±0.37 mg oil/g VSS.day and 107.60±0.51 mg oil/g VSS.day in R3 and R1, respectively. In higher oil concentrations (between 100 to 320 mg/L), oil toxicity ruptured the granules putting down VSS concentration (Fig.2.5c) and oil removal capacity as supported by previous literature (Lohi et al., 2008).

Combined physicochemical and bioreactor processes were able to treat petroleum wastewater above 35 g/L (oil concentration) range (Lohi et al., 2008; Liu and Liu, 2011). But in aerobic granulation, oil removal has been conducted within a range of 5.6–200 mg/L so far where either biodegradation or adsorption was responsible for oil removal. In our AGRs, diesel concentration was much higher than the previous aerobic granular studies and no oil adsorption was visible in microscopic granule images indicating biodegradation of diesel. GC-MS spectra for oily feed and AGR treated effluent are given in Fig.2.9. In untreated oily wastewater presence of oxytridecane, cyclooctasiloxane, nonadecane, hexasiloxane and heptasiloxane peaks were observed. The disappearance of oxytridecane, cyclooctasiloxane, nonadecane *n*-alkane groups from AGR treated effluent indicated degradation of oil molecules by aerobic granules. Influent and effluent pollutant concentrations in R1, R2, and R3 are elaborated in Table 2.4. Statistical analysis of granule characteristics and reactor performance data of the AGRs in phase 2 (Oil degradation phase) has been provided along with standard deviation and F-value in Table 2.5.

Threshold oil concentrations were observed as 170±15, 310±10 and 250±10 mg/L in sewage, refinery and brewery granules, respectively. Granule size, stability and settleability deteriorated beyond the above-mentioned limits. Current study highlighted that stability of granules in AGR depended on threshold oil concentration, which was different for different inoculum. In treatment plants, influent oil concentration sometimes may be higher than the threshold limit due to operational changes in the refinery.

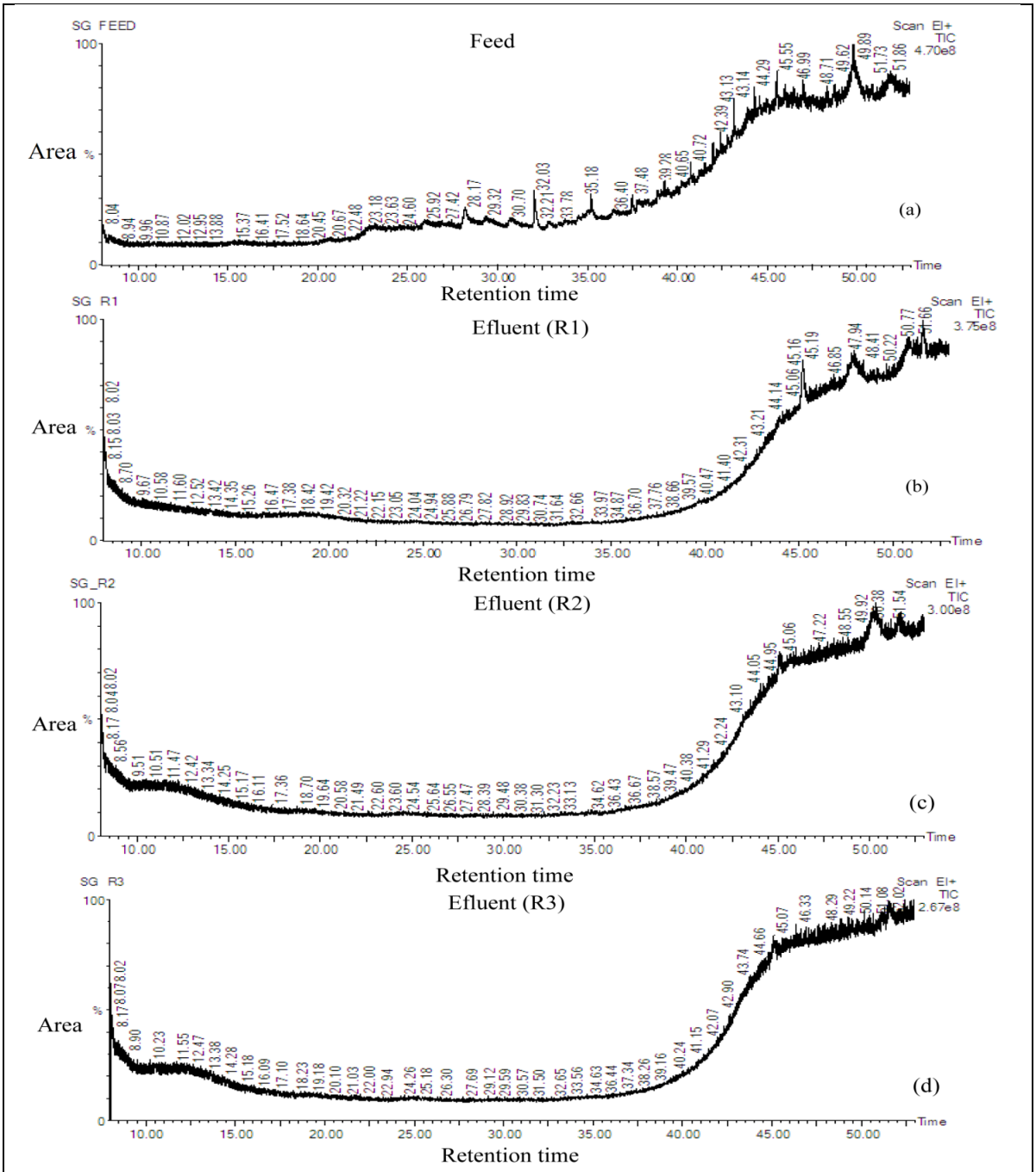

FEED		Effluent (R1, R2, R3)	
Retention time (min)	**Compound name**	**Retention time (min)**	**Compound name**
28.17	Oxytridecane	-	-
32.03	Cyclo-octasiloxane	-	-
35.18	Nonadecane	-	-
45.55	Heptasiloxane	45.55	Heptasiloxane
49.89	hexasiloxane	49.89	hexasiloxane

Fig.2.9 GC-MS spectra for (a) untreated oily feed and treated effluents of (b, c, d) R1, R2, R3.

Table 2.4 Changes in Influent and effluent pollutant concentrations with time in R1, R2 and R3

	Phase	R1						R2						R3					
		COD		NH_4^+-N		Hydrocarbon		COD		NH_4^+-N		Hydrocarbon		COD		NH_4^+-N		Hydrocarbon	
	Time (day)	I [a]	E [b]	I	E	I	E	I	E	I	E	I	E	I	E	I	E	I	E
Phase1	1 – 7			5	0.09					5	0.08					5	0.08		
	8-21			10-20	0.2					10-20	0.28					10-20	0.28		
	22-28	1200	1.2	20-30	0.6	0	0	1200	1.2	20-30	0.58	0	0	1200	1.2	20-30	0.45	0	0
	29-42			30-50	1.221					30-50	0.73					30-50	0.73		
	43-56			50	.22					50	0.73					50	0.73		
Phase2	57-91					10-100	34					10-100	32					10-100	72
	92-156	1200	1.2	50	4.50	110-310	113	1200	1.2	50	3.73	110-310	101	1200	1.2	50	0.59	110-310	63
	157-190					320	125					320	104					320	62
Phase 3	191-246	1200	1.2	50	0.83	0	1.2	1200	1.2	50	0.77	0	0	1200	1.2	50	0.85	0	0

[a] Influent (mg/L)
[b] Effluent (mg/L)

Table 2.5 Statistical analysis of granule characteristics and reactor performance data of the AGRs in phase 2 (Oil degradation phase)

Reactor	**R1**		**R2**		**R3**		**Overall ANOVA**				
Operation time (day)	**57-190**		**57-190**		**57-190**						
	Mean	**SD**	**Mean**	**SD**	**Mean**	**SD**	**R-square**	**Coeff Var**	**Root MSE**	**Mean square**	**F-value**
Granule size (mm)	3.61	0.47	3.80	0.33	3.67	0.93	0.01	0.17	0.63	0.11	0.28
VSS (g/L)	4.74	0.49	6.50	0.38	7.07	0.80	0.74	0.09	0.58	29.53	85.08
SVI_{30} (mL/g)	42.17	2.36	37.28	2.11	34.06	7.19	0.36	0.12	4.54	333.80	16.18
GSV (m/h)	21.17	2.05	27.71	2.77	27.71	12.93	0.14	0.30	7.72	278.49	4.66
EPS (mg/g VSS)	196.71	33.31	254.17	49.89	306.08	88.23	0.35	0.24	61.60	59855.28	15.77
PN (mg/g VSS)	158.33	31.63	208.96	53.84	258.25	84.16	0.32	0.29	60.51	49928.91	13.63
Hydrophobicity (%)	72.22	11.21	74.64	10.776	67.33	18.73	0.04	0.19	14.05	277.75	1.40
COD removal efficiency (%)	99.45	0.97	99.56	0.87	99.61	0.49	0.01	0.01	0.81	0.12	0.19
TPH removal efficiency (%)	65.46	5.24	70.20	6.57	69.01	8.42	0.08	0.10	6.87	273.55	5.79
NH_4^+-N removal efficiency (%)	92.59	1.77	94.41	1.24	93.21	1.60	0.19	0.01	1.55	17.04	1.01

The present study shows that with influent oil concentrations higher than the threshold limit, if granules are ruptured, it could be possible to restore the granules using simple carbon source like acetate. However, in order to be safe, it is recommended to operate AGR with influent oil lower than the threshold limit of specific inoculum.

The study further reflected that high F/M ratio (2.96 g COD/g SS.day) during reactor start-up enhanced granulation. But F/M ratio range was reduced (0.14-0.20 g COD/g SS.day) till day 56 after granule maturation which is supporting the study of Li et al. (2011). In diesel exposure, increase in F/M ratio (0.17 g COD/g SS.day to 0.24 g COD/g SS.day) increased granule rupture but after the AGRs achieved stability, the F/M was observed to be stable between 0.22-028 g COD/g SS.day.

2.3.5 Biomass activity

Biomass activity determines the amount of active biomass present in a reactor (Jawed and Tare, 1999). Approximately 2-5% COD (carbon source: sodium acetate, influent COD: 1200 mg/L) removal was achieved by initial non-granular sludge in more than 20 h of time. Matured granules collected from phase 1 achieved 16.14±0.33 mg COD/mg VSS.day, 17.8±0.35 mg COD/mg VSS.day, 17.12±0.42 mg COD/mg VSS.day of biomass activities in R1, R2 and R3, respectively. Individual and comparative AGR activity profiles (6 h) are described in Fig.2.10.

Consumption of simple sodium acetate, AGR operating conditions, high granule stability and high VSS content were responsible to enhance biomass activity in the AGRs. In phase 2, all three AGRs were able to remove 99.9±0.01% COD in 8 h. But granule instability in presence of diesel reduced biomass activity. On day 91, in presence of 240 mg/L acetate and 100 mg/L diesel in AGRs, maximum 5.13±0.70 mg COD/mg VSS.day biomass activity was found in R2 which further deteriorated to 3.65±0.23 mg COD/mg VSS.day in R1, 4.96±0.54 mg COD/mg VSS.day in R2 and 3.59±0.17 mg COD/mg VSS.day in R3 on day 190 in presence of 320 mg/L diesel. Throughout phase 2, R2 showed maximum biomass activity indicating more oil tolerance of refinery inoculum than sewage (R1) and brewery inoculum (R3), respectively. In phase 3, sodium acetate restored granule biomass activity.

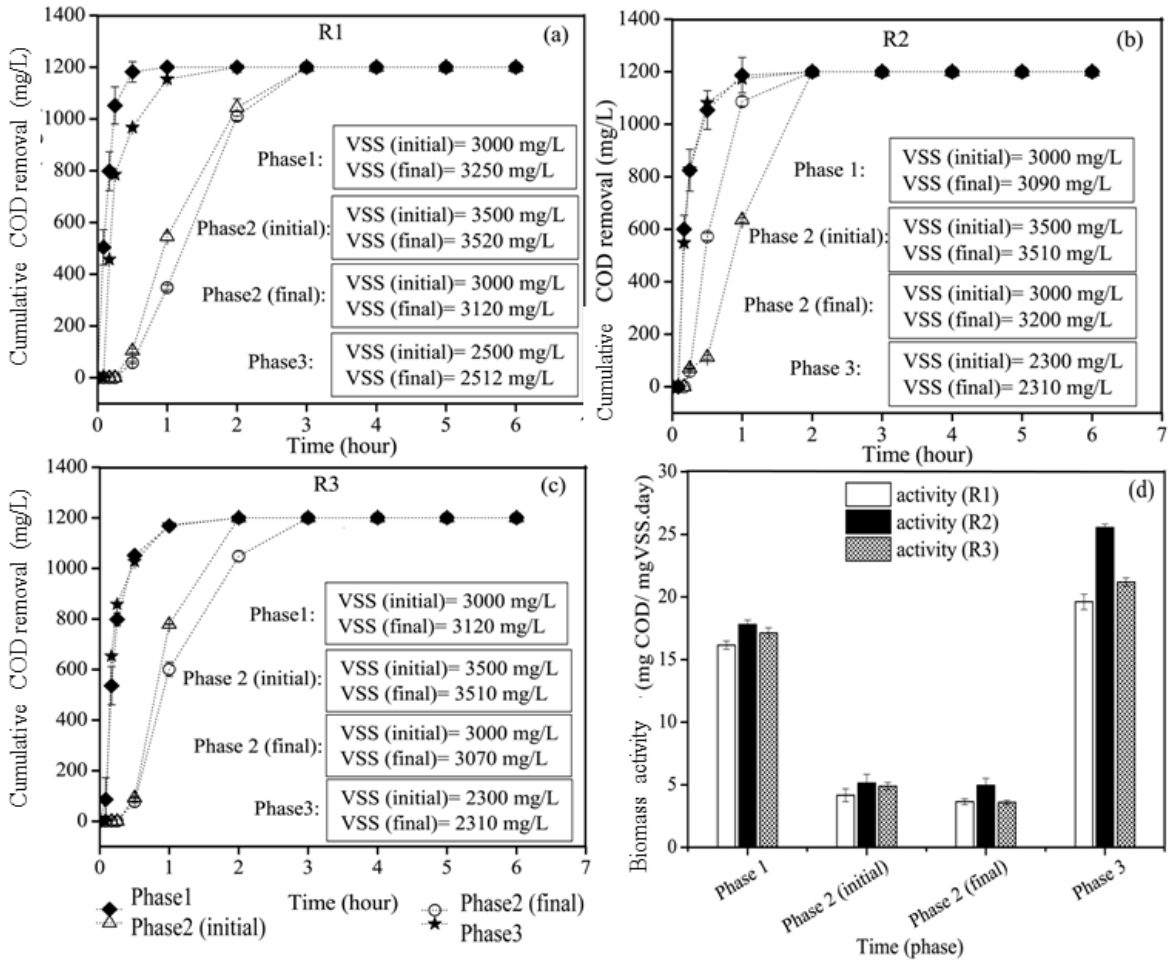

Fig.2.10 (a, b, c) Individual and (d) comparative biomass activity profiles of R1, R2 and R3 in 6 h cycle time. [Phase 2 (initial) stands for day 91 and phase 2 (final) stands for day 190 of study].

2.3.6 Microbial identification

Strain isolated from R1 was rod shaped, Gram positive and showed 99% identity match with *Brevibacterium paucivorans*. Strains isolated from R2 and R3 were spherical and Gram positive showing 99% homology with *Micrococcus aloeverae* and *Staphylococcus hominis*, respectively. They were submitted to NCBI and named as *Brevibacterium paucivorans* strain SG001 (accession no: MK574866), *Micrococcus aloeverae* strain SG002 (accession no: MK574867) and *Staphylococcus hominis* strain SG003 (accession no: MK574868), respectively. Image of isolated DNA bands are shown in Fig.2.11. Pure colonies, FESEM images and phylogenetic trees of the isolated strains are given in Fig.2.12.

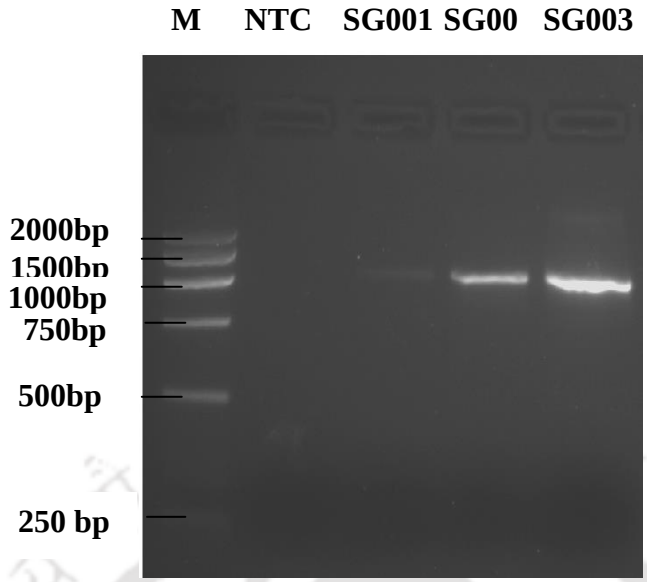

Fig.2.11 16S PCR image: 1% (W/V) Agarose Gel electrophoresis: Lane M: 1 kb DNA marker; Lane NTC: Negative test control; well SG001, SG002, SG003: sample PCR Product.

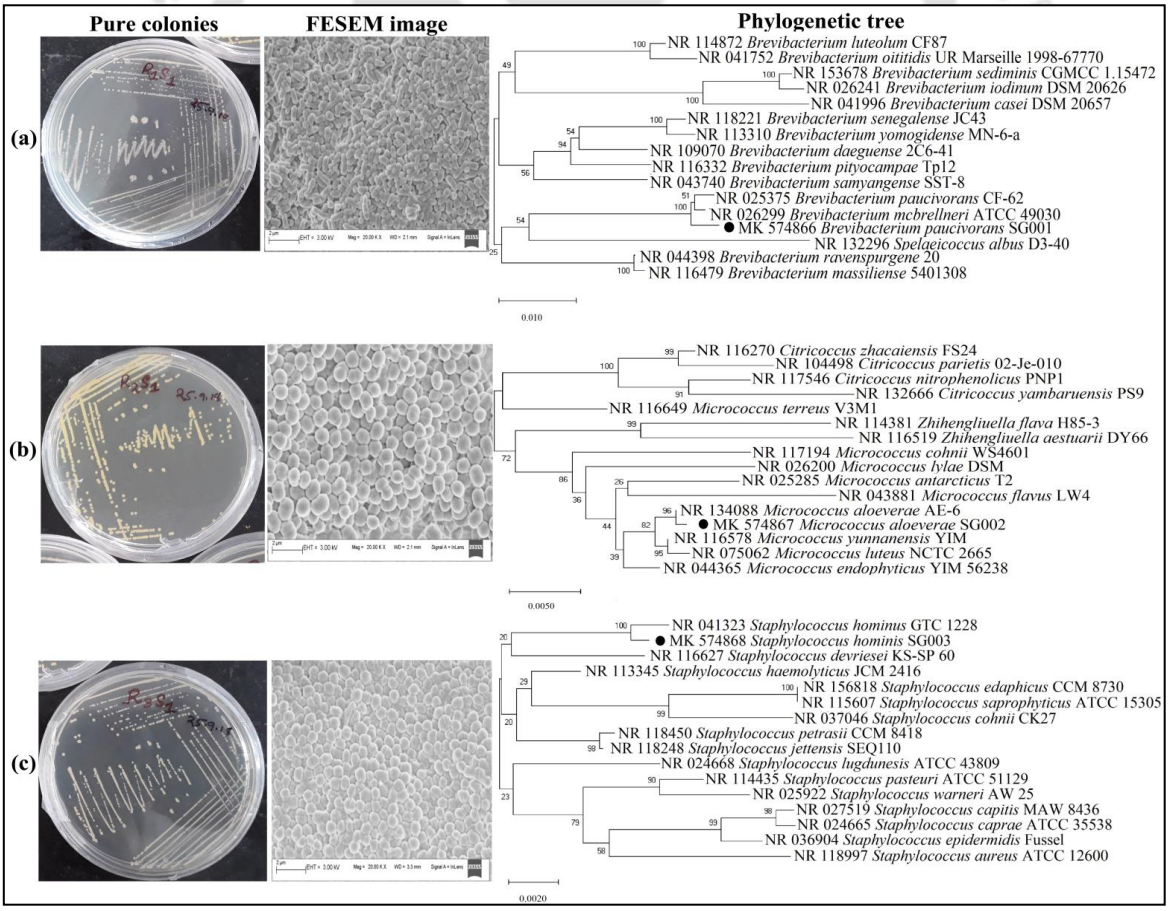

Fig.2.12 Isolated bacterial colonies, FESEM images and phylogenetic trees of (a) *Brevibacterium paucivorans* strain SG001, (b) *Micrococcus aloeverae* strain SG002 and (c) *Staphylococcus hominis* strain SG003.

2.3.7 Pollutant removal by pure strains

Pollutant removal profiles of isolated strains are shown in Fig.2.13. *Micrococcus aloeverae* strain SG002 achieved highest COD removal between 800 to 1200 mg/L influent COD concentrations among the three strains. NH_4^+-N (50 mg/L) was almost completely utilized by all three heterotrophic strains. In 48 h of study, *Micrococcus aloeverae* strain SG002 degraded 88.07±0.68% oil in 50 mg/L and 61.34±0.85% oil in 320 mg/L influent diesel concentrations, respectively. *Brevibacterium paucivorans* strain SG001 and *Staphylococcus hominis* strain SG003 achieved 33.28±0.84% and 38.18±0.90% oil removal efficiencies in 320 mg/L diesel concentration.

This study again proved that refinery origin of *Micrococcus aloeverae* strain SG002 helped them to achieve maximum pollutant removal in diesel environment. This result correlates with the maximum oil removal efficiency of R2 containing refinery granules. All three strains have literature evidences of environmental bioremediation. Ferhat et al. (2011) isolated biosurfactant producing *Brevibacterium sp.* 7G from crude-oil contaminated soil and Esmaeil et al. (2009) isolated *Micrococcus sp*. and *Staphylococcus hominis* from Kuwait coast having 8.57–5.26 and 13–9.7 μg/min of crude oil mineralization rates, respectively. *Micrococcus luteus* strain has been used in both municipal and industrial wastewater treatments (Leung et al., 2000). But, their capabilities of aerobic granule formation and oil removal in petroleum wastewater treatment are being demonstrated for the first time.

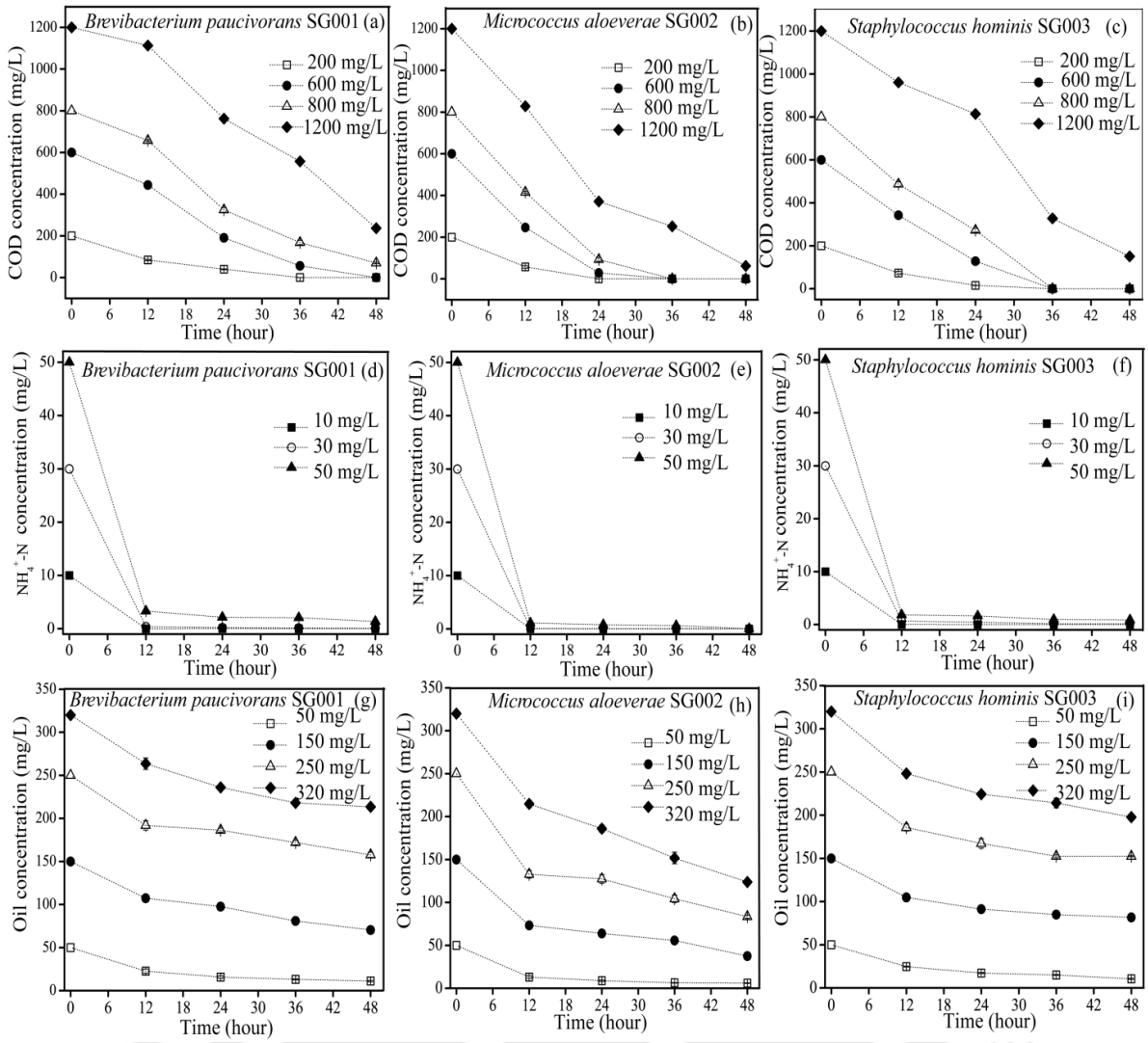

Fig.2.13 (a, b, c) COD, (d, e, f) NH_4^+-N and (g, h, i) oil removal profiles of the isolated strains in 48 h.

2.4 Summary of the chapter

This chapter demonstrated the influences of different inocula in aerobic granulation during oily wastewater treatment. In phase 1, with sodium acetate as feed, brewery inoculum promoted maximum granule size and EPS content. But in phase 2, at 320 mg/L of emulsified diesel concentration, recalcitrance of diesel caused partial rupture in sewage and brewery granules. However, previous oil exposure helped the refinery sludge granules to maintain 23.21±0.58 m/h of GSV and 39.80±0.57 mL/g SVI values. Refinery granules achieved maximum 310±10 mg/L oil tolerance threshold and 67% oil removal efficiency among the AGRs. *Brevibacterium paucivorans* strain SG001, *Micrococcus aloeverae* strain SG002 and *Staphylococcus hominis* strain SG003 were the major oil degrader isolated from sewage, refinery and brewery sludge, respectively. *Micrococcus aloeverae* strain SG002 had maximum oil removal capacity. In order to maintain AGR stability, influent oil loading is

suggested within the threshold limit of 0.26-0.47 kg/m^3.day of a specific inoculum. Ruptured granules due to oil shock loading can be reconstructed by using simple carbon source.

References

Abdullah, N., Yuzir, A., Curtis, T.P., Yahya, A., Ujang, Z. 2013. Characterization of aerobic granular sludge treating high strength agro-based wastewater at different volumetric loadings. Bioresource Technology 127, 181-187.

APHA, 2005. Standard Methods for the Examination of Water and Wastewater, twenty-first ed. American Public Health Association, Washington, DC, USA.

Beun, J., Hendriks, A., Van Loosdrecht, M., Morgenroth, E., Wilderer, P., Heijnen, J., 1999. Aerobic granulation in a sequencing batch reactor. Water Research 33, 2283-2290.

Beun, J., Van Loosdrecht, M., Heijnen, J., 2002. Aerobic granulation in a sequencing batch airlift reactor. Water Research 36, 702-712.

Caluwé, M., Dobbeleers, T., D'aes, J., Miele, S., Akkermans, V., Daens, D., Geuens, L., Kiekens, F., Blust, R., Dries, J., 2017. Formation of aerobic granular sludge during the treatment of petrochemical wastewater. Bioresource Technology 238, 559-567.

Chen, C., Ming, J., Yoza, B.A., Liang, J., Li, Q.X., Guo, H., Liu, Z., Deng, J., Wang, Q., 2019. Characterization of aerobic granular sludge used for the treatment of petroleum wastewater. Bioresource Technology 271, 353-359.

Corsino, S.F., Campo, R., Di Bella, G., Torregrossa, M., Viviani, G., 2015. Cultivation of granular sludge with hypersaline oily wastewater. International Biodeterioration & Biodegradation 105, 192-202.

Corsino, S.F., Capodici, M., Torregrossa, M., Viviani, G. 2016. Fate of aerobic granular sludge in the long-term: the role of EPSs on the clogging of granular sludge porosity. Journal of Environmental Management 183, 541-550.

Corsino, S.F., Di Trapani, D., Torregrossa, M., Viviani, G. 2018. Aerobic granular sludge treating high strength citrus wastewater: Analysis of pH and organic loading rate effect on kinetics, performance and stability. Journal of Environmental Management 214, 23-35.

Dangcong, P., Bernet, N., Delgenes, J.-P., Moletta, R., 1999. Aerobic granular sludge—a case report. Water Research 33, 890-893.

Deng, S., Wang, L., Su, H. 2016. Role and influence of extracellular polymeric substances on the preparation of aerobic granular sludge. Journal of Environmental Management 173, 49-54.

Dubois, M., Gilles, K.A., Hamilton, J.K., Rebers, P.t., Smith, F., 1956. Colorimetric method for determination of sugars and related substances. Analytical Chemistry 28, 350-356.

Esmaeil, A.-S., Drobiova, H., Obuekwe, C., 2009. Predominant culturable crude oil-degrading bacteria in the coast of Kuwait. International Biodeterioration & Biodegradation 63, 400-406.

Ferhat, S., Mnif, S., Badis, A., Eddouaouda, K., Alouaoui, R., Boucherit, A., Mhiri, N., Moulai-Mostefa, N., Sayadi, S., 2011. Screening and preliminary characterization of biosurfactants produced by Ochrobactrum sp. 1C and Brevibacterium sp. 7G isolated from hydrocarbon-contaminated soils. International Biodeterioration & Biodegradation 65, 1182-1188.

Hamza, R.A., Sheng, Z., Iorhemen, O.T., Zaghloul, M.S. and Tay, J.H., 2018. Impact of food-to-microorganisms ratio on the stability of aerobic granular sludge treating high-strength organic wastewater. Water research 147, 287-298.

Jawed, M., Tare, V., 1999. Microbial composition assessment of anaerobic biomass through methanogenic activity tests. Water SA 25, 345-350.

Leung, W.C., Wong, M.-F., Chua, H., Lo, W., Yu, P., Leung, C., 2000. Removal and recovery of heavy metals by bacteria isolated from activated sludge treating industrial effluents and municipal wastewater. Water Science and Technology 41, 233-240.

Li, A.J., Li, X.Y. and Yu, H.Q., 2011. Effect of the food-to-microorganism (F/M) ratio on the formation and size of aerobic sludge granules. Process Biochemistry 46, 2269-2276.

Li, X.Y., Yang, S., 2007. Influence of loosely bound extracellular polymeric substances (EPS) on the flocculation, sedimentation and dewaterability of activated sludge. Water Research 41, 1022-1030.

Liu, C.-W., Liu, H.-S., 2011. Rhodococcus erythropolis strain NTU-1 efficiently degrades and traps diesel and crude oil in batch and fed-batch bioreactors. Process Biochemistry 46, 202-209.

Liu, Y., Tay, J.-H., 2002. The essential role of hydrodynamic shear force in the formation of biofilm and granular sludge. Water Research 36, 1653-1665.

Liu, Y., Tay, J.-H., 2004. State of the art of biogranulation technology for wastewater treatment. Biotechnology Advances 22, 533-563.

Lohi, A., Cuenca, M.A., Anania, G., Upreti, S., Wan, L., 2008. Biodegradation of diesel fuel-contaminated wastewater using a three-phase fluidized bed reactor. Journal of Hazardous Materials 154, 105-111.

Lowry, O.H., Rosebrough, N.J., Farr, A.L., Randall, R.J., 1951. Protein measurement with the Folin phenol reagent. Journal of Biological Chemistry 193, 265-275.

Mallick, S.K., Chakraborty, S., 2017. Treatment of synthetic refinery wastewater in anoxic–aerobic sequential moving bed reactors and sulphur recovery. Jornal of Environmental Science and Health, Part A 52, 1257-1268.

Metcalf, E., Eddy, H.I. 2003. Wastewater engineering; treatment and reuse. McGraw-Hill, Boston.

Milia, S., Malloci, E., Carucci, A., 2016. Aerobic granulation with petrochemical wastewater in a sequencing batch reactor under different operating conditions. Desalination and Water Treatment 57, 27978-27987.

Moy, B.P., Tay, J.H., Toh, S.K., Liu, Y., Tay, S.L., 2002. High organic loading influences the physical characteristics of aerobic sludge granules. Letters in Applied Microbiology 34, 407-412.

Qin, L., Tay, J.-H., Liu, Y., 2004. Selection pressure is a driving force of aerobic granulation in sequencing batch reactors. Process Biochemistry 39, 579-584.

Rosenberg, M., Gutnick, D., Rosenberg, E., 1980. Adherence of bacteria to hydrocarbons: a simple method for measuring cell surface hydrophobicity. FEMS Microbiology Letters 9, 29-33.

Tay, J.H., Ivanov, V., Pan, S., Tay, S.L., 2002. Specific layers in aerobically grown microbial granules. Letters in Applied Microbiology 34, 254-257.

Tijani, H., Abdullah, N., Yuzir, A., Ujang, Z., 2015. Rheological and fractal hydrodynamics of aerobic granules. Bioresource Technology 186, 276-285.

Tomar, S.K., Chakraborty, S., 2018. Characteristics of aerobic granules treating phenol and ammonium at different cycle time and up flow liquid velocity. International Biodeterioration & Biodegradation 127, 113-123.

Val del Rio, A., Figueroa, M., Mosquera-Corral, A., Campos, J.L., Méndez, R., 2013. Stability of aerobic granular biomass treating the effluent from a seafood industry. International Journal of Environmental Research 7, 265-276.

Wan, C., Sun, S., Lee, D.-J., Liu, X., Wang, L., Yang, X., Pan, X. 2013. Partial nitrification using aerobic granules in continuous-flow reactor: rapid startup. Bioresource Technology 142, 517-522.

Wang, S.-G., Liu, X.-W., Gong, W.-X., Gao, B.-Y., Zhang, D.-H., Yu, H.-Q., 2007. Aerobic granulation with brewery wastewater in a sequencing batch reactor. Bioresource Technology 98, 2142-2147.

Yu, G.-H., Juang, Y.-C., Lee, D.-J., He, P.-J., Shao, L.-M., 2009. Enhanced aerobic granulation with extracellular polymeric substances (EPS)-free pellets. Bioresource Technology 100, 4611-4615.

Zhang, H., He, Y., Jiang, T., Yang, F., 2011. Research on characteristics of aerobic granules treating petrochemical wastewater by acclimation and co-metabolism methods. Desalination 279, 69-74.

Chapter 3

Effects of HRTs with oil degradation pathway and phytotoxicity study

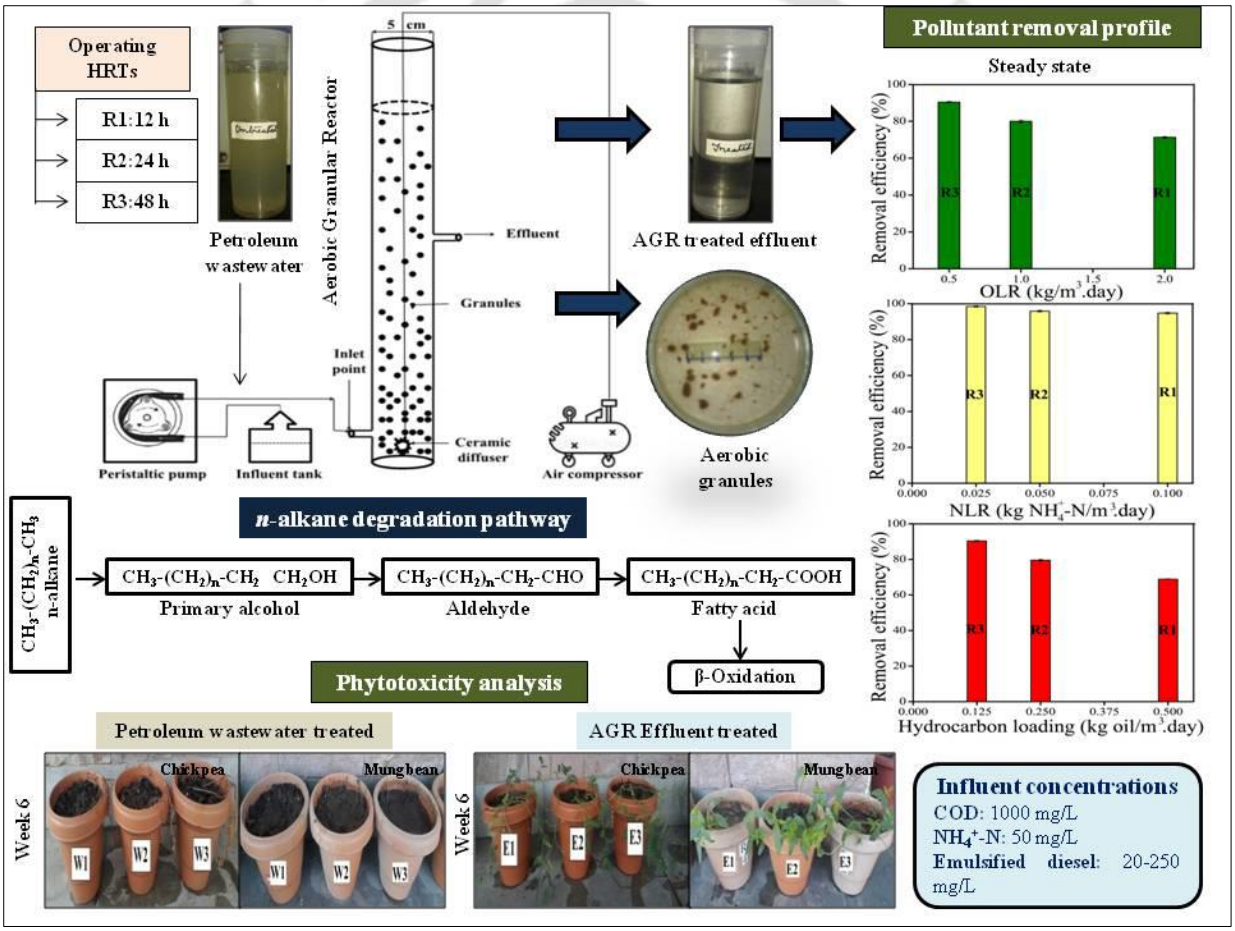

CHAPTER 3

Effects of HRTs with oil degradation pathway and phytotoxicity study

The chapter is about impacts of HRTs on granule characteristics, reactor activity and predicting hydrocarbon removal pathway with phytotoxicity analysis while treating oily wastewater in AGRs.

3.1 Introduction

Hydraulic retention time (HRT) plays an important role in reactor performance. It influences the average contact time between a soluble substrate and aerobic granules which further controls the treatment efficiency of the AGR. Pan et al. (2004) optimized 2 to 12 h HRT for stable granulation and Rosman et al. (2014) observed that low HRT enhanced COD and nitrogen removal in rubber wastewater treatment. Tomar and Chakraborty (2018a) reported that granule size and EPS content were inversely proportional to HRT whereas pollutant removal was independent of the HRT while treating phenol and ammonia in AGRs. Role of HRT on aerobic granules and pollutant removal efficiencies are mostly reported on simple wastewater containing acetate (Moy et al., 2002; Ghangrekar et al., 2005) rather than having hydrocarbon and nitrogen.

Literature are limited on hydrocarbon degradation pathway by aerobic granular sludge, nitrogen removal in presence of hydrocarbons and on nitrogen balance. AGR mediated petroleum wastewater treatment indicated either oil bio-adsorption in granules or oil and co-substrate co-metabolism mechanism for oil removal (Corsino et al., 2015; Zhang et al., 2011a). Corsino et al. (2015), Milia et al. (2016) and Chen et al. (2019) faced deterioration in nitrogen removal and absence of nitrification in AGRs due to lack of autotrophic biomass while treating coal gasification and petroleum wastewater.

Moreover, in agricultural irrigation of oily wastewater, hydrocarbon toxicity can affect crop production contaminating the entire food chain (Yu et al., 2017). Hence, phyto-toxicity study is essential to determine the environmental viability of the AGR treated effluent.

This chapter focuses on the effects of changing HRTs on granule characteristics, reactor activity, COD removal efficiencies with probable hydrocarbon degradation mechanism and pathway and detailed nitrogen balancing during synthetic oily wastewater treatment in AGRs. The study further determined suitable range of HRT and influent loadings for AGR operation

to achieve complete hydrocarbon removal. Phytotoxic effect of AGR treated oily wastewater was also checked on two largely cultivated legume plants *Cicer arietinum* and *Vigna radiata*.

3.2 Materials and methods

3.2.1 Chemicals and reagents

For confocal microscopy, four dyes SYTO 63, fluorescein isothiocyanate (FITC), concanavalin A (Con A) and SYTOX blue were used which were purchased from HiMedia, India. Chemicals for phytotoxicity analysis like potassium sodium tartrate tetrahydrate, magnesium carbonate, guaicol, H_2O_2 were of analytical grade from Himedia, India. Other chemicals and reagents required for effluent analysis and FESEM imaging are given in Chapter 2 (section 2.2.1).

3.2.2 Seed granules

Seed granules were hydrocarbon degrading granules (sewage:refinery:brewery sludge granules in 1:1:1 w/w ratio) having 5.23±0.07 mm average size and 6.68±0.01 g/L VSS maintained in sodium acetate which were previously developed in our laboratory as discussed in Chapter 2.

3.2.3 Feed composition

Literature reported AGR treatment of real hydrocarbon rich wastewater having hydrocarbon concentration between 6.8 to 151 mg/L (Zhang et al., 2011a; Zhang et al., 2011b; Corsino et al., 2015; Campo and Di Bella, 2019) whereas the total petroleum hydrocarbon content in real petroleum refinery wastewater varies within a broad range of 40–250 mg/L (Coelho et al., 2006; Ma et al., 2009; Khaing et al., 2010). Hence to check the AGR performance at high oil concentration we used synthetic wastewater. In start-up phase (day 1-42), a combination of emulsified (emulsifier: nonylphenol ethoxylate; diesel:emulsifier: 200:1 v/v ratio) diesel and sodium acetate provided carbon source to maintain 1000 mg/L influent COD in the AGRs. Diesel concentration increased from 20 to 250 mg/L in 70 days and acetate concentration correspondingly decreased. After reaching 170 mg/L of acetate and 230 mg/L of diesel concentration, sodium acetate supply was stopped and emulsified diesel was used as sole carbon source. AGRs were operated with 250 mg/L of maximum diesel concentration providing 1000 mg/L influent COD for last 28 days to achieve steady state. NH_4Cl (190 mg/L) was used as nitrogen source and phosphate buffer worked as phosphate source which maintained feed pH at 7±0.2. Trace metal solution was applied in 1 mL/L concentration. Buffer and trace metal compositions were maintained according to Chapter 2 (section 2.2.4).

3.2.4 Reactor set-up and operation

Fig.3.1 elaborates AGR schematic and operating conditions. Three acrylic tube reactors (R1, R2, R3) were set up with 3.0 L working volume, 153.0 cm working height and 5.0 cm inner diameter. Air compressor provided 2 L/min aeration into the AGR and peristaltic pump was employed for reactor feeding with 2.07 m/h feed up-flow velocity. R1, R2 and R3 were operated with 12, 24 and 48 h HRTs having 6, 12 and 24 h cycle times, respectively. In each cycle, volume exchange ratio (VER) was 50%, feeding and effluent withdrawal times were maintained at 22 and 3 min, respectively. The initial F/M ratio in the AGRs was 0.15 g COD/g SS.day. The granule settling time changed from 5 to 3 min. detailed cycle durations of the AGRs are given in Table 3.1.

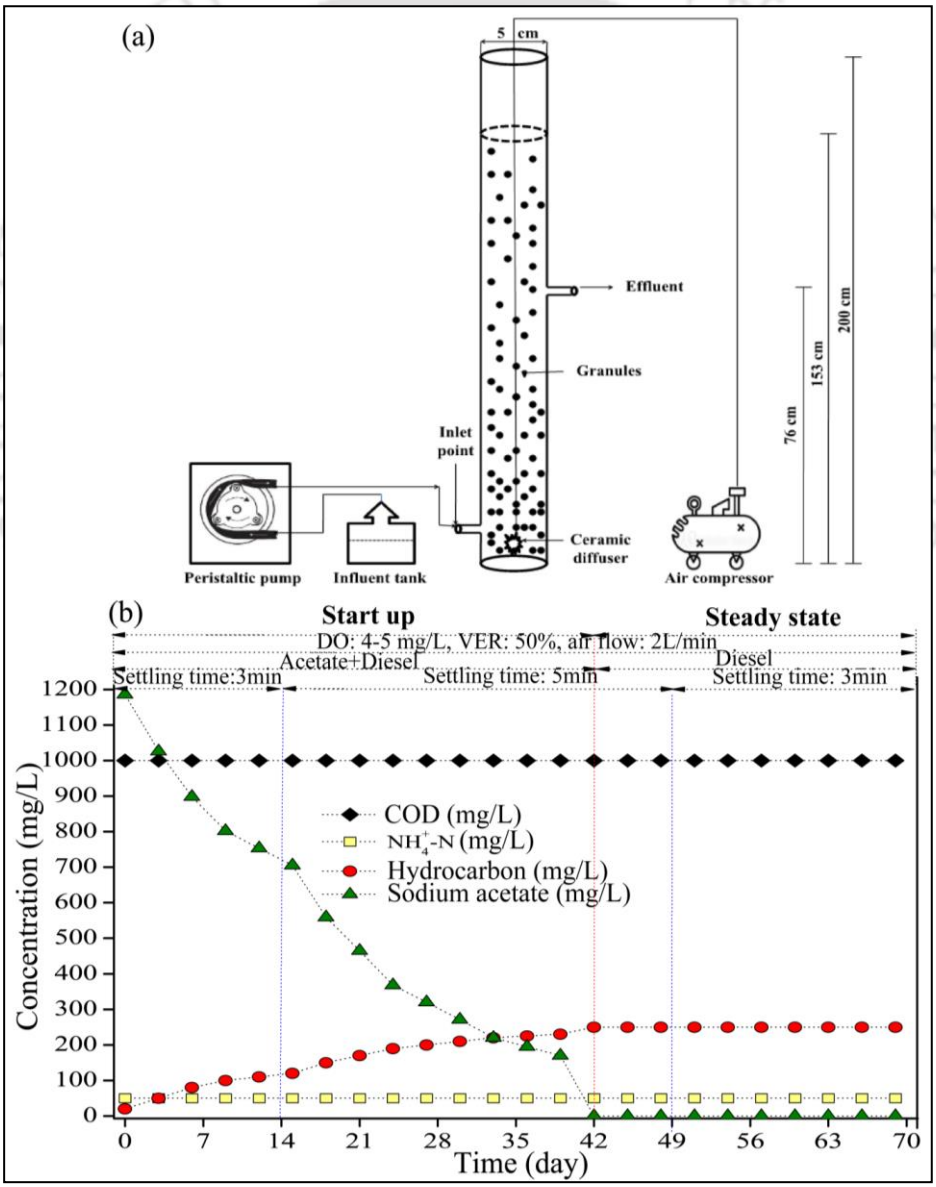

Fig.3.1 (a) Schematic of AGR and (b) AGR operating conditions [AGRs were operated with 50% VER and 12 h, 24 h, and 48 h operating HRTs, respectively].

Table 3.1 Detailed cycle durations of the AGRs

Cycle phases (min)	R1	R2	R3
Filling	22	22	22
Reaction	329	687	1407
Settling	3	5	5
Decanting	3	3	3
Idle	3	3	3
Total cycle time	360	720	1440

*R1, R2 and R3 were operated with 50% VER and 12 h, 24 h, and 48 h operating HRTs, respectively.

HRT and ULV were calculated by equations 2.1 and 2.2 given in Chapter 2 (Metcalf and Eddy, 2003).

3.2.5 Analytical methods

Granule strength was determined in terms of **integrity coefficient** (IC) by calculating the ratio of solids (TSS) present in the supernatant to the total weight (TSS) of the residual granular sludge, expressed in percent (Ghangrekar et al., 2005). Reactor activity study, sludge, effluent and FESEM analysis were carried out according to chapter 2 (section 2.2.6).

3.2.6 Confocal laser scanning microscopy (CLSM)

To observe the distribution of total cells, dead cells, proteins and polysaccharides in hydrated aerobic granules, they were stained by fluorescent dyes according to Yu et al. (2009). SYTO 63 dye (200 µM, 100 µL) was added to granule samples and was shaken for 30 min at 100 rpm. Samples were washed with PBS buffer to remove excess dye. Thereafter, about 100 µL of 0.1 M $NaHCO_3$ buffer was added to it. FITC dye (10 g/L, 10 µL) was further added to the sample and was kept at room temperature (30 °C) for 1 h. After buffer washing 100 µL (250 mg/L) of CON A dye was added to the granules and was incubated for another 30 min. Then, the sample was buffer washed and was stored at 4 °C. Before microscopic observation, sytox blue dye (2.5 µM, 100 µL) dye was added and was kept for 10 min. Finally, stained granules were cut into 30 µm sections and they were analyzed under confocal laser scanning microscopy (CLSM, Model: Leica TCS, SP8, Germeny, software: LASX confocal software) with 10× or 20× objectives.

3.2.7 Phytotoxicity analysis

For phytotoxicity study, 30 pots were prepared containing 2.5 kg local soil in each. Each of the first fifteen pots was planted with six *Cicer arietinum* legumes and the rest fifteen pots were planted with ten *Vigna radiata* legumes. First three pots of both *Cicer arietinum* and *Vigna radiata* were treated with normal tap water, another three pots with untreated oily

wastewater containing 250 mg/L of diesel and the rest nine pots were treated with R1, R2 and R3 treated effluents. Pots were in triplicates for each AGR effluent. Each pot was daily treated with 100 mL water (tap water/untreated oily wastewater/AGR treated effluent). Pots were kept in sunlight at 18±3 °C temperature between 10 to 60% relative humidity and the study continued up to six weeks. Germination percentage was calculated by using equation 3.1.

$$\text{Gemination (\%)} = \frac{\text{no. of seeds germinated}}{\text{total no. of seeds planted in a pot}} \times 100\% \quad (3.1)$$

3.2.7.1 Chlorophyll analysis

Total chlorophyll estimation was conducted according to standard method (APHA, 2005). It was conducted in subdued light to avoid photo-degradation. About 0.5 g of green fresh leaf sample was collected. Chlorophyll was extracted in acetone solution using a tissue grinder. Extract was centrifuged at 5000 rpm for 15 minutes. Supernatant was collected in an opaque container and was stored at 4°C. Extract was transferred to a 1 cm cuvette and absorbance was measured at 750, 664, 647 and 630 nm wavelengths, respectively. The readings observed at 664, 647 and 630 nm were used to determine Chlorophyll *a*, *b* and *c*, respectively. Reading at 750 nm was the correction to the turbidity. Turbidity correction was subtracted from each of the absorbance reading values while using them in the following equations 3.2-3.4 to determine mg chlorophyll/g fresh weight (F.W.) of leaves.

a) C_a= 11.85(OD664)-1.54(OD647)-0.08(OD630) (3.2)

b) C_b= 21.03(OD647)-5.43(OD664)-2.66(OD630) (3.3)

c) C_c= 24.52(OD630)-7.60(OD647)-1.67(OD664) (3.4)

Where, C_a, C_b, C_c= concentrations of chlorophyll *a*, *b*, *c* (mg/L); OD664, OD647, OD630 = corrected OD at respective wavelengths. Then equation 3.5 was used to calculate the amount of chlorophyll per unit volume.

$$\text{Chlorophyll } a, \text{ mg/m}^3 = \frac{C_a \times \text{extract volume,L}}{\text{Volume of the sample,m}^3} \quad (3.5)$$

The chlorophyll content was further converted into mg/g F.W.

3.2.7.2 Cabohydrate and protein measurement

Fresh leaves were weighed and cleaned with distilled water and then dried at 40-45° C temperature. Dried leaves were grinded using 95% ethanol and the viscous solution was centrifuged and the supernatant was finally used for protein and carbohydrate analysis by following the process used for granule protein (PN) and polysaccharides (PS) content measurement mentioned in Chapter 2 (section 2.2.6.1).

3.2.7.3 Catalase analysis

Catalase is an important enzyme for protecting the plant cells from oxidative damage by reactive oxygen species (ROS). Catalase activity was determined according to method described by Aebi (1984). About 0.5 g fresh leaf samples was homogenised in 5 mL of cold 200 mM sodium phosphate buffer (pH 7.8) using mortar and pestle. The homogenates were centrifuged at 12,000 rpm for 20 min at 4 °C temperature, and the supernatant was used for catalase activity assay. A reaction mixture of buffer and hydrogen peroxide was added to the enzyme extract and the enzyme activity was measured by monitoring the decrease in absorbance due to H_2O_2 consumption at 240 nm wavelength in UV visible spectrophotometer. One unit of catalase activity was defined as µ mole H_2O_2 split/mg F.W.

3.2.7.4 Peroxidase analysis

The function of peroxodase is to break down hydrogen peroxide (H_2O_2), which is one of the toxins produced during respiration. A reaction mixture of 25 mM phosphate buffer (pH 7.0), mM H_2O_2, 0.05% guaiacol and 0.1 mM EDTA was added to 0.5 ml enzyme extract. The reaction was initiated by adding H_2O_2 and the increase in the absorbance was monitored at 470 nm wavelength at 1 min intervals up to 4 min in UV visible spectrophotometer (Ambreen et al., 2000). One unit of peroxidase activity was defined as the Δ Absorbance/mg F.W.

3.3 Results and discussion

3.3.1 Effects of HRT on granule size, density, strength and morphology

Initial seed granules were yellowish in colour having 5.23±0.07 mm average diameter, 13.65±0.02 g/L density and 6.69±0.05 g/L of VSS content. Increasing diesel exposure changed granule colour from yellow to brownish (Fig.3.2). Fig.3.3a describes granule size profiles in the AGRs.

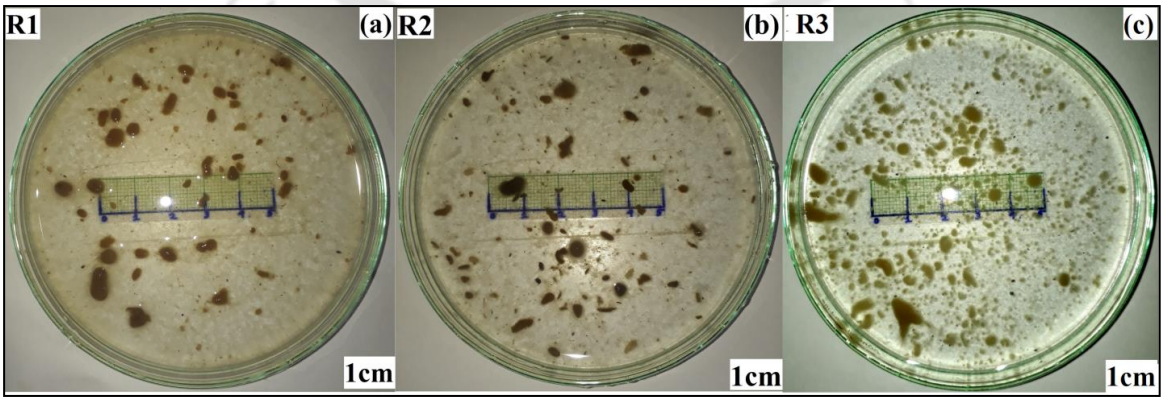

Fig.3.2 Aerobic granules collected from (a) R1, (b) R2 and (c) R3 on day 70

Similarly, granular colour change from yellow to brown was observed by Zhang et al. (2011) in real petrochemical wastewater. With increasing diesel loading, effects of different HRTs became prominent on granule size, density and morphology.

In the first 42 days, combined effect of sodium acetate (1186-170 mg/L) and emulsified diesel (20-230 mg/L) promoted 4.56±0.05 mm average granule size in the AGRs. Between day 43-70, in presence 250 mg/L emulsified diesel, R2 and R3 faced granule size reduction (R2: 4.60±0.04 mm, R3: 4.31±0.21 mm) with decreasing granule density (R2: 12.51±0.05 g/L, R3: 12.52±0.05 g/L) and biomass concentration (VSS: R2: 5.27±0.01 g/L, R3: 4.85±0.01 g/L). But in R1 granule disintegration was comparatively lesser and size, density and VSS content were nearly stable at 4.72±0.05 mm, 13.5±0.01 g/L and 6.47-6.38, g/L respectively. Granule density and VSS profiles are shown in Fig.3.3b and c, respectively.

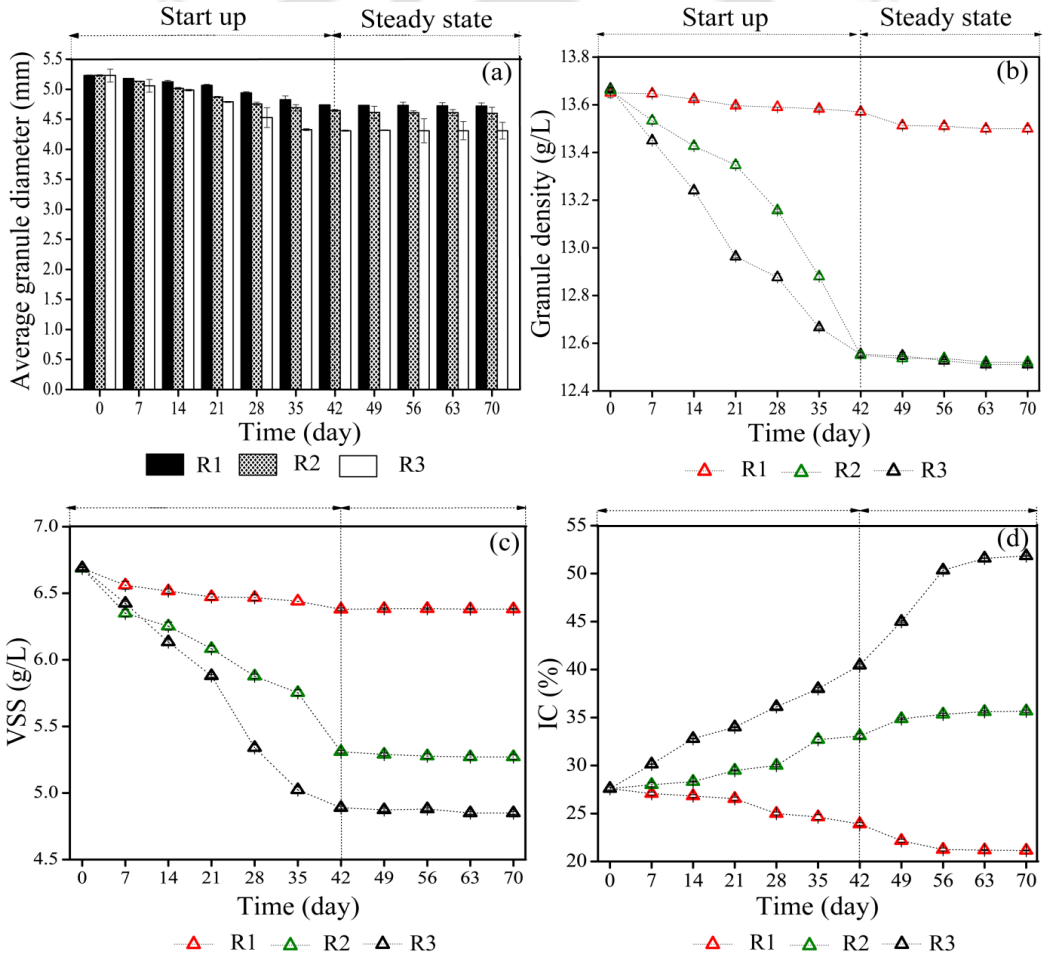

Fig.3.3 (a) Granule size, (b) density, (c) VSS content and (d) integrity coefficient profiles in the AGRs.

Short HRT (12 h) produced high selection pressure on granules by removing loose biomass and high organic loading promoted bigger granules than AGRs operated with higher HRTs (24 h and 48 h) and lower loadings. Similarly, literatures suggested the use of short

HRTs and high organic loadings for bigger and denser granule formation while treating rubber, phenolic, POME and synthetic wastewaters (Rosman et al., 2014; Tomar and Chakraborty, 2018a; Gobi et al., 2011; Morgenroth et al., 1997).

Integrity coefficient (IC) determines microbial integrity and physical strength of granules. Initial seed granules had 27.6±0.15% IC value which reduced up to 21.14±0.04% in R1 and increased up to 35.66±0.11% and 51.85±0.07% in R2 and R3, respectively. Changes in IC values are described in Fig.3.3d. According to Ghangrekar et al. (2005) minimum IC value for short HRT suggested maximum strength and density in R1 granules which is corresponding with maximum biomass content in R1 (Fig.3.3c).

Granule microstructures were largely influenced by HRT values. FESEM images of day 65 proved that R1 granules had dense microbial structures (Fig.3.4) suggesting granule integrity which is agreeing with low IC values in R1 (Fig.3.3d). Whereas, R2 and R3 operated with longer HRTs produced porous granules. Similarly, shorter HRT provided more compact microscopic granule structures than longer HRTs while treating rubber wastewater (Rosman et al., 2014).

CLSM microscopy was carried out on day 60 (Fig.3.5). Extended Fluorescence for SYTO 63 and FITC in R1 granules indicated that 12 h HRT promoted higher amounts of total cells and proteins than R2 and R3 operated with 24 h or 48 h HRTs which is agreeing with maximum biomass concentration and EPS content in R1 among the AGRs (Fig.3.3c and 3.6b). Moreover, high fluorescence for Sytox blue in R2 and R3 granules proved that long HRTs were responsible for more proportion of dead cells than R1.

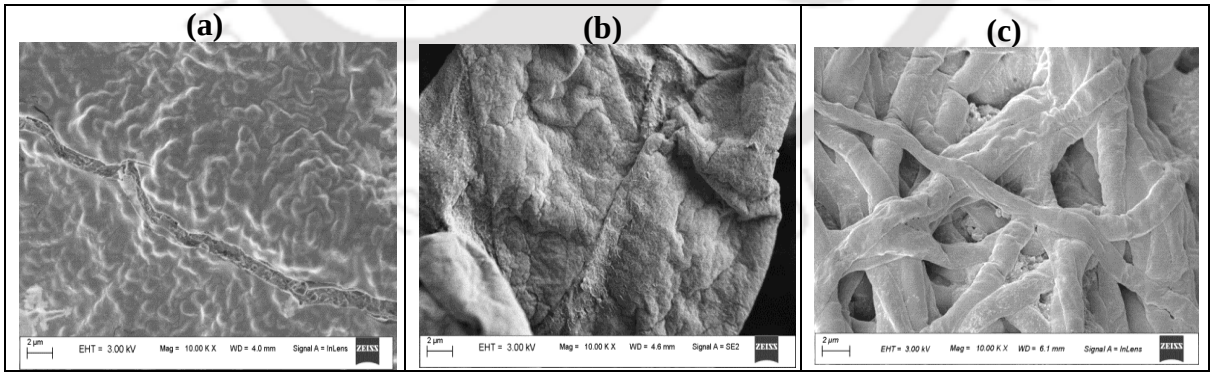

Fig.3.4 FESEM images of (a) R1, (b) R2 and (c) R3 granules in 10000× magnification on day 65.

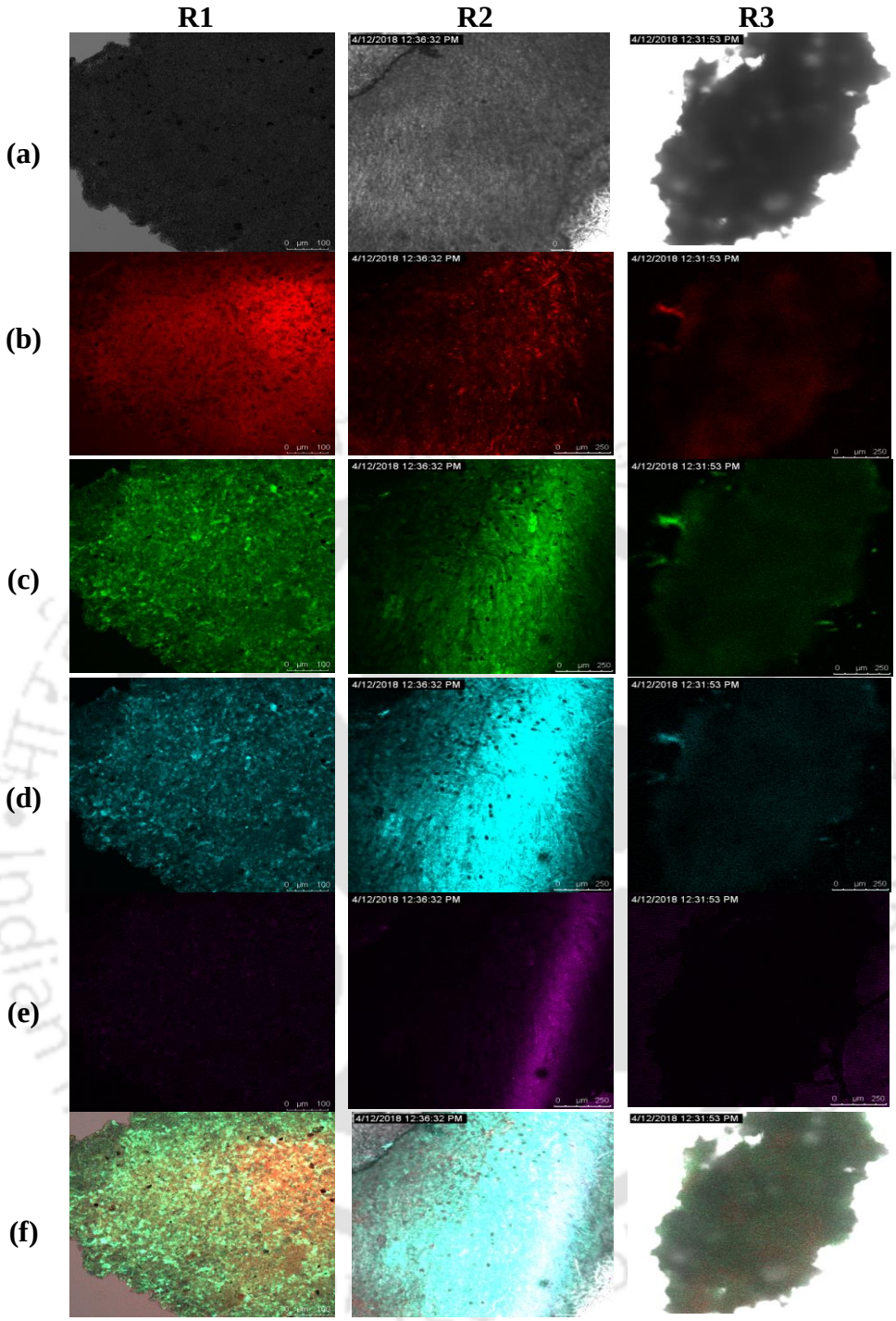

Fig.3.5 CLSM images of R1 (Bar: 100 µm) and R2, R3 (Bar: 250 µm) on day 60: (a) optical microscopic image (b) total cells (Syto 63); (c) proteins (FITC); (d) polysaccharides (Con A); (e) dead cells (Sytox Blue); (f) combined image of (b) and (e).

3.3.2 Effects of HRT on granule characteristics

3.3.2.1 Granule settling behaviour

Approximately, 25-70 m/h GSV and below 50 mL/g SVI_{30} are optimum for granule formation and settleability (Adav et al., 2008; Liu and Tay, 2004). Comparative GSV and

SVI_{30} profiles in the AGRs are given in Fig.3.6a. Seed granules had 41.35±0.02 m/h GSV and 23.75±0.04 mL/g SVI_{30} values. When sodium acetate and diesel were co-substrates, increasing hydrocarbon concentration (20-230 mg/L) and longer HRTs provided less hydraulic pressure on granules which hampered granule settling behaviour in R2 and R3.

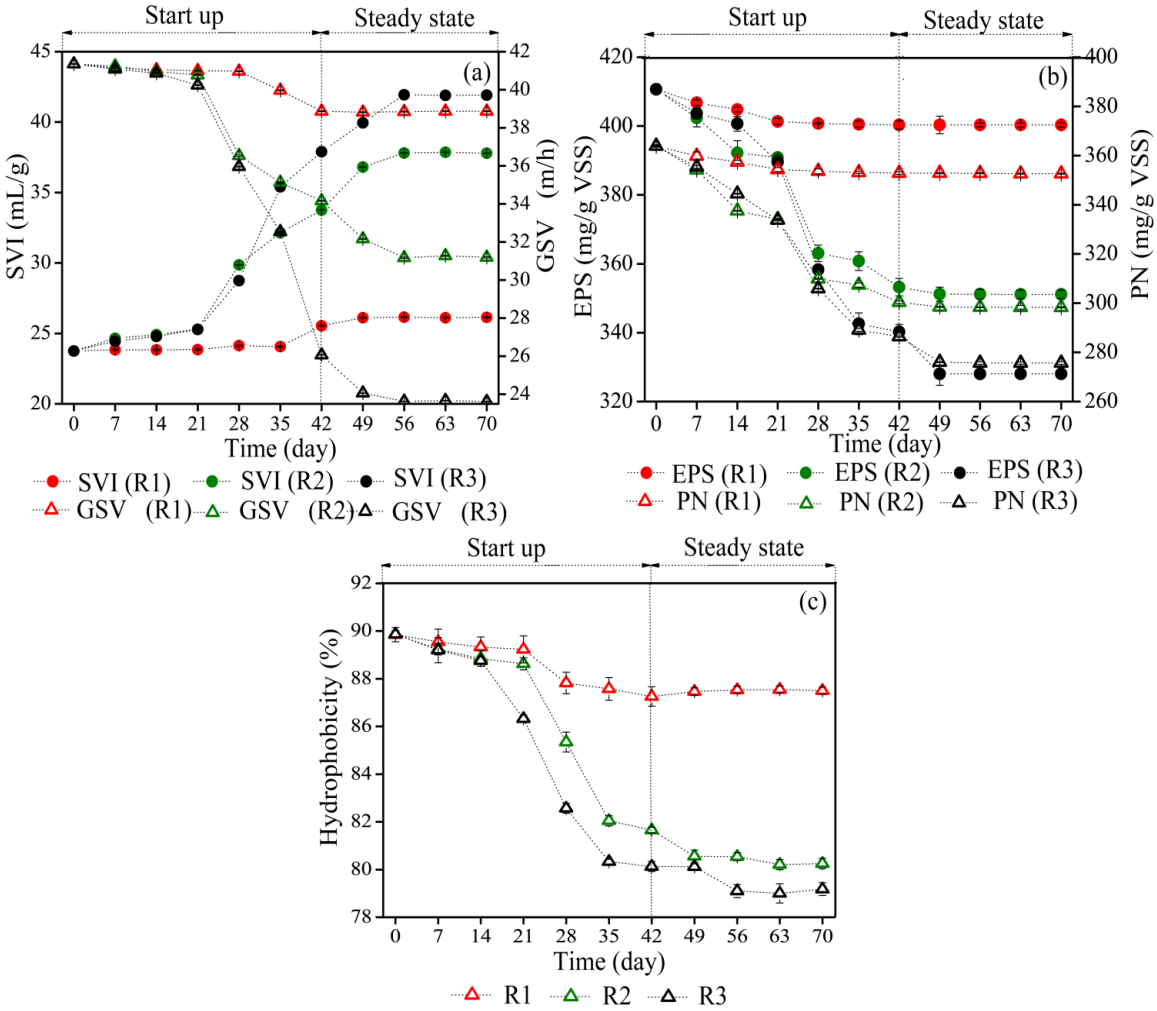

Fig.3.6 Comparative (a) SVI_{30} and GSV, (b) EPS and PN and (c) granule hydrophobicity profiles in the AGRs.

R2 and R3 showed decreasing GSV (R2: 34.16±0.04 m/h, R3: 26.07±0.02 m/h) and increasing SVI_{30} data trends (R2: 33.75±0.02 mL/g, R3: 37.91±0.04 mL/g). But when diesel was used as sole carbon source (250 mg/L), short HRT in R1 helped to achieve highest GSV (38.87±0.02 m/h) and lowest SVI_{30} (26.14±0.04 mL/g) indicating maximum granule settleability among the AGRs. On the other hand, according to Moy et al. (2002) 2 kg COD/m^3.day organic loading rate (OLR) was the main key factor for denser granules with better settling in R1 than R2 and R3 operated with 1 and 0.5 kg COD/m^3.day OLRs, respectively. On day 56 onwards, R2 and R3 acclimatized in diesel environment and achieved stable SVI_{30} (R2: 37.79±0.01 mL/g, R3: 41.92±0.04 mL/g) and GSV (R2:

31.19±0.03 m/h, R3: 23.61±0.02 m/h) values. Similarly, high GSV and low SVI_{30} values were observed in AGRs operated with 6 h and 12 HRTs while treating rubber and simple synthetic wastewaters, respectively (Pan et al., 2004; Rosman et al., 2014).

3.3.2.2 Variation in EPS and hydrophobicity

EPS are the polymeric base materials required for granule formation. EPS contain proteins and polysaccharides responsible for mechanical strength and stability (Liu and Tay, 2002; McSwain et al., 2005). Protein hydrophobicity helps in granular structure formation. Comparative EPS and PN trend and hydrophobicity profiles are described in Fig.3.6b and c, respectively. In presence of 20-170 mg/L emulsified diesel, EPS and PN content had nominal reduction from 410.65±0.43 to 393.91±0.12 and 363.91±0.43 to 340.72±2.7 mg/g VSS, respectively.

During 190-250 mg/L diesel exposure, increased hydrocarbon toxicity changed granule microbial environment which reduced EPS content, protein synthesis and cell hydrophobicity in the AGRs. On day 70 with 250 mg/L diesel exposure, maximum EPS concentration and cell hydrophobicity were observed in R1 (400.31±0.01 mg/g VSS, 87.5±0.51%) followed by R2 (351.12±0.02 mg/g VSS, 80.25±0.21%) and R3 (328.05±0.17 mg/g VSS, 79.18±0.07%), respectively. Short HRT (12 h) was responsible for short cycle time in R1 which increased hydraulic selection pressure in the reactor and enhanced EPS production while compared to R2 and R3 operated with 24 and 48 h HRTs (Rosman et al., 2014).

EPS content in aerobic granules were inversely proportional to HRT while treating phenol and ammonia and about 69.1, 55.9 and 36.39% granule hydrophobicity were reported during synthetic wastewater treatment at 6, 12, 24 h HRTs which are similar to our results (Pan et al., 2004; Tomar and Chakraborty, 2018). Characteristics of aerobic granule and AGR treatment efficiency in varieties of hydrocarbon containing wastewater operated with different HRT and influent loading rates are given in a comparative form in Table 3.2.

With decreasing VSS concentration in AGRs (till day 42), the F/M ratio increased from 0.15 g COD/g SS.day to 0.16, 0.19 and 0.21 g COD/g SS.day in R1, R2 and R3, respectively and remained unchanged till day 70. Hence, granule GSV correspondingly decreased with increasing F/M ratio which is also observed by Hamza et al. (2018) in high strength organic wastewater. The slight increase in F/M ratio and shortest operating HRT (12 h) in R1 maintained EPS concentration nearly 400 mg/g VSS which provided highly stable granules. Similarly, Janga et al. (2007) observed that rise in F/M ratio from 0.13 to 0.29 g COD/g SS.day provided more protein and polysaccharide adsorption in granule EPS matrix increasing EPS content.

Table 3.2 Comparisons of granule characteristics and treatment efficiency in different types of hydrocarbon rich wastewater in AGRs operated with different HRT and influent loading rates

Type of wastewater	Operating HRT (h)	Influent loading ($kg/m^3.day$)	Granule size (mm)	SVI (mL/g)	EPS (mg/g VSS)	Effluent concentration (mg/L)	References
Palm oil mill wastewater	24	OLR: 3-6	0.9	30[a]	-	COD: 300-600	Gobi et al. (2011)
Hypersaline oily wastewater	6, 24	OLR: 3.60, 1.35; HLR: 0.03, 0.007	1.9	28, 30[b]	340, 550	COD:18, 162; hydrocarbon: 0.68 (0.05)	Corsino et al. (2015)
Coal gasification wastewater	8	OLR: 3	0.25-1.3	30 (8)[c]	-	COD: 59.4 (19.8)	Milia et al. (2016)
Petroleum wastewater (real)	12	OLR: 2.0; HLR:0.10	0.06-1.17	26-45[a]	32 (3)	COD: 110-80	Zhang et al. (2011)
Petroleum wastewater (synthetic)	12	OLR:1.2-1.8; HLR: 0.1-0.4	0.46–0.9	30 [a]	128	COD: 30-5; hydrocarbon: 25-20	Chen et al. (2019)
Diesel wastewater	12, 24, 48	OLR: 2, 1, 0.5; HLR: 0.04-0.5, 0.02-0.25, 0.01-0.125	4.72, 4.60, 4.31	26, 37, 41 [a]	400, 351, 328	COD: 1 (0.5); hydrocarbon: 77.87, 51.2, 24.23	Current study

[a] SVI_{30}, [b] SVI_5, [c] SVI_8
OLR: organic loading rate, HLR: hydrocarbon loading rate
Standard deviations are in parenthesis

3.3.3 Effects of HRT on AGR performance

3.3.3.1 COD and organic removal with reactor activity

COD removal patterns are given in Fig.3.7a. Seed granules were cultivated in acetate media with 1.8 kg COD/m^3.day of OLR having 99.9±0.05% COD removal efficiency as mentioned in Chapter 2. From day 1-42, sodium acetate and diesel and from day 43-70 only emulsified diesel were fed as carbon source. HRT and OLR are interlinked parameters which are inversely proportional to each other. With increasing HRT values from 12 h to 24 h to 48 h the OLR values correspondingly decreased from 2 to 1 to 0.5 kg COD/m^3.day in R1, R2 and R3, respectively. We mainly focused on how HRT variation influenced pollutant removal efficiencies of AGRs with mentioning the corresponding changes of the OLR.

In start-up phase, introduction of diesel slightly hampered COD removal up to 97.39±0.02% in R1, 98.36±0.01% in R2 and 98.57±0.02% in R3 till day 28 (influent hydrocarbon: 200 mg/L). After achieving steady state (day 49 onwards), COD removal became proportional to the HRT values of the AGRs. At the end of the study (day 70), R1, R2 and R3 achieved 71.34±1%, 80.02±0.56% and 90.40±0.21% COD removal efficiencies (influent hydrocarbon: 250 mg/L), respectively. In rubber wastewater treatment 98.4% COD removal was observed in AGR with 6 h HRT but in phenolic wastewater 94-96% COD removal (OLR: 2.03 kg COD/m^3.day) was achieved with complete phenol removal irrespective of 6, 12, 24 h of operating HRTs (Rosman et al., 2014; Tomar and Chakraborty, 2018a).

However, in our study, emulsified diesel was used as sole carbon source between day 43-70. Though 5-6.8 g/L granular biomass concentration was maintained in all three AGRs, longer cycle time (12 h, 24 h) in R2 and R3 helped the aerobic granules in more microbial degradation of 250 mg/L recalcitrant hydrocarbon molecules providing 80-90% COD removal efficiency. But in 6 h cycle time, R1 granules were capable of only 71±34% COD removal due to incomplete hydrocarbon degradation.

Hydrocarbon loading rate (HLR) was maintained at 0.04-0.5, 0.02-0.25 and 0.01-0.125 kg/m^3.day in R1, R2 and R3, respectively. Hydrocarbon removal profile is given in Fig.3.7b. With increasing diesel concentration (170-250 mg/L), hydrocarbon removal capacity decreased in granules. Gravimetric analysis showed 98±1% hydrocarbon removal in R1, R2 and R3 till day 20, 26 and 41 in presence of 150, 190 and 230 mg/L, emulsified diesel, respectively.

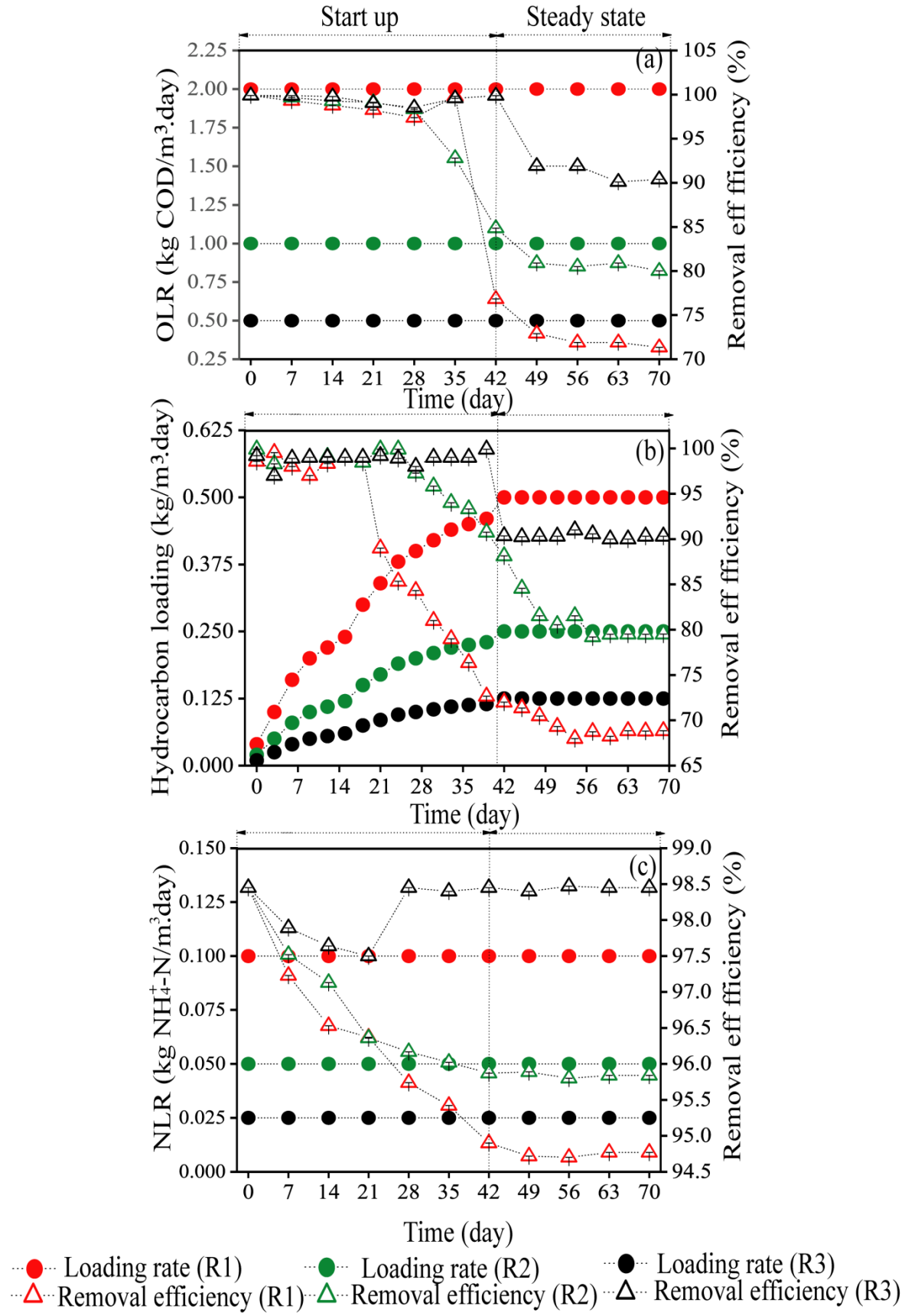

Fig.3.7 (a) COD, (b) hydrocarbon and (c) nitrogen loading with removal profiles in the AGRs.

Between day 51-70, AGRs achieved steady state with 250 mg/L of influent hydrocarbon. According to gravimetric results, at the end of the study (day 70), R3 achieved maximum 90.31±0.26% removal in presence of 250 mg/L of diesel, whereas R1 and R2 achieved 68.85±0.06% and 79.52±0.32% hydrocarbon removal efficiencies, respectively. Final effluent oil concentrations were 77.87±0.11, 51.2±0.02, 24.23±0.12 mg/L in R1, R2 and R3. In Chapter 2 (section 2.3.1), we observed that only 0.021-0.076% emulsified hydrocarbon was removed by air volatilization and dead granule surface adsorption indicating microbial hydrocarbon degradation in aerobic granules.

Till day 42, the increase in F/M ratio (0.15 g COD/g SS.day to 0.21 g COD/g SS.day) indicated amount of excess substrate which exceeded the consumption capacity of the available granule bacteria (Hamza et al., 2018). However, the AGRs achieved steady state after day 42 and F/M ratio remained stable which maintained TPH removal efficiency between 68-90% up to day 70.

Untreated hydrocarbon rich wastewater and the AGR treated effluents were analysed by GC-MS to detect the diesel components in untreated wastewater and the intermediates or final compounds generated after biodegradation of diesel (Fig.3.8a-d). Table 3.3 provides the name and carbon number of the compounds found in influent and effluent samples.

The probable aerobic alkane degradation pathway along with β-oxidation is described in Fig.3.9. Diesel is mainly composed of medium length saturated hydrocarbons between C_{10} to C_{29} (Nkem et al., 2016). GC-FID chromatograms exhibited that influent oily wastewater contained various *n*-alkanes ranging from C_6 to C_{36} carbons (Fig.3.8a and Table 3.3).

After 70 days of AGR operation, fatty acids like tridecanoic acid (C_{13}), octadecanoic acid (C_{18}), octadecadienoic acid (C_{18}) and medium length alkanes like pentadecyne (C_{15}) and octylcyclopropane (C_{11}) compounds were detected in R1 effluent (Fig.3.8b and Table 3.3). GC-MS results indicated that long chain compounds like heptacosane (C_{27}) as well short and medium chain compounds like benzene to heptane (C_6-C_7), nonane to cyclodecane (C_9-C_{10}) and undecane to tridecane (C_{11}-C_{13}), pentadecane to octadecane (C_{15}-C_{18}) were removed by the aerobic granules in R2 and R3 (Fig.3.8c and d and Table 3.3). However, presence of very small peaks of octane (C_8), tetradecane (C_{14}), tetracosane (C_{24}), octacosane (C_{28}) and hexatriacontane (C_{36}) in R2 and R3 effluents, respectively indicated the presence of some non-degraded alkanes (Fig.3.8c and d and Table 3.3).

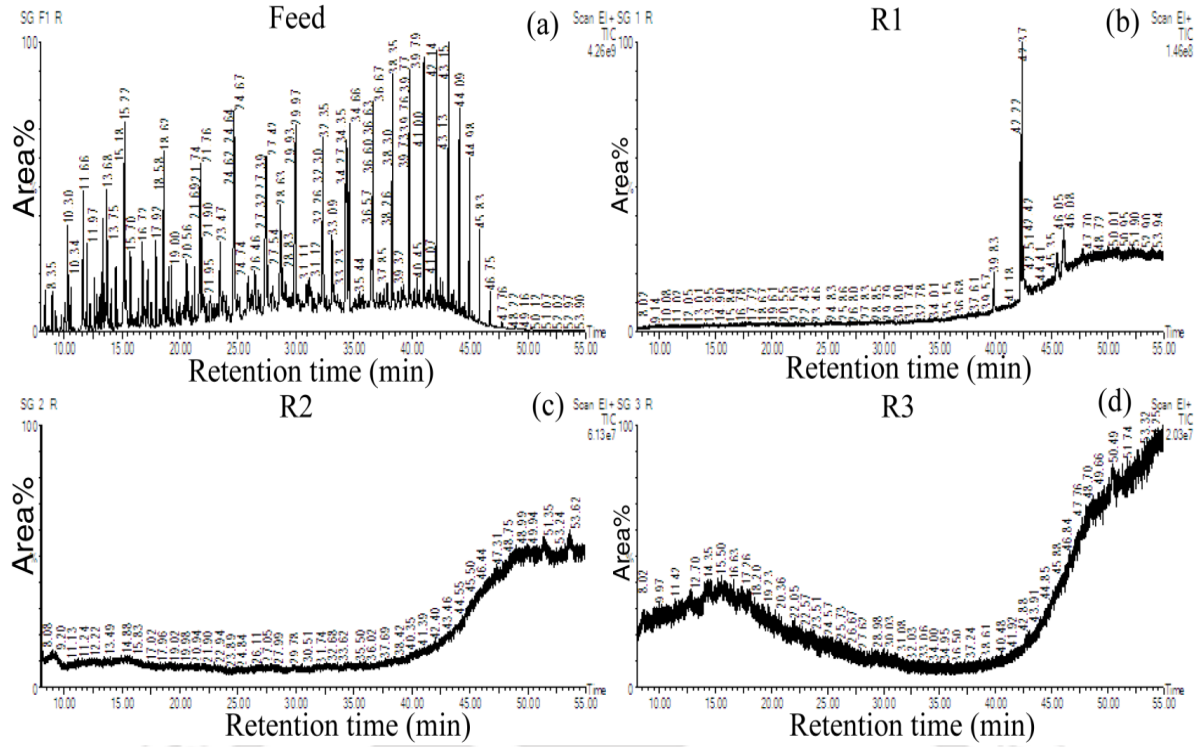

Fig.3.8 GC-MS results for (a) untreated petroleum wastewater and (b) R1, (c) R2 and (d) R3 treated effluent.

Based on literature, *n*-alkanes generally follow degradation pathway where the methyl groups of the *n*-alkane are initially converted to alcohol and then its hydroxyl group is oxidized to aldehydes and finally it is converted into a fatty acid (Kostal et al., 1998; Zhang et al., 2011; Cai et al., 2013). The presence of fatty acids and short chain alkanes in R1 effluent is suggesting that alkanes were degraded following the above-mentioned pathway in the AGRs.

Moreover, for aerobic degradation of polyaromatic hydrocarbons (PAHs), Hadibarata and Kristanti (2012) hypothesized oxidation of aromatics into aromatic acids where intermediates can follow either methyl group oxidation in alkyl-aromatic hydrocarbon or hydrogen substitution in benzene rings. Cai et al. (2013) also observed that 99.0% of *n*-alkanes and 43.03-99.9% of PAHs of petroleum hydrocarbons were aerobically biodegraded by following oxidation of hydrocarbons into fatty acids.

Table 3.3 Compounds detected in influent and R1, R2 and R3 treated effluents in GC-MS analysis

Influent			R1 effluent			R2 effluent			R3 effluent		
Retention time (min)	**Compound name**	**Carbon number**	**Retention time (min)**	**Compound name**	**Carbon number**	**Retention time (min)**	**Compound name**	**Carbon number**	**Retention time (min)**	**Compound name**	**Carbon number**
8.34	Octane	C_8	39.83	Tridecanoic acid	C_{13}	22.99	Octane	C_8	46.48	Hexatriacontane	C_{36}
10.30	Hexyl octyl ether	C_{14}	42.22	Octadecanoic acid	C_{18}	30.51	Tetradecane	C_{14}	47.76	Hexatriacontane	C_{36}
11.66	Nonane	C_9	42.36	Octadecadienoic acid	C_{18}	42.40	Tetracosane	C_{24}	48.70	Octacosane	C_{28}
11.97	Cyclohexane	C_6	45.41	Pentadecyne	C_{15}						
13.33	O-xylene	C_8	46.01	Octylcyclopropane	C_{11}	No sharp peak found			No sharp peak found	-	
13.68	Cyclopentane	C_5									
13.74	Octadecanal	C_{18}									
15.22	Octanol	C_8									
15.70	Heptane	C_7									
16.72	Benzene	C_6									
17.92	Benzene	C_6									
18.61	Undecane	C_{11}									
19.00	Napthalene	C_{10}									
20.55	Cyclodecane	C_{10}									
21.75	Dodecane	C_{12}									
23.47	Octane	C_8									
26.46	Tridecane	C_{13}									
27.42	Hexadecanoic acid	C_{16}									
29.96	Tetradecane	C_{14}									
32.35	Pentadecane	C_{15}									
33.08	Hexadecane	C_{16}									
34.36	Tetradecane	C_{14}									
34.66	Pentadecane	C_{15}									
36.67	Heptadecane	C_{16}									
38.35	Octacosane	C_{28}									
41.04	Octadecane	C_{18}									
42.15	Tetracosane	C_{24}									
43.16	Heptacosane	C_{27}									
44.97	Octadecane	C_{18}									
44.67	Hexatriacontane	C_{36}									
45.83	Octacosane	C_{28}									
46.74	Hexatriacontane	C_{36}									

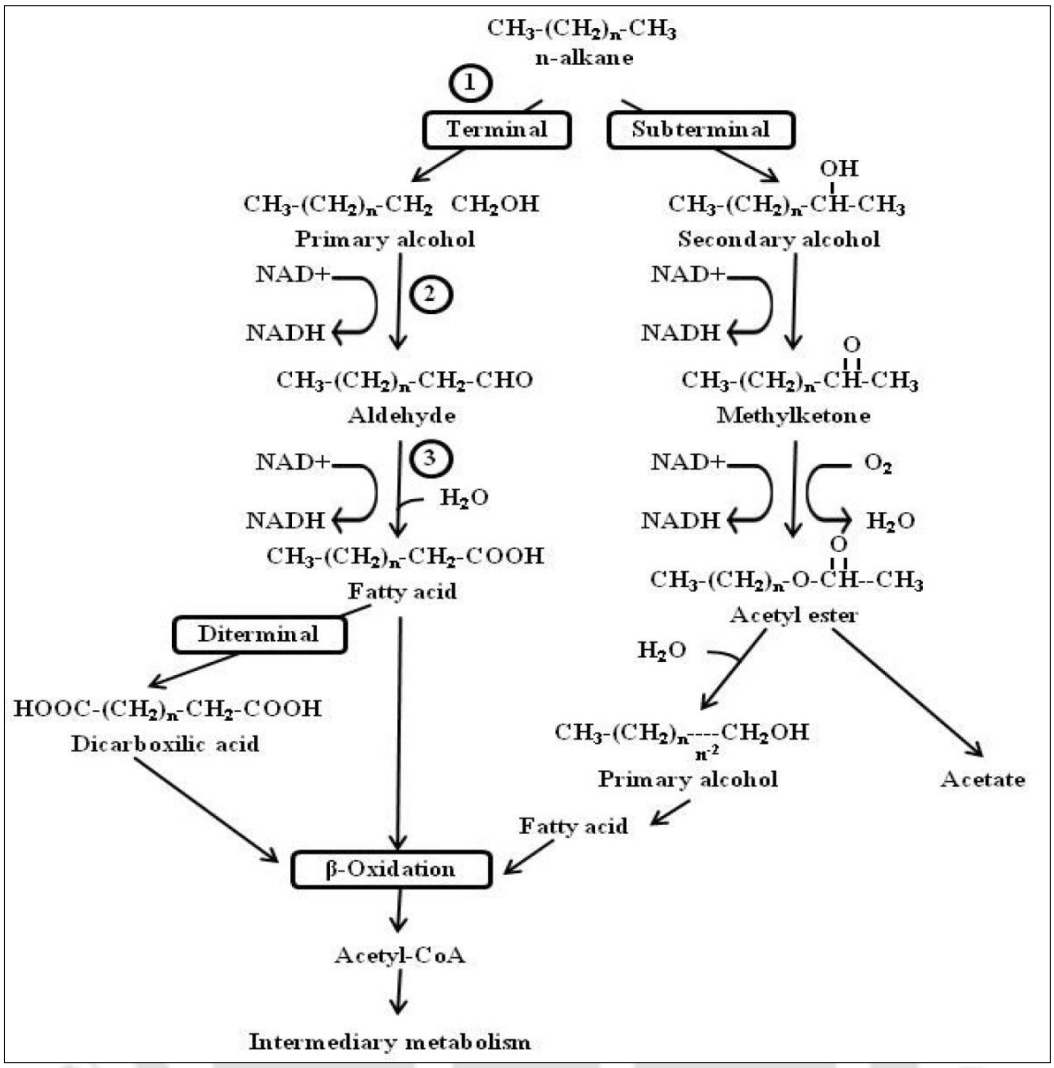

Fig.3.9 Probable alkane degradation pathway where β-oxidation of fatty acids was mediated by enzymes like (1) *n*-alkane monooxygenase, (2) alcohol dehydrogenase, (3) aldehyde dehydrogenase (Fritsche and Hofrichter, 2000).

Due to shorter HRT (12 h) and high hydrocarbon loadings, R1 had insufficient time for complete hydrocarbon degradation. Hence presence of medium length alkanes (C_{11}-C_{15}) and fatty acids in R1 effluent suggested that partial degradation of diesel occurred which produced metabolites like fatty acids. Similarly, Cai et al. (2013) reported the presence of fatty acids in the bacterial culture extracted after 90 days of biodegradation of crude hydrocarbon. The non-degraded part remained as medium chain alkanes (C_{11}-C_{15}) in R1 effluent which resulted into 69% hydrocarbon removal with 77.87±0.11 mg/L effluent hydrocarbon contributing 286.6±0.5 mg/L of effluent COD.

Longer HRT and low hydrocarbon loading provided more contact and reaction time between pollutant and microorganisms favouring more pollutant removal (Pendashteh et al., 2012). Hence, despite of having lower hydrocarbon removal rate in R2 and R3 than R1

(R1:139.65±0.02 mg hydrocarbon/g VSS.day, R2: 112.60±0.08 mg hydrocarbon/g VSS.day and R3: 81.97±0.32 mg hydrocarbon/g VSS.day), longer cycle times (12 h, 24 h) of R2 and R3 helped in 79-90% hydrocarbon removal. The unutilized hydrocarbon in the effluents of R2 and R3 were 51.2±0.02 mg/L and 24.23±0.12 mg/L, respectively which were identified by the nondegraded alkane residues (C_8, C_{14}, C_{24}, C_{28}, C_{36}) in GC-MS spectra (Fig. 3.8c and d and Table 3.3). These compounds provided effluent COD of 199.8±0.33 and 96±1 mg/L, respectively in R2 and R3. Absence of major alkane (C_6-C_7, C_9-C_{10}, C_{11}-C_{13}, C_{15}-C_{18}, C_{27}) peaks for R2 and R3 effluents suggested that diesel degradation followed the fatty acid production pathway and further took part in β-oxidation of fatty acids (Cai et al., 2013).

In our previous study in Chapter 2, *Brevibacterium paucivorans* strain SG001, *Micrococcus aloeverae* strain SG002 and *Staphylococcus hominis* strain SG003 were isolated as major hydrocarbon degraders from aerobic granules (section 2.3.6). Literature suggested probable hydrocarbon degradation mechanisms like specific adhesion of microbial cell with large hydrocarbon droplets, cellular assimilation of small emulsified hydrocarbon droplets or high nutrient (total organic carbon) assisted biodegradation by different *Brevibacterium sp.*, *Micrococcus sp.*, *Staphylococcus sp*. isolated from hydrocarbon contaminated soil or wastewaters (Esmaeil et al., 2009; Ferhat et al., 2011). Similarly, Loureiro et al. (2020) reported 55±3% degradation of the C_{11}-C_{22} *n*-alkanes while treating commercial B10 diesel hydrocarbon with residual sludge of a biogas plant. All studies are suggesting that alkane biodegradation was possible by microorganisms which is supporting our results.

AGR efficiency in hydrocarbon and COD removal with changing HRT can be further justified by reactor activity analysis. Reactor activity is the key factor to determine the amount of active biomass responsible for organics removal inside a reactor which was calculated by equation 2.6 mentioned in Chapter 2 (Jawed and Tare, 1999). Impacts of different HRTs also reflected in variation of biomass activity in the AGRs. Fig.3.10 represents the 6 h cumulative COD removal profile with individual reactor activity profile of R1, R2 and R3.

After 70 days of HRT study, maximum granular biomass activity of 8.33±0.21 mg COD/mg VSS.day was achieved by R1. R2 and R3 achieved 2.72±0.30 mg COD/mg VSS.day and 2.46±0.15 mg COD/mg VSS.day, of activities respectively. Shortest HRT (12 h) inside R1 produced higher shear force which promoted more granules density (13.5±0.01 g/L) with more biomass concentration (6.38±0.05 g/L) providing maximum microbial activity while compared to R2 and R3 operated with higher HRTs (24 h, 48 h) promoting less VSS (5.27±0.01 and 4.85±0.01 g/L) and selection pressure on granules. Similarly, Tomar and

Chakraborty (2018b) also reported that high shear force was responsible to enhance granular biomass activity in AGR for treating phenol, thiocyanate and ammonium. High hydrocarbon loading in R1 provided rapid biomass growth which corresponds to low SRT (11 day) value of the AGR. It further helped in achieving maximum granule size, hydrocarbon removal rate and reactor activity in R1. But, long cycle time duration (24 h) was the main factor in R3 to achieve maximum hydrocarbon removal (90.31±0.26%) compensating the low reactor activity and (2.46±0.15 mg COD/mg VSS.day) and low hydrocarbon removal rate (81.97±0.32 mg hydrocarbon/g VSS.day). This study proved that reactor activity was proportional to biomass concentration and hydrocarbon removal rate but inversely proportional with HRT of an AGR.

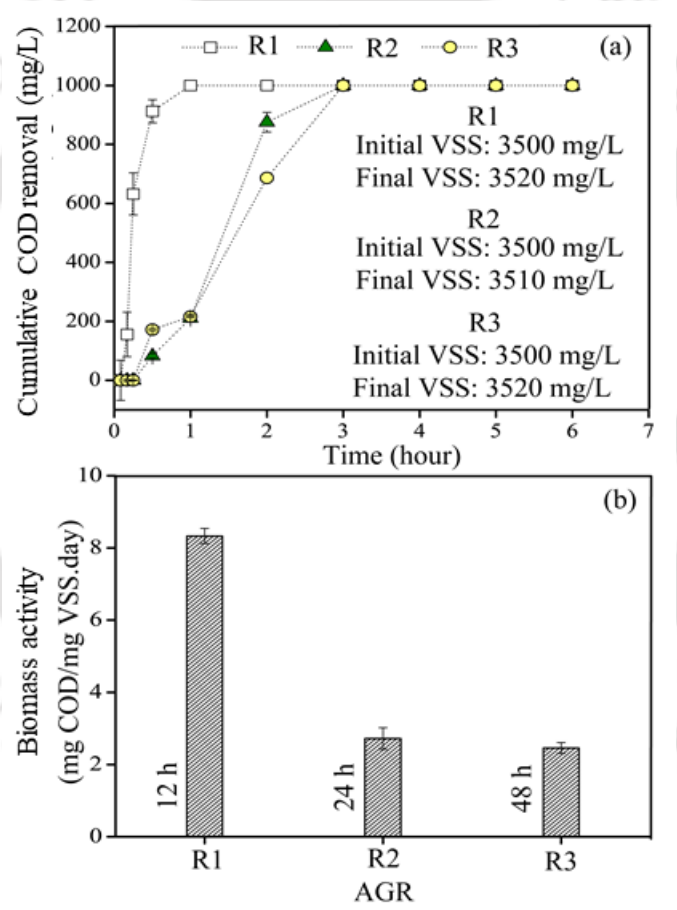

Fig.3.10 (a) Cumulative COD removal profile in the AGRs with (b) individual reactor activity profile in R1, R2 and R3.

Though shorter HRT (12 h) and high hydrocarbon loading provided maximum granule size and stability it provided poor hydrocarbon removal. So, for environmental aspects, use of medium (24 h) and longer (48 h) HRTs are recommended to achieve more hydrocarbon

removal with better quality effluent maintaining optimum granule stability in hydrocarbon rich wastewater treatment.

3.3.3.2 Nitrogen removal

The NH_4^+-N removal efficiencies of the AGRs are described in Fig.3.7c. Nitrogen loading rate (NLR) was fixed at 0.1, 0.05, 0.025 kg NH_4^+-N /m^3.day in R1, R2 and R3, respectively. An aerobic process first oxidizes NH_4^+-N to nitrites (NO_2^-) by ammonia-oxidizing bacteria (AOB) and further converts to nitrates (NO_3^-) by nitrite-oxidizing bacteria (NOB) as described in equation 1.2a-c in Chapter 1. The rest part of nitrogen is consumed for biomass growth (Metcalf and Eddy, 2003).

Recalcitrance of diesel initially caused partial granule rupture disrupting the outer ammonia oxidizing bacterial layer reducing NH_4^+-N removal efficiency in the AGRs (Tay et al., 2002). Similarly, NH_4^+-N removal decreased from 97 to 93% in aerobic granules in presence of real petrochemical wastewater (Zhang et al., 2011). Maximum HRT in R3 provided longer time for maximum 98.45±0.06% NH_4^+-N removal efficiency followed by R2 (95.84±0.04%) and R1 (94.77±0.31%), respectively. Effluent NH_4^+-N concentrations were 2.62±0.1 mg/L, 2.08±0.01 mg/L and 0.78±0.12 mg/L in R1, R2 an R3, respectively. Nitrite-nitrogen (NO_2^--N) production was almost negligible and 1.22±0.03 mg/L, 5.6±0.47 mg/L and 11.7±0.58 mg/L of nitrate-nitrogen (NO_3^--N) was produced in R1, R2 and R3 treated effluents. Granule rupture increased biomass washout which decreased SRT (equation 2.7, Chapter 2) from 15 days to 11 days in R1 and 10 days in R2 and R3, respectively.

Nitrogen utilized for biomass growth in R1, R2 and R3 were calculated as 46.4±0.12 mg/L, 42.16±0.05 mg/L and 39±0.02 mg/L by using equation 2.8 in Chapter 2 (Metcalf and Eddy, 2003). Flow rates inside R1, R2 and R3 were 6, 3 and 1.5 L/day, respectively.

Maximum 1.74 mg VSS/day of biomass wasted per day ($P_{X,bio}$) was found in R1 which was calculated by equation 2.9 (Chapter 2) determining maximum biomass growth and activity corresponding to the results of reactor activity. According to literature, shorter SRT inhibits growth of NOB population (Wan et al., 2013). Nitrite nitrogen production was almost negligible. Theoretical nitrogen oxidized was calculated by equation 3.6 (Metcalf and Eddy, 2003). Theoretical and actual nitrogen (NO_3^--N+NO_2^--N) oxidized were estimated as 0.98±0.01 mg/L, 5.76±0.21 mg/L, 10.22±0.41 mg/L and 1.22±0.03 mg/L, 5.6±0.47 mg/L, 11.7±0.58 mg/L in R1, R2 and R3, respectively.

$$\text{Theoretical nitrogen oxidized (mg/L)} = [\text{influent nitrogen (mg/L)} - \text{Effluent } NH_4^+ - \text{N (mg/L)} - \text{Nitrogen used for biomass growth (mg/L)}] \quad (3.6)$$

As nitrification is considered to be a longer process, nitrification was higher in R3 having 48 h HRTs than R1 and R2 with shorter HRTs. About 78-92% NH_4^+-N was consumed for new biomass synthesis. Hence nitrification was only 2-20% of the influent concentration. The less evidence of nitrification provided less scope for subsequent denitrification in the AGRs.

During rubber wastewater treatment maximum NH_4^+-N removal (92.7%) was observed at shortest (6 h) HRT (Rosman et al., 2014) whereas, aerobic granules achieved 99% NH_4^+-N removal for both higher and lower HRTs during phenol and ammonia treatment (Tomar and Chakraborty, 2018a, 2018b). However, current study proved that NH_4^+-N removal depends on operating HRT. The statistical analysis of granule characteristics and reactor performance data of the AGRs has been provided along with standard deviation and F-value in Table 3.4.

3.3.4 Phytotoxicity analysis

Fig.3.11 describes germination, chlorophyll content and comparative catalase and peroxidase profiles in *Cicer arietinum* and *Vigna radiata.* Photographs of tap water, untreated oily wastewater and R1, R2 and R3 effluent treated plants obtained on 1st and 6th week of the study are shown in Fig.3.12.

Untreated hydrocarbon rich wastewater (diesel: 250 mg/L) had high phytotoxicity providing only 38.8±0.01 and 16.67±0.55% germinations in *Cicer arietinum* and *Vigna radiata*. Tap water provided 93±0.05 and 99.02±0.01% and AGR treated effluent provided approximately 80±0.50 and 95±0.2% germination percentages in *Cicer arietinum* and *Vigna radiata*, respectively. Hydrocarbon containing wastewater treated plants became yellowish and in 6 weeks they almost died with negligible chlorophyll contents. Diesel toxicity can be a possible reason to block electron transport of photosynthesis and causing iron, magnesium or zinc deficiencies slowing down chlorophyll production (Tripathi et al., 2013; Chow et al., 2018). In contrast, R3 effluent having 24.23±0.12 mg/L of hydrocarbon concentration provided maximum 0.53±0.045 and 0.74±0.021 mg/g F.W. cholorophyll in *Cicer arietinum* and *Vigna radiata* suggesting least phytotoxic effluent among the AGRs.

The study proved that AGR treated water having 24-77 mg/L hydrocarbon concentration had less phytotoxic effects which provided almost similar results as the non-toxic tap water treated plants. According to GC-MS results (Fig.3.8) degradation of diesel hydrocarbons ensured less phytotoxicity in AGR effluents. Similarly, incidents of enhanced plant germination index due to 71.6-73% removal of polyphenols and total petroleum hydrocarbons (C_6-C_{22}) from petroleum sludge (Aguelmous et al., 2018) and increased chlorophyll *a* synthesis in *Triticum aestivum* L. grown in bioremediated soil than untreated

Table 3.4 Statistical analysis of granule characteristics and reactor performance data of the AGRs

Reactor	**R1**		**R2**		**R3**		**Overall ANOVA**				
Operation time (day)	**1-70**		**1-70**		**1-70**						
	Mean	**SD**	**Mean**	**SD**	**Mean**	**SD**	**R-square**	**Coeff Var**	**Root MSE**	**Mean square**	**F-value**
Granule size (mm)	4.90	0.20	4.79	0.22	4.59	0.35	0.20	0.05	0.27	0.29	3.94
VSS (g/L)	6.46	0.09	5.76	0.52	5.43	0.70	0.43	0.08	0.51	2.98	11.44
SVI_{30} (mL/g)	24.87	1.12	31.33	5.87	33.27	7.87	0.30	0.19	5.70	213.21	6.54
GSV (m/h)	39.98	1.13	35.99	4.37	32.09	8.00	0.22	0.15	5.30	170.77	6.06
EPS (mg/g VSS)	402.40	3.48	370.70	23.36	359.80	34.31	0.38	0.06	24.05	24.05	9.31
PN (mg/g VSS)	355.10	3.72	318.23	24.65	307.45	35.13	0.42	0.07	24.87	6866.31	11.09
Hydrophobicity (%)	88.24	1.01	84.28	4.11	83.14	4.46	0.29	0.04	3.55	78.74	6.24
IC (%)	24.29	2.53	31.87	3.26	39.81	8.74	0.58	0.17	5.58	31.19	21.21
COD removal efficiency (%)	87.12	13.63	90.57	9.03	96.44	4.30	0.14	0.10	9.76	244.56	2.56
TPH removal efficiency (%)	81.32	12.64	90.71	8.55	95.31	4.32	0.29	0.10	9.16	1220.58	14.53
NH_4^+-N removal efficiency (%)	95.78	1.24	96.44	0.87	98.23	0.36	0.59	0.01	0.90	17.66	21.69

hydrocarbon-contaminated soil (Shen et al., 2016) suggested lesser phytotoxicity which is agreeing with our study.

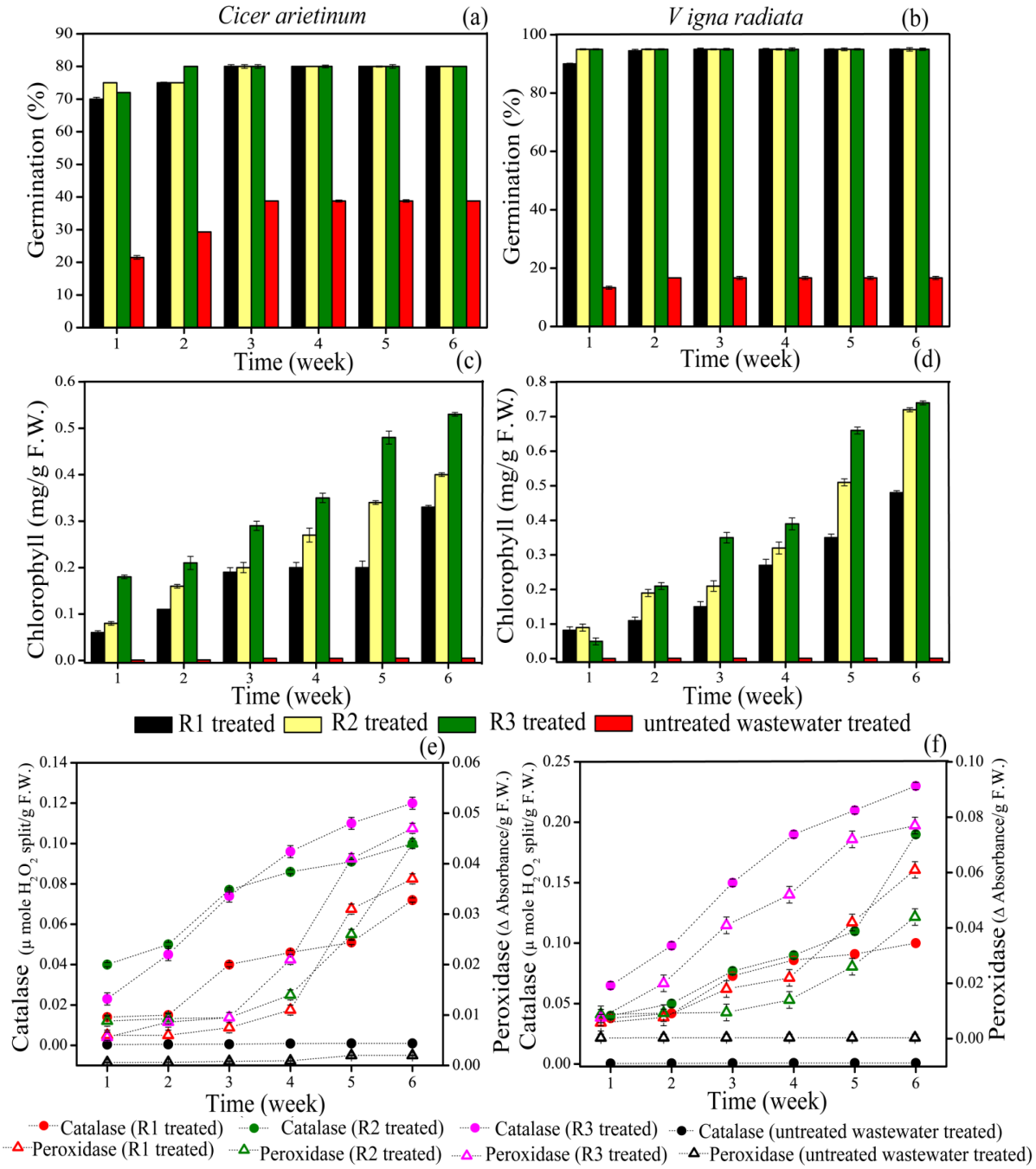

Fig.3.11 (a, b) Seed germination, (c, d) total chlorophyll and (e, f) comparative catalase and peroxidase profiles in *Cicer arietinum* and *Vigna radiata.*

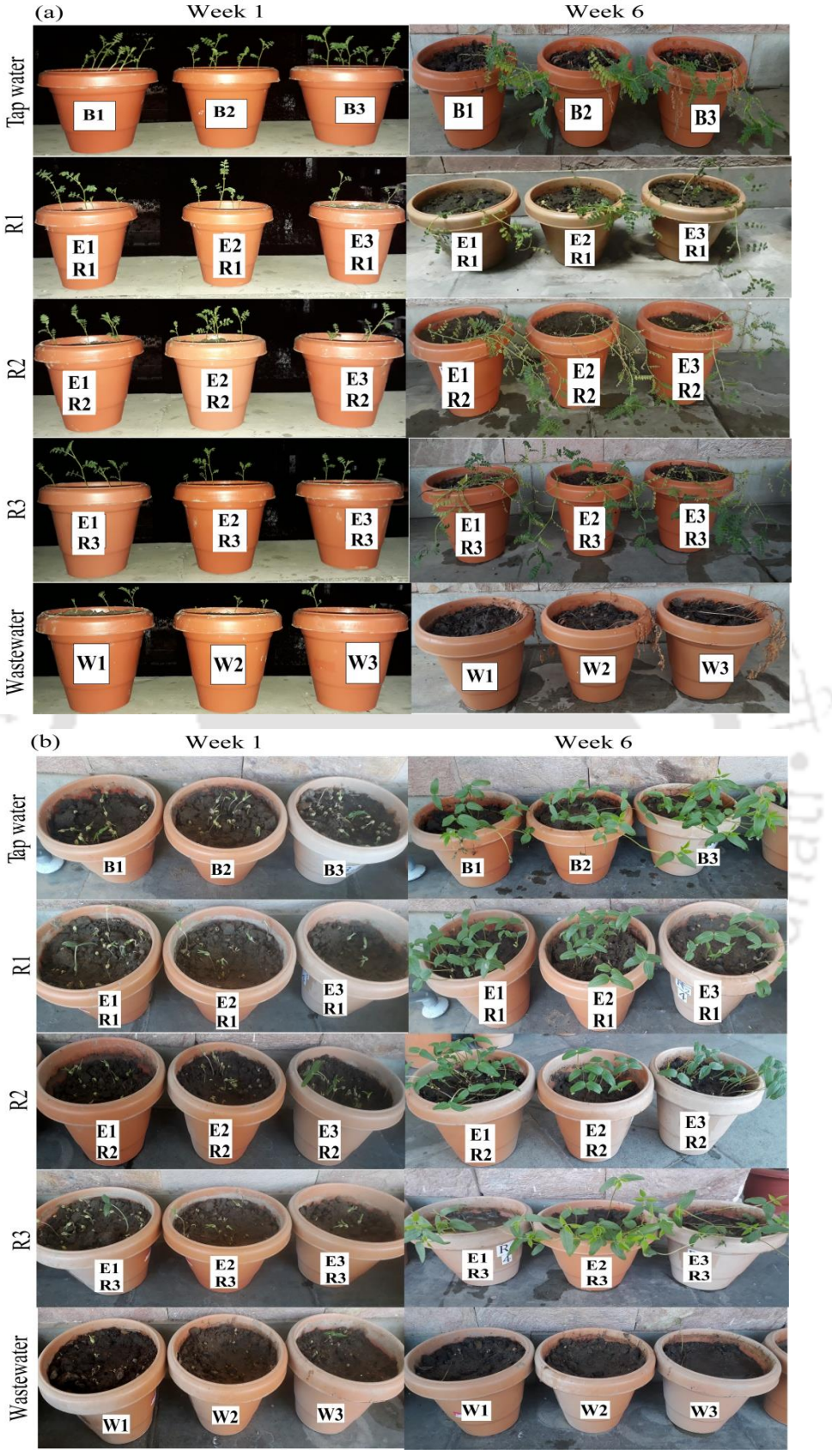

Fig.3.12 Tap water treated, untreated oily wastewater treated and R1, R2 and R3 effluent treated (a) *Cicer arietinum* and (b) *Vigna radiata*. [B, E and W stand for tap water treated, AGR effluent treated and oily wastewater treated plants, respectively].

Catalase and peroxidase are the two most important antioxidants and H_2O_2 scavengers. Six weeks phytotoxicity study provided highest catalase and peroxidase contents in tap water treated plants due to absence of toxic diesel whereas, diesel (250 mg/L) toxicity might have reduced in iron supply in plant system and iron translocation from active plant enzyme sites resulting into severe damage in antioxidant content (Chaterjee and Chaterjee, 2000). R1, R2 and R3 effluent treated plants (having 77-24 mg/L oil concentrations) obtained 0.1-0.23 µ mole H_2O_2 split/mg F.W. catalase and 0.037-0.077 Δ Absorbance/mg F.W. peroxidase contents providing minimum oxidative plant damage.

According to literature, poor biomass content in untreated diesel (250 mg/L) wastewater treated plants might have disrupted plant nitrogen metabolism hampering the synthesis of essential biomolecules like proteins, nucleic acids, coenzymes and nitrogen bases (Chow et al., 2018; Chaterjee and Chaterjee, 2000). But, R3 effluent provided maximum 10.89±0.28 and 8.65±0.04 mg/g F.W. protein contents in *Cicer arietinum* and *Vigna radiata* where low hydrocarbon content (24.23±0.12 mg/L) might be a possible reason of higher protein contents.

Six weeks of diesel exposure further affected the iron metabolism in oily wastewater treated plants reducing total carbohydrate content up to 0.03±0.01 mg/g F.W. in *Cicer arietinum and* 0.035±0.01 mg/g F.W. in *Vigna radiata*, respectively (Chaterjee and Chaterjee, 2000). Whereas, in tap water and AGR treated plants obtained carbohydrates between 1.39-1.17 mg/g F.W. in *Cicer arietinum* and 2.3-2.0 mg/g F.W. in *Vigna radiata*, respectively due to absence or reduced diesel (77-24 mg/L) content.

3.4 Summary of the chapter

Shortest HRT (12 h) and highest hydrocarbon loadings in R1 promoted maximum granule size and EPS content. COD removal efficiency varied between 71.34±1 to 90.40±0.21% which was proportional to the operating HRT and hydrocarbon removal efficiency of the AGRs. Maximum nitrogen was utilized for biomass growth and only 2-20% complete nitrification took place in the AGRs. In R1 short HRT was responsible for partial degradation of medium chain alkanes (C_{11}-C_{15}) which probably converted into fatty acids (C_{13}-C_{18}) and in R2 and R3 longer HRTs (24 h, 24 h) allowed 79–90% degradation of hydrocarbon (C_6-C_7, C_9-C_{10}, C_{11}-C_{13}, C_{15}-C_{18}, C_{27}) which further followed the β-oxidation of the fatty acids. In phytotoxicity assay, AGR effluent treated plants achieved 80-95% germination. Hence, for better hydrocarbon removal AGR should be maintained between 24 to 48 h HRTs with 0.125-0.25 kg/m^3.day hydrocarbon loadings where effluent hydrocarbon should be approximately within 77 to 24 mg/L to avoid phytotoxicity after disposal.

References

Adav, S.S., Lee, D.-J., Show, K.-Y., Tay, J.-H., 2008. Aerobic granular sludge: recent advances. Biotechnology Advances 26, 411-423.

Aebi, H., 1984. Catalase in vitro. *Methods in Enzymology* 105, 121-126.

Aguelmous, A., El Fels, L., Souabi, S., Zamama, M., Yasri, A., Lebrihi, A., Hafidi, M., 2018. Petroleum sludge bioremediation and its toxicity removal by landfill in gunder semi-arid conditions. Ecotoxicology and Environmental Safety 166, 482-487.

Ambreen, S., Rehman, K., Zia, M.A., Habib, F., 2000. Kinetic studies and partial purification of peroxidase in soybean, Pakistan Journal of Agricultural Sciences 37, 119-122.

APHA, 2005. Standard Methods for the Examination of Water and Wastewater, twenty-first ed. American Public Health Association, Washington, DC, USA.

Cai, M., Yao, J., Yang, H., Wang, R., Masakorala, K. 2013. Aerobic biodegradation process of petroleum and pathway of main compounds in water flooding well of Dagang hydrocarbon field. Bioresource Technology 144, 100-106.

Campo, R., Di Bella, G. 2019. Petrochemical slop wastewater treatment by means of aerobic granular sludge: effect of granulation process on bio-adsorption and hydrocarbons removal. Chemical Engineering Journal 378, 122083.

Chen, C., Ming, J., Yoza, B.A., Liang, J., Li, Q.X., Guo, H., Liu, Z., Deng, J., Wang, Q., 2019. Characterization of aerobic granular sludge used for the treatment of petroleum wastewater. Bioresource Technology 271, 353-359.

Chatterjee, J., Chatterjee, C., 2000. Phytotoxicity of cobalt, chromium and copper in cauliflower, Environmental Pollution 109, 69-74.

Chow, Y., Lee, L., Zakaria, N., Foo, K., 2018. Phytotoxic effects of trivalent chromium-enriched water irrigation in *Vigna unguiculata* seedling. Journal of Cleaner Production 202, 101-108.

Coelho, A., Castro, A.V., Dezotti, M., Sant'Anna Jr, G. 2006. Treatment of petroleum refinery sourwater by advanced oxidation processes. Jornal of Hazardous Materials 137, 178-184.

Corsino, S.F., Campo, R., Di Bella, G., Torregrossa, M., Viviani, G., 2015. Cultivation of granular sludge with hypersaline oily wastewater. International Biodeterioration & Biodegradation 105, 192-202.

Esmaeil, A.-S., Drobiova, H., Obuekwe, C., 2009. Predominant culturable crude hydrocarbon-degrading bacteria in the coast of Kuwait. International Biodeterioration & Biodegradation 63, 400-406.

Ferhat, S., Mnif, S., Badis, A., Eddouaouda, K., Alouaoui, R., Boucherit, A., Mhiri, N., Moulai-Mostefa, N., Sayadi, S., 2011. Screening and preliminary characterization of biosurfactants produced by Ochrobactrum sp. 1C and Brevibacterium sp. 7G isolated from hydrocarbon-contaminated soil. International Biodeterioration & Biodegradation 65, 1182-1188.

Fritsche, W., Hofrichter, M. 2000. Aerobic degradation by microorganisms. Biotechnology. New York: John Wiley & Sons, 11, 146-164.

Ghangrekar, M., Asolekar, S., Joshi, S., 2005. Characteristics of sludge developed under different loading conditions during UASB reactor start-up and granulation. Water Research 39, 1123-1133.

Gobi, K., Mashitah, M., Vadivelu, V., 2011. Development and utilization of aerobic granules for the palm oil mill (POM) wastewater treatment. Chemical Engineering Journal 174, 213-220.

Hadibarata, T., Kristanti, R.A. 2012. Identification of metabolites from benzo [a] pyrene oxidation by ligninolytic enzymes of *Polyporus sp*. S133. Journal of Environmental Management 111, 115-119.

Hamza, R.A., Sheng, Z., Iorhemen, O.T., Zaghloul, M.S. and Tay, J.H., 2018. Impact of food-to-microorganisms ratio on the stability of aerobic granular sludge treating high-strength organic wastewater. Water research 147, 287-298.

Janga, N., Ren, X., Kim, G., Ahn, C., Cho, J. and Kim, I.S., 2007. Characteristics of soluble microbial products and extracellular polymeric substances in the membrane bioreactor for water reuse. Desalination 202, 90-98.

Khaing, T.-H., Li, J., Li, Y., Wai, N., Wong, F.-s. 2010. Feasibility study on petrochemical wastewater treatment and reuse using a novel submerged membrane distillation bioreactor. Separation and Purification Technology 7, 138-143.

Kostal, J., Suchanek, M., Klierova, H., Demnerova, K., Kralova, B., McBeth, D.L. 1998. *Pseudomonas* C12B, an SDS degrading strain, harbours a plasmid coding for degradation of medium chain length n-alkanes. International Biodeterioration & Biodegradation 42, 221-228.

Li, X.Y., Yang, S., 2007. Influence of loosely bound extracellular polymeric substances (EPS) on the flocculation, sedimentation and dewaterability of activated sludge. Water Research. 41, 1022-1030.

Liu, Y., Tay, J.-H., 2002. The essential role of hydrodynamic shear force in the formation of biofilm and granular sludge. Water Research 36, 1653-1665.

Liu, Y., Tay, J.-H., 2004. State of the art of biogranulation technology for wastewater treatment. Biotechnology Advances 22, 533-563.

Loureiro, D.B., Olivera, C., Tondo, M.L., Herrero, M.S., Salvatierra, L.M., Pérez, L.M. 2020. Microbial characterization of a facultative residual sludge obtained from a biogas plant with ability to degrade commercial B10 diesel oil. Ecological Engineering 144, 105710.

Ma, F., Guo, J.-b., Zhao, L.-j., Chang, C.-c., Cui, D. 2009. Application of bioaugmentation to improve the activated sludge system into the contact oxidation system treating petrochemical wastewater. Bioresource Technology 100, 597-602.

McSwain, B., Irvine, R., Hausner, M., Wilderer, P., 2005. Composition and distribution of extracellular polymeric substances in aerobic flocs and granular sludge. Applied and Environmental Microbiology 71, 1051-1057.

Metcalf, E., Eddy, H.I. 2003. Wastewater engineering; treatment and reuse. McGraw-Hill, Boston.

Milia, S., Malloci, E., Carucci, A., 2016. Aerobic granulation with petrochemical wastewater in a sequencing batch reactor under different operating conditions. Desalination and Water Treatment 57, 27978-27987.

Morgenroth, E., Sherden, T., Van Loosdrecht, M., Heijnen, J., Wilderer, P., 1997. Aerobic granular sludge in a sequencing batch reactor. Water Research 31, 3191-3194.

Moy, B.P., Tay, J.H., Toh, S.K., Liu, Y., Tay, S.L., 2002. High organic loading influences the physical characteristics of aerobic sludge granules. Letters in Applied Microbiology 34, 407-412.

Nkem, B.M., Halimoon, N., Yusoff, F.M., Johari, W.L.W., Zakaria, M.P., Medipally, S.R., Kannan, N. 2016. Isolation, identification and diesel-oil biodegradation capacities of indigenous hydrocarbon-degrading strains of *Cellulosimicrobium cellulans* and *Acinetobacter baumannii* from tarball at Terengganu beach, Malaysia. Marine Pollution Bulletin 107, 261-268.

Pan, S., Tay, J.H., He, Y.X., Tay, S.L., 2004. The effect of hydraulic retention time on the stability of aerobically grown microbial granules. Letters in Applied Microbiology 38, 158-163.

Pendashteh, A.R., Abdullah, L.C., Fakhru'l-Razi, A., Madaeni, S.S., Abidin, Z.Z., Biak, D.R.A., 2012. Evaluation of membrane bioreactor for hypersaline oily wastewater treatment. Process Process Safety and Environmental Protection 90, 45-55.

Rosman, N.H., Anuar, A.N., Chelliapan, S., Din, M.F.M., Ujang, Z., 2014. Characteristics and performance of aerobic granular sludge treating rubber wastewater at different hydraulic retention time. Bioresource Technology 161, 155-161.

Shen, W., Zhu, N., Cui, J., Wang, H., Dang, Z., Wu, P., Luo, Y., Shi, C., 2016. Ecotoxicity monitoring and bioindicator screening of hydrocarbon-contaminated soil during bioremediation. Ecotoxicology and Environmental Safety 124, 120-128.

Tay, J.H., Ivanov, V., Pan, S., Tay, S.L. 2002. Specific layers in aerobically grown microbial granules. Letters in Applied Microbiology 34, 254-257.

Tomar, S.K., Chakraborty, S., 2018a. Characteristics of aerobic granules treating phenol and ammonium at different cycle time and up flow liquid velocity. International Biodeterioration & Biodegradation 127, 113-123.

Tomar, S.K., Chakraborty, S., 2018b. Effect of air flow rate on development of aerobic granules, biomass activity and nitrification efficiency for treating phenol, thiocyanate and ammonium. Journal of Environmental Management 219, 178-188.

Tripathi, P., Singh, P.C., Mishra, A., Chaudhry, V., Mishra, S., Tripathi, R.D., Nautiyal, C.S., 2013. Trichoderma inoculation ameliorates arsenic induced phytotoxic changes in gene expression and stem anatomy of chickpea (*Cicer arietinum*). Ecotoxicology and Environmental Safety 89, 8-14.

Wan, C., Sun, S., Lee, D.-J., Liu, X., Wang, L., Yang, X., Pan, X. 2013. Partial nitrification using aerobic granules in continuous-flow reactor: rapid startup. Bioresource Technology 142, 517-522.

Yu, G.-H., Juang, Y.-C., Lee, D.-J., He, P.-J., Shao, L.-M., 2009. Enhanced aerobic granulation with extracellular polymeric substances (EPS)-free pellets. Bioresource Technology 100, 4611-4615.

Yu, L., Han, M., He, F., 2017. A review of treating hydrocarbony wastewater. Arabian journal of chemistry 10, S1913-S1922.

Zhang, H., He, Y., Jiang, T., Yang, F., 2011 (a). Research on characteristics of aerobic granules treating petrochemical wastewater by acclimation and co-metabolism methods. Desalination 279, 69-74.

Zhang, Z., Hou, Z., Yang, C., Ma, C., Tao, F., Xu, P. 2011 (b). Degradation of n-alkanes and polycyclic aromatic hydrocarbons in petroleum by a newly isolated *Pseudomonas aeruginosa* DQ8. Bioresource Technology 102, 4111-4116.

Chapter 4

Refinery wastewater treatment by bioaugmenting *Micrococcus aloeverae* strain SG002

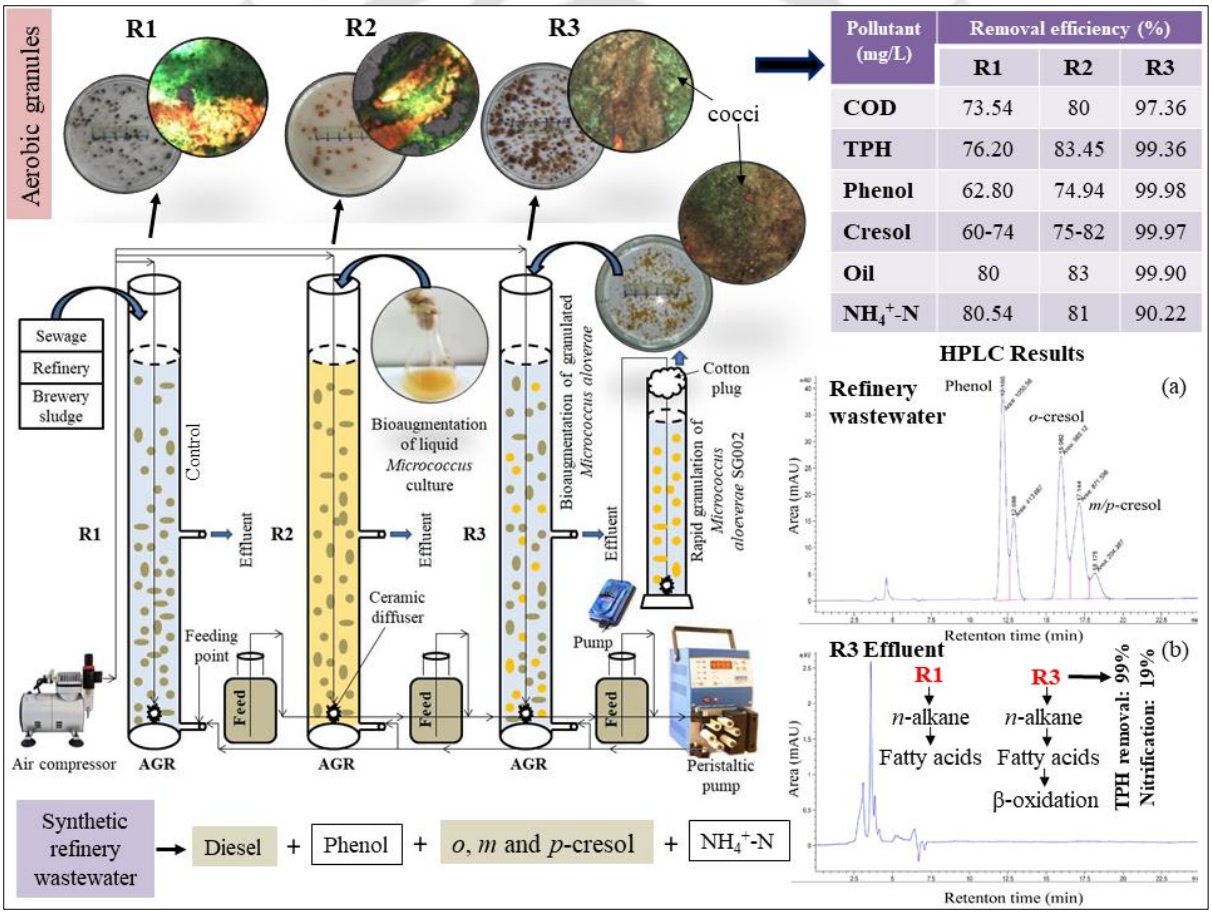

Pollutant (mg/L)	Removal efficiency (%)		
	R1	R2	R3
COD	73.54	80	97.36
TPH	76.20	83.45	99.36
Phenol	62.80	74.94	99.98
Cresol	60-74	75-82	99.97
Oil	80	83	99.90
NH_4^+-N	80.54	81	90.22

CHAPTER 4

Refinery wastewater treatment by bioaugmenting *Micrococcus aloeverae* strain SG002

This chapter is about rapid granulation of oil degrader *Micrococcus aloeverae* strain SG002 and its most efficient mode of bioaugmentation in AGRs in multiple hydrocarbon laden refinery wastewater treatment.

4.1 Introduction

Petroleum refining process produces wastewater containing hazardous contaminants like oil, phenols, cresols and dissolved minerals (Karray et al., 2020). The slow biodegradability, chemical complexity and toxicity of the refinery wastewater are the hitches to successful bioremediation.

Aerobic granular system faced initial granule rupture in recalcitrant hydrocarbon exposure and breakage of ammonia oxidizing layer promoted poor nitrogen removal (30-50%) while treating petrochemical, coal gasification or hypersaline oily wastewater containing 5.6-250 mg/L of influent oil (Zhang et al., 2011; Chen et al., 2019; Milia et al., 2016; Corsino et al., 2015). Remediation of individual contaminants like oil, phenol or cresols are reported in AGRs (Campo and Di Bella, 2019; Tomar and Chakraborty, 2020; Jeemat at al., 2014), but aerobic granulation in high strength (with >300 mg/L of hydrocarbon) refinery wastewater laden with multiple hydrocarbons (like, phenol, cresol and oils) is not well investigated. In most of the studies, matured granulation from mixed sludge inoculum took approximately 30 to 50 days of AGR operation (Zhang et al., 2011; Chen et al., 2019). Hence, slow granulation is another problem which can be solved with rapid and cost-effective development of hydrocarbon degrading aerobic granules.

Bioaugmentation process enhances the process efficiency of a rector by augmenting a particular microorganism or a consortium with pollutant degrading properties. Researchers used either liquid culture of pure strain, consortium, flocculent activated sludge or genetic mode of bioaugmentation in AGRs. Liquid culture augmentation of *Rhizobium* sp. NJUST18 and a combination of *Rhizobium* and *Shinella granuli* NJUST29 enhanced pyridine removal efficiencies in AGRs (Liu et al., 2015; Liang et al., 2018). Jiang et al. (2006, 2007) used liquid culture of two coaggregating and similar bacterial strains for bioaugmentation whereas, Ma et al. (2012) reported plasmid pJP4 mediated bioaugmentation in AGR system. In another study, Jemaat et al. (2013) bioaugmented *p*-nitrophenol (PNP) degrading flocculent sludge in

AGR for phenol, 2,4-dichlorophenoxyacetic, chlorophenol and PNP removal, respectively. Moreover, bioaugmentation of *Enterobacter cloacae* and a hydrocarbon degrading liquid consortium successfully accomplished 7.9-75% total phenolic hydrocarbon (TPH) degradation in diesel and petroleum contaminated soil (Bento et al., 2005; Hua et al., 2010). However, the most appropriate approach of bioaugmentation in AGR is not well explored. We isolated *Micrococcus aloeverae* strain SG002 from petroleum sludge biogranules which was discussed in Chapter 2. *Micrococcus* had almost 61% oil degrading capacity in 48 h indicating bioaugmentation potential in oily wastewater treatment.

The aim of the study was to establish a rapid and cost-effective granulation of oil degrader *Micrococcus aloeverae* outside AGR and to thoroughly investigate on the most efficient approach of biougmentation to reduce granule disintegration and increase organics removal efficiency with biodegradation analysis including higher nitrification efficiency in multi-pollutant laden refinery wastewater.

4.2 Materials and methods

4.2.1 Chemicals and reagents

Chemicals required for feed preparation, microbial staining, sludge and effluent analysis are described in Chapter 2 and Chapter 3 (section 2.2.1 and 3.2.1). For HPLC study, HPLC grade acetonitrile was procured from Merck, India and 99% pure phenol, *o*-cresol, *m*-cresol and *p*-cresol were purchased from HiMedia, India and Sisco Research Laboratories Pvt. Ltd.

4.2.2 Characterization of refinery wastewater

Wastewater sample was collected from the effluent treatment plant of Indian Oil Corporation Limited (IOCL), Guwahati, India. It was a combined wastewater of effluents generated from different units of the refinery which was collected after gravitational separation of heavy oil and just before entering into the dissolved air floatation (DAF) unit for chemical treatment. Sample was stored at 4 °C in an air tight container for characterization. COD and total phenolic hydrocarbon (TPH) values in the wastewater were within 1300-1450 mg/L and 300-350 mg/L, respectively. Presence of emulsified oil and other aromatic hydrocarbons like, phenol and three isomers (ortho, meta, para) of cresols were found above the permissible limit. Trace amount of heavy metals like Fe, Co, Cu, Ni, Cr, Zn and Cd were also detected. pH of the wastewater was nearby 7.33±0.1. To conduct the AGR process, a synthetic refinery wastewater was composed according to the above characteristics. Real and synthetic refinery wastewater compositions are elaborated in Table 4.1. Diesel oil was emulsified in nonylphenol ethoxylate in 200:1 v/v ratio. About 1 mg/L of diesel oil, phenol and cresol contributed influent COD of 4, 2.3 and 2.5 mg/L, respectively. In

112 days of the study, COD and total phenolic hydrocarbon (TPH) concentrations gradually increased between 800-1300 mg/L and 200-330 mg/L, respectively. Phosphate buffer maintained influent pH 7 and trace metal solution provided mineral sources to the granules. Influent phenol and cresol concentrations were gradually increased between 20-50 mg/L.

Table 4.1 Real and synthetic refinery wastewater compositions

Real refinery wastewater			
Parameters	**Concentration**	**Parameters**	**Concentration**
Physical properties		Cl^-	250 mg/L
pH	7.33	S^{-2}	59.20 mg/L
Conductivity	9.44 mS/cm	*Metallic properties*	
Total dissolved solids (TDS)	445 mg/L	Na	116.26 mg/L
Total solid (TS)	0.89 mg/L	K	108.04 mg/L
Alkalinity	32.66 mg/L as $CaCO_3$	Ca	0.26 mg/L
Turbidity	62.2-62.8 NTU	Fe	3.09 mg/L
Petroleum properties		Mn	0 mg/L
Total phenolic hydrocarbon	300-350 mg/L	Co	1.79 mg/L
Phenol	39-50 mg/L	Pb	0 mg/L
o-cresol	40-41 mg/L	Cu	0.015 mg/L
m, p-cresol	30-32 mg/L	Ni	0.24 mg/L
COD	1300-1450 mg/L	Cr	0.55 mg/L
NH_4^+-N	50-51 mg/L	Zn	0.22 mg/L
NO_3^-	0 mg/L	As	0 mg/L
PO_4^{-3}	250 mg/L	Cd	0.113 mg/L
SO_4^{-4}	100 mg/L		

Synthetic refinery wastewater			
Parameters	**Concentration**	**Parameters**	**Concentration**
Emulsified diesel	145-233 mg/L	*m, p*-cresol	20-30 mg/L
NH_4Cl	50 mg/L	Phosphate buffer[a]	1 mg/L
Phenol	30-50 mg/L	Trace metal solution[b]	1 mg/L
O-cresol	20-40 mg/L	$NaHCO_3$	As per requirement

[a]Phosphate buffer contained (g/L): 72.3 KH_2PO_4 and 104.5 K_2HPO_4.
[b]Trace metal solution contained (mg/L): 10,000 $MgSO_4.7H_2O$, 10,000 $CaCl_2.2H_2O$, 5000, $FeCl_3.6H_2O$, 1000 $CuCl_2$, 1000 $ZnCl_2$, 500 $NiCl_2.6H_2O$ and 500 $CoCl_2$.

4.2.3 Rapid small-scale granulation of *Micrococcus*

Pre-isolated *Micrococcus aloeverae* strain SG002 cells were grown overnight in 100 mL nutrient broth inside 250 mL conical flasks at 180 rpm shaking incubation at 37 °C temperature. Culture was centrifuged at 8000 rpm for 15 min to collect biomass (Ho et al., 2009). About 3 g/L of fresh biomass was used as initial seed of granulation. We have used sterilized measuring cylinders, media, aeration pipes and cotton plugging for the study. Biomass was taken inside two measuring cylinders with 500 mL working volume. Continuous aeration (2 L/m) was provided into the cylinders through air pumps and volume

exchange ratio (VER) was maintained at 50%. In every 3 days, the cylinders were fed with fresh feed (synthetic refinery wastewater) containing 1300 mg/L COD, 50 mg/L ammonia nitrogen, 234 mg/L emulsified diesel, 50 mg/L of phenol, 40 mg/L *o*-cresol, 30 mg/L of *m* and *p*-cresol, respectively. Trace metal and phosphate buffer were also provided for bacterial growth.

4.2.4 AGR set-up and operation

Three AGRs (R1, R2, R3) were configured with 3 L working volume, 5 cm diameter, 153 cm working height with 30.56 height to diameter ratio. AGR operation started with hydrocarbon degrading pre developed mixed inoculum (sewage:refinery:brewery sludge in 1:1:1 w/w ratio) aerobic granules discussed in Chapter 3. R1 was kept as blank reactor without bioaugmentation whereas liquid culture and granular bioaugmentation of *Micrococcus aloeverae* strain SG002 was studied in R2 and R3, respectively.

They were operated with 16 h HRT and 50% VER with 3 cycles per day comprising 22 min feeding, 450 min aeration and 5-3 min of granule settling time in each cycle. About 2 L/min airflow velocity by a compressor and 2.07 m/h of feed up-flow velocity through a peristaltic pump were maintained throughout the study. The first 21 days of AGR operation was the start-up phase and from day 22 to 112 was considered as the steady-state when influent COD was stable at 1300 mg/L.

4.2.5 Bioaugmentation

Bioaugmentation process with AGR schematic is described in Fig.4.1. About 500 mL of liquid culture of hydrocarbon degrading *Micrococcus aloeverae* strain SG002 with 3.6 g/L of VSS was augmented in R2 which was 10% of the existing biomass (6.03±0.05 g/L) of the AGR. Granulated *Micrococcus* (grown in 15 days) was bioaugmented into R3 reactor containing mixed sludge granules for their performance improvement. About 200 mL of *Micrococcus aloeverae* granules having 9 g VSS/L concentration was added into R3 which was also 10% of the reactor biomass. Though literature suggested biomass application of 5% (w/w) of reactor biomass for successful bioaugmentation, we kept it 10% to avoid washout from AGRs in toxic refinery wastewater (Jemaat et al., 2013). Bioaugmentation was repeated in every 21 days interval and the study continued up to 112 days. Table 4.2 describes the bioaugmentation doses in chronological order in R2 and R3.

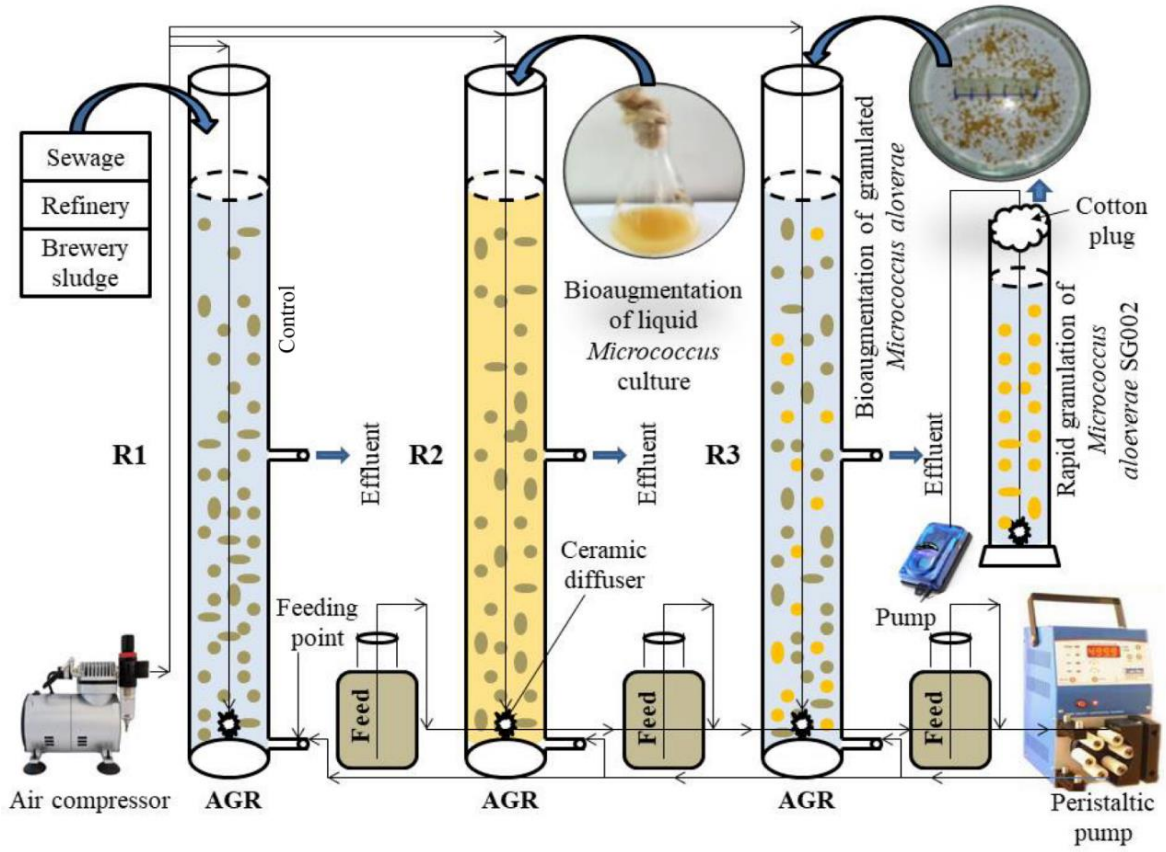

Fig.4.1 Control mixed granular sludge in R1 and bioaugmentation of liquid and granulated *Micrococcus aloeverae* strain SG002 in R2 and R3.

Table 4.2 Details of liquid and granular *Micrococcus* bioaugmentation doses applied to R2 and R3

Day	No. of dose	R2			R3		
		VSS inside reactor (g/L)	Augmented liquid biomass (g)	Percentage of augmentation (%)	VSS inside reactor (g/L)	Augmented granular biomass (g)	Percentage of augmentation (%)
21	1	5.81±0.07	1.74±0.12	10	7.23±0.07	2.17±0.01	10
42	2	5.8±0.12	1.74±0.02	10	8.37±0.21	2.51±0.05	10
63	3	6.67±0.25	2±0.01	10	8.37±0.25	2.51±0.01	10
84	4	6.66±0.05	1.99±0.13	10	8.4±0.05	2.52±0.02	10
105	5	6.67±0.04	2±0.01	10	8.3±0.09	2.49±0.12	10

4.2.6 Analytical procedure

The blank studies to check the pollutant removal by air volatilization and adsorption on dead granule surfaces were done according to chapter 2 (section 2.2.6.3). Effluent nitrate (NO_3^-) and nitrite (NO_2^-) concentrations along with SO_4^{-2}, PO_4^{-3} and Cl^- in the refinery wastewater were checked by ion chromatography (792 Basic IC, Metrohm) using anion column (Metrosep A Supp 5, 250/4.0 mm) and carbonate eluent maintaining a flow-rate of 0.7 mL/min and column pressure of 11-13 MPa. Heavy metals were detected in atomic

adsorption spectroscopy (Make: Varian, Netherlands, model: AA240). Flame photometer was used to detect Na, K and Ca (Make: Systronics, model: 128). Turbidity of the wastewater was measured by Nephelometric Turbidity meter (Systronics, model: 132) by calibrating with 100 and 50 NTU standard turbidity solutions. Procedures of reactor activity study, FESEM along with GC-MS, sludge and effluent analysis are discussed in Chapter 2 (section 2.2.6). CLSM analysis was conducted according to Chapter 3 (section 3.2.6).

4.2.7 Phenol and cresol detection by high-performance liquid chromatography (HPLC)

Phenol and cresol concentrations were measured by using HPLC technique. Feed and effluent samples were centrifuged and filtered through 0.2 µm syringe filters and then analyzed in HPLC (Agilent Technologies) having C-18 reverse phase column (250 mm × 4.6 mm; 5 µm pore size) and UV-vis detector operated at 275 nm wavelength. The mobile phase was a mixture of acetonitrile and water (40:60 v/v) which was applied at 0.5 mL/min flowrate at 27 °C temperature. For instrument calibration, standard curves of phenol and cresols were prepared (Fig.A4-A6) by using known concentration of 99% pure phenol, *o*-cresol, *m*-cresol and *p*-cresol purchased from HiMedia and Sisco Research Laboratories Pvt. Ltd.

In steady state, AGR effluents were taken out in 2 h intervals of a cycle for gravimetric and chromatography analysis to check hydrocarbon and NH_4^+-N degradation kinetics.

4.3 Results and discussion

4.3.1 *Micrococcus* granulation in refinery wastewater

Images of *Micrococcus* originated, control and bioaugmented granules are given in Fig.4.2. After 7 days of inoculation, *Micrococcus* granulation was initiated in synthetic refinery wastewater inside the measuring cylinders. Spherical or rod shaped, light yellowish matured granules (Fig.4.2a) were formed in 15 days having 0.5±0.02 mm diameter and 4.8±0.5 g/L VSS content. The initial F/M ratio was 0.76 g COD/g SS.day which decreased up to 0.27 g COD/g SS.day in 15 days suggesting better granule biomass density and settling properties (Hamza et al., 2018). Granules were highly settleable with 36±1.3 mL/g SVI_{30} value. EPS concentration increased up to 63.22±1.5 mg/g VSS and integrity coefficient (IC) reached 15±1% determining high granule strength. We utilized the day 15 granules for AGR augmentation and continued the study till day 30 to check maximum granule efficiency.

Granulated *Micrococcus* achieved 80-90% COD removal. NH_4^+-N and TPH removal efficiency varied between 62-95% in 30 days. Table 4.3 provides details of *Micrococcus* biomass characteristics and pollutant removal efficiencies before and after granulation.

Table 4.3 Characteristics and pollutant removal efficiencies of *Micrococcus aleoverae* SG002 granules in refinery wastewater

Granule Characteristics	**Values**			**Pollutants (mg/L)**	**Influent**	**Removal (%)**		
	Day 0	**Day 15**	**Day 30**			**Day 0**	**Day 15**	**Day 30**
Diameter (mm)	0.07±0.002	0.5±0.02	0.62±0.2	COD	1300	60±1	78.12±0.2	90.52±1
VSS (g/L)	1.7±0.12	4.8±0.5	6.72±0.43	NH_4^+-N	50	80±1.2	90±1.43	99±1.5
GSV (m/h)	20±0.7	29±1.3	39±1	TPH	330	62±0.7	81±1.4	90.48±1.3
SVI (mL/g)	63±1.2	36±1.2	28.4±1	Phenol	50	56±0.54	90.1±1	99±1
EPS (mg/g VSS)	27.21±0.56	63.22±1.5	120.50±2.7	*o*-cresol	40	57±0.23	91±0.76	99±0.77
PN (mg/g VSS)	20.40±0.55	49.22±2	96.56±1.5	*m*-cresol	30	56±0.67	91±1	99±0.67
PS (mg/g VSS)	6.8±0.12	14±0.5	24.12±0.45	*p*-cresol	30	56±1	91±1.5	99±1
IC (%)	36±0.23	15±1	9±0.4	Emulsified diesel	230	61±0.8	77.4±1.5	87±1.4
Hydrophobicity (%)	42±1	75±1.5	82±1					

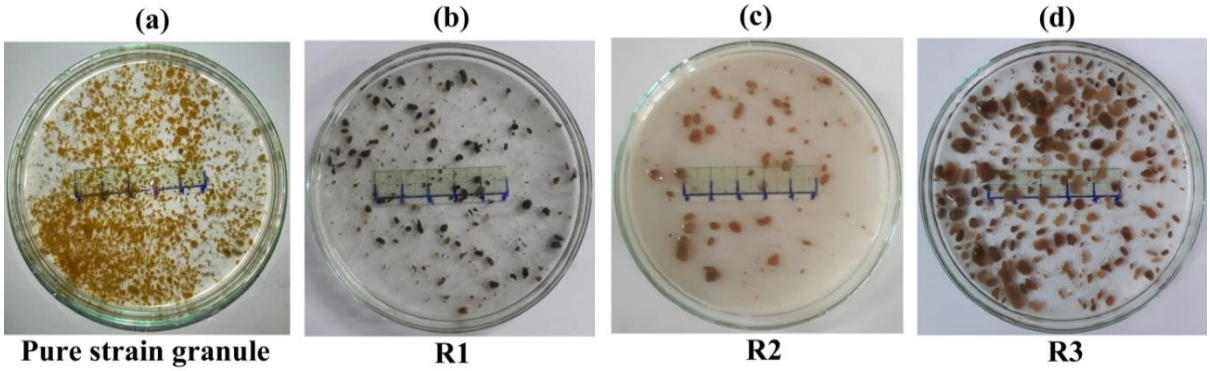

Fig.4.2 Images of (a) *Micrococcus* strain originated, (b) non-augmented, (c, d) liquid and granular culture bioaugmented granules cultivated in the steady state of R1, R2 and R3 (scale: 1 unit =1 cm).

Corynebacterium sp. DJ1, *Acinetobacter calcoaceticus* and other auto or coaggregator strains took almost 60-150 days for matured granulation to degrade 250-2000 mg/L of single pollutant phenol (Jiang et al., 2006, 2007; Adav and Lee, 2008; Ho et al., 2009). However, rapid (15 days) small-scale matured granulation of *Micrococcus aloeverae* in multiple hydrocarbons laden refinery wastewater achieving above 80% organics removal is reported for the first time. Removal of operational cost for air compressor and peristaltic pump were the added benefits of this process.

4.3.2 Characterization of granules without bioaugmentation

Granule size, VSS, IC, Comparative SVI_{30} with GSV, EPS with PN and granule hydrophobicity trends in the AGRs are described in Fig.4.3. The initial mixed sludge granules had 4.51±0.05 mm average size with 6.03±0.05 g/L VSS and 400±0.5 mg/g VSS of EPS content. In control R1, presence of recalcitrant oil, phenol and cresols turned the granules blackish with size reduction up to 3.33±0.45 mm in 63 days of AGR operation (Fig.4.2b). Due to flocculent biomass washout F/M ratio reached 0.35 g COD/g SS.day, which affected granule settleability (Hamza et al., 2018). Reduced settleability further increased granule SVI_{30} between 40-45 mL/g and hampered the GSV values till 26±1 m/h. IC was 30-40% and granule hydrophobicity reduced up to 64±07% due to decreasing granule strength in refinery wastewater.

Till day 63, hydrocarbon toxicity affected the EPS secretion (Fig.4.3e) leading to granule disintegration and less compact microscopic structure (Fig.4.4) in R1. Initial granule breakage and instability phenomena observed in petroleum wastewater treatment in Chapter 2 and in previous literature (Zhang et al., 2011) supported our current results. However,

between day 63-112, gradually the granule diameter, VSS, GSV and EPS achieved stability at 3.14±0.07 mm, 3.70±0.5 g/L, 26.65±0.67 m/h and 270.87±1.2 mg/g VSS, respectively.

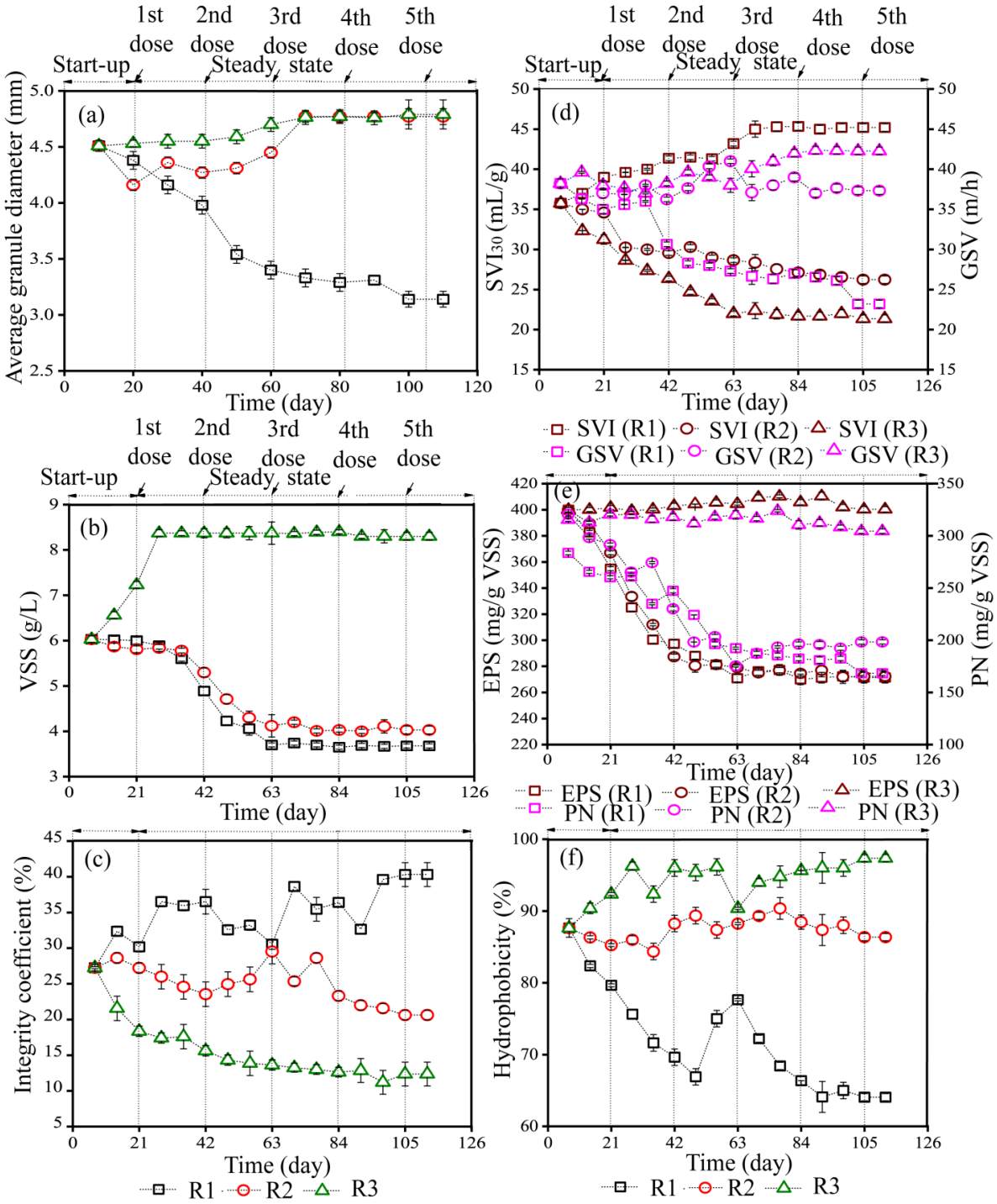

Fig.4.3 (a) Granule diameter, (b) VSS, (c) integrity coefficient, (d) comparative SVI_{30} with GSV, (e) EPS with PN and (f) hydrophobicity trends in R1, R2, R3 AGRs during refinery wastewater treatment. [Dose determines *Micrococcus* bioaugmentation in every 21 days interval].

4.3.3 Properties of bioaugmented granules

The first two doses of liquid *Micrococcus* augmentations (on day 21 and 42) had no significant effect in R2 in controlling the granule rupture due to hydrocarbon exposure. Granule size and VSS followed similar declining trend as in R1 at 200-330 mg/L of influent TPH till day 63 (Fig.4.3a-b). After day 63, the third dose of bioaugmentation resulted into less granule rupture decreasing effluent VSS from 0.64 to 0.30 g/L and granules became light brownish (Fig.4.2c). The fourth (day 84) and fifth dose (day 105) of augmentation provided no further improvement in granule properties. However, as an effect of oil tolerant liquid *Micrococcus* culture augmentation, at 330 mg/L of TPH concentration, (day 63 onwards) R2 achieved nearly stable granule size, VSS and EPS content of 4.77±0.11 mm, 4.11±0.25 g/L and 272.32±1.7 mg/g VSS, respectively. Granule settleability was improved with 26-27 mL/g SVI_{30} and 37-38 m/h GSV in R2. As low IC determines more microbial integrity, 20-25% IC in R2 denoted moderate granule strength with 86-88% of cell hydrophobicity (Ghangrekar et al., 2005). PN concentration moderately increased within 175-198 mg/g VSS and PN:PS ratio was 3.5-4 till day 112 in R2. Literature evidences of activated sludge or liquid *Rhizobium* culture augmentations to enhance granule structural stability and settling by maintaining about 40 m/h GSV and 14-25 mL/g SVI in *o*-cresol and pyridine wastewaters are similar to our results in R2 (Jemaat et al., 2014; Liu et al., 2015).

In R3, the second granular *Micrococcus* augmentation imposed remarkable improvement in granule characteristics. Between day 63 to 84, granule diameter, VSS and EPS concentration rapidly increased and achieved stability at 4.76±0.07 mm, 8.37±0.14 g/L and 404.65±1.45 mg/g VSS, respectively (Fig.4.3a, b, e). After fourth augmentation, IC value reached 12±1% indicating high granule integrity (Fig.4.3c). On day 105, about 97% hydrophobicity with 304-310 mg/g VSS PN content maintained 3.7-4 PN:PS ratio in R3 (Fig.4.3f). Bigger (4.79±0.06 mm), denser (8.3±0.08 g/L) granules with compact microstructure (Fig.4.4) enhanced settling with maximum 42.28±0.47 m/h of GSV and 21.37±1 mL/g and SVI_{30} values. On day 105, lower F/M ratio in R3 (0.16 g COD/g SS.day) than R2 (0.32 g COD/g SS.day) was responsible for providing highly stable granules in R3 (Hamza et al., 2018).

Table 4.4 Impacts of different bioaugmentation techniques on granule properties and pollutant removal efficiencies in AGRs treating various industrial wastewaters

Wastewater	Mode of bioaugmentation	Reactor operating conditions	AG characteristics after bioaugmentation	Pollutant removal	Reference
Phenol wastewater	(i) About 2% (w/w) VSS of mono and coculture of coaggregating strains *Propioniferax*-like PG-02 and *Comamonas* sp. PG-08 were augmented into AGR	Volume of AGR: 2 L, cycle time: 4 h, VER: 50%, air flowrate: 1 L/min, settling time: 15 min, [a]F/M ratio: 1.5 g phenol/L.day	Size: 0.2-0.3 mm, biomass concentration: 6-7 g [b]SS/L, SVI: 34.7-47.9 L/g SS, F/M ratio: 0.24 g phenol/g SS.day.	The coculture of PG-02 and PG-08 helped in complete removal of 250 mg/L phenol in 2 days of AGR operation	Jiang et al. (2006)
	(ii) A mixture of phenol degrading *Pandoraea* sp. PG-01 (0.051 g dry weight/L) and *Rhodococcus erythropolis* PG-03 (0.112 g dry weight/L) was bioaugmented into AGR	Volume of AGR: 2 L, dia: 50 mm, cycle time: 4 h, HRT: 8 h, VER: 50%, air flowrate: 3 L/min, settling time: 5, 30 min	Size: 1-1.8 mm, SVI: 34.7-47.9 ml/g SS, biomass concentration: 5-6 g SS/L, SRT: 10-17 day	Strain PG-01 and PG-03 coexisted in the aerobic granules providing compact structure and almost complete removal of 250 mg/L of phenol	Jiang et al. (2007)
p-nitrophenol wastewater	About 15% (w/w) VSS of PNP degrading floccular sludge was augmented in the airlift reactor on day 0, day 7 and day 14 of the study	Volume of airlift reactor: 2.6 L, riser height: 750 mm, dia: 42.5 mm, downcomer dia: 62.5 mm, bottom to downcomer: 8 mm, air flowrate: 125-500 mL/min	Size: 1.5±0.2 mm, Biomass concentration: 2.4-3.2 g VSS/L, GSV: 70±5 m/h, SVI_5: 13±2 mL/g TSS, EPS: 60±7 mg/g VSS PN: 24±1 mg/g VSS, PS: 36±6 mg/g VSS, PS/PN: 1.50	Complete removal of 15 mg/L of PNP, 85% ammonium oxidation and less than 0.3% NO_3^--N in bioaugmented AGR with predominant *Acinetobacter*	Jemaat et al. (2013)
o-cresol wastewater	About 12% (w/w) VSS of PNP degrading activated sludge (Jemaat et al., 2014) was augmented into the reactor	Volume of airlift reactor: 2.6 L, riser height: 750 mm, dia: 42.5 mm, downcomer dia: 62.5 mm, bottom to downcomer: 8 mm, HRT: 0.85-2.3 day, upflow velocity: 0.4 cm/s, air flowrate: 250±50 mL/min	Size: 1.5±1.2 mm, biomass concentration: 40-90 mg/L, GSV: 40-70 m/h, SVI_5: 7-14 mL/g, SVI_{30}/SVI_5: 1, EPS: 38±6 mg/g VSS, PS/PN: 2.2	Partial nitration and complete *o*-cresol (100 mg/L) degradation in 150 days, shock loading resistance: 300-1000 mg/L	Jemaat et al. (2014)
2,4-dichlorophen-oxyacetic acid wastewater	(i) *Pseudomonas putida* SM1443 carrying plasmid pJP4 was augmented in 27 and 11% inoculation ratio in microcosm and AGR system, respectively.	Volume of AGR: 1.7 L, height: 87 cm, dia: 5 cm, cycle time: 6 h, VER: 50%, air flowrate: 3 L/min.	Size: 0.45-0.65 mm, biomass concentration: 5.8-7.5 g [c]MLSS/L, SVI: 24-32 mL/g, compact granules formed transconjugant after pJP4 transfer in the AGR	Nearly 83-99% COD and complete removal of 8-385 mg/L of 2,4-D following Haldane model.	Quan et al. (2010)
	(ii) *Pseudomonas putida* SM1443 carrying plasmid pJP4 was augmented in 10% inoculation ratio	Volume of AGR: 1.7 L, height: 87 cm, dia: 5 cm, cycle time: 6 h and 4 h, VER: 50%, air flowrate: 3 L/min,	Size: 0.6-0.72 mm, biomass concentration: 6 g MLSS/L, SVI: 20-30 mL/g,	Bioaugmented AGR had about 90% COD and 100% 2,4-D (500 mg/L) removal	Quan et al. (2011)

Chlorophenol wastewater	Previously pJP4 plasmid augmented 2,4-D degrading aerobic granules were used as AGR seed	Volume of AGR: 1.5 L, height: 80 cm, dia: 5 cm, cycle time: 4 h and 3 h, VER: 50%, air flowrate: 1.5-2 L/min, settling time: 5 min.	Size: 0.4-0. mm, biomass concentration: 6 g MLSS/L, SVI: 20-35 mL/g, EPS layered rod-shaped bacteria populated compact granules	About 99% degradation of 2,4-D (400 mg/L), 4-chlorophenol (45 mg/L), 2,4-dichlorophenol (25 mg/L) and 2,4,6-trichlorophenol (20 mg/L)	Ma et al. (2012)
Pyridine wastewater	(i) AGR was seeded with about 2 g (dry weight) of pyridine degrading and autoaggregating *Rhizobium sp*. NJUST18	Volume of AGR: 2.2 L, height: 100 cm, dia: 6 cm, VER: 50%, volumetric flowrate: 0.2 m^3/h, air velocity: 0.02 m/s.	Size: 0.5-1 mm, MLSS: 5.12±0.13 g/L, [d]MLVSS: 4.61± 0.17 g/L, SVI: 25±3.6 mL/g, GSV: 37.2 ± 2.7 m/h.	Full pyridine removal: 2600 m/L in pure *Rhizobium* and 4000 mg/L in aerobic granules in 7.5 h with 17-74 mg/L residual TOC in effluent	Liu et al. (2015)
	(ii) AGR was inoculated with 2 g (dry weight) of pyridine degrading or coaggregating *Rhizobium sp.* NJUST18, *Shinella granuli* NJUST29 and *Paracoccus versutus* NJUST32	Volume of AGR: 2.2 L, height: 100 cm, dia: 6 cm, VER: 50%, volumetric flowrate: 0.2 m^3/h, air velocity: 0.02 m/s.	Size: 0.2-0.5 mm, EPS: 232.79 mg/g VSS, [e]c-di-GMP content: 268.56 mg/g VSS, coaggregation index: 62.08%	NJUST18+NJUST29 combination had the strongest coaggregation achieving complete 1000 mg/L pyridine removal in AGR within 50 h	Liang et al. (2018)
Refinery wastewater	About 10% (w/w) VSS of liquid and granulated *Micrococcus aloeverae* SG002 was augmented in two AGRs 21 days intervals	Volume of AGR: 3 L, H/D: 30.56, cycle time: 8 h, HRT: 16 h, VER: 50%, feed up-flow velocity: 2.07 m/h, air flowrate: 2 L/min	Size: 4.77, 4.79 mm, VSS: 4.03. 8.3 g/L, GSV: 37.33, 42.28 m/h, SVI_{30}: 26.23, 21.37 mL/g, EPS: 272.32, 400.36 mg/g VSS, PS/PN: 3.5-4, IC: 20.63, 12.36 hydrophobicity: 86.36, 97.36%	About 80-97.36% COD, 81-90.22% NH_4^+-N, 83-99% TPH removal with 1-19% complete nitrification in *Micrococcus* augmented granules (influent TPH: 330 mg/L).	Current study

[a]F/M: Food/microorganism
[b]SS: Suspended solids
[c]MLSS: Mixed liquor suspended solids
[d]MLVSS: Mixed liquor volatile suspended solids
[e]c-di-GMP: cyclic diguanylate.

Moreover, the introduction of oil tolerant *Micrococcus* granules reduced granule rupture providing dark brownish stable granules in R3 (Fig.4.2d). Though granule size range (4.5-4.7 mm) was similar in R2 and R3, granulated *Micrococcus* helped in significant improvement of granule biomass concentration and strength validating that 10% granular bioaugmentation is more effective for granule characteristics than liquid culture in refinery wastewater treatment in AGR. Table 4.4 provides comparative impacts of several modes of bioaugmentations in granule quality and pollutant removal efficiencies in AGRs treating different recalcitrant wastewaters.

4.3.4 Granule micrograms

FESEM images (Fig.4.4) provided cocci dominated very dense *Micrococcus* granules grown in measuring cylinders on day 20 (at 5000×). On day 95, control granules in R1 had partially filamentous structure. Sparse distribution of *Micrococcus* on R2 granule surfaces signified that liquid culture augmentation had moderate impacts in improving granule microstructure. However, granular augmentation of *Micrococcus* in R3 provided dense cocci population on granule surfaces providing strong microbial granules with 11% IC which was similar to dominance of *Acinetobacter* and *Rhizobium* on bioaugmented *o*-cresol and pyridine degrading aerobic granules (Jemaat et al., 2014; Liu et al., 2015).

CLSM microscopy was carried out on day 100 of AGR steady-state (Fig.4.5). Extended fluorescence for SYTO 63, CON A and FITC in *Micrococcus*, R1, R2 and R3 granules indicated presence of good amounts of total cells, polysaccharides and proteins. Presence of cocci bacteria was more prominent in granule augmented R3 granules than liquid culture augmented R2 granules. High fluorescence for Sytox blue in R1 granules proved that absence of oil degrader *Micrococcus* was responsible for more proportion of dead cells in R1 than R2 and R3.

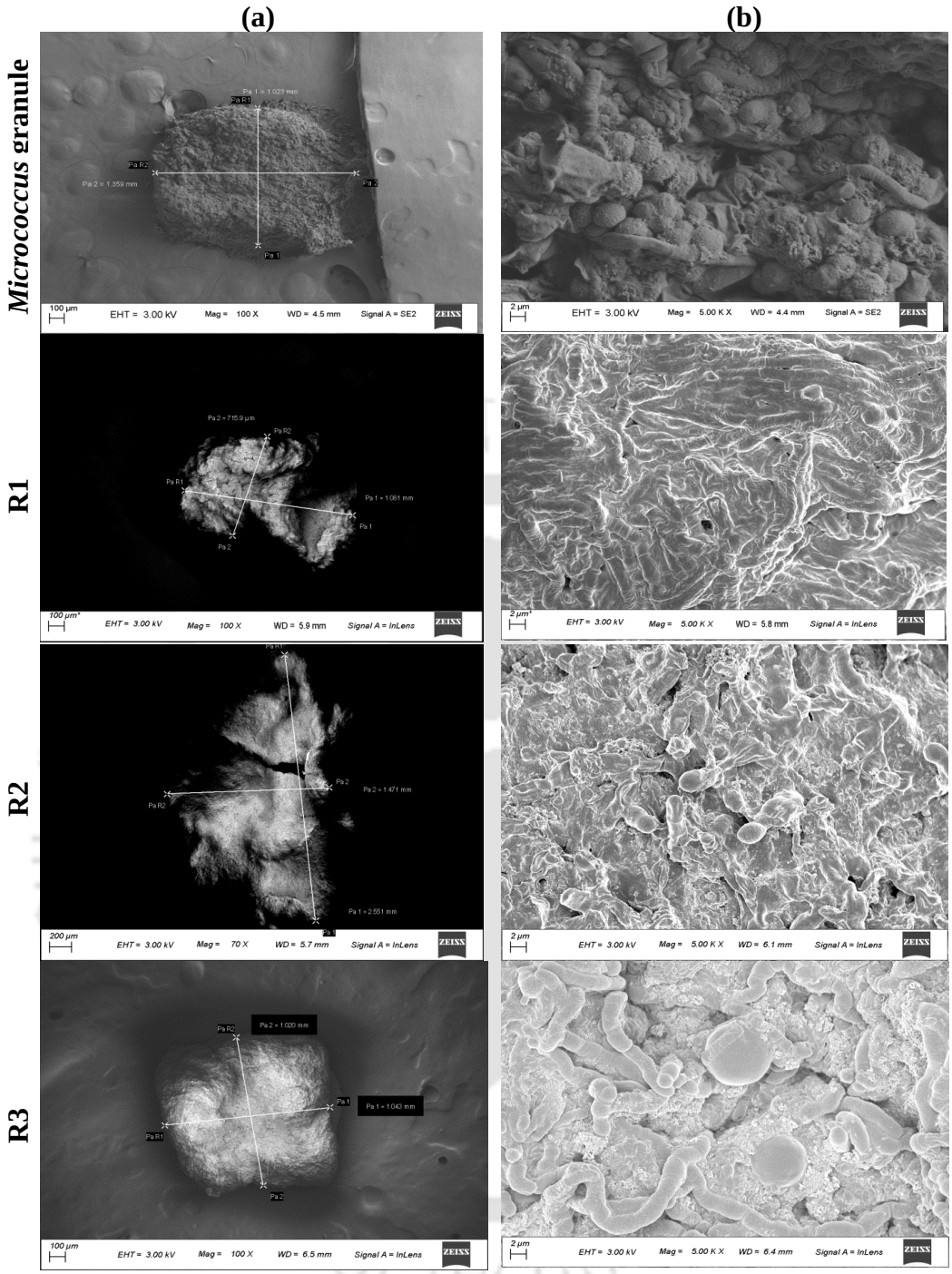

Fig.4.4 FESEM images of pure strain granules of *Micrococcus aloeverae* strain SG002 and non-bioaugmented R1 and bioaugmented R2 and R3 granules on day 95 of study (magnification: 5000×).

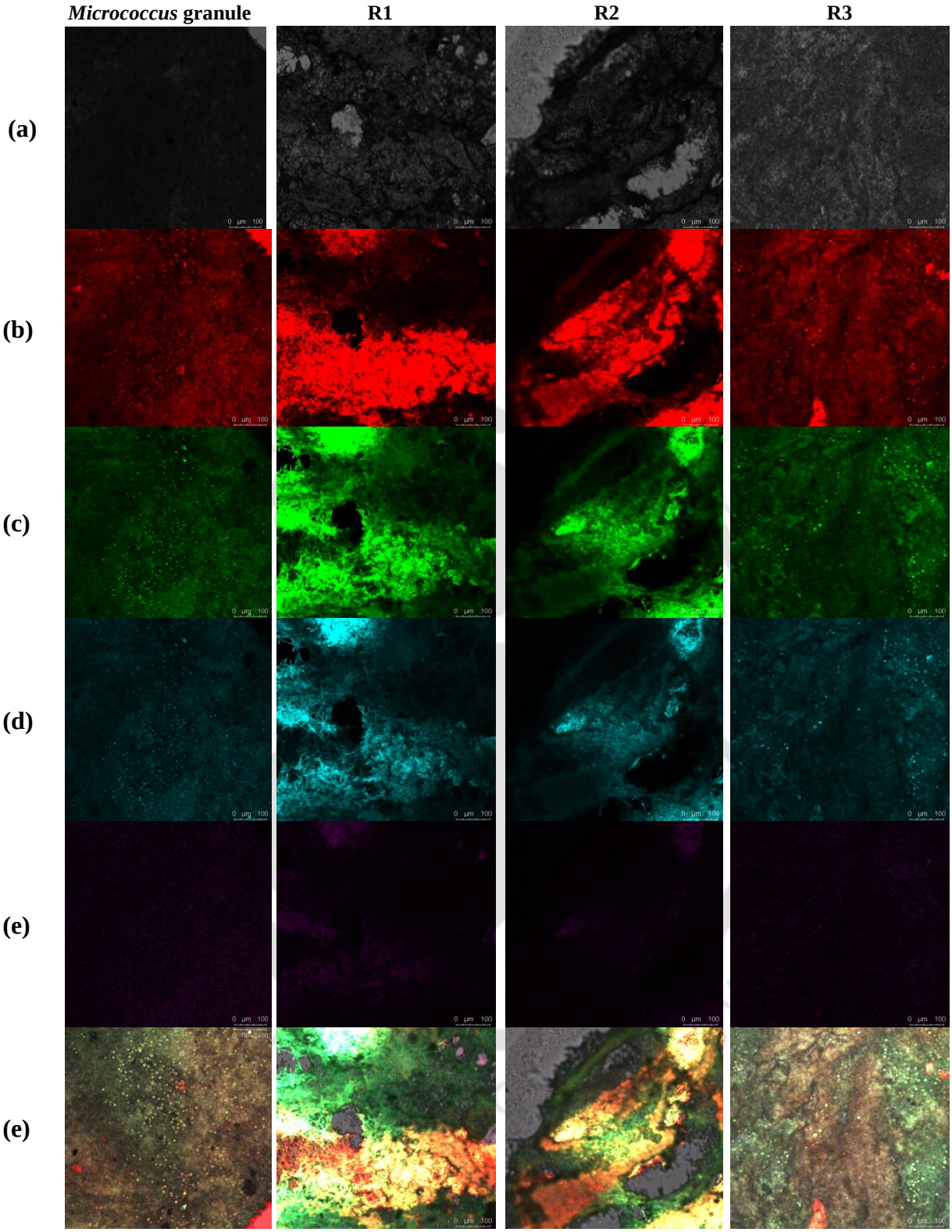

Fig.4.5 CLSM images of granules of *Micrococcus aloeverae* strain SG002 and R1, R2 and R3 AGRs on day 100 (Bar: 100 µm): (a) optical microscopic image (b) total cells (Syto 63); (c) proteins (FITC); (d) polysaccharides (Con A); (e) dead cells (Sytox Blue); (f) combined image of (b) and (e).

4.3.5 Evaluation of AGR performances

4.3.5.1 Organics removal efficiency with mechanism and reactor activity in AGRs

COD, TPH, phenol, cresols and emulsified diesel removal profiles are described in Fig.4.6. Organic loading rate (OLR) and influent TPH increased within 1.2-1.95 kg COD/m^3.day and 200-330 mg/L till achieving reactor stability (day 21) and remained constant at 1.95 kg COD/m^3.day till day 112. Hydrocarbon loading varied in 0.3-0.495 kg/m^3.day range. Corsino et al. (2015) observed oil inclusion in granule surfaces and Campo and Di Bella (2019) reported enhanced TPH bioadsorption in granule EPS layers during hypersaline oily wastewater treatment. Whereas, in steady state (day 22-112) of current study, about 0.5-1% hydrocarbon was removed by volatilization and adsorption in autoclaved granules indicating hydrocarbon degradation was a microbial phenomenon in the AGRs as observed in Chapter 2 (section 2.3.1).

GC-MS spectra and compounds of TPH removal are elaborated in Fig.4.7 and Table 4.5. HPLC data for the phenol and cresol profiles in feed and AGR effluents in every 2 h interval of a reactor cycle are given in Fig.4.8-4.10.

Control reactor R1 removed 89±1% COD at 200-250 mg/L TPH, 145-173 mg/L diesel, 30-40 mg/L phenol and 20-35 mg/L cresol concentrations. COD and TPH removal gradually decreased within 77-74% with increased recalcitrance of TPH (330 mg/L) and biomass washouts. However, according to HPLC data, R1 achieved stability in 63 days removing 62.8% phenol and 59-74% cresols.

GC-MS spectra indicated the presence of more than 27 *n*-alkanes with various short to long carbon chain (C_6-C_{44}) groups in refinery wastewater. After day 63, R1 treated effluent showed disappearance of some short and medium chain alkanes (C_8-C_{10}, C_{12}-C_{13}, C_{15}) suggesting 76.2% TPH removal in gravimetric results. Presence of benzene (C_6), tetradecane to hexadecane (C_{14}-C_{16}) and heptacosane to tetratetracontane (C_{27}-C_{44}) peaks accounted for 344 and 78.54 mg/L of remaining COD and TPH concentration in R1 effluent.

R1 also produced a fatty acid octadecadienoic acid (C_{18}) predicting a pathway where the methyl groups in *n*-alkanes are oxidized to alcohols and further transformed to aldehydes and fatty acids, respectively. Finally, the fatty acid forms acetyl-CoA which may take part in β-oxidation producing metabolic energy to the granule microorganisms (Cai et al., 2013).

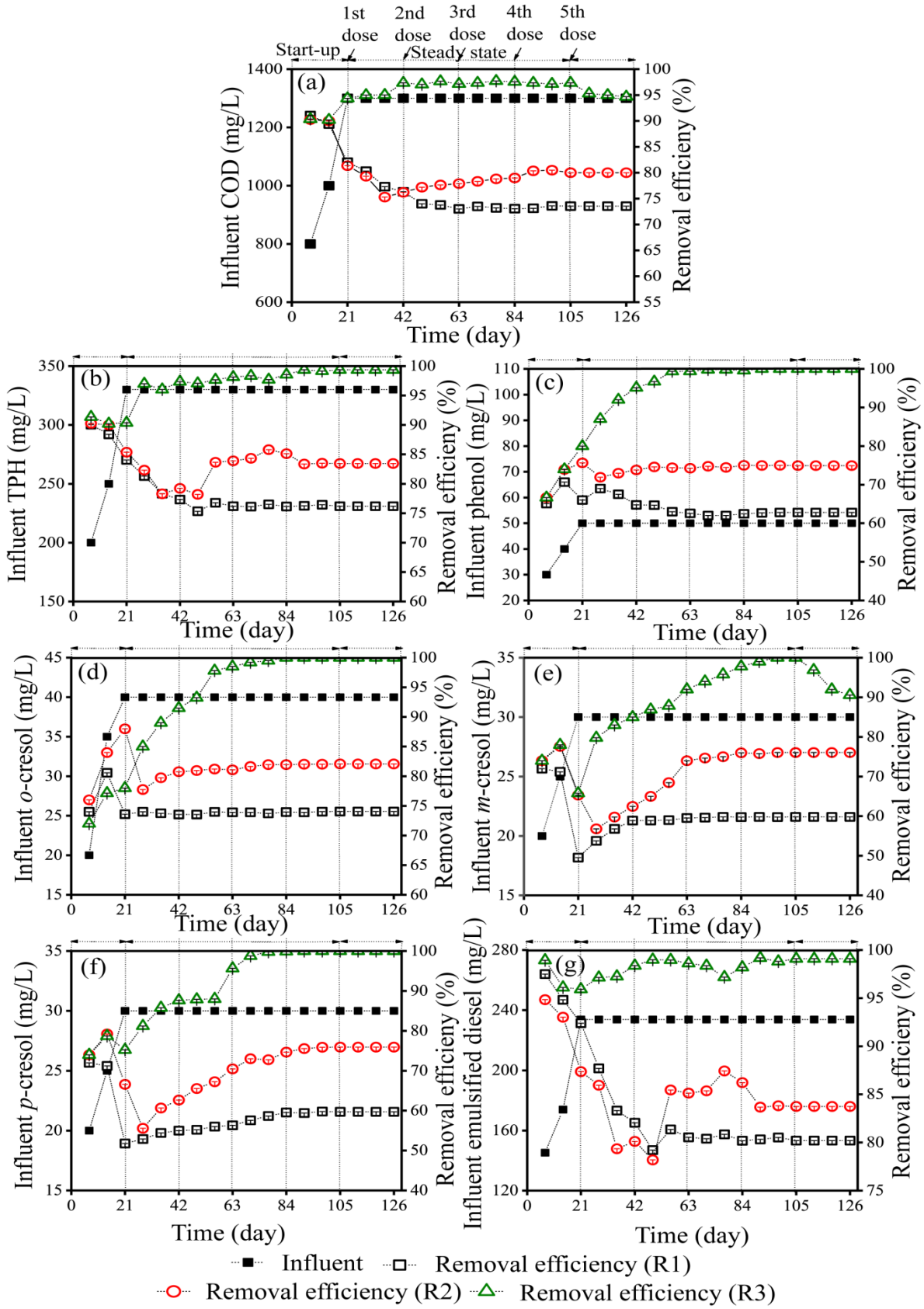

Fig.4.6 (a) COD, (b) TPH, (c) phenol, (d) *o*-cresol, (e) *m*-cresol, (f) *p*-cresol and (g) emulsified diesel removal performances of R1, R2 and R3. [Dose determines *Micrococcus* bioaugmentation in every 21 days interval].

Octadecadienoic acid (C_{18}) remained as a proof intermediate of alkane aerobic biodegradation pathway in R1 effluent. The pathway is discussed in details in section 3.3.3.1 and illustrated in Fig.3.9 of Chapter 3. AGR performances were further evaluated by reactor activity which is the amount of active biomass present in a reactor and was calculated by using equation 2.6 given in Chapter 2 (Jawed and Tare, 1996). Cumulative COD removal profile with individual reactor activity profile in R1, R2 and R3 are illustrated in Fig.4.11. Seed granules had 8.33±0.21 mg COD/mg VSS.day activity which was deteriorated up to 3.02±0.19 mg COD/mg VSS.day in R1 with 91.22±1.32 mg/g VSS.day TPH removal rate in 112 days due to initial granule breakage and VSS reduction for not augmenting oil degrader *Micrococcus.* As R1 had the highest F/M ratio (0.35 g COD/g SS.day) among the AGRs, granule bacteria were not capable of consuming the excess hydrocarbon in the AGR achieving 73% organics removal and the lowest AGR activity (Hamza et al., 2018).

In R2, second dose (day 42) of liquid *Micrococcus* culture augmentation, could not improve COD removal efficiency more than 76.21%. As the third and fourth dose of augmentation (day 63 and 84) reduced granule rupture, COD removal reached 79% which remained nearly stable till day 112. HPLC results provided maximum 75, 82, 76.07 and 75.9% of phenol, *o*, *m* and *p*-cresol removals in R2. Sparse distribution of *Micrococcus* on R2 granule surfaces (Fig.4.4) enabled 7-8% hike in TPH degradation than R1 which is corresponding with the removal medium (C_{11}-C_{12}, C_{14}-C_{15}) and long chain (C_{16}-C_{28}) *n*-alkanes from effluent. The remaining small peaks of octane (C_8), decane (C_{10}), tridecane (C_{13}), hexatriacontane (C_{36}) and tetratetracontane (C_{44}) were corresponding with 260±1 mg/L of residual COD in R2 treated wastewater (Fig.4.7, Table 4.5). About 124.87±2.19 mg/g VSS.day TPH removal rate and 3.70±0.26 mg COD/mg VSS.day reactor activity (Fig.4.11) in R2 further suggested that liquid culture augmentation had moderate improvement in granule stability to perform above 80% hydrocarbon removal in high strength refinery wastewater.

Impact of the granular *Micrococcus* augmentation was very significant in R3 in hydrocarbon removal. The first and second doses (on day 21 and 42) of granular culture augmentation provided 97.36% COD removal with improved granule settling and VSS content (Fig.4.3b). Abundance of oil degrader *Micrococcus* on granule surfaces might be a possible reason in R3 to enhance 23-24% COD removal than R1. After day 42, HPLC and gravimetric analysis ensured about 98.37±0.06% diesel, 99.30±0.03% phenol, 98.28±0.5% *o*-cresol and 97.8±0.43% *m* and *p*-cresol degradations which followed a steady state up to day 112 in presence of 330 mg/L TPH.

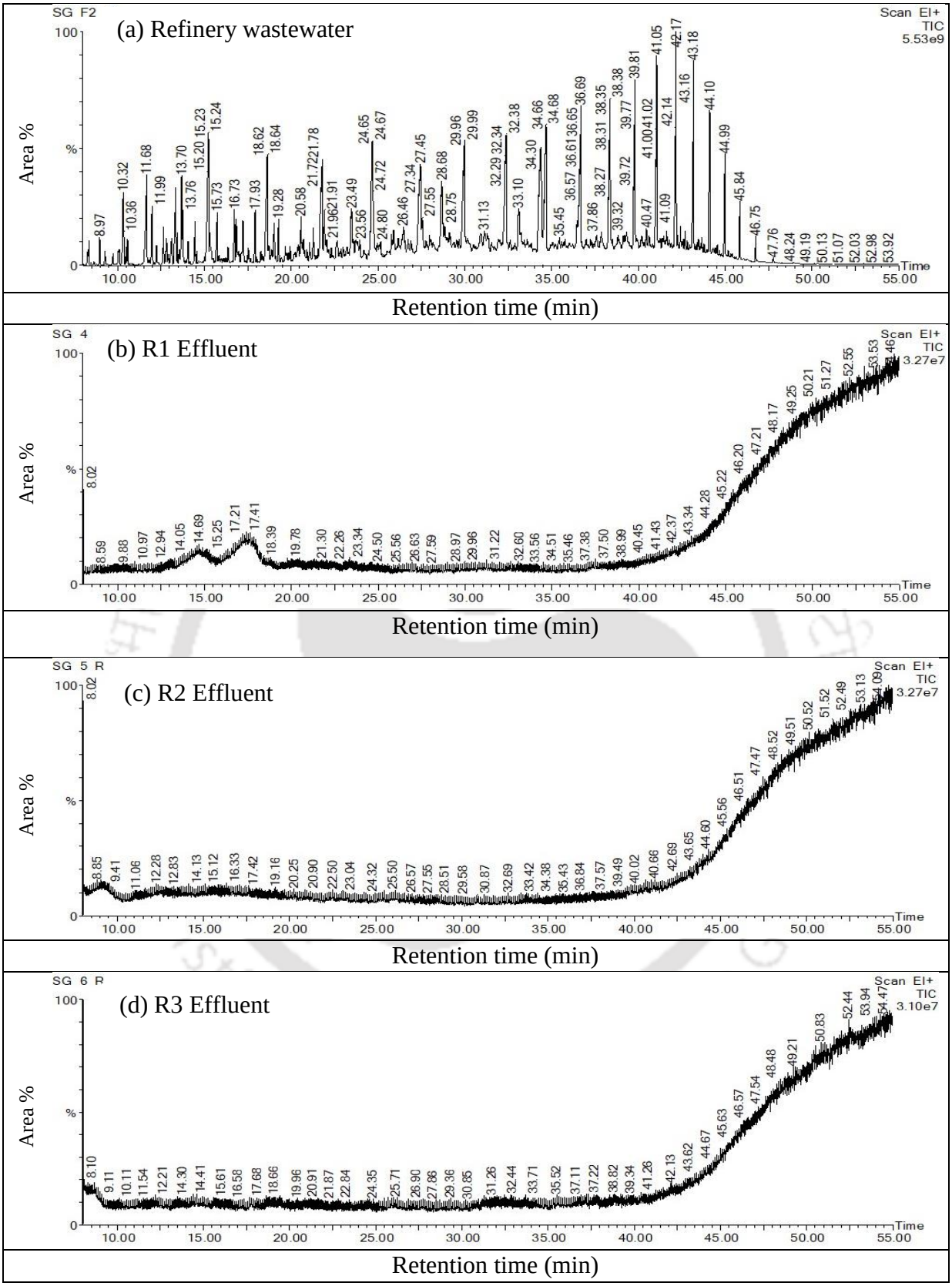

Fig.4.7 GC-MS spectra for (a) untreated refinery wastewater and (b) R1, (c) R2 and (d) R3 treated effluents in steady state.

Table 4.5 Alkanes detected in GC-MS spectra of refinery wastewater and R1, R2 and R3 treated effluents in steady state

Refinery wastewater		R1 effluent (control)		R2 effluent (liquid augmented)		R2 effluent (Granule augmented)	
RT (min)	**Compound**	**RT (min)**	**Compound**	**RT (min)**	**Compound**	**RT (min)**	**Compound**
8.97	Decane (C_{10})	14.69	Hexadecane (C_{16})	8.88	Octane (C_8)	44.67	Tetratetracontane (C_{44})
10.57	Nonane (C_9)	17.21	Benzene (C_6)	9.41	Decane (C_{10})		
11.68	Tridecane (C_{13})	17.41	Benzene (C_6)	11.06	Tridecane (C_{13})		
13.76	Octadecane (C_{18})	18.39	Tetradecane (C_{14})	12.83	Cyclododecane (C_{10})		
15.23	Tetradecane (C_{14})	37.50	Tetratetracontane (C_{44})	45.56	Tetratetracontane (C_{44})		
16.73	Benzene (C_6)	41.43	Octacosane (C_{28})	46.51	Hexatriacontane (C_{36})		
18.64	Tridecane (C_{13})	42.37	Octadecadienoic acid (C_{18})				
21.72	Hexadecane (C_{16})	45.22	Pentadecyne (C_{15})				
23.49	Heptadecane (C_{17})	46.20	Heptacosane (C_{27})				
24.67	Tridecane (C_{13})						
27.45	Tetradecane (C_{14})						
29.99	Pentadecane (C_{15})						
32.38	Octacosane (C_{28})						
33.16	Dodecane (C_{12})						
34.68	Heptadecane (C_{17})						
36.69	Hexatriacontane (C_{36})						
38.38	Heneicosane (C_{21})						
39.77	Eicosane (C_{20})						
39.81	Hexatriacontane (C_{36})						
41.05	Tetratetracontane (C_{44})						
42.17	Heptacosane (C_{27})						
43.18	Hexatriacontane (C_{36})						
44.16	Docosane (C_{22})						
44.99	Tetratetracontane (C_{44})						
45.84	Octacosane (C_{28})						
46.75	Heptacosane (C_{27})						
47.76	Hexatriacontane (C_{36})						

*RT: Retention time

Disappearance of major alkane peaks in effluent spectra suggested almost complete TPH removal in R3 leaving only 2-3 mg/L residual TPH (tiny peak of tetratetracontane (C_{44})) in effluent which was within the permissible effluent discharge limit of 10 mg/L framed by Environmental Protection Act, 2002, India. It suggested almost complete conversion of alkane to fatty acids and its further participation in β-oxidation leaving small alkane fractions in R3 treated effluent.

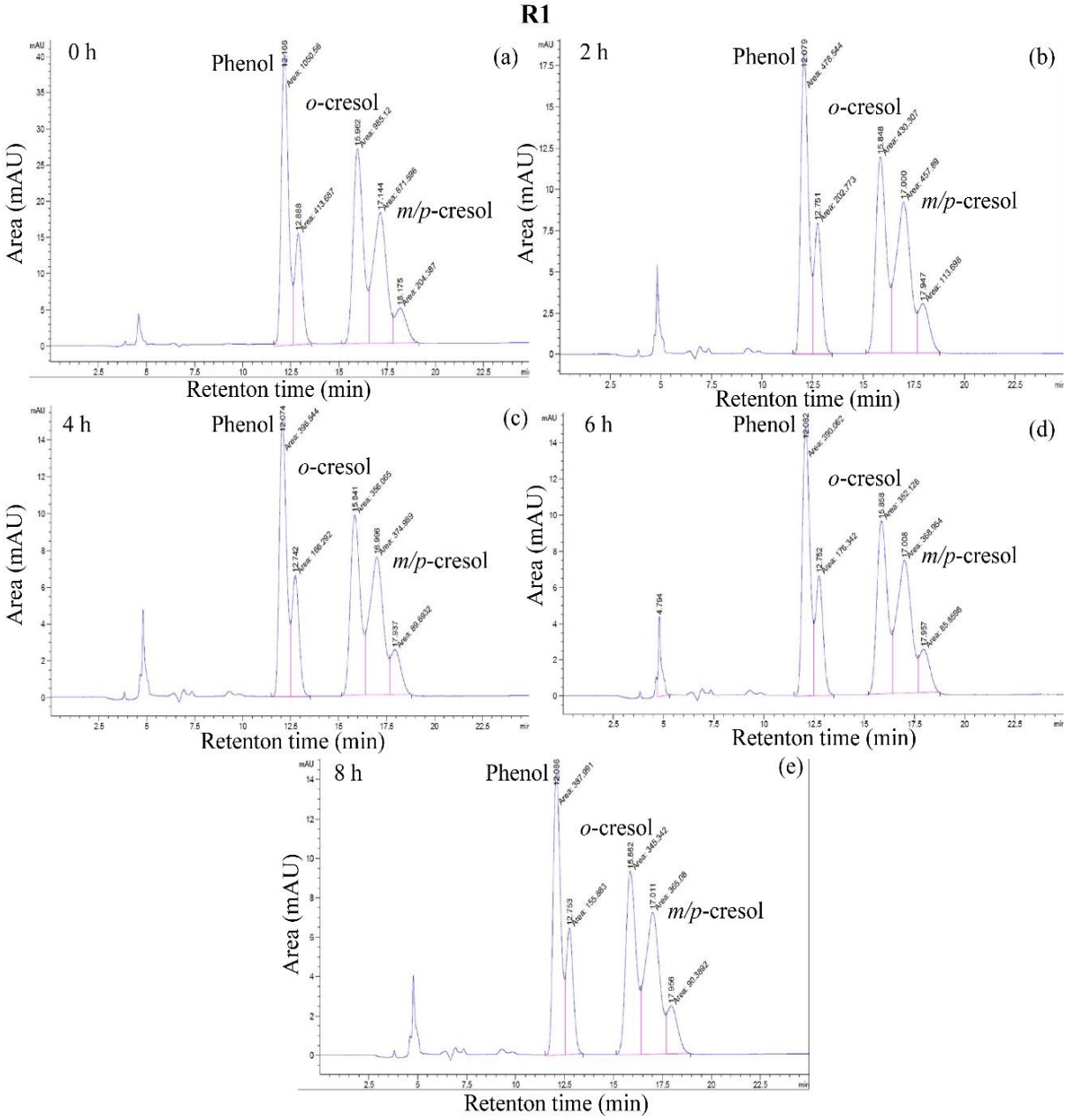

Fig.4.8 HPLC results in R1 (control) for phenol and cresol concentrations in (a) 0 h, (b) 2 h, (c) 4 h, (d) 6 h and (e) 8 h of the AGR cycle.

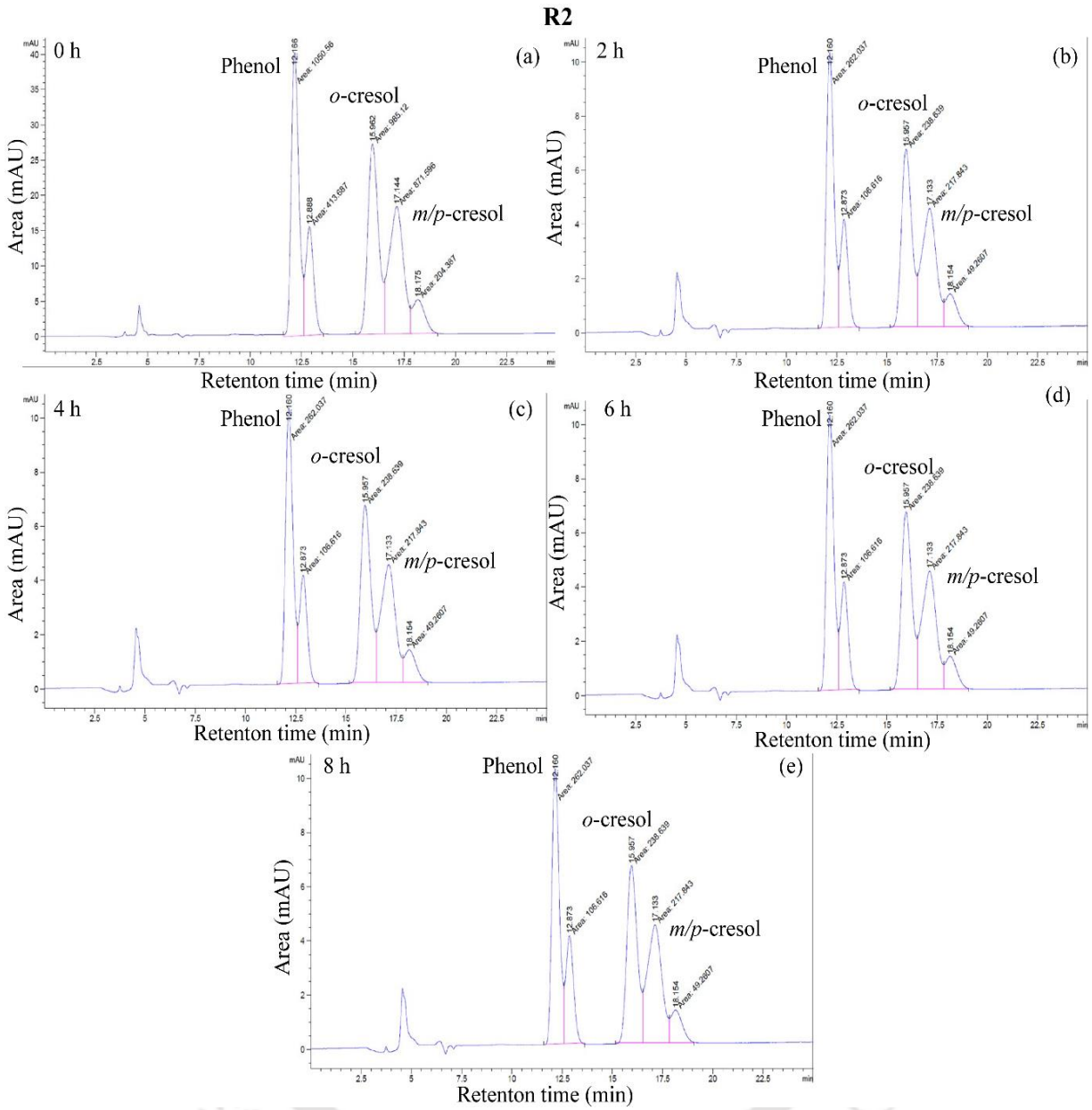

Fig.4.9 HPLC results in liquid *Micrococcus* augmented R2 for phenol and cresol concentrations on (a) 0 h, (b) 2 h, (c) 4 h, (d) 6 h and (e) 8 h of the AGR cycle.

As, aerobic granules are clusters of billions of bacterial population and contains higher amount of bioactive VSS with shock resistant EPS layer than liquid or flocculent biomass culture, accomplishment of complete TPH removal by correct approach of granulated *Micrococcus* augmentation and prediction of alkane to fatty acid conversion in control reactor and its further removal by β-oxidation in bioaugmented AGR were the main takeaway of this study. Literature also suggested conversion of phenols to catechols (1, 2-hydroxybenzene) in AGR systems (Basheeer and Farooqi, 20012). The probable aerobic phenol biodegradation reaction is given in equation 1.1 (Chapter 1) which might justify the complete phenol and cresol removal occurred in R3.

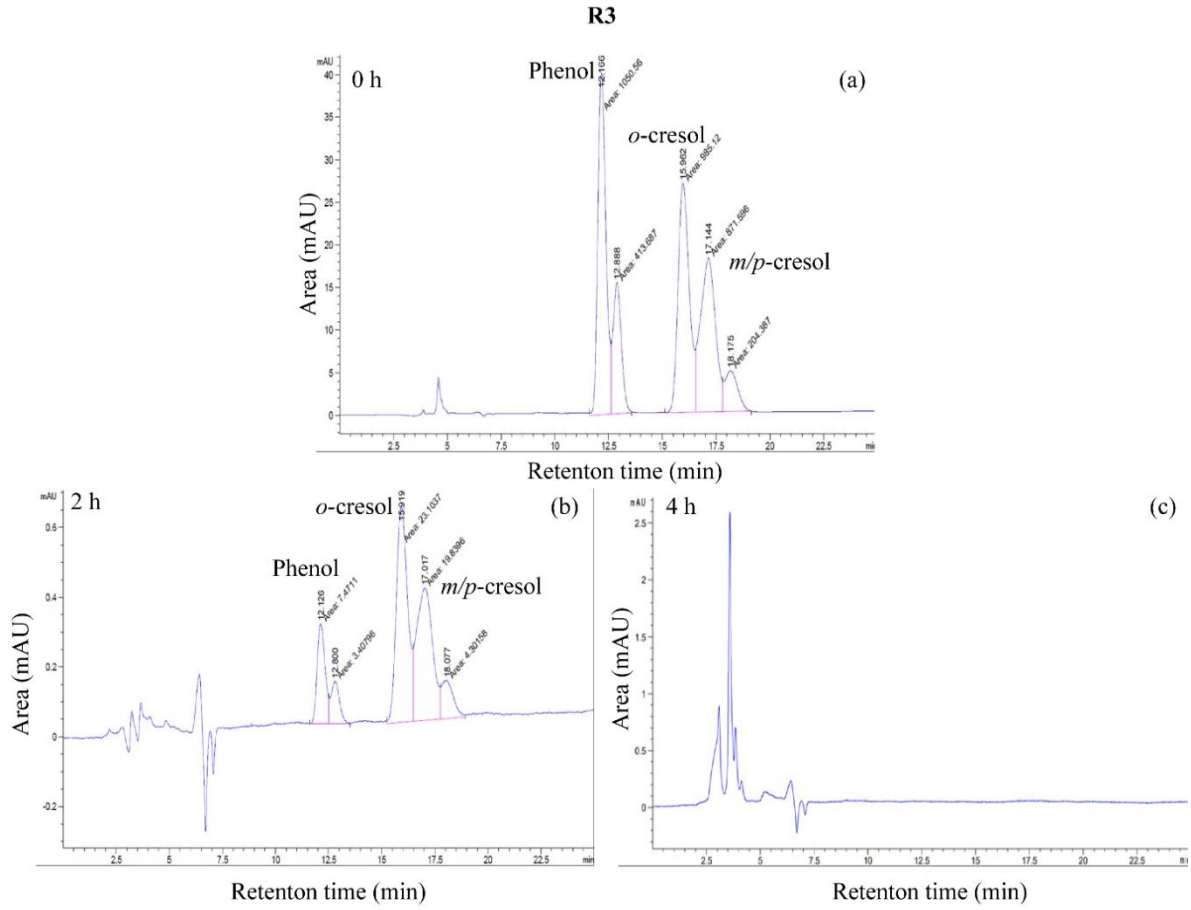

Fig.4.10 HPLC results in granulated *Micrococcus* augmented R3 for phenol and cresol concentrations on (a) 0 h, (b) 2 h, (c) 4 h of AGR cycle.

In *ortho* pathway of cathechol, cis, cis-muconate is produced via catechol-1,2-dioxygenase which can be further utilized in TCA cycle. In *meta* pathway, catechol ring is cleaved by catechol-2,3-dioxygenase to 2-hydroxymuconic semialdehyde (HMSA). HMSA can be either oxidized or hydrolyzed to 4-oxalocrotonate and 2-oxopent-4-enoate and cis-muconate is finally converted to muconolactone (Bera et al., 2017). In steady state, R3 achieved maximum 152.32±3.1 mg/g VSS.day TPH removal rate with 7.63±0.41 mg COD/mg VSS.day biomass activity (Fig.4.11) which was the highest among the AGRs for having most stable and dense granules. Similar biomass activity pattern was obtained in stable and dense granules during HRT studies in Chapter 3 (section 3.3.3.1).

Granulated *Micrococcus* addition promoted the lowest F/M ratio (0.16 g COD/g SS.day) in R3 among the AGRs, which denoted presence of sufficient amount of microorganisms to degrade about 99% phenolic compounds and 97% COD.

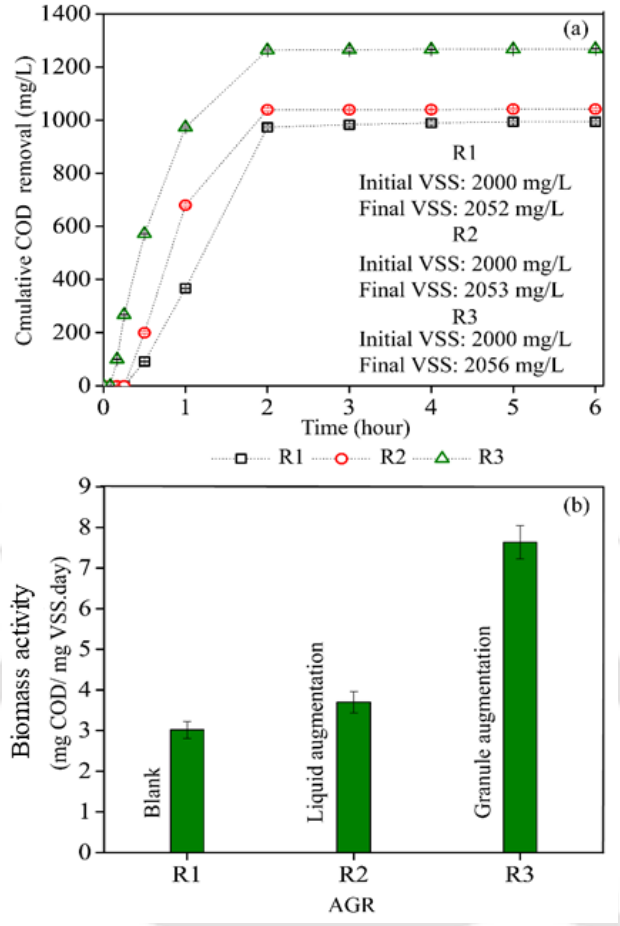

Fig.4.11 (a) Cumulative COD removal profile with (b) individual reactor activity profile in R1, R2 and R3.

Chapter 2 and previous literature reported the use of glucose, sodium acetate or propionate to initiate or reconstruct granulation process or to enhance hydrocarbon removal in co-metabolism mechanism (Zhang et al., 2011; Chen et al., 2019). But the current AGR operation was entirely conducted with refinery wastewater as sole substrate indicating operational feasibility in real refinery wastewater treatment plants. About 90% phenol, cresol and pyridine removals were observed in liquid culture bioaugmented AGRs treating a single pollutant by Adav et al. (2007), Jemaat et al. (2014) and Liu et al. (2015). Whereas, our study suggested use of 2-3 doses of 10% (w/w) granulated *Micrococcus* bioaugmentation to achieve 99% TPH removal at 330 mg/L of multiple hydrocarbon laden refinery wastewater.

4.3.5.2 Variation in nitrogen removal

Nitrogen loading rate and influent NH_4^+-N concentrations were 0.075 kg NH_4^+-N/m^3.day and 50 mg/L throughout the study. NH_4^+-N removal with NO_3^--N and NO_2^--N concentrations in effluents are described in Fig.4.12. Till day 63, granule disintegration might be a probable reason of outer ammonia oxidizing layer depletion which provided only 73-78% NH_4^+-N

removal in R1 (Tay et al., 2002). R1 achieved 80.54% removal with partial nitrification producing 0.5 and 5.3 mg/L of NO_3^--N and NO_2^--N in effluent within 63 days. In R2 and R3 *Micrococcus* augmentation improved NH_4^+-N removal up to 81 and 90.22% in complex refinery wastewater. Day 63 onwards, maximum 1.5, 9.45 and 4.5, 0.44 m/L NO_3^--N and NO_2^--N were generated in R2 and R3, respectively. The statistical analysis of granule characteristics and reactor performance data of the AGRs has been provided in Table 4.6.

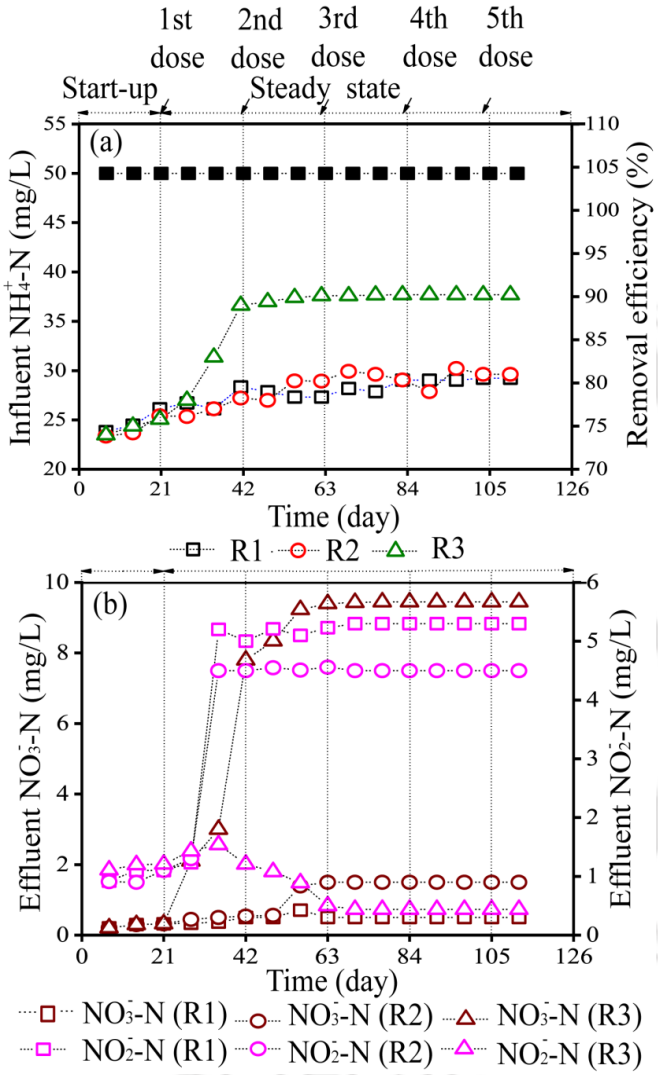

Fig.4.12 (a) NH_4^+-N removal performances and (b) nitrate-N and nitrite-N accounts in the AGR effluent in refinery wastewater treatment. [Dose determines *Micrococcus* bioaugmentation in every 21 days interval].

Nitrosomonas, an ammonia-oxidizing bacteria (AOB) generally helps in aerobic transformation of NH_4^+-N to NO_2^- and nitrite-oxidizing bacteria (NOB), *Nitrobacter* can further covert NO_2^- to NO_3^- (Metcalf and Eddy, 2003). After 63 days of study, R1, R2 and R3 had 0.36, 0.30, 0.21 mg/L effluent VSS concentrations providing 8, 9.3 and 19 days of solid retention times (SRT) which were calculated by equation 2.7 (Chapter 2).

Table 4.6 Statistical analysis of granule characteristics and reactor performance data of the AGRs

Reactor	**R1**		**R2**		**R3**		**Overall ANOVA**				
Operation time (day)	**1-126**		**1-126**		**1-126**						
	Mean	**SD**	**Mean**	**SD**	**Mean**	**SD**	**R-square**	**Coeff Var**	**Root MSE**	**Mean square**	**F-value**
Granule size (mm)	3.49	0.59	4.49	0.22	4.62	0.11	0.66	0.08	0.37	4.93	35.96
VSS (g/L)	4.39	1.02	4.64	0.85	7.98	0.69	0.79	0.15	0.86	72.46	96.15
SVI_{30} (mL/g)	42.63	3.29	29.90	2.84	25.24	4.22	0.82	0.10	3.50	1457.56	118.79
GSV (m/h)	28.71	5.36	36.91	2.49	40.39	2.35	0.65	0.10	3.67	647.67	47.88
EPS (mg/g VSS)	295.49	42.52	294.98	47.69	403.17	3.81	0.66	0.11	36.95	69906.86	51.18
PN (mg/g VSS)	203.07	47.28	213.54	55.51	312.36	8.32	0.58	0.17	42.37	65463.52	36.45
Hydrophobicity (%)	68.31	11.71	84.97	6.64	93.64	2.75	0.64	0.09	7.93	2982.02	47.32
IC (%)	37.32	7.58	27.51	6.36	15.83	3.88	0.68	0.22	6.14	2084.33	55.22
COD removal efficiency (%)	74.61	8.01	79.25	4.48	95.75	2.32	0.74	0.06	5.47	2222.73	74.24
TPH removal efficiency (%)	76.95	6.54	82.89	3.80	96.34	2.92	0.76	0.05	4.68	1775.59	80.82
NH_4^+-N removal efficiency (%)	77.26	3.27	78.27	2.47	86.42	6.17	0.49	0.05	4.27	453.70	24.77

Nitrogen uptake for biomass growth was calculated by equation 2.8 (Chapter 2) which was found to be 34.47, 34.50, 35.22 mg/L in R1, R2 and R3, respectively and the rest took part in nitrification (Metcalf and Eddy, 2003). About 4.5 L/day flowrate was found in AGRs. Longer SRT (10-30 days) is ideal for NOB growths for complete nitrification (Wan et al., 2013). Comparative shorter SRTs and presence of toxic *n*-alkanes in influent caused high biomass washouts in R1 and R2 inhibiting NOB population (Chen et al., 2019). Hence, AOB and NOB could not outcompete the heterotrophic oil degraders in aerobic granules producing 9-10.6% partial and only 1-3% complete nitrification in R1 and R2, respectively (Jemaat et al., 2013). On other hand, according to Jemaat et al. (2014), the bioaugmented heterotrophic *o*-cresol degraders prevailed on the outer layer of granules and acted as a shield for the AOBs ensuring nitrification in cresol treatment. Similarly, in current study granulated *Micrococcus* augmentation in R3 provided cocci dominated compact granular surface which can be predicted as a protector of nitrifying bacteria in the core of granules promoting maximum 18.9% complete nitrification among the AGRs.

In previous literature, co-substrate feeding strategy was employed to recover nitrification in AGRs in hydrocarbon recalcitrance (Zhang et al., 2011; Chen et al., 2019) whereas, R3 was capable of 19% nitrification by using refinery wastewater as the sole carbon source. Hence, granular *Micrococcus* augmentation is recommended over liquid culture in AGRs to achieve simultaneous hydrocarbon and NH_4^+-N (90%) removal where 70% nitrogen was consumed by biomass and 19% achieved complete nitrification.

4.3.6 Pollutant degradation kinetics in steady state

Fig.4.13 provides hydrocarbon and NH_4^+-N removal profiles in 2 h time intervals in R1, R2 and R3 in AGR cycle (8 h). AGRs achieved 75-98% TPH removal within 2 h providing 77.78±1.31, 54.45±0.73 and 2.7±0.04 mg/L effluent TPH in R1, R2 and R3, respectively which are corresponding to cumulative COD removal (Fig.4.11) for biomass activity. Existence of above 27 alkanes enhanced recalcitrance of refinery wastewater. GC-MS revealed that with incomplete biodegradation of C_8-C_{15} *n*-alkanes, R1 also produced octadecadienoic acid (C_{18}) indicating alkane to fatty acid conversion as described in Chapter 3. In R2, *Micrococcus* culture facilitated about 80% degradation of C_{11}-C_{28} in 2 h and the remaining 2% was degraded in next 6 h whereas, 98-99% alkane degradation was observed within 2 h in granule augmented R3.

HPLC peaks for phenol and *o*-cresol were observed at 12.5 min, 15.9 min, respectively and *m* and *p*-cresol peaks appeared together at 17.2 min (Fig.4.8-4.10). R1 was able to degrade 58-62% phenolics within 4 h generating 18.97±0.5 mg/L phenol and 10.71-12.45

mg/L cresol in effluent and about 0.5-1% phenolics was further degraded in next 4 hours. Liquid *Micrococcus* augmentation in R2 facilitated maximum 74.93% phenol and 82.07-75.9% removals of *o*, *m*, and *p*-cresols providing 7-12.53 mg/L residual phenolics within 2 h which remained constant throughout the 8 h cycle. In R3, granulated *Micrococcus* promoted 99% phenolics removal in 2 h and complete degradation occured in 4 h.

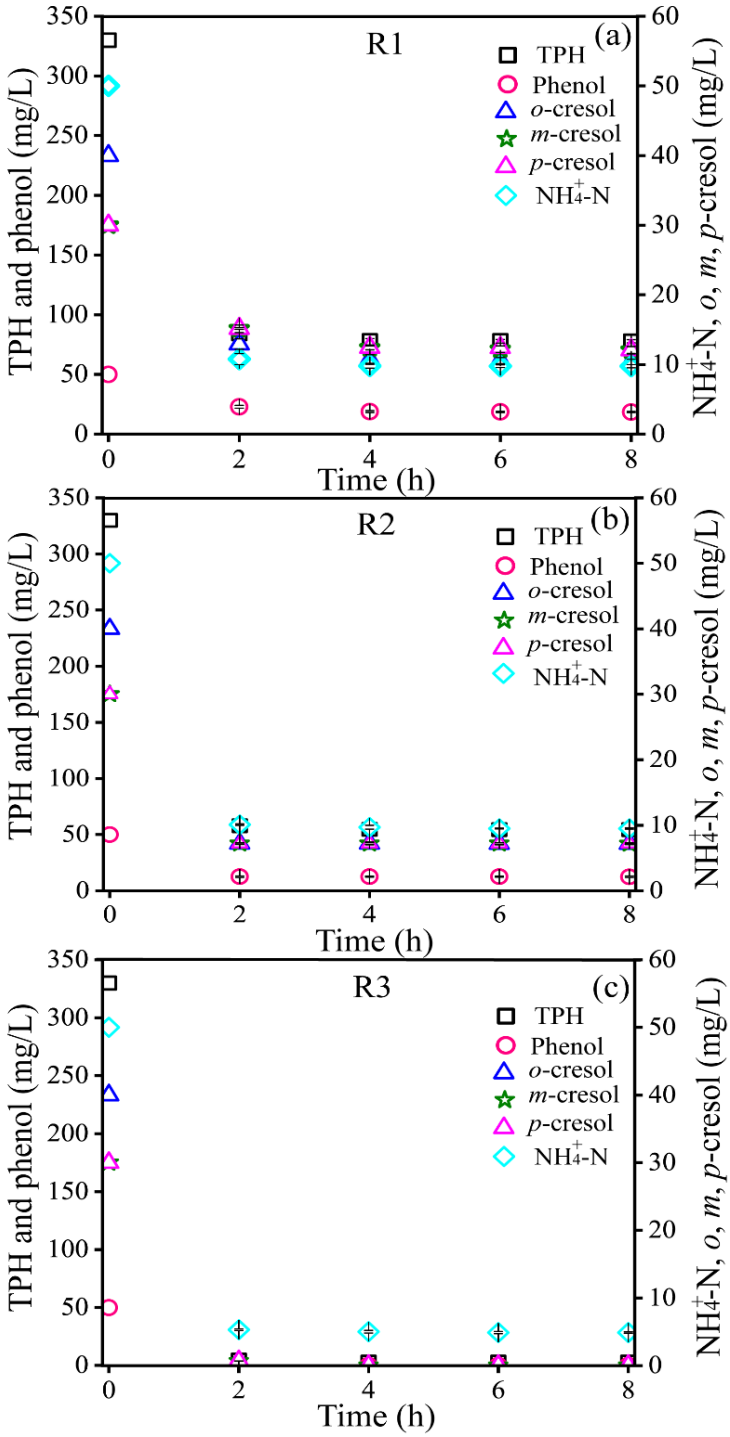

Fig.4.13 TPH, NH_4^+-N, phenol and cresol removal kinetics profiles in (a) R1, (b) R2 and (c) R3 in 8 h cycle (steady state).

The NH_4^+-N concentration was reduced between 4-12 mg/L in 8 h (Fig.4.13a-c) in the AGRs suggesting simultaneous growth of AOB and oil degrading heterotrophs in AGR cycle with 1-19% complete nitrification (Jemaat et al., 2014). Granular *Micrococcus* again emphasized its augmentation benefit in AGR system achieving the 90% nitrogen removal with almost complete TPH removal in 2 h treating high strength refinery wastewater.

4.4 Summary of the chapter

The study fulfilled the target of rapid granulation of *Micrococcus* strain along with developing appropriate bioaugmentation procedure solving slow granulation and granule rupture problems with enhanced pollutant removal efficiencies in refinery wastewater treatment. Control AGR faced granule disintegration in refinery effluent. Liquid *Micrococcus* augmentation had minimal impact on granule characteristics whereas granular culture augmentation significantly improved the granule size, settling and integrity coefficient. Dense and sparse cocci population in bioaugmented granules facilitated 7-24% hike in TPH removal than control reactor. Two doses of granular augmentation ensured simultaneous AOB and heterotroph growth achieving 99% hazardous phenolics removal with 19% complete nitrification. Degradation of C_8-C_{15} *n*-alkanes with fatty acid conversion took place in control and removal of C_6-C_{36} predicted β-oxidation of fatty acids in bioaugmented AGRs. Hence, about 2 kg COD/m^3.day OLR with 10% (w/w) granular *Micrococcus* augmentation is recommended in AGR for complete hydrocarbon removal with improved nitrification efficiency treating refinery wastewater within permitted discharge limit.

References

Adav, S.S., Chen, M.Y., Lee, D.J. and Ren, N.Q., 2007. Degradation of phenol by Acinetobacter strain isolated from aerobic granules. Chemosphere 67, 1566-1572.

Adav, S.S., Lee, D.J., 2008. Single-culture aerobic granules with *Acinetobacter calcoaceticus*. Applied microbiology and biotechnology 78, 551-557.

Basheer, F. and Farooqi, I.H., 2012. Biodegradation of p-cresol by aerobic granules in sequencing batch reactor. Journal of Environmental Sciences 24.

Bento, F.M., Camargo, F.A., Okeke, B.C. and Frankenberger, W.T., 2005. Comparative bioremediation of soils contaminated with diesel oil by natural attenuation, biostimulation and bioaugmentation. Bioresource Technology 96, 1049-1055.

Bera, S., Roy, A.S. and Mohanty, K., 2017. Biodegradation of phenol by a native mixed bacterial culture isolated from crude oil contaminated site. International Biodeterioration & Biodegradation 121, 107-113.

Cai, M., Yao, J., Yang, H., Wang, R., Masakorala, K. 2013. Aerobic biodegradation process of petroleum and pathway of main compounds in water flooding well of Dagang hydrocarbon field. Bioresource Technology 144, 100-106.

Chen, C., Ming, J., Yoza, B.A., Liang, J., Li, Q.X., Guo, H., Liu, Z., Deng, J., Wang, Q., 2019. Characterization of aerobic granular sludge used for the treatment of petroleum wastewater. Bioresource Technology 271, 353-359.

Corsino, S.F., Campo, R., Di Bella, G., Torregrossa, M., Viviani, G., 2015. Cultivation of granular sludge with hypersaline oily wastewater. International Biodeterioration & Biodegradation 105, 192-202.

Environmental protection act, 2002, Regulations made by the Minister under sections 39 and 96 of the Environment Protection Act 2002.

Ghangrekar, M., Asolekar, S., Joshi, S., 2005. Characteristics of sludge developed under different loading conditions during UASB reactor start-up and granulation. Water Research 39, 1123-1133.

Hamza, R.A., Sheng, Z., Iorhemen, O.T., Zaghloul, M.S. and Tay, J.H., 2018. Impact of food-to-microorganisms ratio on the stability of aerobic granular sludge treating high-strength organic wastewater. Water Research 147, 287-298.

Ho, K. L., Lin, B., Chen, Y. Y., & Lee, D. J., 2009. Biodegradation of phenol using Corynebacterium sp. DJ1 aerobic granules. Bioresource Technology 100, 5051-5055.

Hua, X., Wang, J., Wu, Z., Zhang, H., Li, H., Xing, X. and Liu, Z., 2010. A salt tolerant Enterobacter cloacae mutant for bioaugmentation of petroleum-and salt-contaminated soil. Biochemical Engineering Journal 49, 201-206.

Jawed, M., Tare, V., 1999. Microbial composition assessment of anaerobic biomass through methanogenic activity tests. Water SA 25, 345-350.

Jemaat, Z., Suárez-Ojeda, M.E., Pérez, J. and Carrera, J., 2013. Simultaneous nitritation and p-nitrophenol removal using aerobic granular biomass in a continuous airlift reactor. Bioresource Technology 150, 307-313.

Jemaat, Z., Suárez-Ojeda, M.E., Pérez, J. and Carrera, J., 2014. Partial nitritation and o-cresol removal with aerobic granular biomass in a continuous airlift reactor. Water Research 48, 354-362.

Jiang, H.L., Maszenan, A.M. and Tay, J.H., 2007. Bioaugmentation and coexistence of two functionally similar bacterial strains in aerobic granules. Applied Microbiology and Biotechnology 75, 1191.

Jiang, H.L., Tay, J.H., Maszenan, A.M. and Tay, S.T.L., 2006. Enhanced phenol biodegradation and aerobic granulation by two coaggregating bacterial strains. Environmental Science & Technology 40, 6137-6142.

Karray, F., Aloui, F., Jemli, M., Mhiri, N., Loukil, S., Bouhdida, R., Mouha, N. and Sayadi, S., 2020. Pilot-scale petroleum refinery wastewaters treatment systems: performance and microbial communities' analysis. Process Safety and Environmental Protection 141, 73-82.

Liang, J., Li, W., Zhang, H., Jiang, X., Wang, L., Liu, X. and Shen, J., 2018. Coaggregation mechanism of pyridine-degrading strains for the acceleration of the aerobic granulation process. Chemical Engineering Journal 338, 76-183.

Liu, X., Chen, Y., Zhang, X., Jiang, X., Wu, S., Shen, J., Sun, X., Li, J., Lu, L. and Wang, L., 2015. Aerobic granulation strategy for bioaugmentation of a sequencing batch reactor (SBR) treating high strength pyridine wastewater. Journal of Hazardous Materials 295, 153-160.

Ma, J.Y., Quan, X.C., Yang, Z.F. and Li, A.J., 2012. Biodegradation of a mixture of 2, 4-dichlorophenoxyacetic acid and multiple chlorophenols by aerobic granules cultivated through plasmid pJP4 mediated bioaugmentation. Chemical Engineering Journal 181, 144-151.

Metcalf, E., Eddy, H.I. 2003. Wastewater engineering; treatment and reuse. McGraw-Hill, Boston.

Milia, S., Malloci, E., Carucci, A., 2016. Aerobic granulation with petrochemical wastewater in a sequencing batch reactor under different operating conditions. Desalination and Water Treatment 57, 27978-27987.

Quan, X.C., Ma, J.Y., Xiong, W.C. and Yang, Z.F., 2011. Effects of gene-augmentation on the formation, characteristics and microbial community of 2, 4-dichlorophenoxyacetic acid degrading aerobic microbial granules. Journal of Hazardous Materials 196, 278-286.

Quan, X.C., Tang, H., Xiong, W.C. and Yang, Z.F., 2010. Bioaugmentation of aerobic sludge granules with a plasmid donor strain for enhanced degradation of 2, 4-dichlorophenoxyacetic acid. Journal Hazardous Materials 179, 1136-1142.

Tay, J.H., Ivanov, V., Pan, S., Tay, S.L. 2002. Specific layers in aerobically grown microbial granules. Letters in Applied Microbiology 34, 254-257.

Wan, C., Sun, S., Lee, D.-J., Liu, X., Wang, L., Yang, X., Pan, X. 2013. Partial nitrification using aerobic granules in continuous-flow reactor: rapid startup. Bioresource Technology 142, 517-522.

Zhang, H., He, Y., Jiang, T., Yang, F., 2011. Research on characteristics of aerobic granules treating petrochemical wastewater by acclimation and co-metabolism methods. Desalination 279, 69-74.

Chapter 5

Production of polyhydroxyalkanoates (PHA) from aerobic granules of refinery sludge and *Micrococcus aloeverae* strain SG002

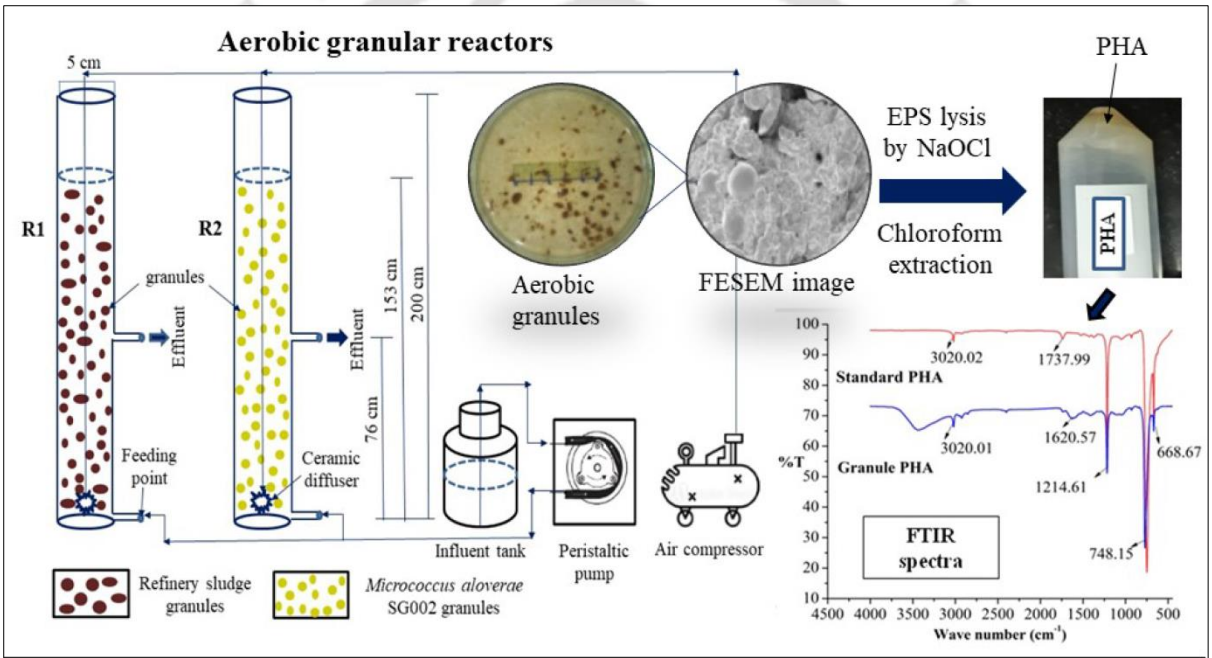

PHA production

PHA yield	R1	R2
% Yield	71±1	47±1
$Y_{PHA/biomass}$ (mg PHA/mg biomass)	0.71± 0.04	0.47± 0.04
$Y_{PHA/COD}$ (mg PHA/mg COD)	0.897± 0.1	0.38± 0.02

- EPS trend was proportional to PHA yield.
- PHB:PHV ratio was within 3.5 to 4.5.
- C_6-C_{10} and C_{16}-C_{36} hydrocarbons were biotransformed into PHA.
- Granulated pure strains and mixed culture granules were suitable for PHA accumulation.

Pollutant removal

Pollutants	R1	R2
COD	90.00%	80.67%
TPH	90.23%	81.40%

CHAPTER 5

Production of polyhydroxyalkanoates (PHA) from aerobic granules of refinery sludge and *Micrococcus aloeverae* strain SG002

This chapter investigates on accumulation of PHA biopolymers in aerobic granules of mixed sludge and specific strain inoculum while treating oily wastewater in AGRs.

5.1 Introduction

Polyhydroxyalkanoates (PHAs) are thermoplastic natural polyesters having hydroxyacid groups in their structure which is very similar in properties to the conventional plastics (Raza et al., 2018). More than 90 genera of both Gram-positive and negative bacteria have been reported as bioplastic producers so far (Kim et al., 2007). To avoid the use of costly sugar-substrate and pure culture bacteria, researchers are focusing to utilize the wastewater as a renewable feedstock and mixed microbial culture (MMC) to simultaneously treat wastewater and produce PHAs (Mannina et al., 2020).

Acetate wastewater and palm oil mill effluent (POME) have been majorly used for aerobic granule mediated PHA production. Implementation of high C/N ratio, aerodynamic feeding, modifying feast-famine ratio were proved to be effective generating stress conditions to enhance PHA accumulation in the AGRs (Fang et al., 2009; Wang et al., 2014; Gobi and Vadivelu, 2014; Vijayan and Vadivelu, 2017). Single strain bacteria (*Haloferax mediterranei*, *Bacillus megaterium*, *Ralstonia eutropha*, *Pseudomonas aeruginosa*, *Pseudomonas putida* etc.), MMC and activated sludge process were reported for PHA production in acetate as well as in hexadecane, POME or olive mill wastewaters (Bhattacharyya et al., 2012; Raza et al., 2016, 2018; Mohan et al., 2010; Amulya et al., 2016; Campanari et al., 2017).

However, PHA accumulation in aerobic granule originated from single strain inoculum is largely unknown. A comparative study on PHA production between oil degrading single strain granules and mixed culture granules using recalcitrant hydrocarbon (100–300 mg/L of oil) or petroleum refinery wastewater is not conducted. Biotransformation of hydrocarbon into PHAs is also not well investigated.

So, the aim of this study was to provide a comparative scenario of granulation and PHA accumulation in two AGRs operated with refinery mixed sludge granules and previously isolated oil degrading *Micrococcus aloeverae* strain SG002 granules using high strength hydrocarbon wastewater as substrate. COD removal and hydrocarbon biotransformation into

PHA at changing organic loading rate (OLR) and C/N ratio in both reactors were studied. The granule derived PHA was characterized and its correlation with EPS was established.

5.2 Materials and methods

5.2.1 Chemicals and reagents

Analytical grade chloroform, sodium hypochlorite and methanol were purchased from HiMedia, India and were used for PHA extraction. Standard P (3HB-*co*-3HV) and solvent $CDCl_3$ were procured from Sigma-Aldrich, USA. Other chemicals used in feed preparation, FESEM imaging, sludge and effluent analysis are discussed in Chapter 2 (section 2.2.1).

5.2.2 Inoculum sludge

Two types of seed sludge were used in the study. AGR R1 was inoculated with oil degrading refinery sludge granules having 3.49±0.01 mm diameter, 5.84±0.03 g/L VSS and 67.39±0.15% oil removal capacity as discussed in Chapter 2. R2 was operated with 3 g/L of oil degrading *Micrococcus aloeverae* strain SG002 culture (isolated from refinery granules mentioned in Chapter 2, section 2.3.6) which developed aerobic granules in 21 days of AGR operation. We have used sterilized reactor, aeration pipes, media and cotton plugging till granule formation in the R2 by following Ho et al. (2009) who used sterile media and additives while cultivating aerobic granules from phenol degrading *Corynebacterium* sp. DJ1. However, after 21 days of AGR operation, 0.46 mm sized *Micrococcus* granules were formed and in order to maintain real wastewater composition and environment, we have used non-sterile synthetic oily wastewater for the rest of the study.

5.2.3 Characteristics of wastewater

Table 5.1 provides detailed AGR feed compositions. AGRs were fed with synthetic oily wastewater where COD concentration was gradually increased from 400 to 1200 mg/L by regulating the diesel concentration from 100 to 300 mg/L.

Table 5.1 Composition of the oily wastewater

Component	Concentration	Component	Concentration
Emulsified diesel	100-300 mg/L	Trace metal solution	1 mL/L
NH_4^+-N	50 mg/L	$MgSO_4.7H_2O$	10,000 mg/L
Phosphate buffer	1 mL/L	$CaCl_2.2H_2O$	10,000 mg/L
KH_2PO_4	72.3 mg/L	$FeCl_3.6H_2O$	5000 mg/L
K_2HPO_4	104.5 mg/L	$CuCl_2$	1000 mg/L
$NaHCO_3$	Added as per requirement	$ZnCl_2$	1000 mg/L
		$NiCl_2.6H_2O$	500 mg/L
		$CoCl_2$	500 mg/L

Diesel oil was emulsified in nonylphenol ethoxylate (300:1 v/v ratio). In start-up phase (day 1-21), 100-250 mg/L diesel was delivered to the AGRs as carbon source. In steady state (day 22-70), diesel concentration was kept stable at 300 mg/L. However, influent ammonia nitrogen was fixed at 50 mg/L throughout the study. Phosphate buffer was added as a feed pH buffer (pH 7±0.2) and about 1 mL/L of trace metal solution was added as trace element supplement for microbial growth.

5.2.4 Reactor fabrication and operational conditions

Fig.5.1 provides AGR schematic diagram. Two AGRs (R1, R2) with 3 L working volume and 153 cm working height were fabricated using acrylic tubes. The height to diameter (H/D) ratio of the AGRs was 30.56. Reactors were operated in 3 cycles per day with 16 h hydraulic retention time (HRT) and 50% volume exchange ratio (VER). Aeration was given by air compressor by regulating air flow rate at 2 L/min by rotameter. Double channel peristaltic pump was used for AGR feeding. Feeding and aeration times were 22 min and 450 min, respectively and granule settling time varied between 5 to 3 min. R1 granules had 0.44 g COD/g SS.day F/M ratio for start-up and R2 operation was initiated with high F/M ratio of 0.61 g COD/g SS.day for granulation (Li et al., 2011).

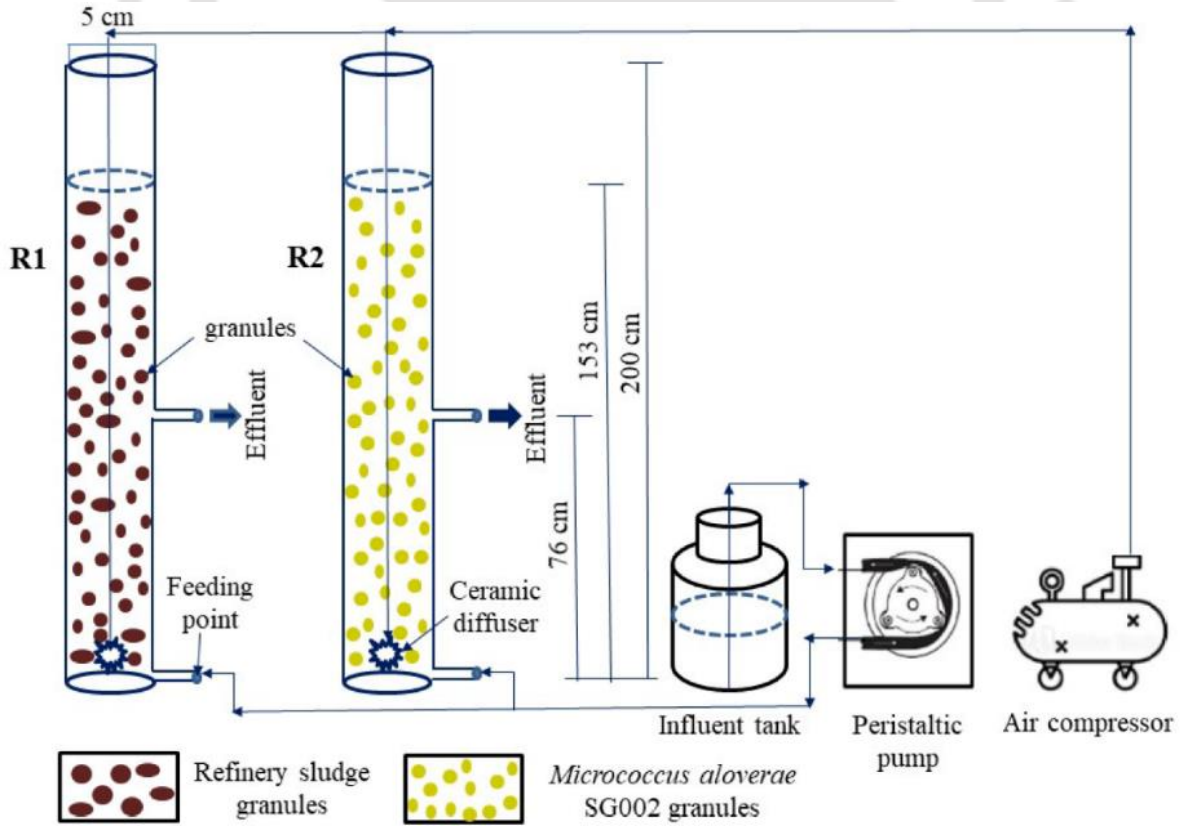

Fig.5.1 Schematic diagram of aerobic granular reactor (AGR).

5.2.5 Analytical procedures

Dissolved oxygen (DO) concentration in the AGRs was measured by using DO meter. Determination of granule characteristics, FESEM, GC-MS and effluent quality analysis are discussed in Chapter 2 (section 2.2.6).

5.2.6 PHA extraction and estimation

Aerobic granules were taken out from the AGRs at the end of feast phase (within 2 h of a cycle time). Samples were centrifuged at 7000 rpm for 15 min. Supernatant was discarded and the biomass was kept at -70 °C temperature for 6 h. Samples were collected in an ice tray and were put inside the lyophilizer (Make: Labconco). A mixture of 12.5 mL of sodium hypochlorite and 12.5 mL of chloroform was added to each gram of the lyophilized granules. Mixture was incubated in a water bath shaker at 37 °C temperature for 90 min after a thorough vortexing. The solution was further centrifuged at 4400 rpm for 30 min and three different layers formed. The top layer consisting sodium hypochlorite was pipetted out. The remaining two layers containing cell debris and PHA fractions were dissolved in chloroform and filtered through glass fibre filter (0.45 µm pore size). Presence of PHA in the chloroform extract was confirmed by FTIR and ^{1}H NMR spectroscopy. About five volume of ice-cold methanol was added to one volume of the chloroform solution (filtrate) to precipitate the PHA. The mixture was evaporated in a fume hood to separate the PHA (Gobi and Vadivelu, 2015b). PHA yield was calculated by equation 5.1 from the dried remaining residue by comparing with the cell dry weight (CDW) of aerobic granules (Gobi and Vadivelu, 2014).

$$Y_{PHA/CDW} = \frac{\text{Total amount of PHA,mg}}{\text{CDW of aerobic granules,mg}} \quad (5.1)$$

PHA yield was further expressed in terms of the mg of COD consumption per litre of the wastewater in the AGR by using equation 5.2.

$$Y_{PHA/COD} = \frac{\text{Total amount of PHA,mg}}{\text{Amount of COD converted,mg/L}} \quad (5.2)$$

5.2.7 PHA characterization

5.2.7.1 Crotonic acid assay

The PHA extraction process with crotonic acid assay flowchart is given in Fig.5.2. For spectrophotometric analysis of PHA, the filtrate was dried at 80 °C temperature inside a hot air oven to evaporate chloroform from the filtrate. About 10 mL of sulfuric acid (98%) was added to the residue and the solution was heated at 100 °C temperature in a water bath for 10 min so that sulfuric acid could dehydrogenate PHA into crotonic acid.

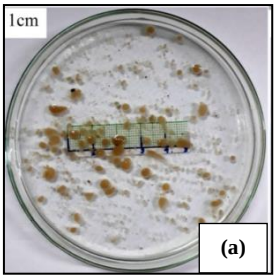

Aerobic granules collected at the end of feast phase of AGR

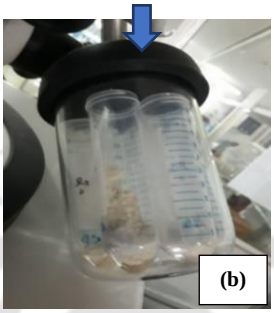

Lyophilized granules

Mixture of granule+chloroform+ sodium hypochlorite formed three distinct layers after incubation (at 37 °C), vortexing and centrifugation. Chloroform was evaporated to separate PHA.

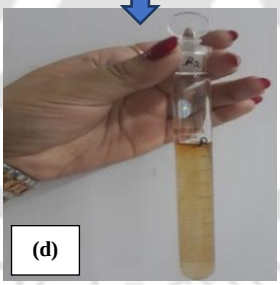

Crotonic acid formed by adding 10 mL sulfuric acid with dried PHA and boiling at 100 °C

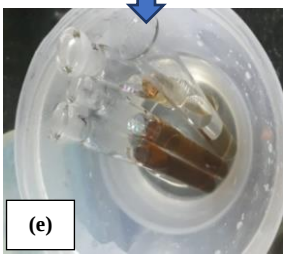

Corotonic acid solution was cooled down at room temperature and the absorbance of the solution was measured at 235 nm and 285 nm wavelengths for determining PHB and PHV

Fig.5.2 A flowchart for PHA extraction and crotonic acid assay

After cooling down at room temperature, the absorbance of the solution was measured at 235 nm and 285 nm wavelengths for determining the hydroxybutyrate (HB) and hydroxyvalerate (HV) concentration, respectively (Amulya et al., 2016). Standard curve was prepared by using pure commercial co-polymer, P (3HB-*co*-3HV) purchased from Sigma-Aldrich (USA) and sulfuric acid was used as blank (Fig.A7-A8).

5.2.7.2 FTIR

Fourier transmission infrared spectroscopy (FTIR, model: PerkinElmer Spectrum 2) was employed to determine the presence of P (3HB-*co*-3HV) in the granule accumulated PHA samples and to further compare it with the spectra obtained by standard PHA (Sigma-Aldrich). The FTIR spectra were recorded in the range of 500-4500 cm^{-1} and with 16 scans at 0.4 cm^{-1} resolution (Gobi and Vadivelu, 2014).

5.2.7.3 ^{1}H NMR

The chemical composition of PHA was further confirmed by ^{1}H NMR analysis of granule derived PHA and 12 mol% standard P (3HB-*co*-3HV) from Sigma-Aldrich (USA). Both types of PHA samples were dissolved in 1 mL $CDCl_3$ by heating at 60 ◦C before analysing in 400 MHz ^{1}H NMR Spectrometer (Bruker 400 MHz NMR) (Mahansaria et al., 2015).

5.3 Results and discussion

5.3.1 Characterization of aerobic granules

In R1, seed refinery granules were light brownish (Fig.5.3a) having average 3.49±0.01 mm diameter with 5.84±0.03 g/L VSS values (discussed in Chapter 2). In start-up phase, at 100-250 mg/L diesel exposure, granule size and biomass concentration (VSS) varied between 4.51-4.22 mm and 6.03-5.89 g/L, respectively. In steady state, granules became dark brownish and achieved stability in diameter (4.51±0.13 mm) and biomass concentration (7.54±0.15 g/L) with less flocculent biomass than the start-up phase (Fig.5.3b). Granule diameter, VSS and IC profiles in R1 and R2 are given in Fig.5.4a-c.

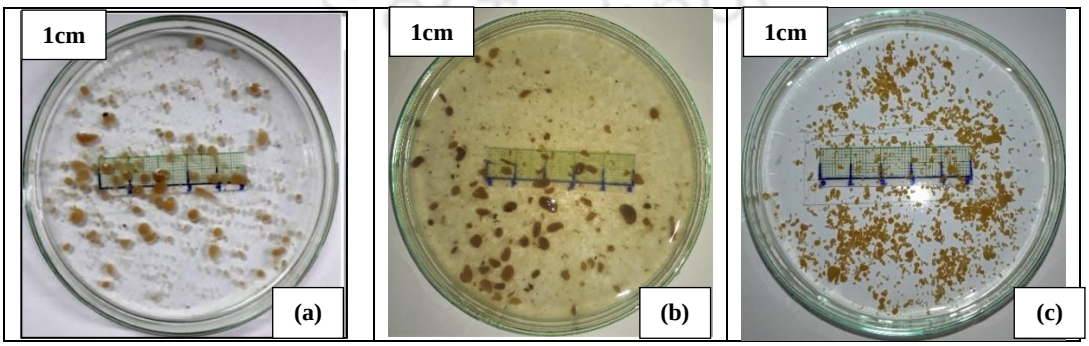

Fig.5.3 Photographs of initial and final refinery sludge granules after AGR treatment in R1 on (a) day 0 and (b) day 65, respectively and of (c) *Micrococcus* granules in R2 on day 65.

In R2, *Micrococcus* strain took almost 21 days for granule formation at 100-250 mg/L of emulsified diesel as influent carbon. During AGR start-up, *Micrococcus* granules were dark yellow in colour (Fig.5.3c) with initial characteristics of 0.46±0.07 mm diameter and 4.8±0.06 g/L VSS content. In steady state, at constant 300 m/L diesel exposure, R2 attained stability with bigger (diameter: 0.71±0.04 mm) and denser (VSS: 6.77±0.12 g/L) granules.

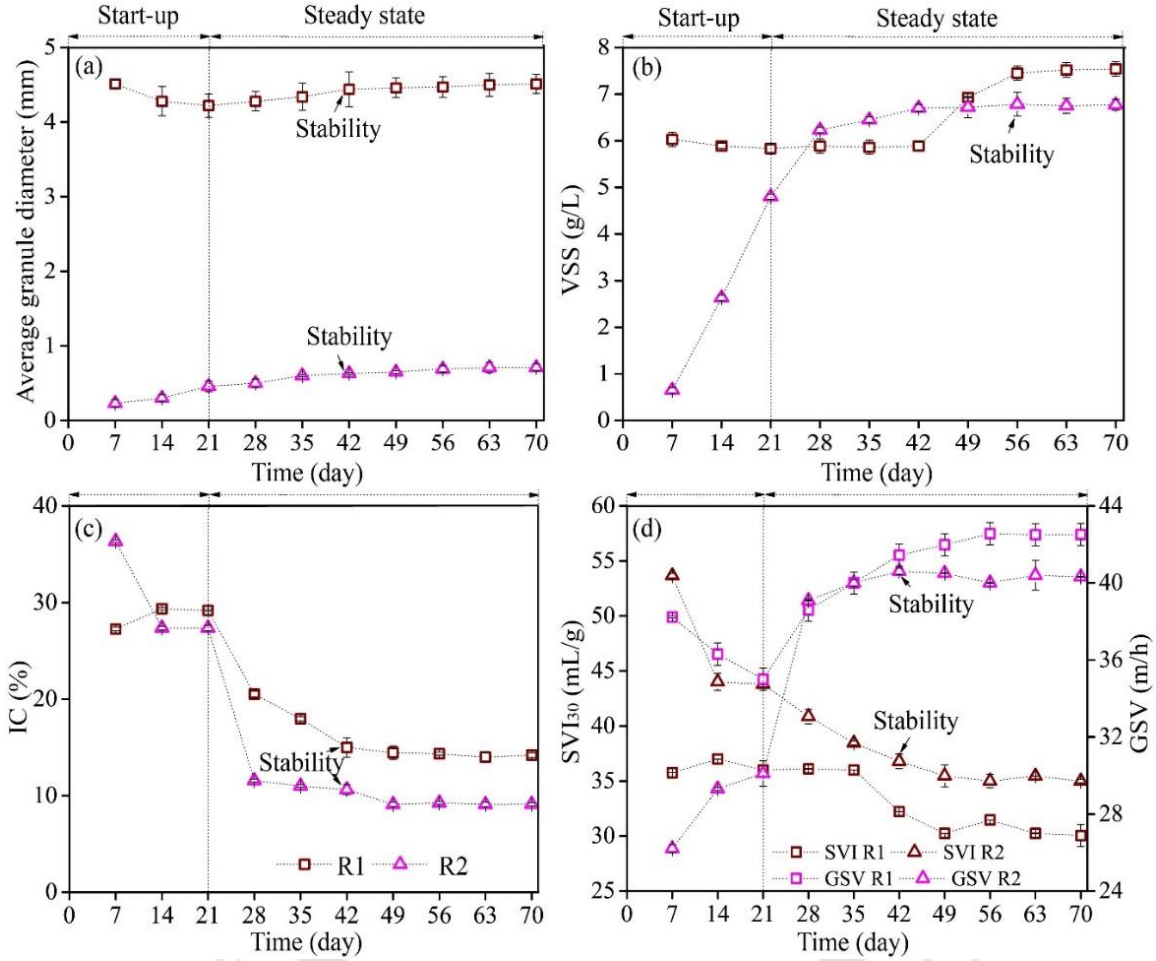

Fig.5.4 (a) Granule diameter, (b) VSS content, (c) IC and (d) comparative SVI_{30} and GSV profile in R1 and R2. [Stability means parameter became stable after the particular data point].

Fang et al. (2009) and Gobi and Vadivelu (2014) reported PHB and PHA productions in 1.5-3 mm sized granules cultivated in POME and acetate wastewater. But Gobi and Vadivelu (2015a) observed decreasing PHA accumulation with increasing granule diameter due to decreasing surface area. On other hand, about 4-fold increase in organic loading rate (OLR) promoted 1.3-fold increase in PHA yield in POME treatment (Gobi and Vadivelu, 2015a). Hence, increasing OLR (0.6-1.8 kg COD/m^3.day) and high C/N (24) conditions overcame the surface area limitation providing 40–71% PHA yield in R1 and R2. Fang et al. (2009)

suggested that granule VSS was proportional to C/N ratio of feed which is supporting our increasing VSS trends of the AGRs.

Low IC value denotes high granule strength and microbial compactness which is closely related to high VSS values of granular sludge (Ghangrekar et al., 2005). Refinery sludge granules had maximum 24±0.55% IC value which slightly increased up to 29.17±0.01% in start-up phase (day 21) due to instability in R1. But in steady state, IC value decreased and became almost stable at 14±0.5% indicating granule compactness which is further supported by the improved VSS (Fig.5.4b and c) till day 70. IC values varied within 13-9% in R2 determining high microbial strength of *Micrococcus* granules which is visible in FESEM images (section 5.3.3 and Fig.5.5). Though mixed sludge promoted PHA accumulating bigger and denser granules, *Micrococcus* granules acquired more integrity due to strong microbial structure.

5.3.2 Granule settleability

About 30-70 m/h of GSV and below 50 mL/g SVI_{30} values are optimum criteria for aerobic granulation (Qin et al., 2004; Liu and Tay, 2004). Fig.5.4d describes the comparative SVI_{30} and GSV trends in the AGRs. In R1, seed refinery granules possessed about 40 m/h of GSV and 25 mL/g of SVI_{30} values. In start-up phase, increasing oil concentration produced loose biomass providing 0.34±0.12 g/L of effluent VSS. Hence, granule settling slightly decreased up to 35±0.01 m/h and SVI_{30} increased up to 36±0.58 mL/g. In steady state, R1 had highly settleable bigger granules having 42.52±0.02 m/h and 30.04±1 mL/g of GSV and SVI_{30} values, respectively (day 70).

After matured granulation in R2 (day 21), *Micrococcus* granules achieved good settling properties with 30.1±0.66 m/h GSV and 43.8±0.67 mL/g SVI_{30} values. In steady state, GSV and SVI_{30} values gradually improved and reached stability at 40.32±0.57 m/h and 35±0.02 mL/g, respectively. Hence, bigger size provided slightly better settleability in mixed culture granules than pure strain originated granules during PHA accumulation in hydrocarbon-rich wastewater. Between day 22-70 the F/M ratio reached 0.20-0.15 and 0.19-0.18 g COD/g SS.day in R1 and R2, respectively. As increase in F/M ratio corresponds with deterioration of granule settleability, the opposite incident of declining F/M ratio trend further suggested the improvement in granule settling in our AGRs (Hamza et al., 2018).

Similarly, aerodynamic feeding in POME wastewater promoted 25-40 mL/g SVI_{30} with 90% COD removal in PHA accumulating granules which is supporting our study on highly settleable PHA producing oil degrading granules (Gobi and Vadivelu, 2014).

5.3.3 Microstructure observation

FESEM analysis provided microscopic granule structures at 5000× magnification on day 65 (Fig.5.5). R1 granule images revealed that in steady state, mixed culture refinery granules had dense non-filamentous formation which is supported by high VSS values (Fig.5.4b). But the presence of cocci on *Micrococcus* (R2) granules ensured strong microbial structure. The low IC profile (9-13%) further supported the increasing granule integrity in R2 granules (Fig. 5.4c).

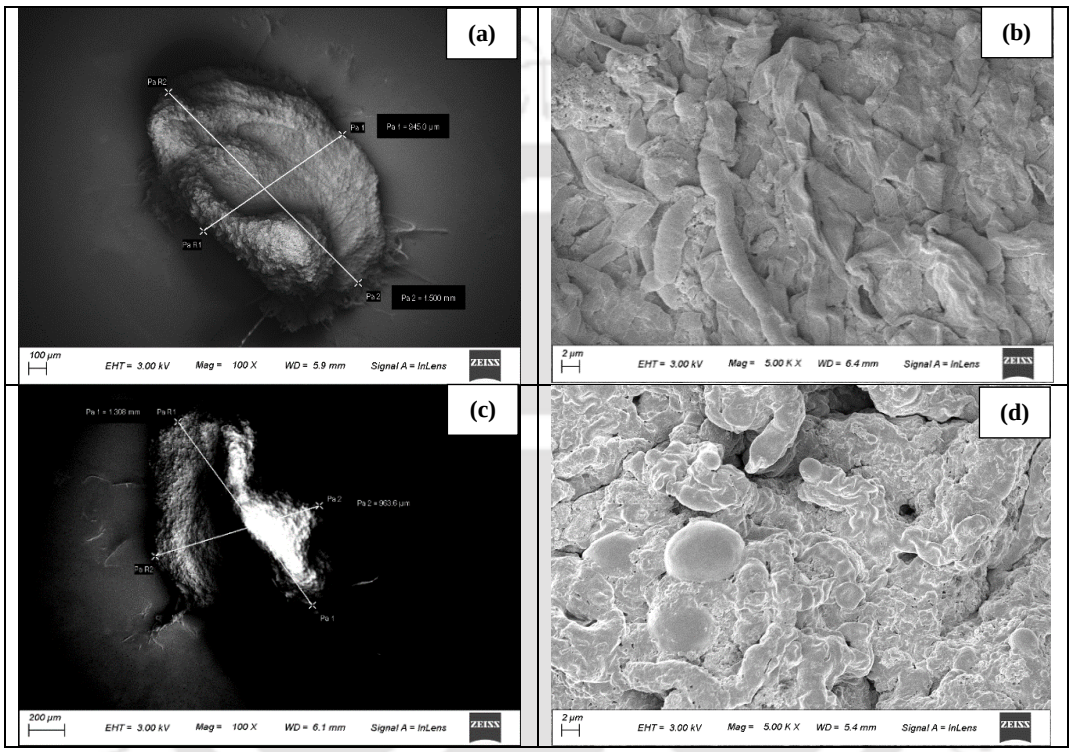

Fig.5.5 FESEM image of (a, b) non-filamentous dense refinery sludge granule and (c, d) *Micrococcus* granule with visible presence of cocci on surfaces. (Image was captured on day 65 at 5000× magnification).

5.3.4 PHA accumulation inside aerobic granules

5.3.4.1 Refinery sludge granules

The COD, DO and PHA production patterns in 8 h cycle of mixed sludge (R1) and *Micrococcus* granules (R2) are described in Fig.5.6. About 4.5-6.7 mg/L of DO concentration prevailed inside the AGRs at constant 2 L/min of air flow velocity. The initial refinery sludge granules had maximum capacity of producing 0.056±0.01 mg PHA/mg CDW. However, in start-up phase, R1 granules almost accumulated 68.34±0.12% COD in presence of 100-250 mg/L of diesel as sole carbon source providing 0.056-0.203 mg PHA/mg CDW yield which further increased up to 0.67±0.01 mg PHA/mg CDW in the initial steady sate (day 40).

Finally, on day 70, R1 had 130 mg/L effluent COD ensuring 87±2% COD removal within 2 h (feast phase) of the AGR operation (Fig.5.6a). The remaining COD either remained as nondegradable hydrocarbon fraction (12±2%) in effluent or slowly degraded (2±1%) in famine phase. Literature suggested that as maximum COD was consumed by the mixed culture granules, the excessive substrate would have been accumulated as PHA to be utilized as energy source in the rest 6 h of famine phase (Gobi and Vadivelu, 2014; Vijayan and Vadivelu, 2017). During POME treatment, Gobi and Vadivelu (2015a) and Vijayan and Vadivelu (2017) also observed that DO concentration was within 6-8.5 mg/L at 1.82 kg COD/m^3.day OLR and 2 L/min air flow rate, respectively which are corresponding with our DO trend in AGRs (Fig.5.6a).

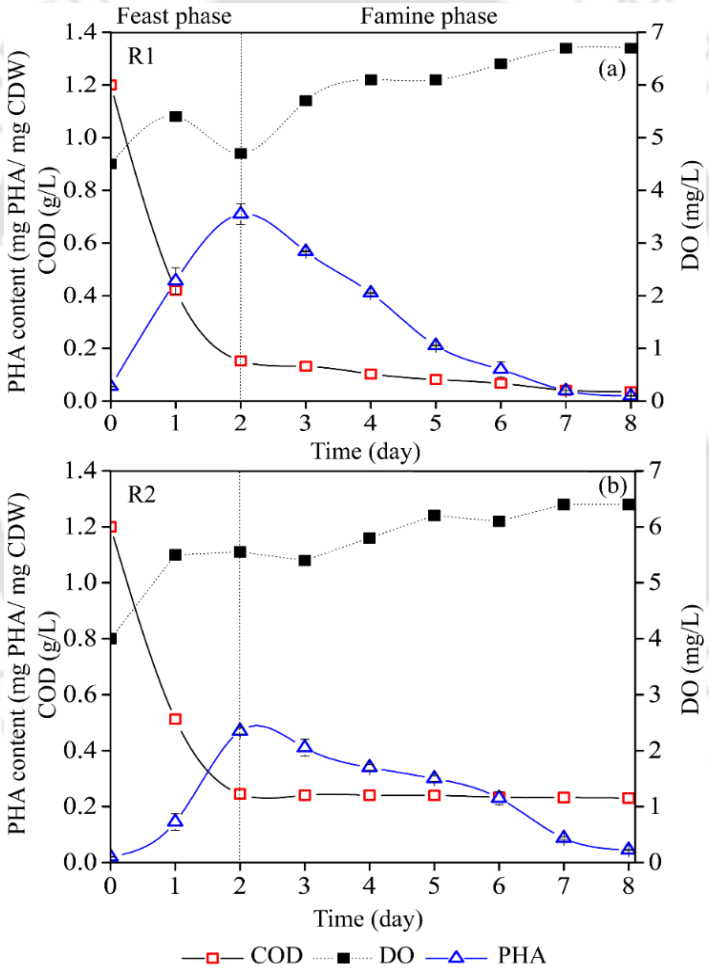

Fig.5.6 DO concentration, PHA accumulation and COD concentration in (a) R1 and (b) R2 in steady state in one complete cycle (8 h).

After day 56, PHA yield was further triggered up to 70-71% CDW which provided maximum 0.71±0.04 mg PHA/mg CDW (71±1% CDW) on day 70 with increasing biomass concentration and stability in refinery sludge granules (Fig.5.9a). In steady state, feast phase

provided maximum 0.7±0.04 mg PHA/mg CDW accumulation which gradually exhausted to 0.4-0.2 mg PHA/mg CDW at the end of famine phase (Fig.5.6a).

Similarly, Gobi and Vadivelu (2014) and Vijayan and Vadivelu (2017) observed maximum 0.56-0.683 mg PHA/mg biomass accumulation at the end of AGR feast phase treating POME consisting several volatile fatty acids (acetic, propionic, butyric, and valeric acids) which are proven precursors of PHA production. However, utilization of diesel wastewater having recalcitrant medium and long chain (C_{10}-C_{29}) alkanes are not yet well reported for PHA production in aerobic granules.

The increasing trend in PHA and COD accumulation helped to reach 0.68-0.89 mg PHA/mg COD yield in R1 (Fig.5.9c). Moreover, the intermittent feeding of AGR and high C/N (24) ratio provided the optimum scenario for high PHA accumulation (Fang et al., 2009). Corotonic acid assay showed that R1 had 0.044-0.58 and 0.012-0.13 mg PHA/mg CDW of PHB and PHV fractions providing 3.5-4.5 of PHB:PHV ratios which was supported by previous literature of PHA production by *H. mediterranei* utilizing waste vinasse (Bhattacharyya et al., 2012). Photographs of granule extracted PHA are given in Fig.5.7.

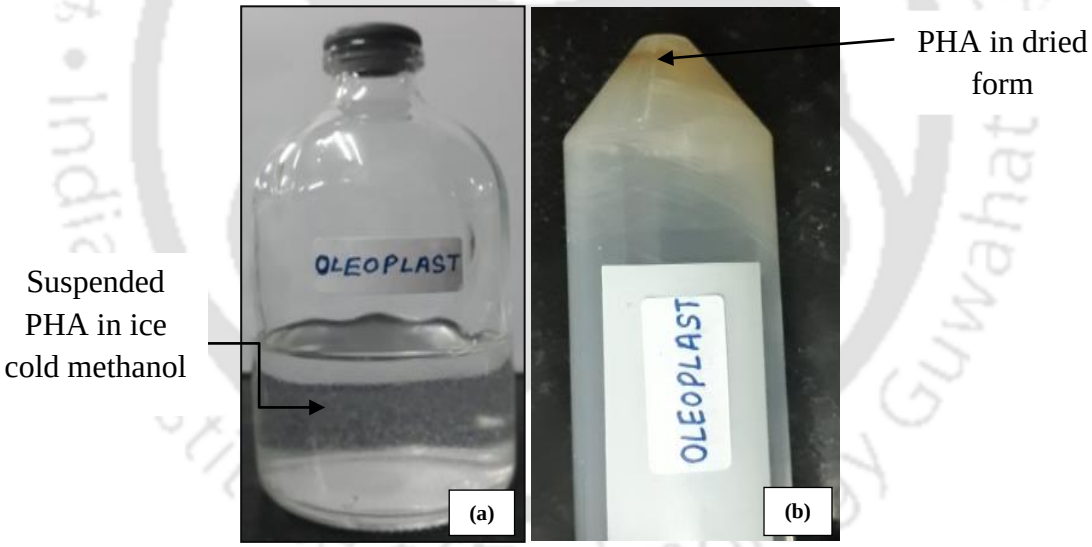

Fig.5.7 Extracted PHA from oil-fed aerobic granules in (a) suspended and (b) dried form.

Comparative representation of wastewater, inoculum, operating strategy, granule properties and PHA yield of recent AGR mediated studies are discussed in Table 5.2 which reflected the use of acetate wastewater or POME in AGRs as PHA synthesis substrates in previous literature whereas current study is about PHA accumutation in aerobic granules from wastewater containing recalcitrant diesel oil. Table 5.3 provides details of PHA production with % yield, mg PHA per mg of COD removal and PHB:PHV ratio at different phases of R1 and R2.

Table 5.2 Comparative study on PHA accumulation of aerobic granules in AGRs operated with different inoculum, wastewater and PHA enhancement strategies

Wastewater	Initial inoculum	Operational approach	PHA enhancement strategy	Granule characteristics	COD removal	PHA yield	References
Acetate wastewater	Anaerobic granular sludge from an up-flow anaerobic sludge blanket reactor	AGR volume: 2 L, HRT: 12 h, cycle time: 6 h, COD: 750 mg/L, NH_4^+-N: 8.5 mg/L.	Varying COD and ammonia concentration (COD/N: 20 to 90)	Size: 1.5 mm, [1]MLSS: 4-8 g/L, [2]MLVSS: 4.5-10 g/L, SVI_{30}: 30-40 mL/g	80-99%	PHB: 44% of CDW[3]	Fang et al. (2009)
Acetate wastewater	Municipal sewage sludge	AGR volume: 2 L, HRT: 12 h, cycle time: 6 h, COD/N: 48-72	i) Ammonium deficient condition (COD/N: 48 to 72) ii) Adjusting granule settling time (5 to 15 min)	Size: 1-3.8 mm, MLVSS: 3-9 g/L, SVI_{30}: below 40 mL/g, EPS: 6-30 mg/g VSS	90%	PHB: 40±4.6% of CDW	Wang et al. (2014)
Palm oil mill effluent (POME)	Activated sludge from POME treatment plant	Cycle time: 6 h, VER: 25%, H/D ratio: 10, flowrate: 3 L/min, OLR: 2.25 kg COD/m^3.day	Aerodynamic feeding (by maintaining feast-famine ratio between 0.15 to 0.36)	Size: 3 mm, SVI_{30}: 25-40 mL/g, EPS: 40–45 µg/mL	90%	PHA: 0.6833 mg PHA/mg biomass.	Gobi and Vadivelu (2014)
Palm oil mill effluent (POME)	Aerobic granules developed by Gobi and Vadivelu (2014)	AGR volume: 2 L, cycle time: 24 h, VER: 25%, OLR: 0.91-3.64 kg COD/m^3.day	Growth disintegration cycle varied on granule sizes between 0.35-2 mm, OLR between 0.91-3.64 kg COD/m^3.day and aeration between 1-4 L/min	size: 0.35-2 mm	90%	PHA: 0.66 to 0.87 g PHA/g CDW	Gobi and Vadivelu (2015a)
Palm oil mill effluent (POME)	Activated sludge from POME treatment plant (Gobi et al., 2011)	AGR volume: 8 L, cycle time: 6 h, VER: 25%, air flowrate: 5 L/min, OLR: 3-6 kg COD/m^3.day	Effects of sodium hypochlorite, acetone, sodium hydroxide, sodium chloride were checked in PHA extraction	size: 0.9-3.1 mm, MLSS: 3.7 mg/L, SVI_{30}: 30 mL/g	90%	PHA: 89% of CDW	Gobi and Vadivelu (2015b)
Palm oil mill effluent (POME)	Aerobic granules developed by Gobi and Vadivelu (2014)	AGR volume: 2 L, cycle time: 8 h, VER: 50%, air flowrate: 0-2 L/min, OLR: 2.25 kg COD/m^3.day	Varying aeration in the famine phase (2, 1, 0.5 and 0 L/m flowrates)	Size: 1.03-1.3 mm, SVI_{30}: 20-41 mL/g	90%	PHA: 0.56 and 0.17 g PHA/g CDW (in feast and famine phase)	Vjayan and Vadivelu (2017)

Oily wastewater	Refinery sludge granules (developed in Chapter 2) and *Micrococcus aloverae* SG002 granules	AGR volume: 3 L, cycle time: 8 h, VER: 50%, air flowrate: 2 L/min, OLR: 0.6-1.8 kg COD/m^3.day	Comparative study on PHA accumulation in mixed culture and pure strain granules varying OLR and C/N	Size: 4.51, 0.71 mm, VSS: 7.54, 6.77 g/L, SVI_{30}: 30, 35 mL/g, GSV: 42.52, 40.32 m/h, EPS: 409.36, 281.09 mg/g VSS, IC: 14, 9%.	90.34, 80.67%	71±0.04, 0.47±0.04 mg PHA/mg CDW	Current study

[1]MLSS: Mixed liquor suspended solids (g/L)
[2]MLVSS: Mixed liquor volatile suspended solids (g/L)
[3]CDW: Cell dry weight (mg)

Table 5.3 Details of PHA production with PHB and PHV ratio at different phases of R1 and R2 granules

PHA Yield	***Micrococcus aloverae* SG002 culture (liquid)**				**R1 Initial (Seed refinery granules)**				**R1 Final (Refinery granules on day 70)**				**R2 (*Micrococcus* granules on day 70)**			
	PHB	**PHV**	**PHA (Total)**	**PHB: PHV**	**PHB**	**PHV**	**PHA (Total)**	**PHB: PHV**	**PHB**	**PHV**	**PHA (Total)**	**PHB: PHV**	**PHB**	**PHV**	**PHA (Total)**	**PHB: PHV**
% yield	1.6±0.01	0.5±0.01	2.1± 0.1	3.2	4.4± 0.5	1.2± 0.2	5.6±1	3.5	58.1± 1	12.9±0.5	71±1	4.5	38.5± 0.5	8.5±0.02	47±1	4.4
$Y_{PHA/biomass}$ (mg PHA/mg CDW)	0.016± 0.002	0.005 ±0.002	0.021± 0.001	3.2	0.044± 0.01	0.012± 0.01	0.056±0.01	3.5	0.58 ± 0.02	0.13±0.01	0.71± 0.04	4.5	0.38 ±0.01	0.85 ±0.02	0.47± 0.04	4.4
$Y_{PHA/COD}$ (mg PHA/mg COD)	-	-	0.032±0.02	-	-	-	0.041±0.001	-	-	-	0.897±0.1	-	-	-	0.38±0.02	-

5.3.4.2 *Micrococcus aloeverae* SG002 granules

The liquid culture of oil degrading *Micrococcus aloeverae* strain SG002 provided a nominal 0.021±0.001 mg PHA/mg CDW yield after being fed with 300 mg/L emulsified diesel having 1200 mg/L influent COD and 50 mg/L NH_4^+-N with 2 L/min aeration in a 500 mL shake flask for 7 days. However, after 21 days of AGR operation, *Micrococcus* granules removed about 70.23±0.52% COD with 20.55±1% PHA accumulation having 3.2-3.5 of PHB:PHV fractions. The steady state provided constant 300 mg/L oil and 1200 mg/L COD concentration in R2 which helped the granules to achieve 80.67±0.43% COD removal accumulating maximum 0.47±0.04 mg PHA/mg CDW (Fig.5.9b).

In R2, maximum COD removal (80%) was observed in feast phase (2 h of the AGR cycle) ensuring 0.47±0.01 mg PHA/mg CDW accumulation in granules to be used as energy storage (Fig.5.6b). The PHB fraction was always higher than the PHV fractions in both AGRs. In R2 the final PHB:PHV ratio was 4.4 on day 70 promoting 0.23-0.38 mg PHA/mg COD yield (Fig.5.9c).

Non-granulated liquid biomass of *P. putida*, *P. aeruginosa* and *H. mediterranei* were cultivated in different substrates (corn oil, soybean oil, n-hexadecane, waste vinasse) in both shake flask or reactor conditions which promoted about 80-90% COD removal to reach nearly 40% PHA yield (Bhattacharyya et al., 2012; Raza et al., 2016, 2018). Hence, in 70 days AGR operation, granular biomass of *Micrococcus* and refinery sludge were proved to be effective in increasing 45-65% PHA yields than liquid biomass and seed granules.

5.3.5 PHA characterization

The aerobic granule derived PHA was analysed in FTIR and ^{1}H NMR to determine the chemical compositions. Fig.5.8a and b are providing FTIR and ^{1}H NMR spectra of PHA produced in the AGRs. The FTIR spectra of R1 and R2 granule accumulated PHA (day 60) produced several peaks which indicated that the PHA was in P (3HB-*co*-3HV) which was similar with the peaks observed in commercial PHA (Sigma Aldrich, USA).

The presence of adsorption bands at 3436.59 and 3435.63 cm^{-1} in R1 and R2 accumulated PHA corresponded to the asymmetric methyl (-CH_3) stretching which was similar to the P (3HB-*co*-3HV) reported in the work by Reddy et al. (2012). The peak at 1737.99 cm^{-1} represented the carbonyl (C=O) group which was found to be present in PHA. Meanwhile, the peaks at 1214, 1215, 1217 cm^{-1} indicated the presence of the C–O stretching of polymer ester and the bands at 1421.80 and 3020.01 cm^{-1} suggested the probable presence of methyne (-CH) group and methylene (-CH_2) vibrations, respectively (Gobi and Vadivelu, 2014; Amulya et al., 2016).

The ^{1}H NMR results (Fig.5.8b) further suggested that the granule PHA was a co-polymer P (3HB-*co*-3HV) of two monomers hydroxybutyrate (HB) and hydroxyvalerate (HV). The PHA sample of both R1 and R2 provided similar ^{1}H NMR spectra and chemical groups irrespective of the type of inoculum and granule characteristics. So, we have given only the ^{1}H NMR result of R2 sample in Fig.5.8b. The resonances observed at 0.88-0.90, 1.26-1.29, 1.586, 2.54-2.64 and 5.22-5.28 ppm determined the presence of the $–CH_3$ (HV side group), $–CH_3$ (HB side group), $–CH_2$ (HV side group), $–CH_2$ (HB and HV bulk structure) and –CH (HB and HV bulk structure) groups, respectively (Bhattacharyya et al., 2012; Gobi and Vadivelu, 2015b). The sharp peaks near 3.12 ppm indicated the methyl ester group ($-CH_3O$) and 6.25 ppm signified the PHA dissolving solvent $CDCl_3$ (Amulya et al., 2016).

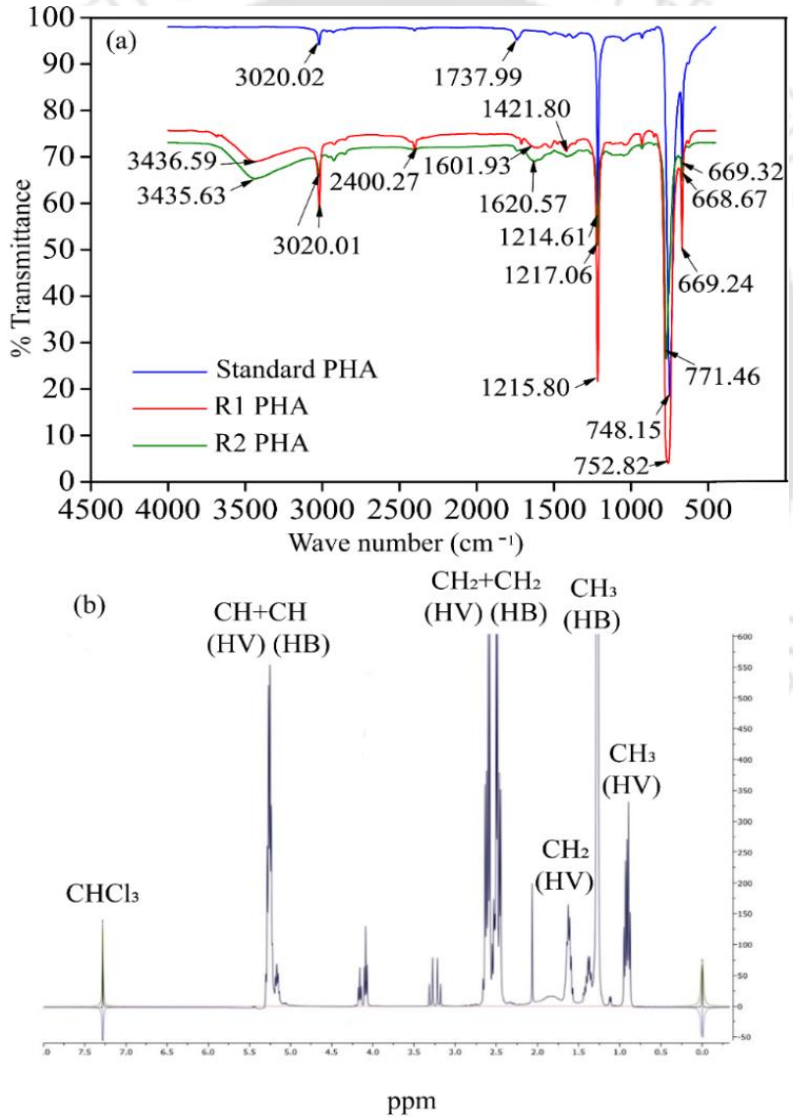

Fig.5.8 (a) FTIR spectra of standard and R1, R2 granule derived PHA and (b) ^{1}H NMR spectra of R2 derived PHA (as R1 and R2 samples had similar spectra) cultivated in hydrocarbon-rich wastewater.

5.3.6 EPS and PHA correlation in the AGRs

EPS and PHA correlation trends in R1 and R2 are given in Fig.5.9a and b and PHA yield in terms of COD removal are given in Fig.5.9c. EPS are proteins (PN) and polysaccharides (PS) which form the outer granule layer providing more stability and hydrophobicity (Liu and Tay, 2002). They play a major role in cell aggregation and granule formation.

The mixed culture seed refinery granules in R1 had 400.04±1.74 mg/g VSS of EPS content with approximately 0.056±0.01 mg PHA/mg CDW yield. In start-up phase (up to day 21), the changing OLR (0.6-1.5 kg COD/m^3.day) and C/N ratio (8-24) caused EPS fluctuation which varied between 400 to 385 mg/g VSS in R1. PHA production also ranged between 0.056 and 0.21 mg PHA/mg CDW (Fig.5.9a).

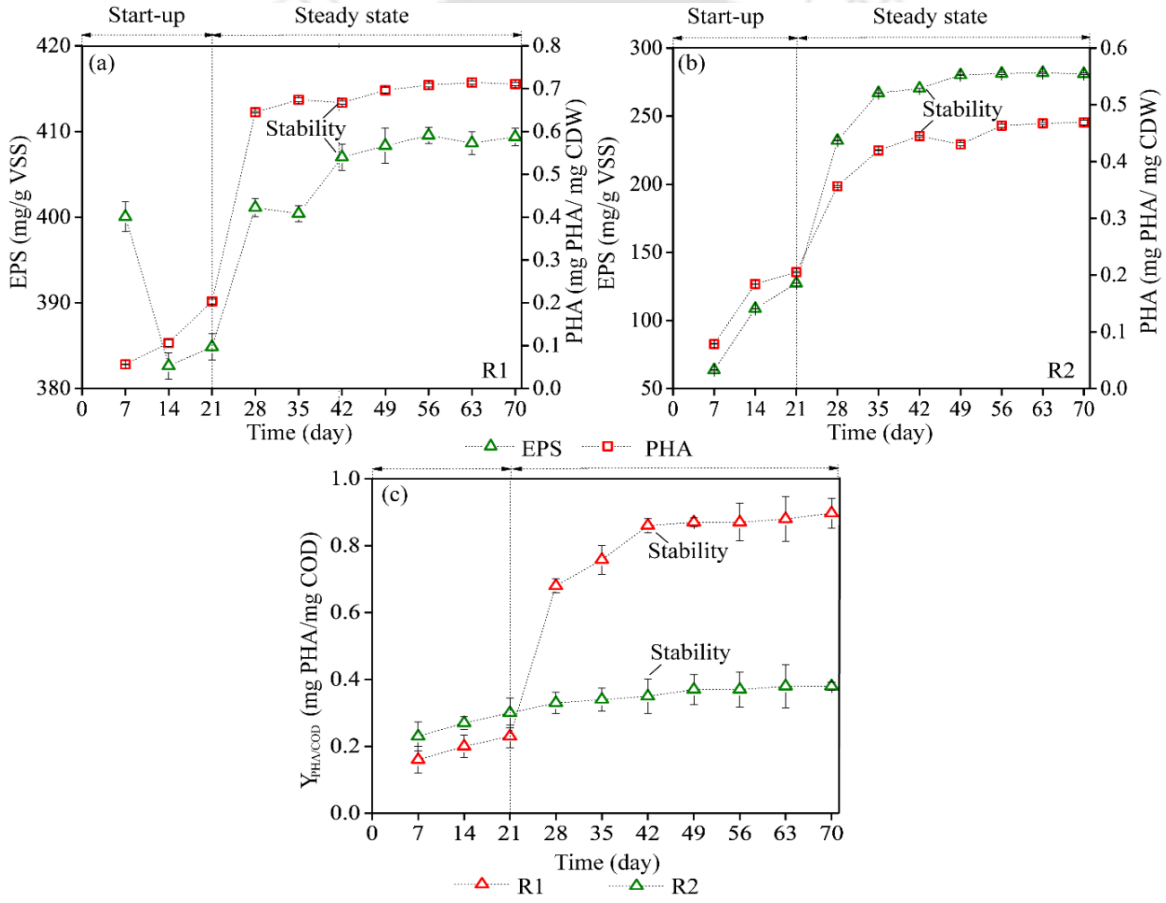

Fig.5.9 EPS and PHA correlation in (a) R1 and (b) R2 and (c) PHA accumulation per mg COD removal in steady state of the AGRs. [Stability means parameter became stable after the particular data point].

Initially in steady-state (day 28-42), 0.6-1.5 kg COD/m^3.day OLR and constant airflow velocity (2 L/min) promoted stress increasing the EPS concentration up to 407±1.52 mg/g VSS in R1. It simultaneously increased PHA accumulation till 0.64–0.66 mg PHA/mg CDW (Nichols et al., 2004). Eventually, the final EPS and PHA yield reached stability at 409.36±1

mg/g VSS and 0.71±0.04 mg/mg CDW, respectively on day 70. Increasing VSS content is equivalent to more active biomass in the AGR as observed in Chapter 3 (section 3.3.3.1). In current study, active biomass proliferated more EPS on the granule surfaces. Increasing EPS content enhanced the polymeric interaction of flocculent biomass to form matured compact granules and also increased the granule surface energy (Tsuneda et al., 2003; Artelt et al., 2005). The study ensured that EPS and PHA concentrations were proportional to each other. Wang et al. (2014) also observed that granule EPS and PHA yield in acetate wastewater was influenced by reactor operating conditions like HRT, C/N and shear force and followed similar trend which is supporting our results.

In R2 also, granule EPS and PHA increased and decreased correspondingly to each other. In start-up phase, *Micrococcus* granules achieved maximum 127.34±0.15 mg/g VSS of EPS accumulating 0.205±0.013 mg PHA/mg CDW. PHA and EPS profile were proved to be interlinked and they gradually increased together with increasing biomass concentration in both mixed and pure strain aerobic granules. On day 70 at 300 mg/L of constant diesel exposure, R2 granules finally had 281.09±0.53 mg/g VSS of EPS concentration with 0.47±0.04 mg PHA/mg CDW of maximum yield (Fig.5.9b). PN:PS ratio was observed to be 3.5-4.5 in both AGRs which was within the optimum range suggested in literature for stable granulation (Adav and Lee, 2008).

5.3.7 Organics removal by the AGRs

Seed refinery granules and liquid culture of *Micrococcus aloeverae* SG002 were capable of 67.39±0.15% and 61.34±0.85% of TPH removal after 8 h and 48 h of inoculation, respectively in 320 mg/L of diesel concentration.

Fig.5.10 provides the COD and TPH removal patterns in R1 and R2. In start-up phase, influent COD and OLR values gradually increased from 400-1000 mg/L and 0.6-1.5 kg COD/m^3.day in the AGRs. The hydrocarbon loading rate (HLR) ranged between 0.15 to 0.37 kg/m^3.day till day 21. In start-up phase (day 21), R1 and R2 granules achieved maximum 68.34±0.44, 70.23±0.12% COD and 70.41±0.21, 72±0.50% of TPH removal, respectively. Steady state provided constant 1.8 kg COD/m^3.day of OLR and 0.45 kg/m^3.day of HLR with 1200 mg/L of COD concentration. Both AGRs achieved a stable COD and TPH removal pattern after day 42 of the study. Similarly in Chapter 3, increased granule stability and biomass concentration further helped the mixed sludge granules in R1 in almost 90±1% COD and TPH removal after 70 days of AGR operation. In R2 also granulated *Micrococcus* reached 80.67±0.5% COD and 81.40±0.2% TPH removal in 70 days. The declining trend in

F/M ratio from 0.2-0.17 g COD/g SS.day (in average) indicated presence of adequate amount of microorganisms to consume 80-90% organics from the substrate (Hamza et al., 2018).

GC-MS spectra revealed the presence of short chain compounds like cyclohexane to octane (C_6-C_8), medium chain like dodecane to octadecane (C_{12}-C_{18}) and long chain like tetracosane to hexatriacontane (C_{24}-C_{36}) *n*-alkane peaks in the untreated oily wastewater (Fig.5.11a). The major long and medium chain *n*-alkane peaks (C_{16}-C_{36}) almost disappeared (sample collected on day 65) and some small and medium chain alkane peaks (C_8, C_{15}) were sparsely detected in the R1 effluent (Fig.5.11b) denoting TPH degradation by the mixed culture refinery granules.

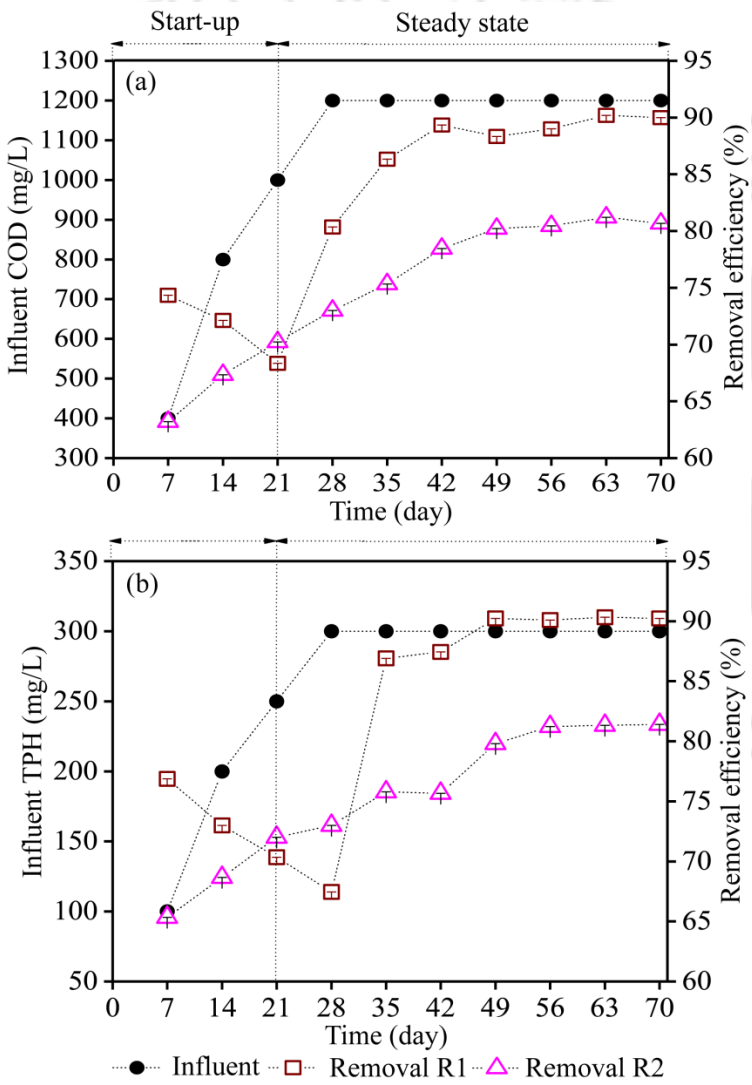

Fig.5.10 (a) COD and (b) TPH removal profile in the AGRs.

However, in R2, *Micrococcus* granules were capable of removing short chain (C_6-C_{10}) alkanes from the effluent (sample collected on day 65). Some medium and long chain *n*-alkanes like heptasiloxane (C_{17}), octacosane (C_{28}), hexatriacontane (C_{36}) and hexasiloxane (C_{16}) were identified as non-degraded hydrocarbon residues in R2 (Fig.5.11c).

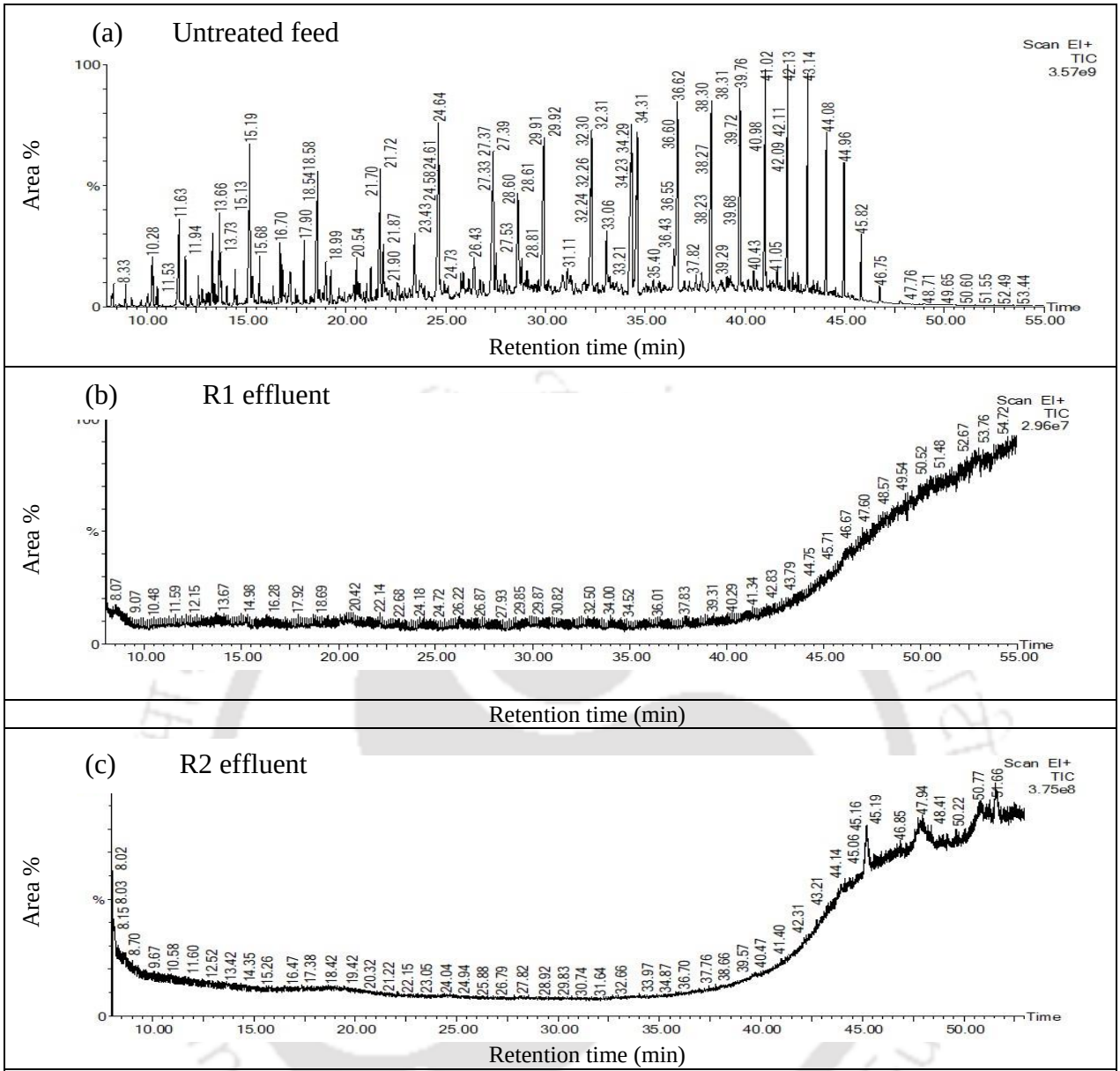

FEED		R1 EFFLUENT		R2 EFFLUENT	
RT (min)	**Compounds**	**RT (min)**	**Compounds**	**RT (min)**	**Compounds**
10.27	Hexyl octyl ether (C_{14})	22.14	Octane (C_8)	45.55	Heptasiloxane (C_{17})
11.94	Cyclohexane (C_6)	34.00	Pentadecane (C_{15})	47.60	Octacosane (C_{28})
15.18	Octanol (C_8)			49.54	Hexatriacontane (C_{36})
21.72	Dodecane (C_{12})			49.89	Hexasiloxane (C_{16})
24.64	Octane (C_8)				
27.36	Hexadecanoic acid (C_{16})				
29.99	Tetradecane (C_{14})				
32.31	Pentadecane (C_{15})		Major peaks		Major peaks
34.6	Pentadecane (C_{15})		disappeared		disappeared
38.33	Octacosane (C_{28})				
41.07	Octadecane (C_{18})				
42.17	Tetracosane (C_{24})				
45.81	Octacosane (C_{28})				
46.14	Hexatriacontane (C_{36})				

Fig.5.11 GC-MS spectra and detected compounds in (a) untreated oily wastewater and (b) R1, (c) R2 treated effluent.

Similarly, in our previous study, we reported about 69-90% TPH removals at various operating HRTs (12, 24 and 48 h) in mixed sludge granules (mixture of sewage, refinery and brewery sludge) which probably followed an alkane degradation pathway where hydrocarbon was mostly converted to fatty acids which undergone β-oxidation and other part remained in effluents (as mentioned in Chapter 3, section 3.3.3.1). As emulsified diesel was the sole carbon source in R1 and R2, COD removal was correlated to TPH removal. Hence, the nondegraded 30 and 55.8 mg/L of TPH in R1 and R2 effluent accounted for the 120 and 232 mg/L of remaining COD in effluent which is visible as alkane fraction peaks in R1 and R2 effluent spectra (Fig.5.11b and c). The study predicted biotransformation of C_{16}-C_{36} and C_6-C_{10} *n*-alkanes into P (3HB-*co*-3HV) by refinery sludge granules and *Micrococcus* granules, respectively.

P. aeruginosa was capable of biotransformation of hexadecane into 40% PHA yield where substrate utilization varied between 80 to 40% in presence of 1%, 2% and 3% hexadecane concentration (Raza et al., 2016). Previous literature reported 80-90% COD removal by both mixed sludge aerobic granules and single strain liquid culture which were cultivated in simple wastewater or low strength POME having less PHA accumulation than current study (Song et al., 2008; Wang et al., 2014; Vijayan and Vadivelu, 2017).

Hence, current study showed that in 70 days AGR operation, *Micrococcus* granules in R2 achieved almost 19% improvement in TPH removal than non-granulated liquid culture and about 23% TPH removal was enhanced in R1 while compared to the seed refinery sludge granules. So firstly, use of mixed inoculum is suggested for bigger, denser and settleable granules to achieve 70% PHA accumulation with 90% hydrocarbon removal efficiencies. Secondly, use of single strains in granulated form is proved to be beneficial to increase microbial integrity, TPH removal as well as 45% of PHA accumulation.

5.3.8 Ammonia nitrogen removal

Refinery seed granules had 94.34±0.01% NH_4^+-N removal efficiency. The nitrogen loading rate (NLR) in AGR was 0.075 kg NH_4^+-N/m^3.day throughout the study. NH_4^+-N removal patterns in R1 and R2 are described in Fig.5.12. R1 granules faced slight granule disintegration in start-up phase reducing granule size. Hence the ammonia oxidizing layer depletion hampered ammonia removal up to 91.34±0.03% in start-up phase (Tay et al., 2002). However, in steady state, R1 achieved stable 99±0.5% removal with improved granule biomass concentration and EPS content. In R2, *Micrococcus* granules achieved maximum 97±0.51% final removal in steady state (day 70).

Ion chromatography results showed that nitrite-nitrogen (NO_2^--N) production was almost negligible and about 0.7 and 1 mg/L nitrate-nitrogen (NO_3^--N) were detected in R1 and R2 treated effluent. The overall nitrification reaction is described in equation 1.2a-c in Chapter 1.

In steady state (day 22-70), the average SRT values for R1 and R2 were calculated as 10 and 9 days by using equation 2.7 (Chapter 2) and the effluent VSS values were 0.21 and 0.34 g/L, respectively. As low F/M ratio is correlated with high SRT values, R1 had longer SRT than R2 (Hamza et al., 2018). Nitrogen balancing was carried out according to Chapter 3. Nitrogen uptake for biomass growth was calculated by equation 2.8 (Chapter 2) which was found to be 48.7 mg/L in R1 and 47.2 mg/L in R2 at 4.5 L/day of flow rate in AGRs.

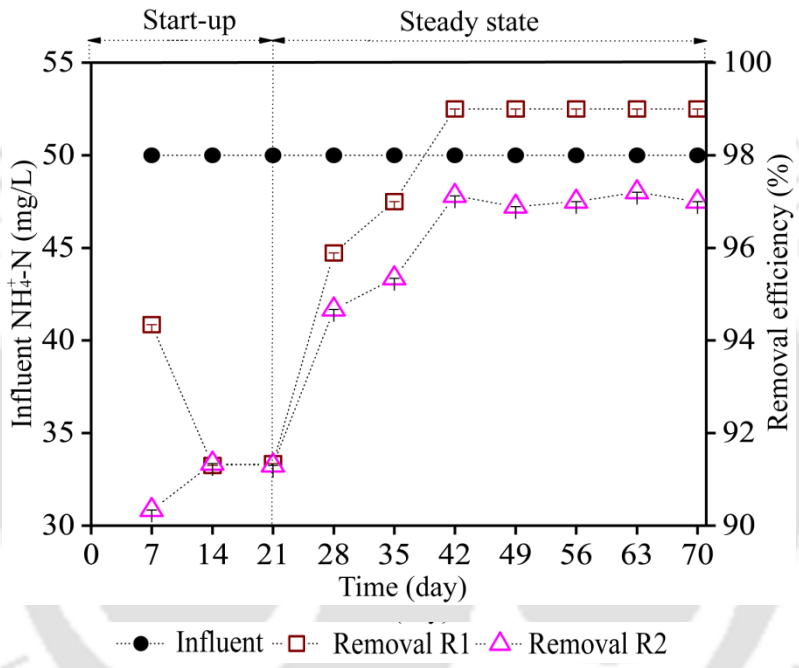

Fig.5.12 NH_4^+-N removal profile in the AGRs

On day 70, the effluent NH_4^+-N concentration in R1 and R2 were found to be 0.5 and 1.5 mg/L, respectively. The amount of theoretical and actual nitrogen oxidised were found to be 0.8 and 0.7 mg/L, 1.3 and 1 mg/L in R1 and R2, respectively. Theoretical nitrogen utilized was calculated according to equation 3.6 given in Chapter 3.

The study showed that about 97-99% was utilized for biomass growth and with only 1-1.5% complete nitrification occurred in irrespective of type of inoculum in R1 and R2 which is corresponding with nitrification results of our previous study in Chapter 3 on AGR mediated oily wastewater treatment in different HRTs. However, as the nitrification was observed to be very less in the reactors chance of denitrification was almost negligible.

The statistical analysis of granule characteristics, reactor performance, and PHA yield of the AGRs has been provided along with standard deviation and F-value in Table 5.4.

Table 5.4 Statistical analysis of granule characteristics, reactor performance, and PHA yield of the AGRs

Reactor	**R1**		**R2**		**Overall ANOVA**				
Operation time (day)	**1-70**		**1-70**						
	Mean	**SD**	**Mean**	**SD**	**R-square**	**Coeff Var**	**Root MSE**	**Mean square**	**F-value**
Granule size (mm)	4.40	0.11	0.54	0.17	0.99	0.05	0.14	74.22	3570.08
VSS (g/L)	6.48	0.77	5.45	2.14	0.10	0.27	1.61	5.35	2.06
SVI_{30} (mL/g)	33.51	2.89	39.84	5.97	0.33	0.12	4.69	201.04	9.11
GSV (m/h)	39.914	2.76	36.65	5.70	0.12	0.11	4.48	53.17	2.64
EPS (mg/g VSS)	401.97	9.94	219.34	85.16	0.71	0.19	60.63	165350.02	44.97
IC (%)	19.62	6.54	16.08	10.18	0.04	0.47	8.56	62.74	0.85
PHA yield (mg PHA/ mg CDW)	401.19	9.94	219.34	85.16	0.71	0.19	60.63	165350.022	44.97
COD removal efficiency (%)	82.83	8.37	75.01	6.36	0.23	0.09	7.43	306.23	5.53
TPH removal efficiency (%)	82.29	9.30	75.42	5.66	0.18	0.09	7.69	236.12	3.98
NH_4^+-N removal efficiency (%)	96.48	3.16	94.82	2.78	0.08	0.03	2.97	13.89	1.56

5.4 Summary of the chapter

The study provided a simultaneous oil removal and bioplastic production process in two AGRs operated with mixed sludge granules and *Micrococcus* originated granules. AGR operation enhanced 23% hydrocarbon removal with strong, settleable and EPS enriched granules developed from mixed refinery sludge. *Micrococcus* strain granulated in 21 days with 81% and 47% TPH removal and PHA yield capacities, respectively. Changing OLR and high C/N ratio provided stress in AGR for maximum 0.71±0.04 mg PHA/mg CDW accumulation in refinery granules. Aerobic granules consumed 80-90% COD in 2 h promoting PHA accumulation as excess energy source for carbon deficient phase (6 h). Granule derived biopolymer P (3HB-*co*-3HV) with 3.5-4.5 PHB:PHV fractions were comparable with commercial PHA (Sigma-Aldrich, USA). Most of the long chain (C_{16}-C_{36}) and short chain (C_6-C_{10}) alkanes were biotransformed into PHAs. Use of bigger, denser mixed culture granules and biogranulated *Micrococcus aloeverae* strain SG002 are the two eco-friendly strategies which are recommended in the current study to achieve 50–70% biodegradable PHA yield and 80–90% removal of recalcitrant hydrocarbons.

References

Adav, S.S., Lee, D.-J., 2008. Extraction of extracellular polymeric substances from aerobic granule with compact interior structure. Journal of Hazardous Materials 154, 1120-1126.

Amulya, K., Reddy, M. V., Rohit, M. V., Mohan, S. V., 2016. Wastewater as renewable feedstock for bioplastics production: understanding the role of reactor microenvironment and system pH. Journal of Cleaner Production 112, 4618-4627.

Artelt, C., Schmid, H.J., Peukert, W., 2005. On the impact of accessible surface and surface energy on particle formation and growth from the vapour phase. Journal of Aerosol Science 36, 147–172.

Bhattacharyya, A., Pramanik, A., Maji, S. K., Haldar, S., Mukhopadhyay, U. K., Mukherjee, J., 2012. Utilization of vinasse for production of poly-3-(hydroxybutyrate-co-hydroxyvalerate) by *Haloferax mediterranei*. AMB express 2, 1-10.

Campanari, S., Augelletti, F., Rossetti, S., Sciubba, F., Villano, M. and Majone, M., 2017. Enhancing a multi-stage process for olive oil mill wastewater valorization towards polyhydroxyalkanoates and biogas production. Chemical Engineering Journal 317, 280-289.

Fang, F., Liu, X. W., Xu, J., Yu, H. Q., Li, Y. M., 2009. Formation of aerobic granules and their PHB production at various substrate and ammonium concentrations. Bioresource Technology 100, 59-63.

Ghangrekar, M., Asolekar, S., Joshi, S., 2005. Characteristics of sludge developed under different loading conditions during UASB reactor start-up and granulation. Water Research 39, 1123-1133.

Gobi, K., Vadivelu, V. M., 2014. Aerobic dynamic feeding as a strategy for in situ accumulation of polyhydroxyalkanoate in aerobic granules. Bioresource Technology 161, 441-445.

Gobi, K., Vadivelu, V. M., 2015a. Dynamics of polyhydroxyalkanoate accumulation in aerobic granules during the growth–disintegration cycle. Bioresource Technology 196, 731-735.

Gobi, K., Vadivelu, V. M., 2015b. Polyhydroxyalkanoate recovery and effect of in situ extracellular polymeric substances removal from aerobic granules. Bioresource Technology 189, 169-176.

Hamza, R.A., Sheng, Z., Iorhemen, O.T., Zaghloul, M.S. and Tay, J.H., 2018. Impact of food-to-microorganisms ratio on the stability of aerobic granular sludge treating high-strength organic wastewater. Water Research 147, 287-298.

Ho, K. L., Lin, B., Chen, Y. Y., & Lee, D. J., 2009. Biodegradation of phenol using Corynebacterium sp. DJ1 aerobic granules. Bioresource Technology 100, 5051-5055.

Kim, D.Y., Kim, H.W., Chung, M.G., Rhee, Y.H., 2007. Biosynthesis, modification, and biodegradation of bacterial medium-chain-length polyhydroxyalkanoates. Journal of Microbiology 45, 87–97.

Li, A.J., Li, X.Y. and Yu, H.Q., 2011. Effect of the food-to-microorganism (F/M) ratio on the formation and size of aerobic sludge granules. Process Biochemistry 46, 2269-2276.

Liu, Y., Tay, J.-H., 2002. The essential role of hydrodynamic shear force in the formation of biofilm and granular sludge. Water Research 36, 1653–1665.

Liu, Y., Tay, J.-H., 2004. State of the art of biogranulation technology for wastewater treatment. Biotechnology Advances 22, 533–563.

Mahansaria, R., Choudhury, J. D., Mukherjee, J., 2015. Polymerase chain reaction-based screening method applicable universally to environmental haloarchaea and halobacteria for identifying polyhydroxyalkanoate producers among them. Extremophiles 19, 1041-1054.

Mannina, G., Presti, D., Montiel-Jarillo, G., Carrera, J., Suárez-Ojeda, M. E., 2020. Recovery of polyhydroxyalkanoates (PHAs) from wastewater: A review. Bioresource Technology 297, 122478.

Mohan, S. V., Reddy, M. V., Subhash, G. V., Sarma, P. N., 2010. Fermentative effluents from hydrogen producing bioreactor as substrate for poly (β-OH) butyrate production with simultaneous treatment: An integrated approach. Bioresource Technology 101, 9382-9386.

Nichols, C.A.M., Garon, S., Bowman, J.P., Raguenes, G., Guezennec, J., 2004. Production of exopolysaccharides by Antarctic marine bacterial isolates. Journal of Applied Microbiology 96, 1057–1066.

Qin, L., Tay, J.-H., Liu, Y., 2004. Selection pressure is a driving force of aerobic granulation in sequencing batch reactors. Process Biochemistry 39, 579–584.

Raza, Z. A., Abid, S., Banat, I. M., 2018. Polyhydroxyalkanoates: Characteristics, production, recent developments and applications. International Biodeterioration Biodegradation 126, 45-56.

Raza, Z. A., Abid, S., Rehman, A., Hussain, T., 2016. Synthesis kinetics of poly (3-hydroxybutyrate) by using a Pseudomonas aeruginosa mutant strain grown on hexadecane. International Biodeterioration Biodegradation 115, 171-178.

Reddy, M. V., Nikhil, G. N., Mohan, S. V., Swamy, Y. V., Sarma, P. N., 2012. *Pseudomonas otitidis* as a potential biocatalyst for polyhydroxyalkanoates (PHA) synthesis using synthetic wastewater and acidogenic effluents. Bioresource Technology 123, 471-479.

Song, J. H., Jeon, C. O., Choi, M. H., Yoon, S. C., & Park, W., 2008. Polyhydroxyalkanoate (PHA) production using waste vegetable oil by *Pseudomonas* sp. strain DR2. Journal of Microbiology and Biotechnology 18, 1408-1415.

Tsuneda, S., Aikawa, H., Hayashi, H., Yuasa, A., Hirata, A., 2003. Extracellular polymeric substances responsible for bacterial adhesion onto solid surface. FEMS Microbiology Letters 223, 287–292.

Vjayan, T., Vadivelu, V. M., 2017. Effect of famine-phase reduced aeration on polyhydroxyalkanoate accumulation in aerobic granules. Bioresource Technology 245, 970-976.

Wang, J., Li, W. W., Yue, Z. B., Yu, H. Q., 2014. Cultivation of aerobic granules for polyhydroxybutyrate production from wastewater. Bioresource Technology 159, 442-445.

Chapter 6

Impacts of salinity on *Brevibacterium paucivorans*, *Staphylococcus hominis* and *Micrococcus aloeverae* granules

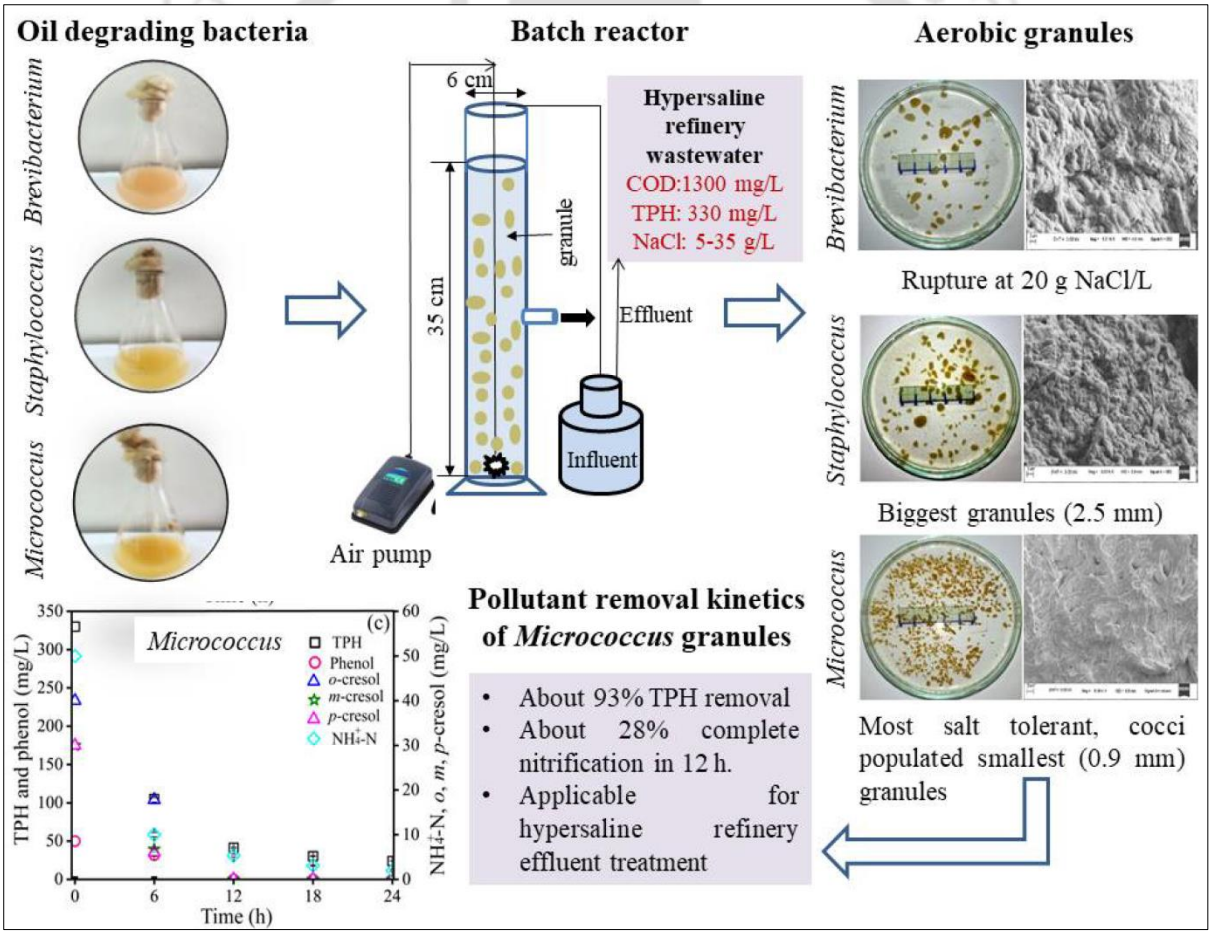

CHAPTER 6

Impacts of salinity on *Brevibacterium paucivorans*, *Staphylococcus hominis* and *Micrococcus aloeverae* granules

This chapter describes a batch scale study on granulation of *Brevibacterium paucivorans*, *Staphylococcus hominis* and *Micrococcus aloeverae* strains separately in refinery wastewater at 5-35 g/L salinity exposure.

6.1 Introduction

Crude oil recovery, distillation and alkylation are the major steps in petroleum refining process to produce hypersaline wastewater. In aquifer zone, saline water is applied to maintain oil reservoir pressure and emulsifier is used for enhanced oil recovery which is a source of wastewater containing emulsified oil, total dissolved solids (TDS), NH_4^+-N and salts (Mallick and Chakraborty, 2020). A mixture of H_2S and alkali commonly known as spent caustic is largely used in alkylation step and can increase salinity of refinery effluent till 300 g/L (Razavi and Miri, 2015).

Membrane separations like reverse osmosis, membrane distillation and pervaporations are the most commonly used techniques for saline wastewater treatment (Castro-Muñoz, 2020). Recent advancements in membrane technology introduced composite hollow fiber membranes, hybrid nanofiltration-reverse osmosis and metal-organic frameworks integrated membranes for desalination purpose (Wang et al., 2021; Du et al., 2020; Abdullah et al., 2021). Even membrane bioreactors were employed in shipboard slop treatment under salinity variation (Di Bella et al., 2015). However, high cost membrane materials, membrane fouling, maintenance of sophisticated reactors and moreover, production of massive volume of refinery wastewater having several oil, phenolics, salts, ammonia and metals are the major challenges of membrane separation for saline oily wastewater (Karray et al., 2020). Biological treatments are considered to be slower, stable but economical than physicochemical processes for emulsified oil removal in refinery wastewater treatments. However, salinity intrusion in floccular sludge reactors resulted into osmotic shock causing biomass washout and reduced organic removal efficiency (Wu et al., 2020).

Aerobic granular reactors (AGRs) were reported to enhance EPS production to achieve saline shock resistant granules with high biomass concentration and reduced biomass washout while treating seawater, fish canning wastewater or fabricated synthetic wastewater in 2-75 g/L salinity range (Corsino et al., 2016; Corsino et al., 2018; Hou et al., 2019, Li et

al., 2020; Wu et al., 2020; Sarvajith and Nancharaiah, 2020). But in hypersaline oily wastewater, prolonged granulation period of 30-50 days, initial granule rupture and depletion of ammonia oxidising layer reducing nitrogen removal were the major problems faced in AGRs (Corsino et al., 2015). Rapid granulation was carried out by adding chemical agents like PAC and biochar or dry granules in AGRs which require processing time and cost with chemical use further indicating necessity of self granulating seed inoculum for rapid granulation in wastewater treatment plants (Liu et al., 2014; Ming et al., 2019; Ogura et al., 2020). AGRs were mostly fed with co-substrates mixed with oily effluent or with lower hydrocarbon concentration (6.8-151 mg/L) than real refinery wastewater (>250 mg/L) (Corsino et al., 2015, Ramos et al., 2015; Campo and Di Bella, 2019). Moreover, nitrogen removal and nitrification are not well explored in dual presence of hydrocarbon recalcitrance and salinity in AGRs.

Role of inoculum and microorganism was another important aspect for salt tolerance in aerobic granules. Literature documented the use of mixed sludge inoculum or salt adapted bio-granules and presence of halophilic bacteria like *Devosia*, *Sphingomonas*, *Muricauda* etc. during petroleum slop or phenol, *o*-cresol and *p*-nitrophenol contaminated saline wastewater treatment (Chen et al., 2019; Campo and Di Bella, 2019; Ramos et al., 2015). However, rapid granulation from specific bacteria along with salt tolerance, nitrification and organics removal in high strength refinery wastewater are not discussed earlier.

The aim of this chapter was to conduct batch scale study on rapid aerobic granulation using three bacterial strains named *Brevibacterium paucivorans* strain SG001, *Staphylococcus hominis* strain SG003 and *Micrococcus aloeverae* strain SG002 for treatment of hyper saline refinery wastewater containing phenol, cresol and diesel oil and to investigate the impacts of salt tolerance on granule characteristics, biomass activity with organics and nitrogen removal efficiency in these three strains to determine their oil and salt tolerance thresholds.

6.2 Materials and methods

6.2.1 Chemicals and reagents

Chemicals and reagents used in feed preparation, FESEM, HPLC, sludge and effluent analysis are discussed in Chapter 2 (section 2.2.1) and Chapter 4 (4.2.1).

6.2.2 Inoculum sources

Brevibacterium paucivorans strain SG001, *Staphylococcus hominis* strain SG003 and *Micrococcus aloeverae* strain SG002 were used as initial inocula of the study. *Brevibacterium*, *Staphylococcus* and *Micrococcus* were previously isolated from aerobic

granules of sewage, brewery and refinery sludge as mentioned in Chapter 2 (section 2.3.6). About 3 g/L of overnight grown culture of *Brevibacterium* and *Staphylococcus* were inoculated in B1 and B2, respectively. B3 was inoculated with pre-developed matured *Micrococcus* granules cultivated in refinery wastewater as mentioned in Chapter 4, section 4.2.3.

6.2.3 Synthetic refinery wastewater

The compositions of the real and synthetic refinery wastewater are given in Table 4.1, Chapter 4. AGRs were fed with same synthetic refinery wastewater used in Chapter 4 having 1300 mg/L COD, 50 mg/L NH_4^+-N and 330 mg/L of total phenolic hydrocarbon (TPH) concentrations containing diesel, phenol, *o*, *m* and *p* cresol as carbon sources. Diesel was emulsified in nonylphenol ethoxylate (200:1 v/v ratio). Phosphate buffer and trace metal solution was added to maintain pH and bacterial growth. NaCl concentration was gradually increased between 5 to 35 g/L in the last 45 days of the study. As salinity of marine water and petroleum slop is reported nearly 35-37 g NaCl/L, we maintained similar salinity range in our feed (Campo and Di Bella, 2019).

6.2.4 Batch operating methodology

Experimental set-up is described in Fig.6.1. Three 1 litre volume measuring cylinders were used to fabricate three batch-scale set-ups B1, B2 and B3. About 35 cm was the working height with 6 cm inner diameter providing 6:1 height/diameter (H/D) ratio of the set-ups. Three aquarium air-pumps were employed for providing 2 L/min of continuous air-flow rate. BI, B2 and B3 were operated with 1 cycle per day with 48 h hydraulic retention time (HRT). Granule settling time varied between 1-2 min. Everyday about 500 mL effluent was decanted from an outlet at 17.5 cm height from the base. Batch feeding and reaction times were 10 and 1418 min, respectively. In last 45 days, feed salinity was increased from 5, 10, 15 to 35 g/L of NaCl concentration in every 7 days interval and was kept constant at 35 mg/L between day 35 to 45. Table 6.1 provides details of day wise increasing NaCl concentration and corresponding conductivity profiles in the batches. Sterilized condition and feeding strategy were maintained inside B1 and B2 till 21-25 days of granulation phase (Ho et al., 2009). However, in order to maintain real wastewater environment, non-sterile synthetic refinery wastewater was used during salinity exposure (day 26-70). About 1.3 g COD/g SS.day F/M ratio was provided to the batches for granulation.

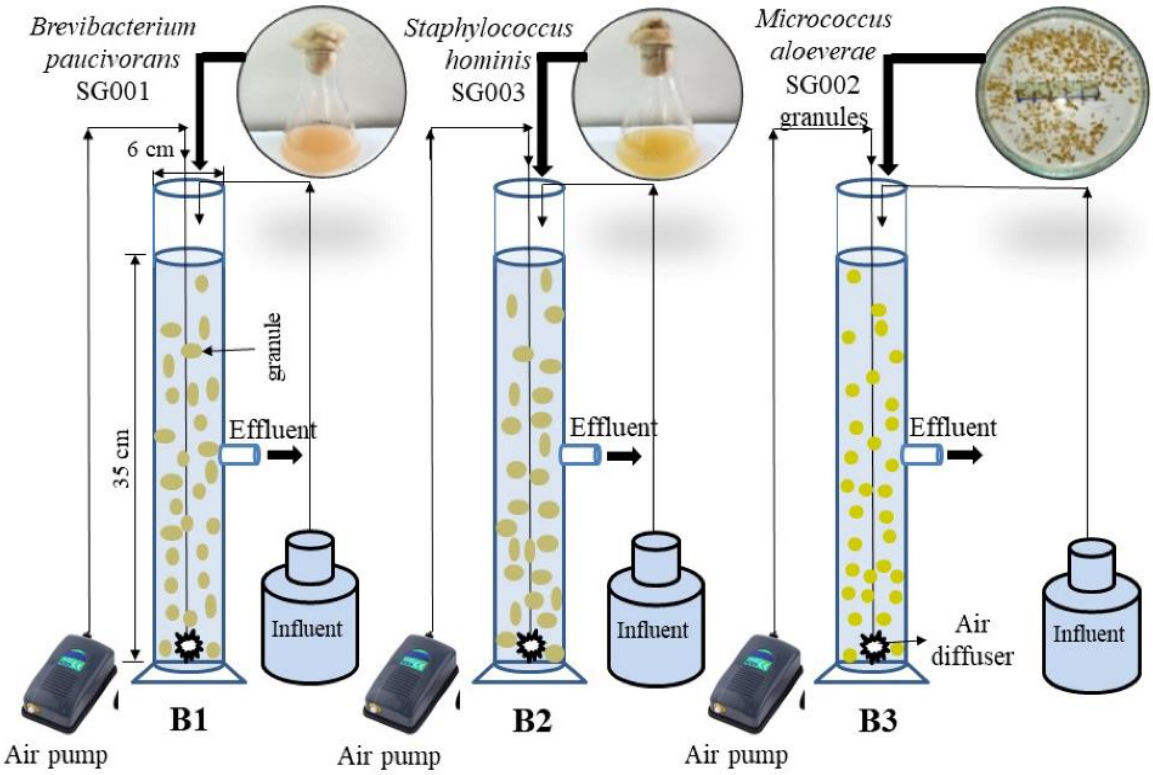

Fig.6.1 Schematics of B1, B2, B3 batches treating saline refinery wastewater

Table 6.1 Increasing NaCl salinity and conductivity profile of the feed

Time (day)	NaCl (g/L)	Salinity (g/L)	Conductivity (mS/cm)	Total dissolved solids (g/L)	Total suspended solids (g/L)	Turbidity (NTU)
1-25	0	4.77±0.34	8.57±0.17	5.4±0.12	6.34±0.14	62±2
28	5	7.72±0.45	13.41±0.2	8.6±0.54	6.78±0.09	62±1
35	10	15.98±0.12	26.16±0.14	16.74±0.23	6.55±0.18	62±2
42	15	23.56±0.65	37.22±0.11	23.83±0.16	6.88±0.02	64±1
49	20	34.32±0.12	52.15±0.34	33.28±0.56	7.22±0.06	65±1
56	25	44.23±0.11	65.25±0.22	41.76±0.23	7.34±0.04	63±2
63	30	50.17±0.21	72.84±0.17	46.57±0.12	7.55±0.51	64±1
70	35	62.9±0.2	88.51±0.19	56.65±0.16	7.55±0.51	63±2

6.2.5 Analytical procedure

Effluent and granule characteristics were measured at the end of each cycle. The total dissolved solids (TDS), salinity and conductivity of the feed and effluent samples were measured by conductivity meter (Thermo Scientific) and turbidity was measured by turbidity meter (Systronics, model: 132). Salinity was measusured after calibrating the instrument with 0.1N KCl solution. Blank volatilization and adsorption study, biomass activity study, sludge, effluent, FESEM and HPLC analysis were carried out according to chapter 2 and 4 (section 2.2.6 and 4.2.7).

6.3 Results and discussion

6.3.1 Granule formation by *Brevibacterium* and *Staphylococcus* strains

Photographs of the aerobic granules are shown in Fig.6.2. Rapid granulation occurred in 10 days of inoculation of *Brevibacterium* and *Staphylococcus* in B1 and B2. Optimum granule size is considered within 0.2 to 16 mm of diameter (Zheng et al., 2006) and in current study the initial granule size was nearly 0.2 to 0.3 mm which was within the mentioned range. After 21-25 days of batch operation, matured yellowish granules were formed having 1.43±0.01 and 1.56±0.05 mm diameter with 4.3±0.01 and 3.47±0.04 g/L of biomass concentration (VSS) in B1 and B2, respectively. Fig.6.3 describes granule size, VSS, IC, settleability and EPS profiles during granulation phase in B1 and B2. The oil degrading nature and granular sludge origin of the strains helped to utilize oily wastewater to granulate and grow (as mentioned in Chapter 2).

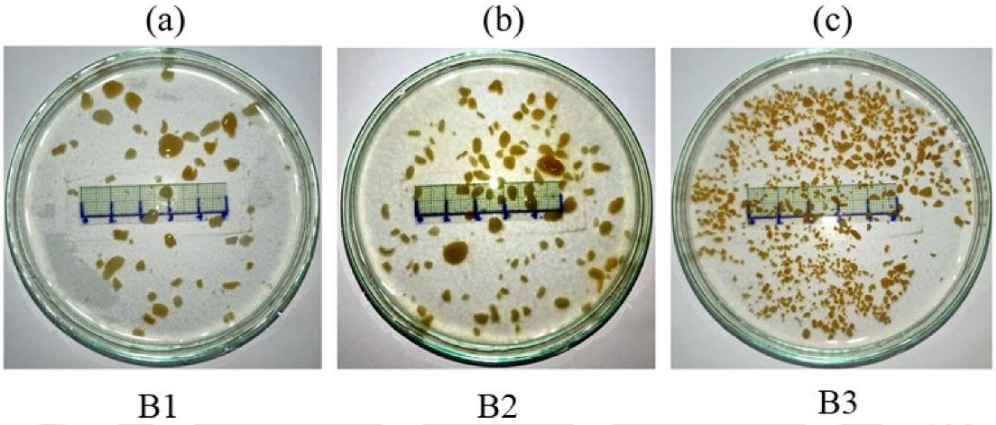

Fig.6.2 Aerobic granules originated from (a) *Brevibacterium*, (b) *Staphylococcus* and (c) *Micrococcus* strains in B1, B2 and B3 treating saline refinery wastewater. (scale: 1 unit =1 cm).

Granule settling behaviour is determined by two parameters GSV and SVI_{30} where GSV is correlated with granule size and SVI_{30} determines volume occupied by settled sludge after 30 min settling time. About 30-70 m/h of GSV range and below 50 mL/g SVI_{30} are essential for matured granulation (Liu and Tay 2004; Qin et al., 2004). In 25 days with increasing size and density, GSV and SVI_{30} increased from 31 to 34 m/h and 53 to 47 mL/g in B1 and 32 to 35 m/h and 41 to 36 mL/g in B2, respectively. High granule strength determines low integrity coefficient (IC) of granules (Ghangrekar et al., 2005). About 37.25±0.56 to 31.9±0.34% IC values indicated initiation of granule structural integrity in *Brevibacterium* and *Staphylococcus* granules. EPS are the polymers containing proteins (PN) and polysaccharides (PS) on outer granule layer enhancing cell surface hydrophobicity for cell aggregation. In 21 days of batch operation EPS concentration triggered up to 73±0.27 and 84±0.12 mg/g VSS in

B1 and B2 with 74-79% hydrophobicity values suggesting stable aerobic granules treating recalcitrant refinery wastewater.

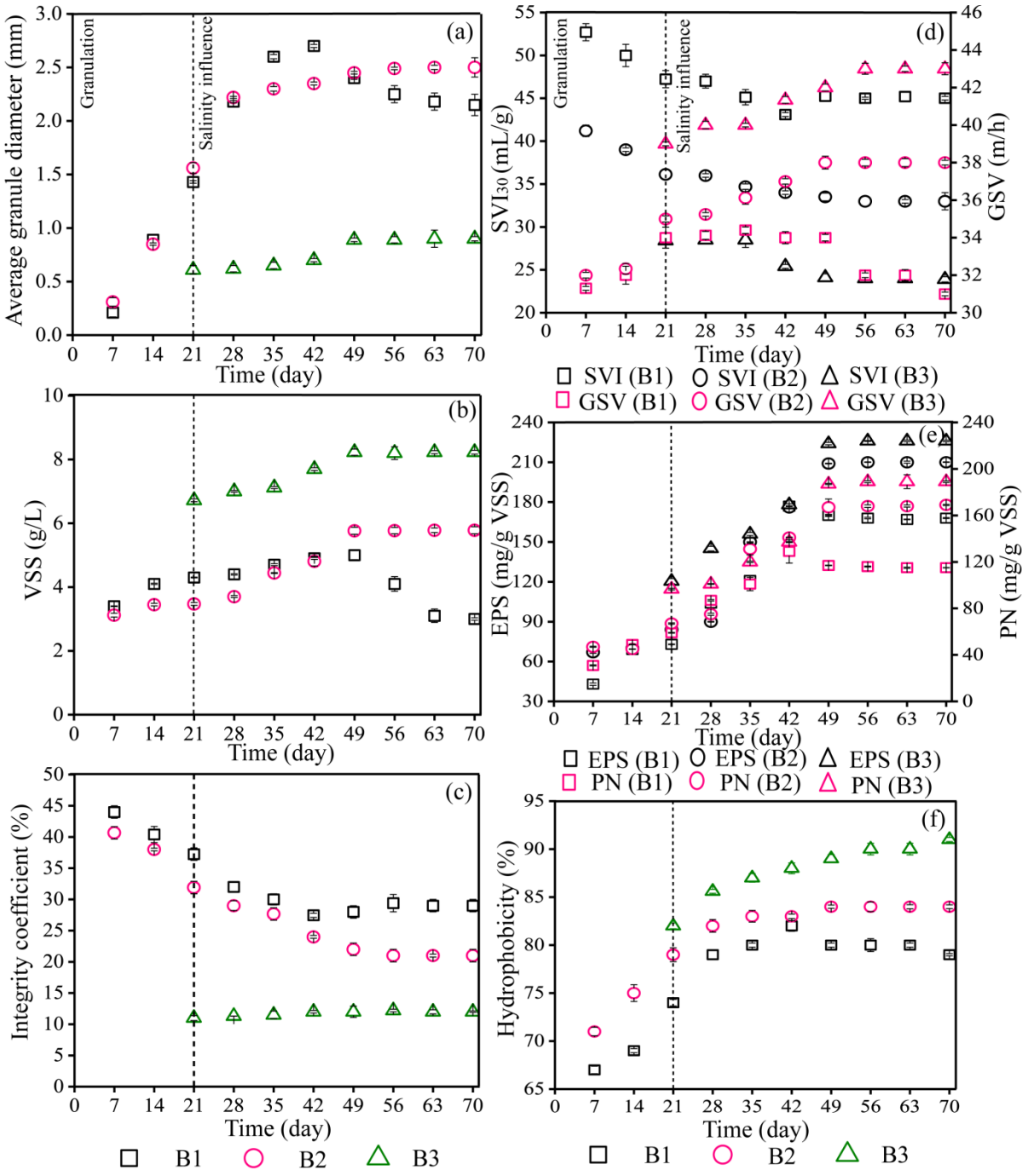

Fig.6.3 (a) Granule size, (b) VSS, (c) IC, (d) comparative SVI_{30} to GSV, (e) comparative EPS to PN and (f) hydrophobicity profiles in B1, B2 and B3 [B3 was operated only in salinity phase and salinity ranged within 5-35 g NaCl/L].

Literature suggested matured granulation from mixed inocula like petrochemical sludge, flocculent municipal wastewater treatment plant sludge and activated sludge in minimum 30-50 days while treating recalcitrant petroleum slop or hypesaline oily wastewater (Chen et al.

2019; Campo and Di Bella, 2019; Corsino et al., 2015). Autochthonous seawater microbes took almost 110 days for granular sludge formation in hypersaline seawater (Sarvajith and Nancharaiah, 2020). However, in current study, rapid granulation in nearly 20 days from single strain bacteria in complex refinery wastewater determines its feasibility to withstand hydrocarbon recalcitrance in real refinery wastewater treatment plants.

6.3.2 Granule characterization in saline refinery wastewater

During the salinity influence phase (day 26-70), a significant variation in granule characteristics was observed in *Brevibacterium*, *Staphylococcus* and *Micrococcus* granules. Changes in granule size, VSS, IC and comparative SVI_{30} to GSV profiles in B1, B2 and B3 are described in Fig.6.3a-d. Between day 26-42 in presence of 330 mg/L TPH and 5-15 g/L NaCl salinity, B1, B2 and B3 promoted granules with 0.7-2.35 mm size, 4.81-7.7 g/L VSS and 176-178 mg/g VSS EPS content.

However, after 20 g/L NaCl exposure, *Brevibacterium* granules faced partial disintegration decreasing size and VSS from 2.7-2.4 mm and 5-4 g/L which gradually increased effluent VSS up to 0.34 g/L. Granule rupture eventually decreased GSV and increased SVI_{30} till 34-32 m/h and 43-45 mL/g, respectively. IC profile hiked from 27 to 29% in B1 indicating reduction in granule strength. Day 49 onwards at 25-35 g/L NaCl, B1 acclimatized in hydrocarbon and saline environment achieving stability at 2.15±0.11 mm diameter and 3±0.04 g/L VSS. B2 granules had moderate granule strength (IC: 21%) in presence of 20-35 g/L NaCl, which stabilized at 2.5±0.09 mm granule size and 5.78±0.09 g/L VSS in 49 days.

Micrococcus had the smallest (size: 0.9±0.03 mm) and strongest granules (IC: 12±0.12%) at 35 g/L NaCl suggesting the most salt tolerant granules among the batches at 330 mg/L TPH exposure. Due to bigger size, *Staphylococcus* granules (B2) achieved 38 m/h GSV but the higher biomass density (VSS: 8.23±0.06 g/L) and microbial strength (IC: 12%) provided maximum 43 m/h GSV in small sized B3 granules (Liu and Tay, 2004). Low SVI_{30} range (41-28 mL/g) in B2 and B3 further indicated highly settleable granules (Qin et al., 2004). On day 70, Due to biomass washout, B1 had maximum F/M ratio of 0.43 g COD/g SS.day whereas, B3 had minimum 0.16 g COD/g SS.day F/M ratio suggesting maximum GSV values (Hamza et al., 2018).

Mixed inoculum promoted 70-80 m/h of GSV and about 30 mL/g of SVI_5 in aerobic granules treating hypersaline oily wastewater containing 5.6 mg/L oil (Corsino et al., 2015) and stepwise increase in salinity till 38 g NaCl/L provided stable aerobic granules with 20 mL/g SVI_5 and SVI_{30} values in 164 days (Campo et al., 2018). Hence, current study indicates

the feasibility of using single strains of *Brevibacterium*, *Staphylococcus* and *Micrococcus* to achieve faster, stronger and more stable granulatiom than the previous studies while treating hypersaline refinery wastewater.

6.3.3 Extracellular polymeric substances

Comparative EPS with PN and hydrophobicity trends in B1, B2 and B3 are illustrated in Fig.6.3e-f. In B1, oil toxicity and salinity shock initially reduced EPS and PN synthesis till 177-170 and 129-117 mg/g VSS. Salt adaptation gradually increased EPS content up to 168±0.33 mg/g VSS with 79% hydrophobicity in *Brevibacterium* granules. Till day 70, B2 granules reached stable EPS and PN concentrations at 210±0.22 and 169±1 mg/g VSS, providing 84% hydrophobicity.

The mechanism behind granule formation and stability in hypersaline refinery wastewater might be the inherited oil tolerance from refinery sludge origin which provided high biomass content to form *Micrococcus* granules and its high EPS content. EPS are the base materials to increase cell-to-cell adhesion for granule formation and stability (Song et al., 2020). According to literature, bigger granules in B1 and B2 might be a possible reason of lower EPS content than smaller granules in B3 under salinity influence (Li et al., 2020) and saline shock promoted osmotic pressure increasing microbial activity for EPS synthesis in granules (Ou et al., 2018). Hence, salinity stress promoted 226 mg/g VSS of EPS layer with 91% hydrophobicity in *Micrococcus* granules which acted as a shield to resist granule rupture. During petroleum slop wastewater treatment, PN/PS values were found near 9 at 11-24 g/L of salinity which deteriorated to a ratio of 3.4 resulting into partial degranulation at 37 g/L salinity (Campo and Di Bella, 2019). In current study, even in presence of hypersalinity (35 g/L) and high hydrocarbon concentration (330 mg/L), PN/PS trend was observed between 4.5 to 9.5 in B2 and B3 suggesting granule robustness and structural stability with higher proportion of bound-proteins. According to Sivasubramanian et al. (2021), higher Na^+ ion concentration might have associated with promoting protein synthesis enzymes in *Micrococcus* and *Staphylococcus* granules but saline exposure increased the hydrophilic polysaccharides production in *Brevibacterium* which reduced PN/PS ratio between 2 to 4 causing granule rupture and hampering granule settleability.

Table 6.2 provides a comparison between two scenarios, mixed sludge inoculated aerobic granules treating saline wastewater and specific strain originated aerobic granules treating refinery wastewater in dual presence of hydrocarbon recalcitrance and saline stress.

Table 6.2 comparative aerobic granular characteristics and pollutant removal performance while treating various saline wastewaters with a focus on role of microorganisms in granules.

Type of wastewater	Salinity concentration	AGR operational strategies	Granule characteristics	Pollutant removal performances	Role of granules/ microorganisms	References
Hypersaline oily wastewater	Chloride concentration: 0.225-25 g/L	AGR volume: 3.5 L, airflow velocity: 3.5 cm/s, cycle time: 3, 12 h, VER: 50%, OLR: 3-6 kg/m^3.day	Size: 1.9 mm, SVI_5: 28-30 mL/g, GSV: 70-85 m/h, EPS: 340-550 mg/g VSS	COD removal efficiency: 98-88%, Total nitrogen: 45-50%, TPH: 90%, phosphorous: 50- 80%	Hydrocarbon adsorption and biodegradation in granules inoculated from municipal sludge	Corsino et al. (2015)
Aromatic wastewater	Salt concentration: 2-29 g/L	AGR volume: 2.6 L, air flow-rate: 150 to 250 mL, influent COD: 2890 mg/L (Phenol, *o*-cresol, *p*-nitrophenol, glucose, sucrose)	Size: 0.22 mm. SVI_{30}: 26 mL/g, SVI_{30}/SVI_5: 1, EPS: 61 g/g VSS	COD removal efficiency: 96%, complete removal of phenolics	Active genera, at high salinity: *Devosia*, *Sphingomonas* and *Muricauda*; low salinity: *Sphingobium*, *Cythophaga* and *Comamona*	Ramos et al. (2015)
Fish canning wastewater	NaCl concentration: 30-75 g/L	AGR volume: 3.5 L, air flow-rate: 3 L/min, cycle time: 12 h, VER: 50%, OLR: 3.22-4 kg/m^3.day	Size: 1.8-2.21 mm, density: 280-236 g ^{1}TSS/L, EPS: 357-316 mg PN/L, 39-16 mg PS/L, GSV: 34-21 m/h	COD removal efficiency: 90%, NH_4^+-N: 98% by nitrification-denitrification process at 50 g/L NaCl	Salt acclimatized granules resisted osmotic and organic matter shocks removing COD and nitrogen.	Viviani (2016)
Petroleum slop wastewater	NaCl concentration: 37.8±1.5 g/L	AGR volume: 3.5 L, air flow-rate: 3.3 cm/s, cycle time: 6 h, VER: 50%, COD: 816 mg/L, TPH: 151 mg/L	Size: 1-1.15 mm, VSS: 2.5 g/L, SVI_5: 10 mL/g, PN: 80-100 mg/g VSS, PS: 5-25 mg/g VSS	COD: 67%, TPH: 83%	Two types of seed sludge: Salt-adapted biogranules and flocculent sludge was exposed to petroleum slop for granulation.	Campo and Di Bella (2019)
Hypersaline seawater	Salinity range: 3.4-12%	AGR volume: 3 L, airflow velocity: 0.2 cm/s, cycle time: 6 h, VER: 70%, influent COD: 80000 mg/L	Size: 1.9-2.2 mm, SVI_5: 8.3-20 mL/g, ^{2}MLSS/ ^{3}MLVSS: 1.21-1.31, density: 1.91 g/mL, GSV: 37-69 m/h, hydrophobicity: 96-98%	TOC removal efficiency: 93%, total nitrogen: 82-99%, total phosphorus: 95-96%	Granules were cultivated from autochthonous seawater-born microbes and *Stappiaceae* (45%) and *Rhodobacteraceae* (21%) were the dominant genera.	Sarvajith and Nancharaiah (2020)
Synthetic wastewater	Short-term saline shock: 0-60 g/L NaCl	AGR volume: 3 L, cycle time: 6h, VER: 60%, anoxic phase: 20 min, aeration: 325 min, settling: 5 min	SVI_{30}: ≤50 mL/g, IC: 87.6%	COD removal efficiency: 87.5% at 40 g/L and 73.8% at 60 g/L saline shock, at 40-60 g/L salinity	DNA leakage of 177.2% had advantages to diminish damages on cell structure	Wu et al (2020)

Synthetic wastewater	Stepwise increase in NaCl concentration: 2-10 and 4-20 g/L	AGR volume: 4 L, cycle time: 4 h, settling time: 12-21 min, VER: 50%, influent COD: 500 g/L, Low temperature: 12 °C	Size: 1.49-2.20 mm, SVI_5: ≤50 mL/g, SVI_5/SVI_{30}: 1, biomass concentration: 0.7-8 g SS/L, Hydrophobicity: 64-74%, density: 50-64 g VSS/L	COD removal efficiency: 90%, ammonium: 95% and total nitrogen: 70%	Enriched strains: *Thauera*, *Azoarcus*, *Nitrosomonas*; Supressed strains: *Flavobacterium* and *Meganema* in salinity	Li et al. (2020)
Synthetic wastewater	Salinity range: 1-4%	CFR volume: 20 L, HRT: 9.5 h, air flow-rate: 18 L/min, light illumination, DO: 7-9 mg/L, room temperature: 23 °C, Influent COD: 600 mg/L	Algal bacterial granule size: 0.6-0.65 mm, MLSS: 3.7-4.5 g/L, SVI_{30}: 15-36 mL/g, chlorophyll *a*: 2-10 mg/g SS, lipid: 45-80 mg/g SS, EPS: 275 mg/g VSS	[4]DOC removal efficiency: 91.5% of, Total phosphorus: 41.8-49.2% and total inorganic nitrogen: 45.6-55.6% at 1-3% saline wastewater	Enriched strains: *Halomonas* and *Nitzschia* but Supressed strains: *Nitrosomonas* and *Flavobacterium* in salinity	Meng et al. (2020)
Low salinity phenolic wastewater	NaCl concentration: 2% (w/v)	AGR volume: 3.6 L, cycle time: 6 h, VER: 50%, Influent COD: 200 mg/L	MLVSS/MLSS: 60%, PS: 18-82 m/g MLVSS, PN:0.81-0.96 mg/g MLVSS	Complete phenol removal (10-100 mg/L), Phenol favoured P removal than N	Major halophiles: *Stappia*, *Luteococcus* and *Formosa*	He et al. (2021)
Saline refinery wastewater	NaCl concentration: 5-35 g/L	AGR volume: 1 L, cycle time: 24 h, air flow-rate: 2L/min, VER: 50%	Size: 0.9-2.5 mm, VSS: 3-8 g/L, SVI_{30}: 23-45 mL/g, GSV: 31-43 m/h, IC: 12-29%, EPS: 168-226 mg/g VSS, hydrophobicity: 79-91%	COD: 71-92% TPH: 72-93% Phenol:70-100%, Cresol: 97-100%, NH_4^+-N: 89-96%, complete nitrification: 1.02-28%	*Micrococcus* (strongest), *Staphylococcus* and *Brevibacterium* inoculated stable granules in salinity exposure	Current study

[1]TSS: Total suspended solids (g/L)
[2]MLSS: Mixed liquor suspended solids (g/L)
[3]MLVSS: Mixed liquor volatile suspended solids (g/L)
[4]DOC: Dissolved organic carbon (mg/L)

The table showed that the previous studies focused on saline water treatment (0-38 g/L salinity) mostly added with co-substrates with or without presence of recalcitrant organic pollutants where salt adapted or mixed sludge inoculated aerobic granules were used in AGRs. Dominance of halophilic bacteria was also evident in aerobic granules. In contrast, current study indicated utility of single strain inoculum for rapid formation of salt tolerant granules by using refinery wastewater as sole substrate with 330 mg/L TPH concentration and about 35 g NaCl/L salinity providing 93% organics removal and improved nitrification than earlier studies.

6.3.4 Microscopic image analysis

Fig.6.4 provides FESEM images providing morphology of B1, B2 and B3 granules taken on day 60 at 5000× magnification. Non filamentous microstructure with rod shaped bacterial population suggested that after initial rupture, *Brevibacteriam* (B1) granules acclimatized in saline environment achieving denser granules. Cocci abundance on *Staphylococcus* and *Micrococcus* granule surfaces ensured strong microbial structure in B2 and B3 which is further justified by their high VSS (5-8 g/L) content and low IC values (12-21%).

CLSM analysis was conducted on day 65 of the study (Fig.6.5). Extended fluorescence of Syto 63 indicated high amount of total cells in B1, B2 and B3 granules. High FITC fluorescence in B3 further signified maximum protein content in *Micrococcus* granules among the three strains. Con A fluorescence was comparatively higher in *Brevibacterium* as polysaccharides content increased in saline environment decreasing PN/PS ratio between 2 to 4 in B1. Higher Sytox blue fluorescence in B1 suggested more number of dead cells in *Brevibacterium* granules than B2 and B3 due to granule rupture in saline shock.

6.3.5 Performances of *Brevibacterium, Staphylococcus* and *Micrococcus* granules

6.3.5.1 Organics removal performances

The COD, TPH, Phenol, *o*, *m*, *p*-cresol and emulsified diesel removal profiles are described in Fig.6.6. The influent COD and TPH concentrations were constant at 1300 mg/L and 330 mg/L providing 0.95 kg COD/m^3.day of organic loading rate (OLR) and 0.495 kg/m^3.day of hydrocarbon loading rates (HLR) throughout 70 days of the study. Emulsified diesel, phenol, *o*, *m* and *p*-cresol feeding were maintained at 234, 50, 40, 30 and 30 mg/L concentrations, respectively.

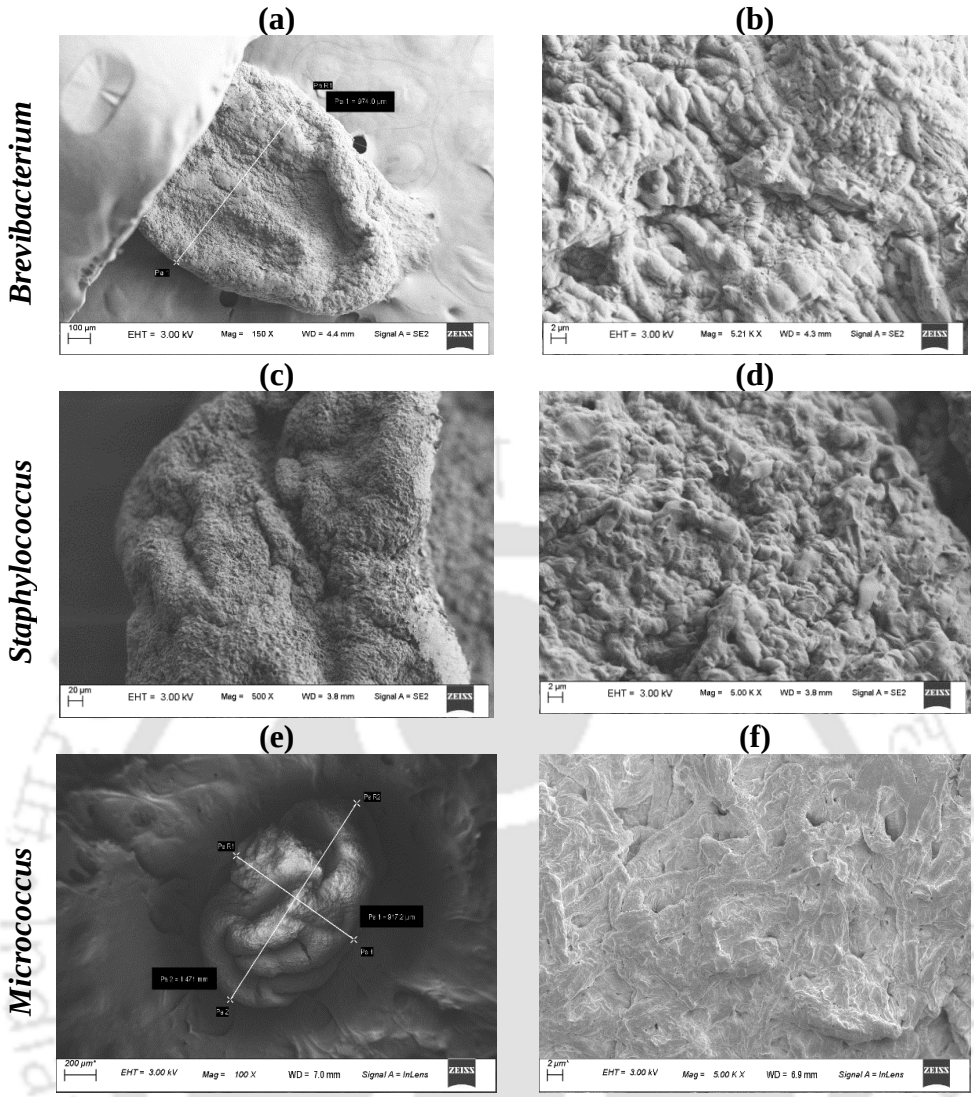

Fig.6.4 FESEM images of (a, b) rod-shaped bacteria dominated *Brevibacterium* granules, cocci abundant dense surfaces of (c, d) *Staphylococcus* and (e, f) *Micrococcus* granules cultivated in saline refinery wastewater. Images were taken at 5000× magnification on day 65 of batch operation.

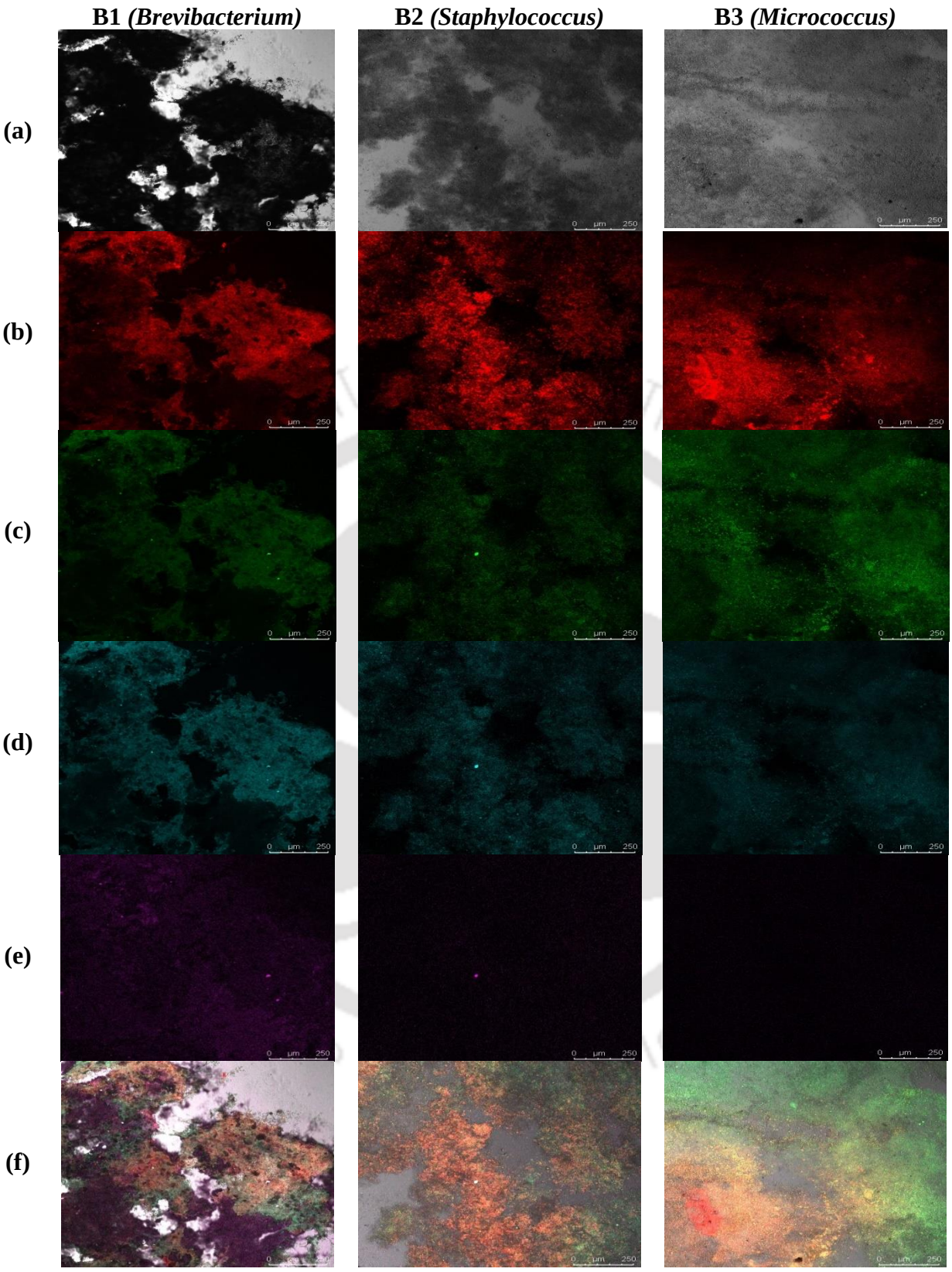

Fig.6.5 CLSM images of B1, B2 and B3 (Bar: 250 µm) granules on day 65 at 35 g/L NaCl salinity influence: (a) optical microscopic image (b) total cells (Syto 63), (c) proteins (FITC), (d) polysaccharides (Con A), (e) dead cells (Sytox Blue), (f) combined image of (b) and (e).

In current study, *Brevibacterium* (B1) and *Staphylococcus* (B2) achieved almost 73-75% COD and TPH removal in granulation phase (day 1-25) confirming granulated strains were more hydrocarbon tolerant and efficient in organics removal than flocculent biomass culture. After 20 g/L NaCl exposure, partial granule rupture and VSS reduction dropped TPH removal from 75 to 70% in B1. In last 20 days (at 25-35 g/L NaCl), B1 reached nearly stable 70-71% COD and TPH removal due to stable VSS and EPS concentration. After 70 days of complete batch operation, B1 provided 15.5, 40.48 and 0.75-5.44 mg/L of effluent phenol, oil and cresol concentrations, respectively.

Till day 49, B2 had 80-81% COD and TPH removals. *Staphylococcus* granules achieved stability at 20-35 g/L NaCl providing 82 and 95-97% of TPH and phenolics removal, respectively. The cocci dominated strong granules with 5.77 g/L VSS ensured salt tolerance with 80.9% COD removal from refinery wastewater. The final oil, phenol and cresol concentrations in B2 effluent were 40.38, 5.35 and 0.9-5.44 mg/L, respectively.

The smallest, strongest *Micrococcus* granules with maximum 8.34 g/L VSS concentration ensured maximum 92.2% COD and 92.7% TPH removal in B3 between day 26-49. It remained stable at 92.8% TPH removal up to 35 g/L NaCl till day 70 indicating the most salt tolerant oil degrading granules among the batches. Almost complete phenolics and 89.7% diesel removal was achieved in B3 on day 70. The hydrocarbon degradation rates were calculated as 14.9±0.32, 25.78±0.12 and 46.34±0.45 mg oil/g VSS.day in B1, B2 and B3, respectively. Maximum F/M ratio value of 0.43 g COD/g SS.day in B1 indicated presence of insufficient biomass to consume hydrocarbon substrate whereas, B3 obtained minimum 0.16 g COD/g SS.day F/M ratio suggesting 93% hydrocarbon removal (Hamza et al., 2018).

Corsino et al. (2015) and Campo and Di Bella (2019) observed that in salinity influence, EPS production enhanced physical bio-adsorption of oil in granules while treating petroleum wastewater. In current study, volatilization and adsorption study confirmed that only 1-2% TPH was removed abiotically or by adsorption on dead granule surface indicating that organics were removed by biodegradation.

The stable hydrocarbon removal in BI, B2 and B3 even in salinity stress can be explained in two ways. Salinity increases water density causing loose biomass washout from reactors whereas bigger and denser granular sludge with good settling property remain inside the reactor (Ramos et al., 2015). The high biomass concentration determines high microbial activity degrading recalcitrant diesel oil, phenol and cresol compounds by aerobic granules. The another possible reason might be the combined impact of salinity stress causing osmotic pressure enhanced EPS synthesis and conversion of hydrocarbons into proteins during feast

phase of the batch operation (nearly 12 h of cycle, discussed in section 6.3.7). The proteins are utilized in famine phase increasing cell surface hydrophobicity of the granules. The hydrophobic EPS layer works as a barrier between cell wall and external environment and protect the granules from harsh saline exposure (Campo et al., 2018).

Corsino et al. (2015) observed 90% hydrocarbon removal by aerobic granules in hypersaline oily wastewater where TPH concentration was only 5.6 mg/L. Zhang et al. (2011) suggested co-metabolism degradation mechanism where oil and sodium acetate were simultaneously degraded in the AGR. In another study, Ramos et al. (2015) achieved complete phenolics removal in AGR treatment of aromatic wastewater having phenol, *o*-cresol and *p*-nitrophenol where glucose and sucrose were simultaneously fed as co-substrates. Moreover, they faced complete granule disintegration at 29 g/L salinity which was reconstructed after adding anaerobic granules. In contrast, in current study recalcitrant diesel and phenolics containing refinery wastewater was used as sole carbon source for granules that too with higher TPH content (330 mg/L) than previous literature which achieved stability between 25-35 g/L salinity providing 71-93% organics removal.

Degradation of diesel oil has been studied in Chapter 3 and 4 (section 3.3.3.1 and 4.3.5.1) where the degradation mainly followed *n*-alkane to fatty acid conversion which further took part in β-oxidation. Aerobic degradation of phenolics can be predicted to follow the phenol to cathecol conversion pathway as previously observed in AGRs during *o*-cresol treatment by Basheer and Farooqi (2012) which is dicussed in details in chapter 4 (section 4.3.5.1).

Literature evidences of halophile dominance (autochthonous halophilic bacteria and other strains like *Devosia*, *Sphingomonas*, *Muricauda*, *Stappiaceae*, *Rhodobacteraceae*, *Halomonas*, *Nitzschia* etc.) in granules helped to achieve stability between 2-60 g/L salt stress in sea water and aromatic saline wastewater treatment (Ramos et al., 2015; Corsino et al., 2018; Meng et al., 2020; Sarvajith and Nancharaiah, 2020). The organics removal profiles in B1, B2 and B3 followed similar trends as observed in sewage, brewery and refinery sludge granules (origin of *Brevibacterium*, *Staphylococcus* and *Micrococcus* strains) discussed earlier in Chapter 2.

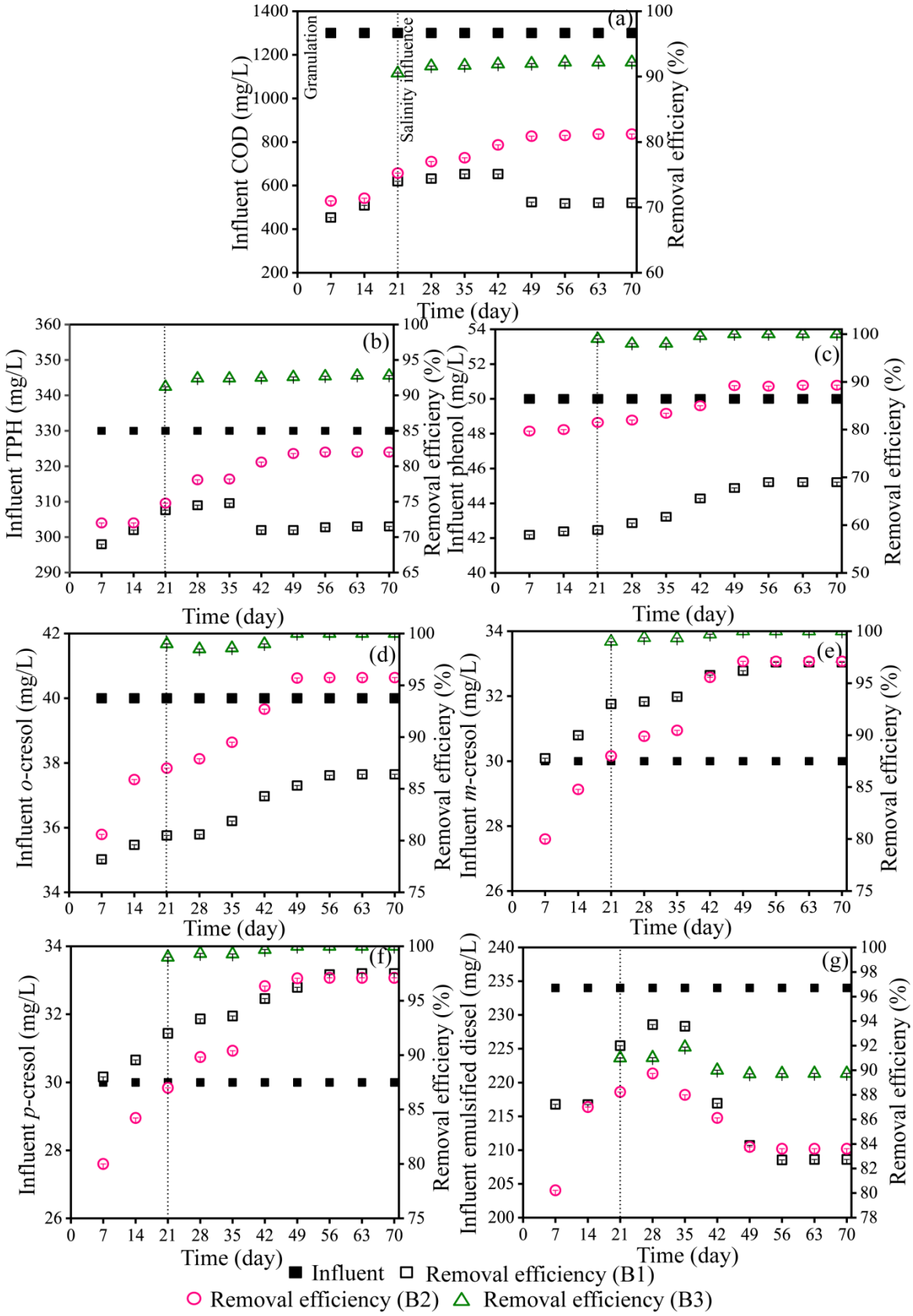

Fig.6.6 (a) COD, (b) TPH, (c) phenol, (d) *o*-cresol, (e) *m*-cresol and (f) *p*-cresol and (g) emulsified diesel removal profiles in B1, B2 and B3 [B3 was operated only in salinity phase and salinity ranged within 5-35 g NaCl/L].

Hence, the refinery sludge origin, oil adaptation and high EPS content were the key factors to resist salinity inhibition for maximum hydrocarbon removal efficiencies in B3 which can be further best fitted in AGR scale treatment of hypersaline (above 30 g/L salinity) refinery wastewater.

6.3.5.2 Nitrogen removal performance

About 190 mg/L of NH_4Cl provided 50 mg/L of influent NH_4^+-N as nitrogen source for the aerobic granules. Nitrogen loading rate was 0.075 kg NH_4^+-N/m^3.day. NH_4^+-N removal patterns and variations in effluent NO_3^--N and NO_2^--N concentrations are described in Fig.6.7. In granulation phase (day1-25), B1 and B2 had 92-94% NH_4^+-N removals which further increseased upto 93 and 95% removals in 15 g/L NaCl exposure with no granule rupture.

However, after day 49, NH_4^+-N removal dropped to 89% in B1 due to partial rupture in 20 g/L salinity. Poor NH_4^+-N removal was previously reported in AGRs treating real petroleum wastewater (Zhang et al., 2011; Chen et al., 2019) as nitrifying bacterial growth in outer aerobic granule layer might have been restricted by hydrocarbon toxicity in salinity exposure (Tay et al., 2002). Finally, after saline stress adaptation, B1 maintained stability with 89% NH_4^+-N removal between 25-35 g/L salinity influene. B2 had stable 95.6% NH_4^+-N removal till day 70 at 25-35 g/L salinity influence due to less granule rupture and high VSS values. The seed *Micrococcus* granules in B3 had 95% NH_4^+-N removal capacity which even followed stable removal pattern in 5-20 g/L of NaCl concentration. The previous oil adaptation, strong microbial integrity (IC: 12%) and highest VSS concentration (8.34 g/L) promoted 96% NH_4^+-N removal in B3 in further salinity of 25-35 g/L NaCl till day 70.

During nitrification, NH_4^+ is initially converted to NO_2^- by ammonia-oxidizing bacteria (AOB) and further tranformed to NO_3^- by nitrite-oxidizing bacteria (NOB). Ion chromatography results provided negligible amount of effluent NO_2^--N concentrations (0.01-0.02 mg/L) indicating nominal partial nitrification in the batches. SRT determines the mean retention time of activated sludge in a wastewater treatment plant which was calculated according to equation 2.7 given in Chapter 2 (Metcalf and Eddy, 2003). The statistical analysis of granule characteristics and pollutant removal performances of the batches has been provided along with standard deviation and F-value in Table 6.3.

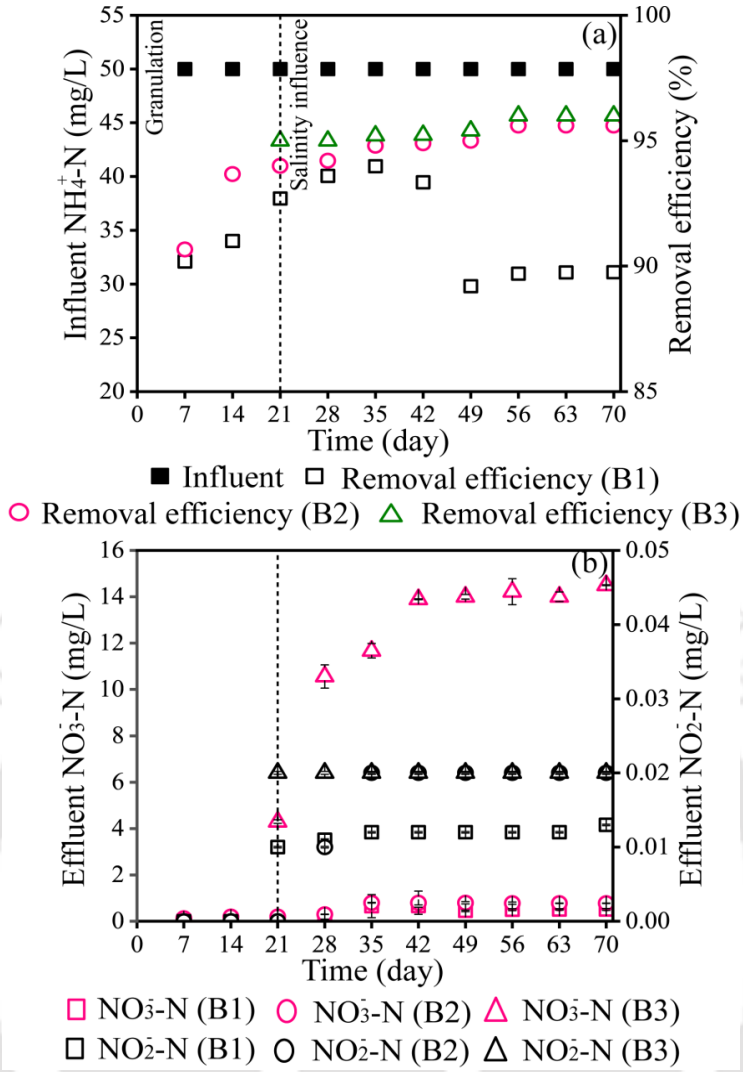

Fig.6.7 (a) NH_4^+-N removal performances and (b) nitrate-N (NO_3^--N) and nitrite-N (NO_2^--N) accounts in B1, B2 and B3 effluent under salinity influence. [B3 was operated only in salinity phase and salinity ranged within 5-35 g NaCl/L].

Granule disintegration increased effluent VSS concentration (0.7-0.74 g/L) in B1 providing 8 days SRT after day 49, followed by 14 and 28 days SRT values in B2 and B3, respectively. As nitrification is a lengthy process and growth of NOBs are favoured by longer SRTs (10-30 days), B3 had maximum 14.5±0.02 mg/L effluent NO_3^--N concentrations indicating maximum complete nitrification among the strains (Wan et al., 2013). B1 and B2 had 0.51±0.04 and 0.78±0.01 mg/L of NO_3^--N concentrations in effluent after achieving steady state (after day 49). Nitrogen utilized for biomass growth was calculated as 45, 42.8 and 34.8 mg/L in B1, B2 and B3 by using equation 2.8 (Chapter 2) at 0.5 L/day of flowrate. Hence, about 60-90% influent nitrogen was consumed in biomass growth leaving 1.02-28% for complete nitrifications and the remaining 4-11% nitrogen provided 5.12, 2.2 and 2 mg/L effluent NH_4^+-N concentration is B1, B2 and B3, respectively on day 70.

Table 6.3 Statistical analysis of granule characteristics and pollutant removal performance of the batch studies

Reactor	**B1**		**B2**		**B3**		**Overall ANOVA**				
Operation time (day)	**1-70**		**1-70**		**1-70**						
	Mean	**SD**	**Mean**	**SD**	**Mean**	**SD**	**R-square**	**Coeff Var**	**Root MSE**	**Mean square**	**F-value**
Granule size (mm)	1.89	0.80	1.95	0.78	0.77	0.13	0.399	0.42	0.67	3.82	8.31
VSS (g/L)	4.10	0.71	4.60	1.11	7.67	0.64	0.77	0.16	0.86	32.22	43.09
SVI_{30} (mL/g)	46.55	2.84	35.35	2.80	25.85	2.21	0.91	0.07	2.66	965.82	135.67
GSV (m/h)	32.88	1.33	35.97	2.30	41.41	1.59	0.80	0.49	1.81	163.49	50.05
EPS (mg/g VSS)	126	50.77	147.61	63.35	187.68	43.35	0.19	0.35	53.84	8564.63	2.95
PN (mg/g VSS)	91.9	33.98	117.8	53.24	151.07	41.83	0.24	0.37	43.89	7780.70	4.04
Hydrophobicity (%)	77	5.18	80.9	4.53	87.82	2.94	0.51	0.05	4.41	263.06	13.49
IC (%)	32.65	5.81	27.62	7.26	11.75	0.42	0.72	0.22	5.58	1029.09	33.02
COD removal efficiency (%)	72.02	2.38	77.60	3.94	91.79	0.56	0.90	0.03	2.78	901.81	116.42
TPH removal efficiency (%)	71.95	1.83	78.35	4.08	92.42	0.51	0.91	0.03	2.70	955.29	131.02
NH_4^+-N removal efficiency (%)	91.32	1.87	94.40	1.48	95.47	0.45	0.62	0.01	1.45	43.31	20.49

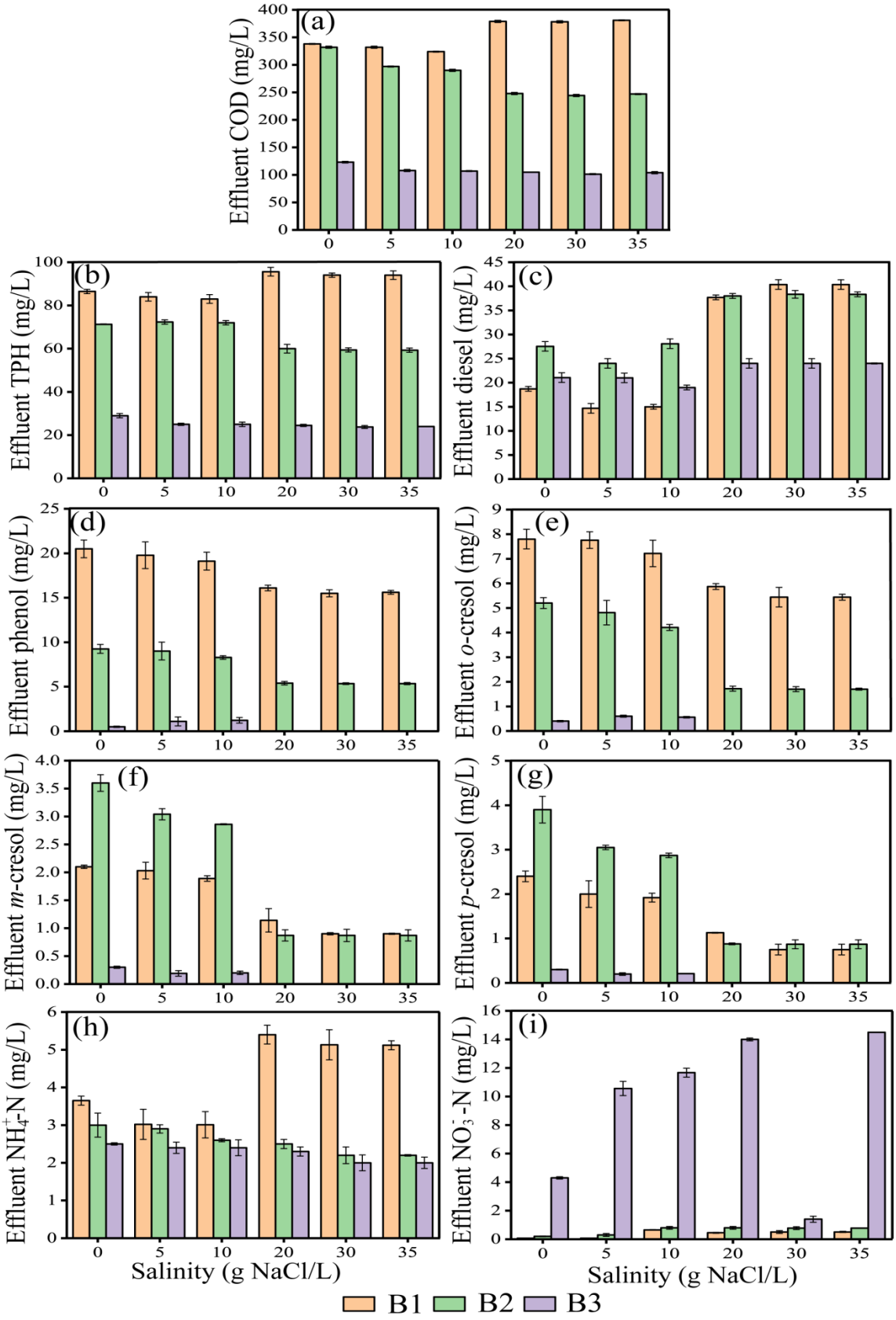

Fig.6.8 Effects of increasing NaCl salinity in effluent quality of B1, B2 and B3. Concentrations of (a) COD, (b) TPH, (c) diesel, (d) phenol, (e) *o*-cresol, (f) *m*-cresol, (g) *p*-cresol, (h) NH_4^+-N and (i) NO_3^--N in B1, B2 and B3 treated effluent.

Recovery of nitrogen removal and nitrification efficiency in AGRs were documented by applying co-substrates while treating petroleum wastewater (Zhang et al., 2011; Chen et al., 2019). In current study, granules were fed with hypersaline refinery wastewater as sole substrate that too in higher TPH content (330 mg/L) than previous literature (5.6-250 mg/L). Single strain *Micrococcus* granules could withstand hydrocarbon and salinity exposure due to high EPS content (226 mg/g VSS) and granule strength (IC: 12%) providing 96% NH_4^+-N removal and 28% nitrification efficiency without adding co-substrates. Influence of changing NaCl salinity in B1, B2 and B3 effluent characteristics are summarized in Fig.6.8.

6.3.6 Granular biomass activity study

Granular biomass activity is the parameter to determine the amount of organic matter present in the system responsible for COD removal calculated by equation 2.6 in Chapter 2 (Jawed and Tare, 1999). The cumulative COD removal profile and the individual biomass activities of B1, B2 and B3 at 35 g/L NaCl are described in Fig.6.9.

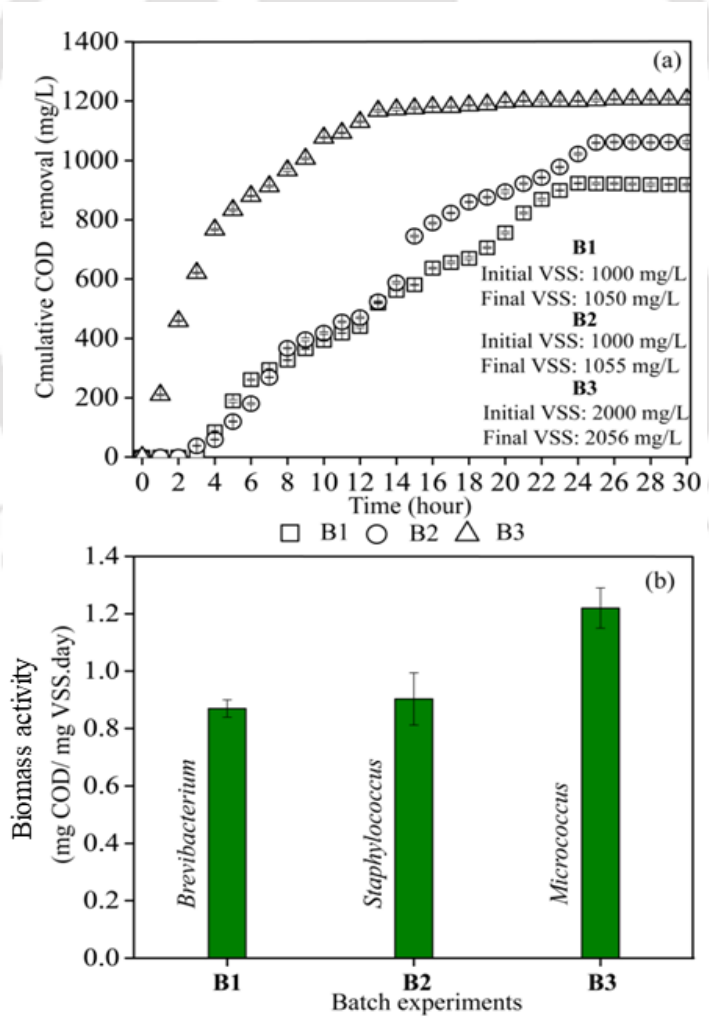

Fig.6.9 (a) Cumulative COD removal profile in the batches with (b) individual biomass activity profile of B1, B2 and B3.

The initial flocculent cultures of *Brevibacterium*, *Staphylococcus* and *Micrococcus* achieved only 0.002 mg COD/ mg VSS.day biomass activity value after 50 h of the study in refinery wastewater. After salt acclimatization, the biomass activity pattern correlated with granule VSS content, salt tolerance and hydrocarbon removal efficiencies of the batches. Aerobic granules achieved a stable (71-93%) COD removal between 20-35 g/L salinity range providing average 0.87±0.03, 0.90±0.09, 1.22±0.07 mg COD/ mg VSS.day of biomass activity values in B1, B2 and B3, respectively. Above 8 g/L VSS and 12% IC value ensured maximum biomass activity in B3. Similarly, in Chapter 3 (section 3.3.3.1), we observed higher biomass activity in granules having 8 g/L VSS and 21% IC developed under 12 h HRT than AGRs operated with longer HRTs providing weaker granules.

6.3.7 Analysis of pollutant removal kinetics

Day 49 onwards, pollutant removals were checked in every 6 h intervals till 24 h. TPH, phenol, cresols and NH_4^+-N removal profiles during a batch cycle are illustrated in Fig.6.10. Fig.6.11-6.13 provides the HPLC data of phenol and cresol concentrations in every 6 h intervals in B1, B2 and B3 treated effluent. HPLC peaks for phenol and *o*-cresol were observed at 12.5 min, 15.9 min, respectively and *m* and *p*-cresol peaks appeared together at 17.2 min.

B1, B2 and B3 achieved 71-93% COD removal within 12-24 h of batch operation at 25-35 g/L NaCl exposure. TPH removal efficiency also varied between 71.5 to 92.7 % in 24 h. HPLC analysis proved that after 24 h of feeding, B1 was capable of removing 70-97% phenol and cresols contributing 381±1 mg/L COD and 94±2 mg/L TPH values in effluent. Reduced VSS (5-3 g/L) and low biomass activity (0.87±0.03 mg COD/mg VSS.day) in *Brevibacterium* granules resulted into no further (effluent sample checked on 30th h) phenolics degradation in B1 after the 24th hour. Stable granules of B2 could remove 68% phenol and 70% cresols in 18 h and complete phenol and cresol degradation occurred in 24 h but remaining 59.3±1 mg/L effluent TPH concentration accounted for the non-degraded diesel fractions in B2.

HPLC peaks for B3 effluent indicated complete removal of phenol, *o*, *m* and *p*-cresol removal within 12 h. B3 had the minimum 24±0.12 mg/L effluent TPH concentration which is corresponding to its strong microstructure (IC: 12%) and highest biomass activity value (1.22±0.07 mg COD/ mg VSS.day) among the batches. Biomass activity (Fig.6.9) and hydrocarbon removal rates were supporting the kinetic data trends in B1, B2 and B3.

Kinetic study evaluated 89, 93 and 96% NH_4^+-N removal efficiencies within 24 h providing 0.75, 3.8 and 2 mg/L of effluent NH_4^+-N concentrations, in B1, B2 and B3,

respectively. The effluent NO_3^--N range varied between 0.51-14.5 mg/L suggesting only 1.02 and 1.56% complete nitrification in B1 and B2 which improved till 28% in B3.

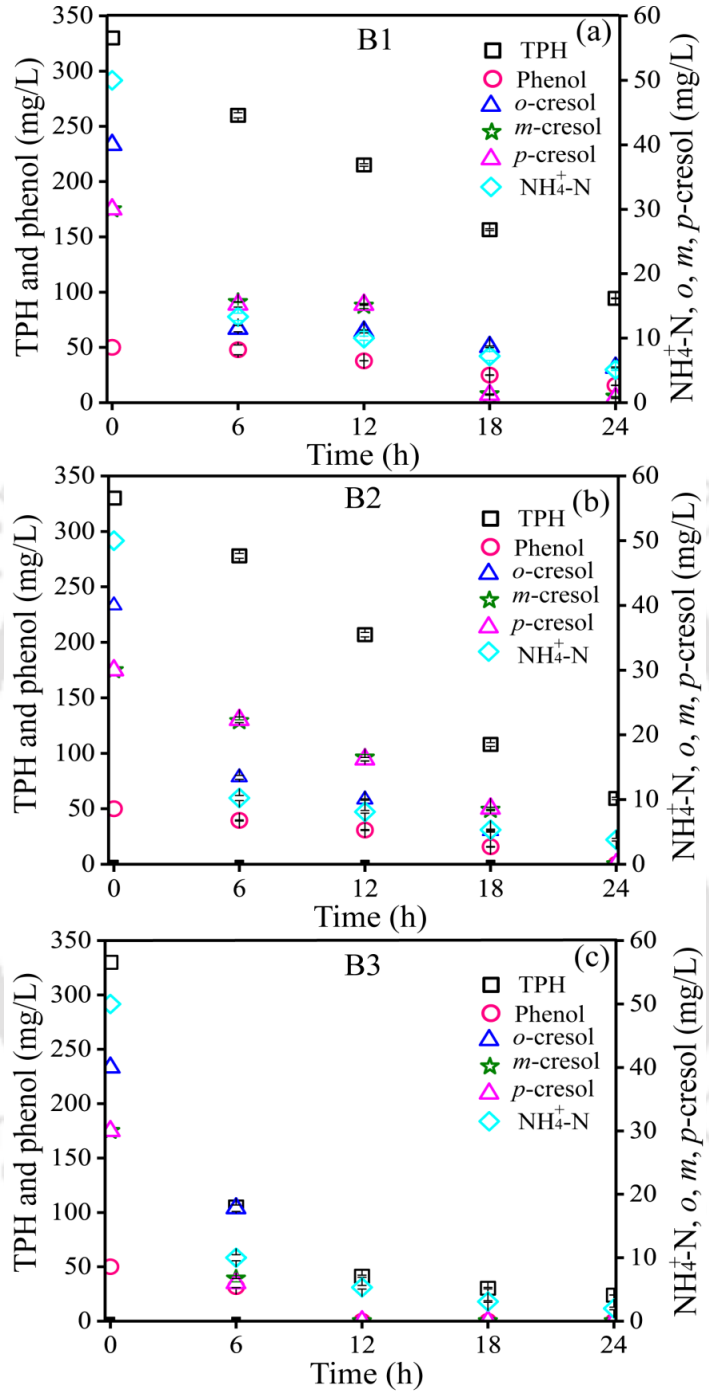

Fig.6.10 TPH, Phenol, o, *m*, *p* cresol and NH_4^+-N removal kinetics in every 6 h intervals in (a) B1, (b) B2 and (c) B3 (day 49 onwards).

The entire study reflected that salt adaptation and high EPS concentration helped to achieve salt tolerant granules in the batches. Previous oil exposure of refinery wastewater treatment plant sludge facilitated 330±10 mg/L hydrocarbon tolerance threshold in B3 with the fastest (12 h) complete phenolics removal among the three strains. As heterotrrophic *o*-

cresol degraders protected AOB population in aerobic granules (Jemaat et al., 2014), cocci dominance on *Micrococcus* granule partially protected nitryfying bacteria enabling 28% complete nitrifications.

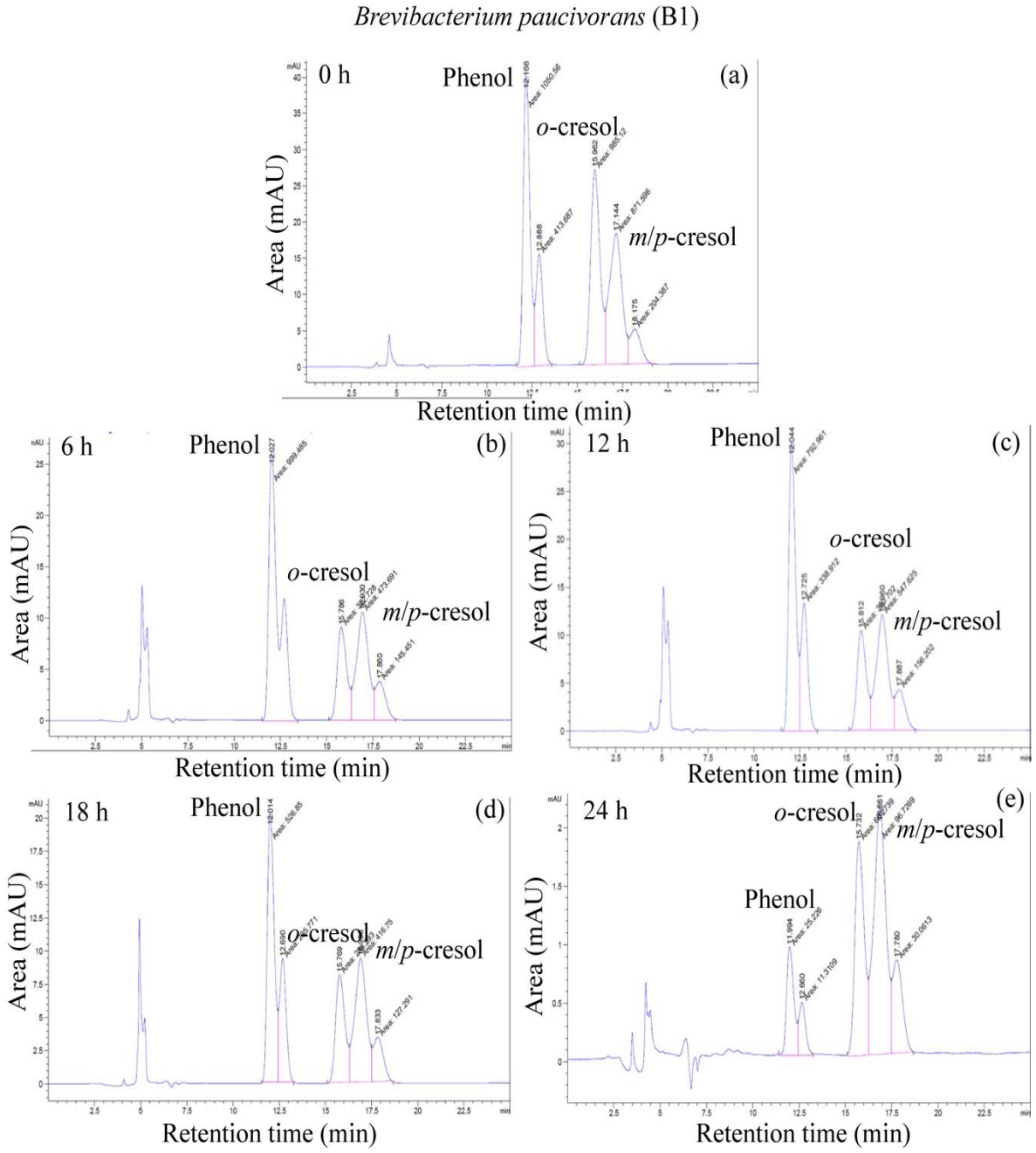

Fig.6.11 HPLC data in B1 (*Brevibacterium* granules) for phenol and cresol concentrations in (a) 0 h, (b) 6 h, (c) 12 h, (d) 18 h and (e) 24 h of the batch cycle.

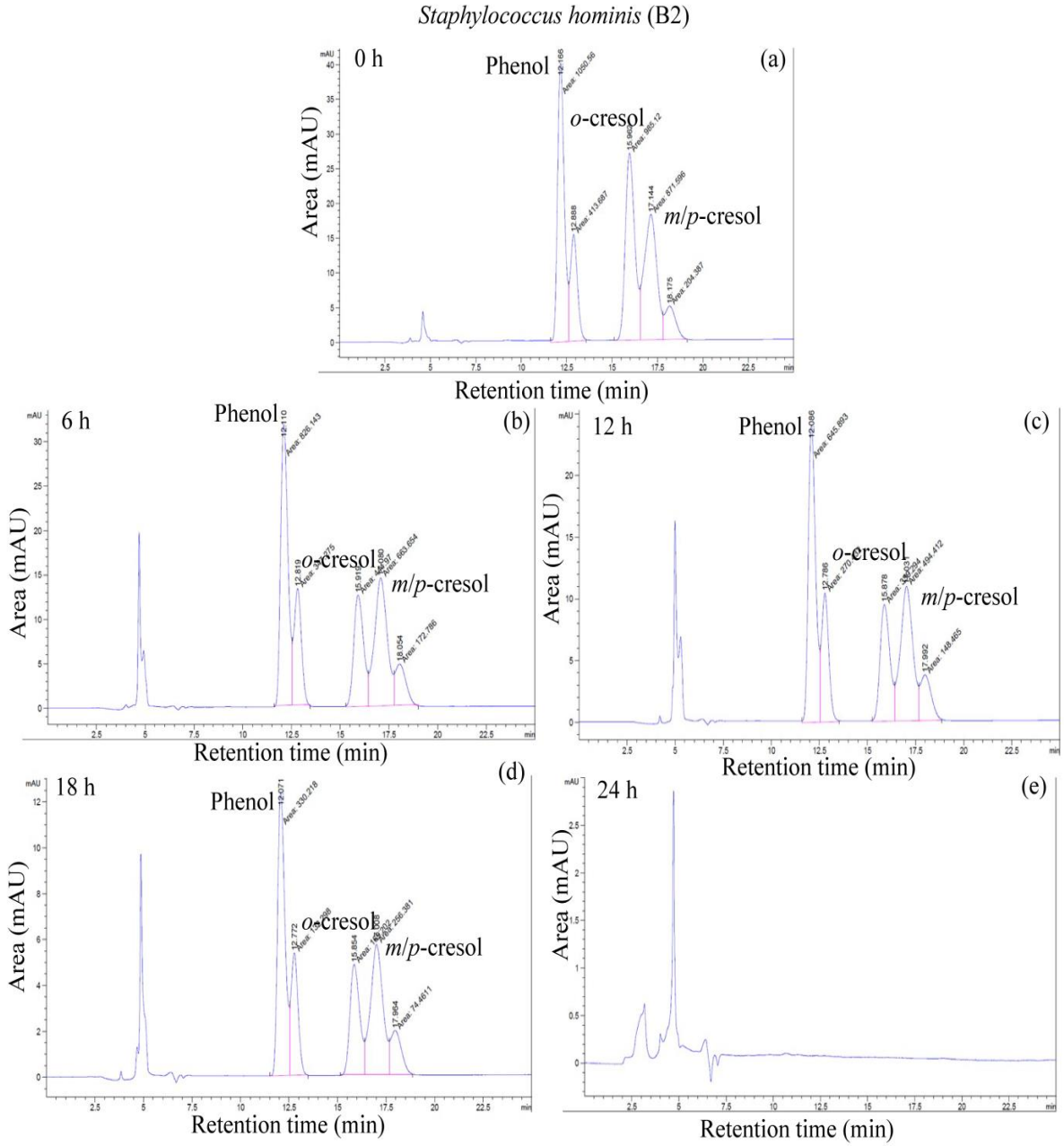

Fig.6.12 HPLC data in B2 (*Staphylococcus* granules) for phenol and cresol concentrations in (a) 0 h, (b) 6 h, (c) 12 h, (d) 18 h and (e) 24 h of the batch cycle.

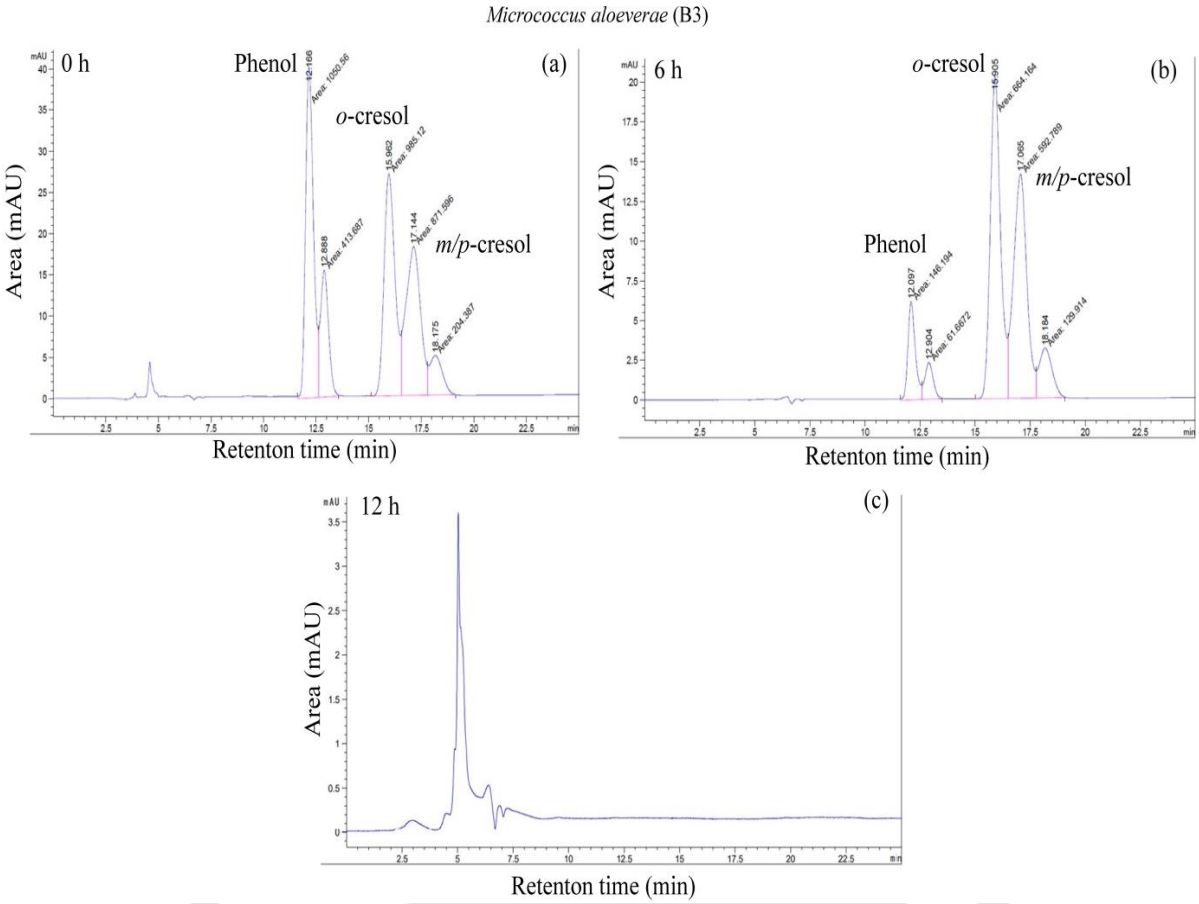

Fig.6.13 HPLC data in B3 (*Micrococcus* granules) for phenol and cresol concentrations in (a) 0 h, (b) 6 h, (c) 12 h of the batch cycle.

6.4 Summary of the chapter

High salinity and high oil concentrations are the major problems faced while treating refinery wastewater. A batch study on biodegradation of hypersaline refinery wastewater having toxic organic pollutants like phenol, cresol, emulsified diesel and ammonia was carried out using three bacterial strains *Brevibacterium paucivorans*, *Staphylococcus hominis* and *Micrococcus aloeverae*. Granular sludge was developed in 21-25 days with each bacterial strain solving slow granulation hitches without adding new sludge or co-substrates. *Brevibacterium* had granule disintegration after 20 g/L NaCl salinity whereas *Staphylococcus* achieved 82% TPH removal at 35 g/L NaCl salinity. *Micrococcus* granules tolerated salinity of 35 g/L NaCl due to refinery sludge origin, dense microstructure and maximum EPS content in sludge among the three strains providing 93% removal of 330 mg/L TPH in 70 days. It also showed fastest phenol and TPH removal kinetics with 28% nitrification in 12 h of batch operation. It is recommended that bioaugmentation of granules prepared from *Micrococcus aloeverae* strain may tolerate high salinity (≥35 g NaCl/L) and capable to degrade organics in high strength refinery wastewater.

References

Abdullah, N., Yusof, N., Ismail, A.F. and Lau, W.J., 2020. Insights into metal-organic frameworks-integrated membranes for desalination process: A review. Desalination 114867.

Basheer, F. and Farooqi, I.H., 2012. Biodegradation of *p*-cresol by aerobic granules in sequencing batch reactor. Journal of Environmental Sciences 24.

Campo, R., Corsino, S.F., Torregrossa, M. and Di Bella, G., 2018. The role of extracellular polymeric substances on aerobic granulation with stepwise increase of salinity. Separation and Purification Technology 195, 12-20.

Campo, R., Di Bella, G., 2019. Petrochemical slop wastewater treatment by means of aerobic granular sludge: effect of granulation process on bio-adsorption and hydrocarbons removal. Chemical Engineering Journal 378, 122083.

Castro-Muñoz, R., 2020. Breakthroughs on tailoring pervaporation membranes for water desalination: A review. Water Research 116428.

Chen, C., Ming, J., Yoza, B.A., Liang, J., Li, Q.X., Guo, H., Liu, Z., Deng, J. and Wang, Q., 2019. Characterization of aerobic granular sludge used for the treatment of petroleum wastewater. Bioresource Technology 271, 353-359.

Corsino, S.F., Campo, R., Di Bella, G., Torregrossa, M., Viviani, G., 2015. Cultivation of granular sludge with hypersaline oily wastewater. International Biodeterioration & Biodegradation 105, 192-202.

Corsino, S.F., Capodici, M., Morici, C., Torregrossa, M. and Viviani, G., 2016. Simultaneous nitritation–denitritation for the treatment of high-strength nitrogen in hypersaline wastewater by aerobic granular sludge. Water Research 88, 329-336.

Corsino, S.F., Capodici, M., Torregrossa, M. and Viviani, G., 2018. A comprehensive comparison between halophilic granular and flocculent sludge in withstanding short and long-term salinity fluctuations. Journal of Water Process Engineering 22, 265-275.

Di Bella, G., Di Prima, N., Di Trapani, D., Freni, G., Giustra, M.G., Torregrossa, M. and Viviani, G., 2015. Performance of membrane bioreactor (MBR) systems for the treatment of shipboard slops: assessment of hydrocarbon biodegradation and biomass activity under salinity variation. Journal of hazardous materials 300, 765-778.

Du, J.R., Zhang, X., Feng, X., Wu, Y., Cheng, F. and Ali, M.E., 2020. Desalination of high salinity brackish water by an NF-RO hybrid system. Desalination 491, 114445.

Ghangrekar, M., Asolekar, S., Joshi, S., 2005. Characteristics of sludge developed under different loading conditions during UASB reactor start-up and granulation. Water Research 39, 1123-1133.

Hamza, R.A., Sheng, Z., Iorhemen, O.T., Zaghloul, M.S. and Tay, J.H., 2018. Impact of food-to-microorganisms ratio on the stability of aerobic granular sludge treating high-strength organic wastewater. Water Research 147, 287-298.

He, Q., Xie, Z., Fu, Z., Wang, H., Chen, L., Gao, S., Zhang, W., Song, J., Xu, P., Yu, J. and Ma, J., Effects of phenol on extracellular polymeric substances and microbial communities from aerobic granular sludge treating low strength and salinity wastewater. Science of The Total Environment 752, 141785.

Ho, K. L., Lin, B., Chen, Y. Y., & Lee, D. J., 2009. Biodegradation of phenol using Corynebacterium sp. DJ1 aerobic granules. Bioresource Technology 100, 5051-5055.

Hou, M., Li, W., Li, H., Li, C. and Wu, X., 2019. Performance and bacterial characteristics of aerobic granular sludge in response to alternating salinity. International Biodeterioration & Biodegradation 142, 211-217.

Jawed, M., Tare, V., 1999. Microbial composition assessment of anaerobic biomass through methanogenic activity tests. Water SA 25, 345-350.

Jemaat, Z., Suárez-Ojeda, M.E., Pérez, J. and Carrera, J., 2014. Partial nitritation and o-cresol removal with aerobic granular biomass in a continuous airlift reactor. Water Research 48, 354-362.

Karray, F., Aloui, F., Jemli, M., Mhiri, N., Loukil, S., Bouhdida, R., Mouha, N. and Sayadi, S., 2020. Pilot-scale petroleum refinery wastewaters treatment systems: performance and microbial communities' analysis. Process Safety and Environmental Protection 141, 73-82.

Li, J., Ma, Z., Gao, M., Wang, Y., Yang, Z., Xu, H. and Wang, X.H., 2020. Enhanced aerobic granulation at low temperature by stepwise increasing of salinity. Science of The Total Environment 137660.

Liu, Y., Tay, J.-H., 2004. State of the art of biogranulation technology for wastewater treatment. Biotechnology Advances 22, 533-563.

Liu, Z., Liu, Y., Zhang, A., Zhang, C. and Wang, X., 2014. Study on the process of aerobic granule sludge rapid formation by using the poly aluminum chloride (PAC). Chemical Engineering Journal 250, 319-325.

Ma, J.Y., Quan, X.C., Yang, Z.F. and Li, A.J., 2012. Biodegradation of a mixture of 2, 4-dichlorophenoxyacetic acid and multiple chlorophenols by aerobic granules cultivated

through plasmid pJP4 mediated bioaugmentation. Chemical Engineering Journal 181, 144-151.

Mallick, S.K. and Chakraborty, S., 2020. Salinity footprint on anoxic-aerobic sequential moving bed reactors during petroleum refinery wastewater treatment: Effects on the dominant species. Journal of Water Process Engineering 37, 101376.

Meng, F., Huang, W., Liu, D., Zhao, Y., Huang, W., Lei, Z. and Zhang, Z., 2020. Application of aerobic granules-continuous flow reactor for saline wastewater treatment: Granular stability, lipid production and symbiotic relationship between bacteria and algae. Bioresource Technology 295, 122291.

Metcalf, E., Eddy, H.I. 2003. Wastewater engineering; treatment and reuse. McGraw-Hill, Boston.

Ming, J., Wang, Q., Yoza, B.A., Liang, J., Guo, H., Li, J., Guo, S. and Chen, C., 2020. Bioreactor performance using biochar and its effect on aerobic granulation. Bioresource Technology 300, 122620.

Ogura, S., Hamza, R.A. and Tay, J.H., 2020. Dried aerobic granules for fast startup of aerobic granular sludge reactors: Reactivation and performance. Journal of Water Process Engineering 36, 101298.

Ou, D., Li, H., Li, W., Wu, X. and Wang, Y.Q., 2018. Salt-tolerance aerobic granular sludge: formation and microbial community characteristics. Bioresource Technology 249, 132-138.

Qin, L., Tay, J.-H., Liu, Y., 2004. Selection pressure is a driving force of aerobic granulation in sequencing batch reactors. Process Biochemistry 39, 579-584.

Ramos, C., Suárez-Ojeda, M.E. and Carrera, J., 2015. Long-term impact of salinity on the performance and microbial population of an aerobic granular reactor treating a high-strength aromatic wastewater. Bioresource Technology 198, 844-851.

Razavi, S.M.R. and Miri, T., 2015. A real petroleum refinery wastewater treatment using hollow fiber membrane bioreactor (HF-MBR). Journal of Water Process Engineering 8, 136-141. 011

Sarvajith, M. and Nancharaiah, Y.V., 2020. Biological nutrient removal by halophilic aerobic granular sludge under hypersaline seawater conditions. Bioresource Technology 318, 124065.

Sivasubramanian, R., Chen, G.H. and Mackey, H.R., 2021. Shock effects of monovalent cationic salts on seawater cultivated granular sludge. Journal of Hazardous Materials 403, 123646.

Song, W., Xu, D., Bi, X., Ng, H.Y. and Shi, X., 2020. Intertidal wetland sediment as a novel inoculation source for developing aerobic granular sludge in membrane bioreactor treating high-salinity antibiotic manufacturing wastewater. Bioresource Technology 314, 123715.

Tay, J.H., Ivanov, V., Pan, S., Tay, S.L. 2002. Specific layers in aerobically grown microbial granules. Letters in Applied Microbiology 34(4), 254-257.

Wan, C., Sun, S., Lee, D.J., Liu, X., Wang, L., Yang, X. and Pan, X., 2013. Partial nitrification using aerobic granules in continuous-flow reactor: Rapid startup. Bioresource Technology 142, 517-522.

Winkler, M.-K.H., Meunier, C., Henriet, O., Mahillon, J., Suárez-Ojeda, M.E., Del Moro, G., De Sanctis, M., Di Iaconi, C., Weissbrodt, D.G., 2018. An integrative review of granular sludge for the biological removal of nutrients and recalcitrant organic matter from wastewater. Chemical Engineering Journal 336, 489–502.

Wu, X., Li, H., Lei, L., Ren, J., Li, W. and Liu, Y., 2020. Tolerance to short-term saline shocks by aerobic granular sludge. Chemosphere 243, 125370.

Zheng, Y.M., Yu, H.Q., Liu, S.J. and Liu, X.Z., 2006. Formation and instability of aerobic granules under high organic loading conditions. Chemosphere 63, 1791-1800.

Wang, C., Chen, Y., Hu, X. and Feng, X., 2021. In-situ synthesis of PA/PVDF composite hollow fiber membranes with an outer selective structure for efficient fractionation of low-molecular-weight dyes-salts. Desalination 503, 114957.

Operational cost analysis and techno-economic assessment of the study

The current study in Ph.D required one time lab-scale AGR establishment cost of approximately Rs.1,01,647.00 which is summarized in Table I.

Table I List of equipment along with the cost of AGR fabrication

Particular	**Quantity**	**Price (Rs.)**
Acrylic pipes	3	4155.00
Acrylic body rotameter	3	5988.00
6 ½ S angles	6	572.00
Bubble stones	10	210.00
Paint, primer, brush, Araldite, M seal, Aluminum strips	10	615.00
Nut-bolts	50	169.00
Silicone rubber tubing	5 m	1938.00
Air compressor	1	20,000.00
Peristaltic pump	1	68,000.00
Total		**1,01,647.00**

The Techno-economic assessment or the cost-benefit analysis of the AGR treatment of refinery wastewater is calculated in terms of treatable wastewater volume, space, time and power requirement while comparing with activated sludge process. Table II provides the techno-economic analysis of our AGRs.

Table II Techno-economic analysis of AGRs and activated sludge process to treat refinery wastewater

Bioreactor	**Reactor volume (L)**	**No of cycle/day**	**Treated water volume (L)**	**Hydrocarbon removal efficiency**	**Energy Requirement (kWh)**	**Operational cost (Rs.)**	**Reference**
Activated sludge process	6	1	3	80-90%	1.92	15.56	Mizzouri et al. (2013), Diya'uddeen et al. (2015)
AGR	3	3	4.5	70-99%	1.92	15.56	Current study

According to the literature, AGR system can reduce up to 75% of space requirement and 25% of energy requirement while compared to activated sludge process (de kruek et al., 2004). In current study, the AGR operational cost involved continuous air supply which was delivered by air compressor at a controlled air flow rate of 2 L/min which required minimum 1.92 kWh or 1.92 unit of energy consumption having electricity cost nearly Rs.15.56/day (considering per unit energy cost as Rs.8). Use of sludge bacteria also reduced the chemical consumption cost of the wastewater treatment process. In return, one lab-scale AGR of 3 L

working volume operated in 3 cycles/ day could produce approximately 4.5 L of treated water which was safe to dispose in agricultural lands. Table II depicts activated sludge process involving SBR or hybrid of Fenton and SBR would require double space for reactor volume, same energy cost and sometimes chemical usage to operate one reactor to produce lesser volume of treated water than AGR (Mizzouri et al., 2013; Diya'uddeen et al., 2015).

Though AGR and activated sludge both are capable of providing similar range of oil removal efficiency (70-90%), AGR is space saving and advantageous to treat more volume of wastewater in same time and operational cost.

The production cost of per unit of 2×2 inches of PHA sheet from aerobic granules by using all chemicals was estimated as Rs.3.75 which is given in Table III.

Table III Estimated cost analysis per unit of PHA production

Ingredients (for 2"×2")	**Price (for 2"×3") in Rs.**
Aerobic sludge granules	0.00
Ethanol	0.40
Acetone	0.75
Chloroform	0.30
Sulfuric acid	1.30
Electricity	1.00
Total cost	**3.75**

Commercial PHA procured from SIGMA-ALDRICH costs around Rs.18,000 for 10 g whereas, extraction of PHA from granular sludge provides an economical sludge management with value added product recovery. Hence the recovery of biodegradable PHA is an added advantage of cost saving in the oi1 refinery waste treatment system.

References

de Kreuk, M.V. and Van Loosdrecht, M.V., 2004. Selection of slow growing organisms as a means for improving aerobic granular sludge stability. Water Science and Technology, 49, 9-17.

Mizzouri, N.S. and Shaaban, M.G., 2013. Individual and combined effects of organic, toxic, and hydraulic shocks on sequencing batch reactor in treating petroleum refinery wastewater. Journal of hazardous materials, 250, 333-344.

Diya'uddeen, B.H., Pouran, S.R., Aziz, A.A., Nashwan, S.M., Daud, W.M.A.W. and Shaaban, M.G., 2015. Hybrid of Fenton and sequencing batch reactor for petroleum refinery wastewater treatment. Journal of Industrial and Engineering Chemistry, 25, 186-191.

Chapter 7

Conclusions and future scope

CHAPTER 7

Conclusions and future scope

The chapter comprises the major findings of the entire work along with the probable future research scope. The study was about investigating the role of different inoculum, isolation of oil degrading bacterial strains, influence of different operating HRTs on granule properties and hydrocarbon removal efficiencies in AGR system while treating oily wastewater. Granule mediated hydrocarbon degradation mechanism was predicted and a probable granule structure restoration technique was explored. Phytotoxic effect of AGR treated effluent was checked on *Cicer arietinum* and *Vigna radiata.* Rapid granulation of *Micrococcus aloeverae* strain SG002 and its most appropriate approach of bioaugmentation were thoroughly studied in AGR treating high strength refinery wastewater laden with oil, phenol and cresols. Recovery of value-added biopolymer P (3HB-*co*-3HV) from oil-fed waste granules was another aim of our study. Effects of salinity on *Brevibacterium*, *Micrococcus* and *Staphylococcus* granules while treating refinery wastewater were also examined. The major conclusions of the study are summarized below:

i) Type of inoculum and its previous exposure to oily wastewater had significant impact in granule formation and stability in AGR. Previous oil exposure helped the refinery sludge granules to achieve maximum granule size and EPS content in presence of 320 mg/L of emulsified diesel. Refinery sludge granules achieved 67% oil removal with maximum 310±10 mg/L diesel oil tolerance whereas the sewage and brewery granules removed 61.02±0.08% and 61.76±0.26% hydrocarbons providing 170±15 and 250±10 mg/L oil tolerance thresholds, respectively. NH_4^+-N removal varied between 91-97% in the AGRs. *Brevibacterium paucivorans* strain SG001, *Micrococcus aloeverae* strain SG002 and *Staphylococcus hominis* strain SG003 were the major pollutant degraders isolated from sewage, refinery and brewery sludge granules. *Micrococcus* had maximum 61% oil removal efficiency among the three species.

ii) Reconstruction of the disintegrated granules was carried out by adding simple substrate like sodium acetate in AGR which was an easier way than adding new sludge in the reactors.

iii) AGR with shortest HRT (12 h) and the highest oil loading of 0.5 kg/m^3.day had biggest and strongest granules but longest HRT (48 h) with the lowest (0.125 kg/m^3.day) loading provided longer contact time between hydrocarbons and granules for 90.31±0.26% TPH removal (250 mg/L). With 12 h HRT, medium chain *n*-alkanes (C_{11}-C_{15}) probably

converted into fatty acids (C_{13}-C_{18}) and longer HRTs (24 h, 24 h) degraded C_6-C_{27} alkanes which further followed the β-oxidation of the fatty acids. NH_4^+-N removal in AGRs with 12, 24 and 48 h HRTs were 94, 95 and 98%, respectively. As nitrification is a longer process, 48 h HRT provided maximum 20% complete nitrification by aerobic granules. The study recommended AGR operation between 24-48 h HRTs with 0.125-0.25 kg/m^3.day hydrocarbon loadings providing 77 to 24 mg/L of effluent TPH concentration to avoid phytotoxicity after disposal.

iv) Rapid granulation of oil degrader *Micrococcus aloeverae* strain in 15 days solved the slow granulation problem faced by mixed sludge inoculum in AGRs.

v) Boiaugmentation of liquid *Micrococcus* in AGR had no significant impact improving granule stability but it increased hydrocarbon removal from 70 to 83.45% than the control AGR. On other hand, only 2 doses of granular culture augmentation of *Micrococcus* facilitated cocci abundant granule microstructure with improved granule size and stability.

vi) Development of the most appropriate bioaugmentation approach by using 10% (w/w) granular *Micrococcus* in AGR reduced granule rupture problem achieving 99% TPH removal in 2 h with 19% complete nitrification while treating oil, phenol and cresol laden refinery wastewater. Degradation of C_8-C_{15} *n*-alkanes with fatty acid conversion was observed in control and removal of C_6-C_{36} predicted β-oxidation of fatty acids in bioaugmented AGRs.

vii) As longer SRT (10-30 days) is ideal for NOB growths for complete nitrification, comparative shorter SRTs (8 and 9.3 days) inhibited NOB population where AOB and NOB could not outcompete the heterotrophic oil degraders in aerobic granules producing 9-10.6% partial and only 1-3% complete nitrification in control and liquid *Micrococcus* augmented AGRs, respectively. But granulated *Micrococcus* augmentation enhanced SRT till 19 days due to reduced granule rupture providing 90% NH_4^+-N removal where 70% nitrogen was consumed by biomass. Cocci dominated granular surface acted as a protector of nitrifying bacteria in the core of granules promoting maximum 19% complete nitrification in granular augmented AGR without adding co-substrates.

viii) About 2 kg COD/m^3.day OLR with 10% (w/w) granular *Micrococcus* augmentation is recommended for stable granulation in AGR to achieve complete hydrocarbon removal from refinery wastewater treatment within permitted discharge limit (10 mg/L).

ix) *Brevibacterium, Staphylococcus* and *Micrococcus* separately achieved batch scale granulation in 15-25 days solving slow granulation hitches in oily wastewater.

Micrococcus achieved the smallest and strongest granules with 330±10 mg/L of TPH and 35 g/L salt tolerance due to formation of thick EPS layer contributing complete phenolics removal in 12 h with improved nitrification up to 28%. It indicated potential use of *Micrococcus* bioaugmentation in treatment plants of hypersaline (≥30 g/L salinity) refinery wastewater.

x) Recovery of biodegradable polymer polyhydroxyalkanoates (PHA) from oil degrading waste sludge granules established a sludge management providing simultaneous oil removal and bioplastic production in AGR. Changing OLR (0.6-1.8 kg COD/m^3.day) and high C/N (8-24) ratio stimulated maximum 0.71 and 0.47 mg PHA/mg CDW accumulation in refinery sludge and *Micrococcus* inoculated granules. PHA was characterized as copolymer P (3HB-*co*-3HV) having 3.5-4.5 of butyrates and valerates (PHB:PHV) ratios. Long and short chain *n*-alkanes (C_{16}-$C_{36,}$ C_6-C_{10}) in oily wastewater were mostly biotransformed into P (3HB-*co*-3HV) by aerobic granules.

- **Future scope**

i) Study on AGR treatment of real refinery wastewater having fluctuating characteristics in seasonal and plant operational variations with exploring biougmentation potential of specific strains to withstand the characteristics variation in wastewater can be performed.

ii) Treatment of BTEX, mercaptan and spent caustic containing refinery wastewater can be conducted in AGRs.

iii) PHA yield can be further improved by varying feast-famine ratio, air-flow rate and by applying bioaugmentation of specific bacteria in AGR.

iv) Hypersaline oily wastewater treatment in AGRs with salinity shock loading and microbial profiling of salt tolerant granules is another future scope of the study.

v) The influence of shifting from sequencing batch reactors (SBR) to continuous-flow stirred tank reactor (CSTR) can be further studied on granule formation, stability and reactor performance treating refinery wastewater.

vi) Pilot scale demonstration of the lab-scale AGR to show the usefulness of the current work in the treatment of oil refinery wastewater, identification of nitrogen oxidizing bacteria (NOB) present in the reactors and phytotoxicity anylysis determining plant uptake of oil and phenol would have been incorporated in future research scope of the study.

APPENDIX I

Table A1 Instruments and equipment used in the present study

Instruments	Parameters measured	Model/manufacturer/specification
^{1}H NMR	PHA charactrization	Bruker, 400 MHz NMR
AAS	metals	Varian, Netherlands
Air compressor	To provide aeration into the AGRs	Tarsons Rocky vac 420
Autoclave	Sterilization of media	Equitron, India
Centrifuge	Separation of suspended solids	REMI, India
CLSM	CLSM imaging	Leica TCS SP8, Leica, Germany
COD digester	COD	HACH, USA
Conductivity meter	Conductivity, salinity, TDS	Thermo Scientific, India
Electronic balance	Weight	Sartorius, Germany
FESEM	Granule microstructure	Zeiss, Sigma, Germany
Flame Photometer	Sodium, potassium, calcium	Systronics 128
FTIR Spectrometer	PHA charactrization	PerkinElmer, Spectrum 2
GC-MS	Hydrocarbons	PerkinElmer Claurus 680, USA
Horizontal Laminar Flow	Maintaining aseptic condition during microbial analysis	Ikon Instruments, India
Hot air oven	TSS and drying	IKON, India
HPLC	Phenol and cresols	Agilent Technologies, 1260 Infinity II
Ion chromatography	Nitrite-N, nitrate-N	Metrohm, Basic IC 792, Switzerland
Lyophilizer	Granule freeze drying	Labconco
Muffle furnace	VSS	Thermo Scientific, Hong Kong
Orbital Shaker	Shaking	Tarsons, India
Peristaltic pump	For reactor feeding	Miclins, PP30 EX 4CC
pH meter	pH	Extech, India
Rotameter	To control air-flow rate in the AGRs	CVG Technocrafts, India
Shaker incubator	Bacterial growth incubation	Scigenics Biotech, India
Turbidity meter	Turbidity	Systronics 132
Ultrapure water purification system	Ultrapure water	Merck, France
UV-Vis Spectrophotometer	NH_4^+-N, PHA, protein, carbohydrate, chlorophyll, catalase, peroxidase	Agilent Technologies, Cary 100 Singapore

APPENDIX II

Liner calibration curve

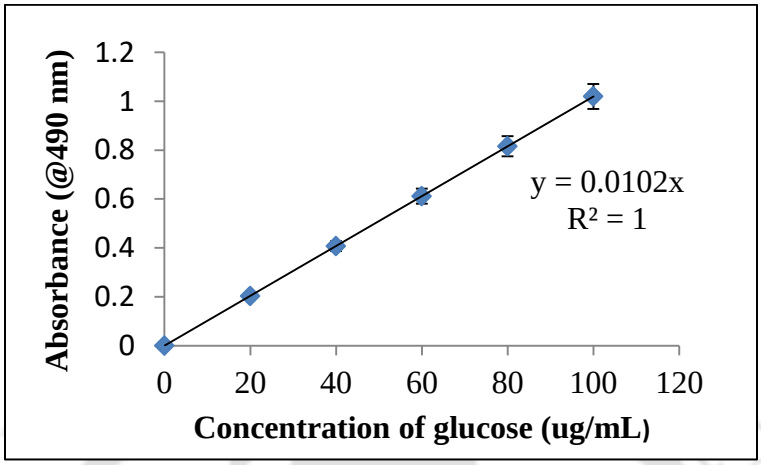

Fig.A1 Calibration curve for polysaccharides (PS)

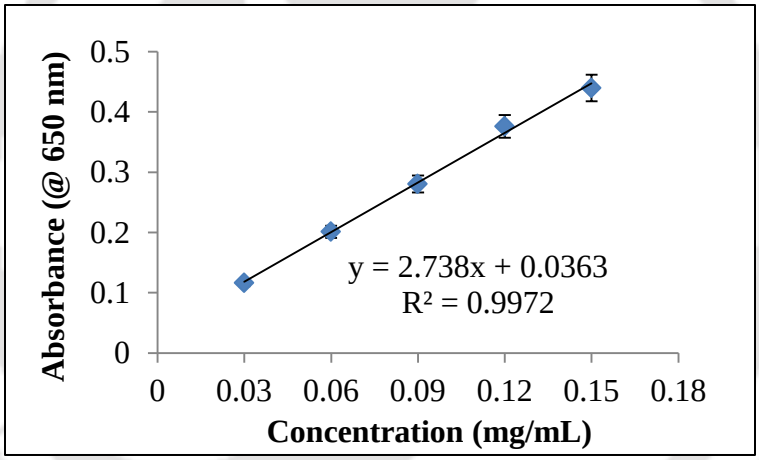

Fig.A2 Calibration curve for protein (PN)

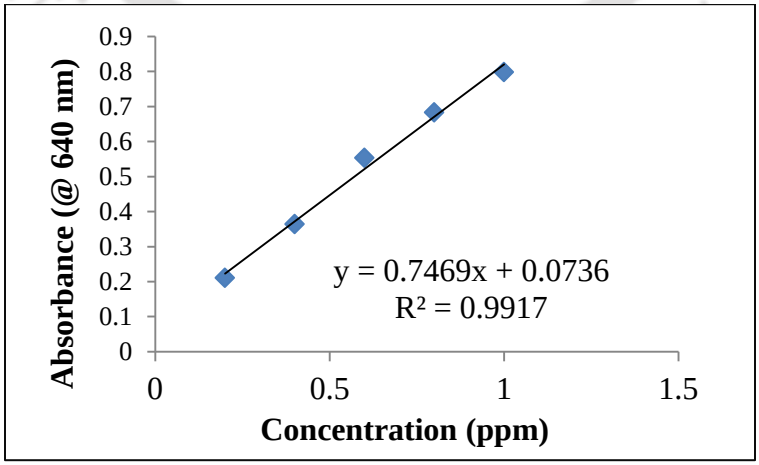

Fig.A3 Calibration curve for ammonia nitrogen (NH_4^+-N)

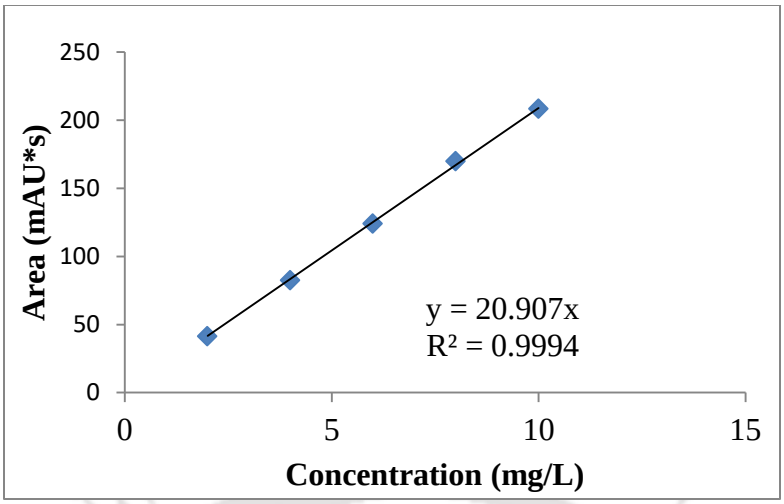

Fig.A4 Calibration curve for Phenol in HPLC

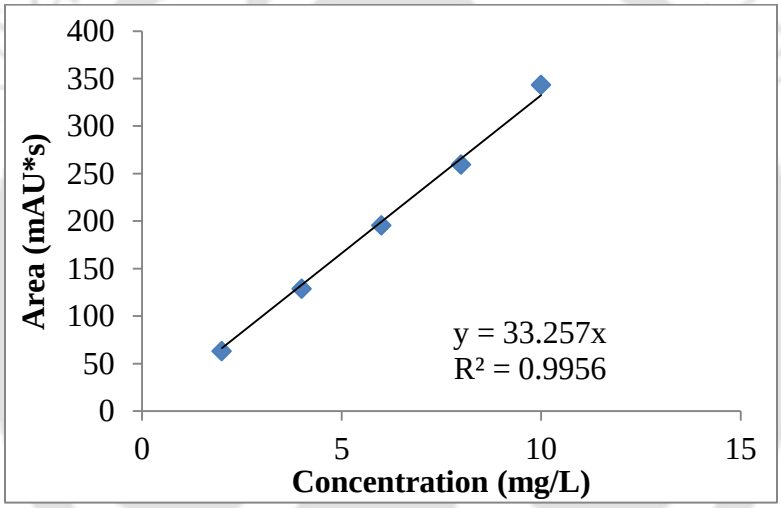

Fig.A5 Calibration curve for *o*-cresol in HPLC

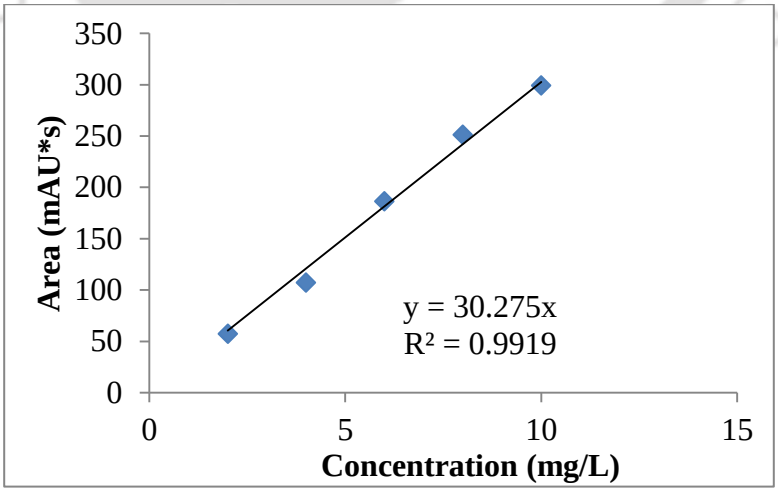

Fig.A6 Calibration curve for *m* and *p*-cresol in HPLC

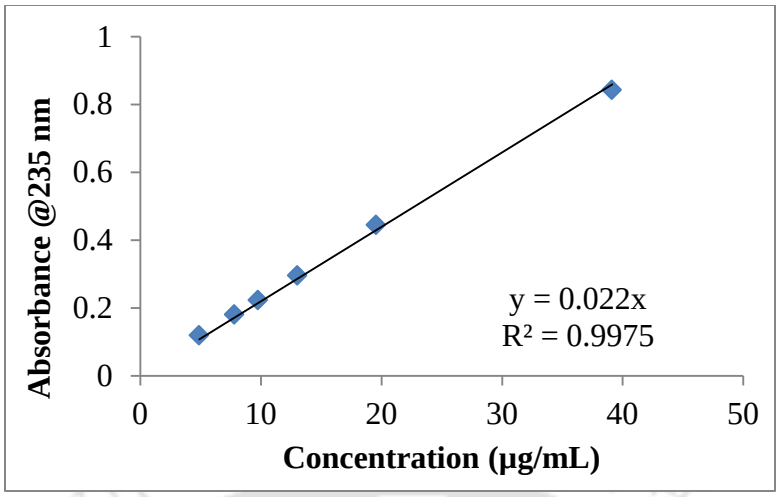

Fig.A7 Calibration curve for commercial PHB

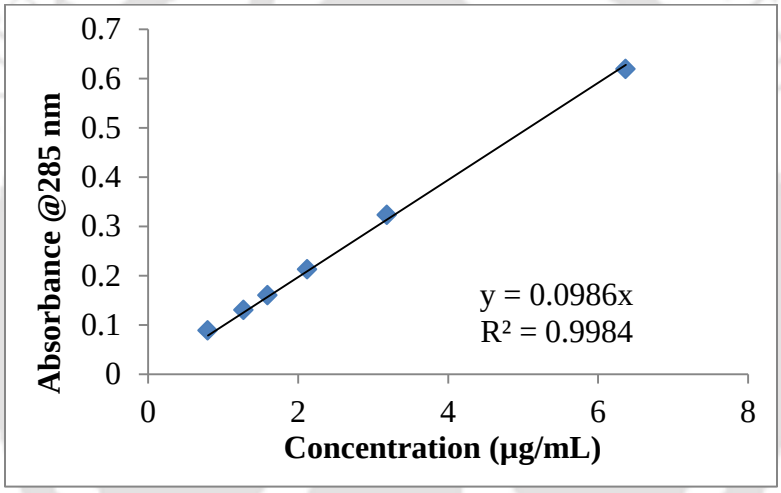

Fig.A8 Calibration curve for commercial PHV

List of Publications

International journal publications

- **Sayanti Ghosh** and Saswati Chakraborty. "Influence of inoculum variation on formation and stability of aerobic granules in oily wastewater treatment." Journal of environmental management 248 (2019): 109239.

- **Sayanti Ghosh** and Saswati Chakraborty. "Impacts of hydraulic retention time on granule behaviour and reactor activity during hydrocarbon degradation in aerobic granular reactors (AGRs) with phytotoxicity analysis". International Biodeterioration & Biodegradation 151 (2020): 104963.

- **Sayanti Ghosh** and Saswati Chakraborty. "Production of Polyhydroxyalkanoates (PHA) from aerobic granules of refinery sludge and *Micrococcus aloverae* strain SG002 cultivated in oily wastewater". International Biodeterioration & Biodegradation 155 (2020): 105091.

- **Sayanti Ghosh** and Saswati Chakraborty. "Aerobic granulation of single strain oil degraders: Salt tolerance enhancing organics and nitrogen removal from high-strength refinery wastewater". Journal of Water Process Engineering 42 (2021): 102104.

Book chapter

- **Sayanti Ghosh** and Saswati Chakraborty. **"**Aerobic Granulation in Hydrocarbon-rich Wastewater Treatment" in **"**Water Pollution and Remediation Technology: Organic Pollutants" (2020). Springer International Publishing. eBook ISBN: 978-3-030-52395-4, DOI: 10.1007/978-3-030-52395-4.

- **Sayanti Ghosh** and Saswati Chakraborty, "Recovery of Biodegradable Bioplastics from Different Activated Sludge Processes during Wastewater Treatment, In: Degradation of Plastics, Materials Research Foundations, Vol. 99, pp 145-162 (2021). DOI: https://doi.org/10.21741/9781644901335-6.

- **Sayanti Ghosh** and Saswati Chakraborty, "Remediation of Emerging Pollutants by Using Advanced Biological Wastewater Treatments". Applied Water Science: Remediation Technologies (2021), 2, pp.623-643. DOI: https://doi.org/10.1002/9781119725282.ch19.

Manuscripts communicated

Articles

- **Sayanti Ghosh** and Saswati Chakraborty. "Bioaugmentation of granulated *Micrococcus aloeverae* strain SG002 in aerobic granular reactors (AGR): novel approach for bioremediation of multiple hydrocarbon laden refinery wastewater". (Submitted).

Book chapters

- **Sayanti Ghosh** and Saswati Chakraborty. "Pollutant removal kinetics of aerobic granular reactors operated with different inocula and hydraulic retention times during diesel wastewater treatment". Springer International Publishing (Accepted, in Press).

- **Sayanti Ghosh** and Anjishnu Biswas. "Endocrine Disruptors in Municipal Wastewater: Occurrence, Characteristics, Effects, and Current Trends of Bioremediation" In: "Bioremediation of Endocrine Disrupting Pollutants in Industrial Wastewater", Elsevier. (Accepted, in press).

International conferences

- **Sayanti Ghosh** and Saswati Chakraborty, 2018. Treatment of Synthetic Oily Wastewater in Aerobic Granular Reactors (AGR). *RECYCLE- 2018,* IIT Guwahati, India, 22-24 February, 2018 **(Best paper award)**.

- **Sayanti Ghosh** and Saswati Chakraborty, 2018. Aerobic granulation in oily wastewater treatment: Granule characterization, pollutant removal, and phyto-toxicity study. *International conference on advanced Technologies for industrial Pollution Control (ATIPC-2018),* IIEST, Shibpur, India, 17-19 December, 2018.

- **Sayanti Ghosh** and Saswati Chakraborty, 2019. Pollutant removal kinetics of aerobic granular reactors operated with different inocula and hydraulic retention times during diesel wastewater treatment. *9th IconSWM-CE,* organized by ISWMAW at KIIT, Bhubaneswar, India, 27-30 November, 2019 **(IconSWM Excellence award 2019 for best paper)**.

- **Sayanti Ghosh** and Saswati Chakraborty, 2019. Aerobic Granulation of *Micrococcus aloeverae* Strain SG002 and its Application in Oil Remediation and Polyhydroxyalkanoates (PHA) Production. *Engineering Sustainable Development Conference 2019* organized by AIChE, Institute for Sustainability and APRU, Korea University, Seoul, South Korea, 12-13 December 2019 **(Received DST-SERB travel assistantship)**.

- **Sayanti Ghosh** and Saswati Chakraborty, 2020. Study on Oily Wastewater Treatment in Aerobic Granular Reactors by Varying Hydraulic Retention Time. *DST-UKIERI supported Workshop cum Symposium-2020 on "Bio-inspired Nanomaterials for Environmental Applications,* IIT Guwahati, India, 12-13 February 2020.

- **Sayanti Ghosh** and Saswati Chakraborty, 2020. Production of Polyhydroxyalkanoates (PHA) from aerobic granules of refinery sludge and *Micrococcus aloverae* strain SG002 cultivated in oily wastewater. *ICBSEE-2020,* NIT Rourkela, India, 5-7 March, 2020.

- **Sayanti Ghosh** and Saswati Chakraborty, 2020. Bioaugmentation approach to enhance aerobic granular reactor (AGR) performance in industrial wastewater treatment: a mini

review. *10th IconSWM-CE*, organized by ISWMAW, India, 2-4 December, 2020 on virtual platform.

- **Sayanti Ghosh** and Saswati Chakraborty, 2021. Bioremediation of hydrocarbon-rich wastewater by aerobic granules of oil degrading bacterial strains in salinity influence. *International web conference in civil engineering for a sustainable planet (ICCESP-2021)*, Organized by ASCE and TKM College of Engineering, India, 5-6 March, 2021.

National conferences

- **Sayanti Ghosh** and Saswati Chakraborty, 2017. Aerobic Granulation in Sequencing Batch Reactor (SBR) and Degradation of Waste Motor Oil. *CHEMCON-2017*, Haldia Institute of Technology, West Bengal, India, 27-30 December, 2017 **(Best poster award)**.

- **Sayanti Ghosh** and Saswati Chakraborty, 2020. Role of seed sludge and oil degrading microorganisms in aerobic granular treatment of hydrocarbon-rich wastewater with phyto-toxicity. *National Conference on Issues & Challenges in Water Treatment and allied research for Sustainable environment (WATER-2020)*, IIT Guwahati, India, 23-25 January, 2020 **(Best paper award)**.

Contest taken part

- **Sayanti Ghosh**, 2018. Presented research proposal on Utilization of Waste Motor Oil & Oily Wastewater: Degradation with Product Formulation. NORTH-EAST BIOSTART-2018. organized by Guwahati Biotech Park, IASST Guwahati, India, 3-5 April, 2018 **(Received 1st prize)**.